



**Northwest and  
Alaska Fisheries  
Center**

**National Marine  
Fisheries Service**

**U.S. DEPARTMENT OF COMMERCE**

**NWAFRC PROCESSED REPORT 87-20**

**Estimation of Egg Production,  
Spawner Biomass,  
and Egg Mortality  
for  
Walleye Pollock,  
*Theragra chalcogramma*,  
in Shelikof Strait  
from Ichthyoplankton Surveys  
during 1981**

**December 1987**

## **NOTICE**

This document is being made available in .PDF format for the convenience of users; however, the accuracy and correctness of the document can only be certified as was presented in the original hard copy format.

Inaccuracies in the OCR scanning process may influence text searches of the .PDF file. Light or faded ink in the original document may also affect the quality of the scanned document.



**Northwest and  
Alaska Fisheries  
Center**

National Marine  
Fisheries Service

U.S. DEPARTMENT OF COMMERCE

## **NWAFRC PROCESSED REPORT 87-20**

Estimation of Egg Production,  
Spawner Biomass,  
and Egg Mortality  
for  
Walleye Pollock,  
*Theragra chalcogramma*,  
in Shelikof Strait  
from Ichthyoplankton Surveys  
during 1981

December 1987



Estimation of Egg Production, Spawner Biomass, and Egg Mortality  
for Walleye Pollock, Theragra chalcogramma, in Shelikof Strait  
from Ichthyoplankton Surveys during 1981 1/

by

Richard Dennis Bates

Resource Assessment and Conservation Engineering Division  
Northwest and Alaska Fisheries Center  
National Marine Fisheries Service  
National Oceanic and Atmospheric Administration  
7600 Sand Point Way Northeast  
Bin C15700, Building 4  
Seattle, Washington 98115-0070

December 1987

1/ A thesis submitted in partial fulfillment  
of the requirements for the degree of

Master of Science

University of Washington

Chairman of the Supervisory Committee  
Dr. Donald R. Gunderson  
Fisheries Resource Institute



## Table of Contents

	Page
List of Figures . . . . .	iv
List of Tables . . . . .	xiii
Chapter 1. Introduction . . . . .	1
Chapter 2. Preliminary analysis of egg catches . . . . .	7
METHODS . . . . .	7
<u>Sampling design</u> . . . . .	7
<u>Field procedures</u> . . . . .	15
<u>Laboratory procedures and incubation time equations</u> . . . . .	16
<u>Tow standardizations</u> . . . . .	20
<u>Station abundance-age plots</u> . . . . .	22
<u>Treatment of hydroacoustic data</u> . . . . .	22
RESULTS . . . . .	22
<u>Egg age frequencies on a sample by sample basis</u> . . . . .	22
<u>Distribution of spawners</u> . . . . .	25
DISCUSSION . . . . .	25
<u>Co-occurrence of eggs and adults within the survey area</u> . . . . .	29
Chapter 3. The estimation of total daily egg abundance . . . . .	33
INTRODUCTION . . . . .	33
METHODS . . . . .	35
<u>Estimators for simple random sampling (SRS)</u> . . . . .	38
<u>Estimators for the delta distribution (DLN), adapted from</u> <u>Aitchison and Brown (1957)</u> . . . . .	39
<u>Estimators for the negative binomial distribution (NB),</u> <u>adapted from Bissel (1972b)</u> . . . . .	40
<u>Total daily egg abundance under the models SRS, DLN, and NB</u> . . . . .	41
<u>Estimators for stratified random sampling (STRS), adapted</u> <u>from Cochran (1977)</u> . . . . .	41
RESULTS . . . . .	43
DISCUSSION . . . . .	45
Chapter 4. Simulations of field sampling . . . . .	48
INTRODUCTION . . . . .	48
METHODS . . . . .	49
<u>General characteristics of egg catch distributions</u> . . . . .	49
<u>Construction of an egg abundance surface</u> . . . . .	51
<u>Simulation of an egg catch</u> . . . . .	58
<u>Survey simulation</u> . . . . .	60
<u>Statistical summary of catch data from simulated egg surveys</u> . . . . .	61
<u>Statistics employed in the comparison of confidence intervals</u> . . . . .	61
RESULTS . . . . .	62

DISCUSSION . . . . .	66
<u>Confidence intervals for the NB model</u> . . . . .	68
<u>Low containment rates and a random sampling design</u> . . . . .	69
<u>High containment rates and a systematic sampling design</u> . . . . .	70
<u>Modeling the spatial trend in egg abundances</u> . . . . .	76
 Chapter 5. A new approach to the estimation of seasonal egg production and egg mortality . . . . .	82
INTRODUCTION . . . . .	82
<u>The pattern of mortality with age</u> . . . . .	83
<u>Conventional approaches to the aggregation of stage         abundance data</u> . . . . .	84
<u>Generalization of the cohort concept</u> . . . . .	86
<u>The constant exponential mortality model and the nonconstant         production curve</u> . . . . .	87
<u>The determination of a date of sampling for a survey</u> . . . . .	90
<u>The representation of age and spawning date for an         instantaneous cohort and for a series of successive         cohorts</u> . . . . .	91
<u>The constant exponential mortality model and the normal         production curve</u> . . . . .	94
<u>Incorporating a nonconstant production function into the         mortality model</u> . . . . .	101
<u>Derivation of the objective function</u> . . . . .	102
METHODS . . . . .	105
<u>Fitting data to the objective function</u> . . . . .	105
<u>The depiction of residuals</u> . . . . .	110
RESULTS . . . . .	111
DISCUSSION . . . . .	114
 Chapter 6. Estimation of seasonal egg production and spawner biomass . . . . .	118
INTRODUCTION . . . . .	118
METHODS . . . . .	119
<u>Integrations over the spawning season</u> . . . . .	119
<u>Estimation of spawner biomass</u> . . . . .	121
RESULTS . . . . .	122
DISCUSSION . . . . .	124
 Chapter 7. Recommendations for survey design and analysis of future sampling efforts . . . . .	126
 Literature Cited . . . . .	129
 Appendix A: Age distributions for eggs of walleye pollock, <u>Theragra chalcogramma</u> , on a catch by catch basis . . . . .	135
 Appendix B: Confidence intervals for simulations of the sampling experiment . . . . .	174





## List of Figures

Number	Page
1. Ichthyoplankton stations and sampling dates for survey 1MF81 (March 11-20). The geographic position of a station is identified by a "+" and stations having the same julian date of sampling (bold number) are located between dashed lines. . . . .	8
2. Ichthyoplankton stations and sampling dates for survey 2MF81 (March 29 - April 08). Stations G001A-G080A were occupied on the first pass through the survey area and stations G081A-G091A were occupied when the survey area was retraced during survey 3 of hydroacoustic cruise MF81-2. The geographic position of a station is identified by a "+" and stations having the same julian date of sampling (bold number) are located between dashed lines. . . . .	9
3. Ichthyoplankton stations and sampling dates for survey 3MF81 (April 26 - May 01). The geographic position of a station is identified by a "+" and stations having the same julian date of sampling (bold number) are located between dashed lines. . . . .	10
4. Ichthyoplankton stations and sampling dates for survey 4MF81 (May 19-24). The geographic position of a station is identified by a "+" and stations having the same julian date of sampling (bold number) are located between dashed lines. . . . .	11
5. Hydroacoustic transect lines and sampling dates for cruise MF81-2, survey 1 (March 06-07 and 11-12). Transects are represented by solid lines and transects having the same julian date of sampling (bold number) are located between dashed lines. The 200 m isobath is shown. . . . .	12
6. Hydroacoustic transect lines and sampling dates for cruise MF81-2, survey 2 (March 24-27). Transects are represented by solid lines and transects having the same julian date of sampling (bold number) are located between dashed lines. The 200 m isobath is shown. . . . .	13
7. Hydroacoustic transect lines and sampling dates for cruise MF81-2, survey 3 (April 04-10). Transects are represented by solid lines and transects having the same julian date of sampling (bold number) are located between dashed lines. The 200 m isobath is shown. . . . .	14
8. Preliminary relationships between incubation temperature (°C) and the cumulative development time (hours to stage endpoint) for the 21 developmental stages recognized for eggs of walleye pollock. . . . .	19
9. An example station abundance-age plot for the eggs of walleye pollock. The logarithms of hourly stage abundances are plotted against the cumulative development times to stage midpoints. A stage number identifies the plotted point for each developmental stage. . . . .	23

10. Distribution of adult walleye pollock as indicated by hydroacoustic echo-integration data, cruise MF81-2 survey 1 (March 06-07 and 11-12).	26
11. Distribution of adult walleye pollock as indicated by hydroacoustic echo-integration data, cruise MF81-2 survey 2 (March 24-27).	27
12. Distribution of adult walleye pollock as indicated by hydroacoustic echo-integration data, cruise MF81-2 survey 3 (April 04-10).	28
13. The recent history of spawning by walleye pollock as indicated by the dominant age groups of eggs from bongo catches, cruise 2MF81 (March 29 - April 08). Solid lines enclose stations with similar spawning histories.	30
14. Geographic boundaries to the survey area and strata. The locations and sizes of strata roughly approximate the distribution of adults as indicated by hydroacoustic echo-integration data.	36
15. Global region A and intermediate regions of the survey area. Intermediate regions were constructed from position and egg abundance data from stations G001A-G083A of survey 2MF81.	52
16. Wire diagram in the form of a prismatic solid depicting the pattern of egg abundances for an intermediate region. An intermediate region was defined by the positions of 3 adjacent sampling stations. The planar surface of abundance models the on-average continuity in egg abundances within the geographic limits of an intermediate region, and the volume of the prismatic solid represents total egg abundance within the region.	53
17. Global abundance surface A. This wire diagram was constructed from position and egg abundance data for stations G001A-G083A of survey 2MF81, with stations G084A-G091A excluded.	56
18. Global abundance surface B. This wire diagram was constructed from position and egg abundance data for stations G001A-G091A, less stations G022A-G024A, of survey 2MF81.	57
19. Hypothetical frequency distributions of potential egg catches from several intermediate regions of the survey area. The distributions for these hypothetical regions are indicated by the numbers 1, 2, 3, and 4. All potential catches for region 1 are indicated by X's. For each region, egg abundances are relatively homogeneous in magnitude and range over only a portion of the total range of abundances for the entire survey area. A single collection is taken from each region out of all the potential sample units available for that region. For intermediate region 1 this particular sample unit is indicated by the encircled X.	72

20. Hypothetical frequency distribution of potential egg catches from all intermediate regions of the survey area. A single collection is systematically taken from each region and the magnitudes are indicated by X's. If a sample frequency distribution was constructed using all collections from every region of the survey area, this distribution would provide a good approximation to the true distribution of egg abundances. A random sampling design would often fail to sample regions having relatively high egg abundances because these regions are so uncommon. However, a systematic sampling throughout the survey area of the systematic trend in egg abundances is often much more successful in obtaining egg abundances in their true proportions. . . . 74

21. The relationship between spawning date, age, and egg abundance within the survey area is shown by this 3-dimensional depiction. The normal curve was assumed to illustrate the seasonal spawning curve, and mortality with age was modeled by a constant exponential decline in egg abundances. Two additional curves for seasonal egg abundance as a function of spawning date and age are shown at the ages associated with hatching and yolk sac absorption. The decline of an egg cohort is depicted by the crosshatched areas on the abundance curves. The totality of all abundance curves from spawning to mature adult forms a 3-dimensional surface which was termed the abundance surface. . . . 88

22. A constant rate of spawning and a constant exponential decline in egg abundance with age are depicted. An egg survey was assumed to center on a specific date of the spawning season (TOS = the time of sampling). The ages of eggs in plankton collections range throughout the entire incubation period, from age 0 to age  $t_3$ . A time transfer line relates the age of an egg to the date of spawning. The age axis was partitioned into 3 hypothetical age groups, denoted A, B, and C. The initial abundance of cohort B is depicted on the seasonal spawning plane and the subsequent abundance of this cohort at the time the survey was conducted is depicted on the sampling plane. The TOS-abundance curve represents the trend in egg abundances with age as of a specific date (TOS) of the spawning season. . . . 92

23. A normal spawning curve and a constant exponential decline in egg abundances are depicted. The time of sampling (TOS) for a hypothetical egg survey was positioned 15 days prior to the date of peak spawning. The age axis was partitioned into 3 hypothetical age groups, denoted A, B, and C. The initial abundance of cohort B is depicted on the seasonal spawning plane and the subsequent abundance of this cohort at the time the survey was conducted is depicted on the sampling plane. The TOS-abundance curve indicates the trend in egg abundances with increasing age. . . . 95

24. A normal spawning curve and a constant exponential decline in egg abundances are depicted. The time of sampling (TOS) for a hypothetical egg survey was partitioned into 3 hypothetical age groups, denoted A, B, and C. The initial abundance of cohort B is depicted on the seasonal spawning plane and the subsequent abundance of this cohort at the time the survey was conducted is depicted on the sampling plane. The TOS-abundance curve indicates the trend in egg abundances with increasing age. . . . . 96

25. A normal spawning curve and a constant exponential decline in egg abundances are depicted. The time of sampling (TOS) for a hypothetical survey was positioned 15 days subsequent to the date of peak spawning. The age axis was partitioned into 3 hypothetical age groups, denoted A, B, and C. The initial abundance of cohort B is depicted on the seasonal spawning plane and the subsequent abundance of this cohort at the time the survey was conducted is depicted on the sampling plane. The TOS-abundance curve indicates the trend in egg abundances with increasing age. . . . . 97

26. A normal spawning curve and a constant exponential decline in egg abundances are depicted. The time of sampling (TOS) for a hypothetical survey was positioned 30 days subsequent to the date of peak spawning. The age axis was partitioned into 3 hypothetical age groups, denoted A, B, and C. The initial abundance of cohort B is depicted on the seasonal spawning plane and the subsequent abundance of this cohort at the time the survey was conducted is depicted on the sampling plane. The TOS-abundance curve indicates the trend in egg abundances with increasing age. . . . . 98

27. The 3-dimensional model for spawning date, age, and egg abundance was rotated approximately 90° to clearly illustrate the shapes of TOS-abundance curves and sampling planes at five moments of the spawning season. The spawning plane is in the background and the hatching plane is in the foreground. The shape of a TOS-abundance curve can be seen to be a complex function of spawning date and age. The estimation of egg mortality is not a simple function of the abundances of a series of successive egg cohorts when the rate of egg production is not constant. . . . . 100

28. The best fitting abundance surfaces for the 1981 egg surveys. Only developmental stages 7 through 20 were used and residuals were weighted. Stage abundance data were from surveys 1MF81, 2MF81 (set A), 3MF81, and 4MF81 (top) and from surveys 1MF81, 2MF81 (set B), 3MF81, and 4MF81 (bottom). . . . . 113

A.1. Station abundance-age plot for eggs of walleye pollock obtained at station G022A of survey 2MF81. The logarithms of hourly stage abundances are plotted against the cumulative development times to stage midpoints. Each stage is identified by a stage number. See Appendix Table A.1 for intermediate values in the computations. . 136

- A.2. Station abundance-age plot for eggs of walleye pollock obtained at station G023A of survey 2MF81. The logarithms of hourly stage abundances are plotted against the cumulative development times to stage midpoints. Each stage is identified by a stage number. See Appendix Table A.2 for intermediate values in the computations. . 138
- A.3. Station abundance-age plot for eggs of walleye pollock obtained at station G024A of survey 2MF81. The logarithms of hourly stage abundances are plotted against the cumulative development times to stage midpoints. Each stage is identified by a stage number. See Appendix Table A.3 for intermediate values in the computations. . 140
- A.4. Station abundance-age plot for eggs of walleye pollock obtained at station G025A of survey 2MF81. The logarithms of hourly stage abundances are plotted against the cumulative development times to stage midpoints. Each stage is identified by a stage number. See Appendix Table A.4 for intermediate values in the computations. . 142
- A.5. Station abundance-age plot for eggs of walleye pollock obtained at station G046A of survey 2MF81. The logarithms of hourly stage abundances are plotted against the cumulative development times to stage midpoints. Each stage is identified by a stage number. See Appendix Table A.5 for intermediate values in the computations. . 144
- A.6. Station abundance-age plot for eggs of walleye pollock obtained at station G066A of survey 2MF81. The logarithms of hourly stage abundances are plotted against the cumulative development times to stage midpoints. Each stage is identified by a stage number. See Appendix Table A.6 for intermediate values in the computations. . 146
- A.7. Station abundance-age plot for eggs of walleye pollock obtained at station G067A of survey 2MF81. The logarithms of hourly stage abundances are plotted against the cumulative development times to stage midpoints. Each stage is identified by a stage number. See Appendix Table A.7 for intermediate values in the computations. . 148
- A.8. Station abundance-age plot for eggs of walleye pollock obtained at station G068A of survey 2MF81. The logarithms of hourly stage abundances are plotted against the cumulative development times to stage midpoints. Each stage is identified by a stage number. See Appendix Table A.8 for intermediate values in the computations. . 150
- A.9. Station abundance-age plot for eggs of walleye pollock obtained at station G069A of survey 2MF81. The logarithms of hourly stage abundances are plotted against the cumulative development times to stage midpoints. Each stage is identified by a stage number. See Appendix Table A.9 for intermediate values in the computations. . 152

- A.10. Station abundance-age plot for eggs of walleye pollock obtained at station G077A of survey 2MF81. The logarithms of hourly stage abundances are plotted against the cumulative development times to stage midpoints. Each stage is identified by a stage number. See Appendix Table A.10 for intermediate values in the computations. . 154
- A.11. Station abundance-age plot for eggs of walleye pollock obtained at station G078A of survey 2MF81. The logarithms of hourly stage abundances are plotted against the cumulative development times to stage midpoints. Each stage is identified by a stage number. See Appendix Table A.11 for intermediate values in the computations. . 156
- A.12. Station abundance-age plot for eggs of walleye pollock obtained at station G079A of survey 2MF81. The logarithms of hourly stage abundances are plotted against the cumulative development times to stage midpoints. Each stage is identified by a stage number. See Appendix Table A.12 for intermediate values in the computations. . 158
- A.13. Station abundance-age plot for eggs of walleye pollock obtained at station G082A of survey 2MF81. The logarithms of hourly stage abundances are plotted against the cumulative development times to stage midpoints. Each stage is identified by a stage number. See Appendix Table A.13 for intermediate values in the computations. . 160
- A.14. Station abundance-age plot for eggs of walleye pollock obtained at station G086A of survey 2MF81. The logarithms of hourly stage abundances are plotted against the cumulative development times to stage midpoints. Each stage is identified by a stage number. See Appendix Table A.14 for intermediate values in the computations. . 162
- A.15. Station abundance-age plot for eggs of walleye pollock obtained at station G087A of survey 2MF81. The logarithms of hourly stage abundances are plotted against the cumulative development times to stage midpoints. Each stage is identified by a stage number. See Appendix Table A.15 for intermediate values in the computations. . 164
- A.16. Station abundance-age plot for eggs of walleye pollock obtained at station G088A of survey 2MF81. The logarithms of hourly stage abundances are plotted against the cumulative development times to stage midpoints. Each stage is identified by a stage number. See Appendix Table A.16 for intermediate values in the computations. . 166
- A.17. Station abundance-age plot for eggs of walleye pollock obtained at station G089A of survey 2MF81. The logarithms of hourly stage abundances are plotted against the cumulative development times to stage midpoints. Each stage is identified by a stage number. See Appendix Table A.17 for intermediate values in the computations. . 168

A.18. Station abundance-age plot for eggs of walleye pollock obtained at station G090A of survey 2MF81. The logarithms of hourly stage abundances are plotted against the cumulative development times to stage midpoints. Each stage is identified by a stage number. See Appendix Table A.18 for intermediate values in the computations. . 170

A.19. Station abundance-age plot for eggs of walleye pollock obtained at station G091A of survey 2MF81. The logarithms of hourly stage abundances are plotted against the cumulative development times to stage midpoints. Each stage is identified by a stage number. See Appendix Table A.19 for intermediate values in the computations. . 172

B.1. Confidence intervals under the DLN model for 100 simulated surveys from abundance surface A, with random sampling, and with 0% local CV. The magnitude of the estimated mean for each survey is indicated by an "X" and the confidence limit extends two standard deviations from the mean. The magnitude of the true mean is indicated by the vertical line. . . . . 175

B.2. Confidence intervals under the DLN model for 100 simulated surveys from abundance surface B, with random sampling, and with 0% local CV. The magnitude of the estimated mean for each survey is indicated by an "X" and the confidence limit extends two standard deviations from the mean. The magnitude of the true mean is indicated by the vertical line. . . . . 176

B.3. Confidence intervals under the SRS model for 100 simulated surveys from abundance surface A, with random sampling, and with 0% local CV. The magnitude of the estimated mean for each survey is indicated by an "X" and the confidence limit extends two standard deviations from the mean. The magnitude of the true mean is indicated by the vertical line. . . . . 177

B.4. Confidence intervals under the SRS model for 100 simulated surveys from abundance surface B, with random sampling, and with 0% local CV. The magnitude of the estimated mean for each survey is indicated by an "X" and the confidence limit extends two standard deviations from the mean. The magnitude of the true mean is indicated by the vertical line. . . . . 178

B.5. Confidence intervals under the NB model for 100 simulated surveys from abundance surface A, with random sampling, and with 0% local CV. The magnitude of the estimated mean for each survey is indicated by an "X" and the confidence limit extends two standard deviations from the mean. The magnitude of the true mean is indicated by the vertical line. . . . . 179

B.6. Confidence intervals under the NB model for 100 simulated surveys from abundance surface B, with random sampling, and with 0% local CV. The magnitude of the estimated mean for each survey is indicated by an "X" and the confidence limit extends two standard deviations from the mean. The magnitude of the true mean is indicated by the vertical line. . . . . 180

B.7. Confidence intervals under the DLN model for 100 simulated surveys from abundance surface A, with grid sampling, and with 0% local CV. The magnitude of the estimated mean for each survey is indicated by an "X" and the confidence limit extends two standard deviations from the mean. The magnitude of the true mean is indicated by the vertical line. . . . . 181

B.8. Confidence intervals under the DLN model for 100 simulated surveys from abundance surface B, with grid sampling, and with 0% local CV. The magnitude of the estimated mean for each survey is indicated by an "X" and the confidence limit extends two standard deviations from the mean. The magnitude of the true mean is indicated by the vertical line. . . . . 182

B.9. Confidence intervals under the DLN model for 100 simulated surveys from abundance surface B, with grid sampling, and with 25% local CV. The magnitude of the estimated mean for each survey is indicated by an "X" and the confidence limit extends two standard deviations from the mean. The magnitude of the true mean is indicated by the vertical line. . . . . 183

B.10. Confidence intervals under the DLN model for 100 simulated surveys from abundance surface B, with grid sampling, and with 50% local CV. The magnitude of the estimated mean for each survey is indicated by an "X" and the confidence limit extends two standard deviations from the mean. The magnitude of the true mean is indicated by the vertical line. . . . . 184

B.11. Confidence intervals under the SRS model for 100 simulated surveys from abundance surface A, with grid sampling, and with 0% local CV. The magnitude of the estimated mean for each survey is indicated by an "X" and the confidence limit extends two standard deviations from the mean. The magnitude of the true mean is indicated by the vertical line. . . . . 185

B.12. Confidence intervals under the SRS model for 100 simulated surveys from abundance surface B, with grid sampling, and with 0% local CV. The magnitude of the estimated mean for each survey is indicated by an "X" and the confidence limit extends two standard deviations from the mean. The magnitude of the true mean is indicated by the vertical line. . . . . 186

B.13. Confidence intervals under the SRS model for 100 simulated surveys from abundance surface B, with grid sampling, and with 25% local CV. The magnitude of the estimated mean for each survey is indicated by an "X" and the confidence limit extends two standard deviations from the mean. The magnitude of the true mean is indicated by the vertical line. . . . . 187

B.14. Confidence intervals under the SRS model for 100 simulated surveys from abundance surface B, with grid sampling, and with 50% local CV. The magnitude of the estimated mean for each survey is indicated by an "X" and the confidence limit extends two standard deviations from the mean. The magnitude of the true mean is indicated by the vertical line. . . . . 188

B.15. Confidence intervals under the NB model for 100 simulated surveys from abundance surface A, with grid sampling, and with 0% local CV. The magnitude of the estimated mean for each survey is indicated by an "X" and the confidence limit extends two standard deviations from the mean. The magnitude of the true mean is indicated by the vertical line. . . . . 189

B.16. Confidence intervals under the NB model for 100 simulated surveys from abundance surface B, with grid sampling, and with 0% local CV. The magnitude of the estimated mean for each survey is indicated by an "X" and the confidence limit extends two standard deviations from the mean. The magnitude of the true mean is indicated by the vertical line. . . . . 190

B.17. Confidence intervals under the NB model for 100 simulated surveys from abundance surface B, with grid sampling, and with 25% local CV. The magnitude of the estimated mean for each survey is indicated by an "X" and the confidence limit extends two standard deviations from the mean. The magnitude of the true mean is indicated by the vertical line. . . . . 191

B.18. Confidence intervals under the NB model for 100 simulated surveys from abundance surface B, with grid sampling, and with 50% local CV. The magnitude of the estimated mean for each survey is indicated by an "X" and the confidence limit extends two standard deviations from the mean. The magnitude of the true mean is indicated by the vertical line. . . . . 192







## List of Tables

Number	Page
<p>1. Sequence of analytical procedures and basic data units. Summarized for each chapter are the main parameters determined by computational procedures; basic units of the estimated parameters; and the chapters in which the estimated quantities are discussed and/or employed in further extrapolations. . . . .</p>	3
<p>2. Summary of activity and timing for ichthyoplankton and hydroacoustic surveys. I denotes an ichthyoplankton survey and H denotes a hydroacoustic survey. At times, both ichthyoplankton and hydroacoustic sampling were conducted on the same dates. . . . .</p>	15
<p>3. Developmental stages for eggs of walleye pollock, <u>Theragra chalcogramma</u> (Matarese, pers. commun.). . . . .</p>	16
<p>4. Preliminary coefficients in the relationship between temperature and cumulative development time for the 21 developmental stages of walleye pollock eggs. Statistics are shown for cumulative development time to the stage endpoint at 5.0°C, stage duration at 5.0°C, fraction of the incubation period represented by the stage, and coefficients for the log-linear relationship between cumulative development time and temperature. . . . .</p>	18
<p>5. Summary of the distributional pattern of adults based on hydroacoustic survey data, and the pattern of egg ages on a station by station basis based on ichthyoplankton data from survey 2MF81. . . . .</p>	31
<p>6. Survey data for eggs of walleye pollock treated as samples from a simple random sampling design (SRS). Statistics shown for each of the 1981 surveys are: n, sample size; m, mean daily abundance (eggs/day /m<sup>2</sup>); se(m), standard error of the mean; CV, coefficient of variation for the mean; and CL, confidence limits for the mean. . . . .</p>	43
<p>7. Survey data for eggs of walleye pollock treated as random samples from a delta distribution (DLN). Statistics shown for each of the 1981 surveys are: n, the number of positive and zero-valued catches, and p, the number of positive catches; p/n, the fraction of the sample units within the survey area having positive egg abundances; m, mean daily abundance (eggs/day/m<sup>2</sup>); se(m), standard error of the mean; CV, coefficient of variation for the mean; CL, confidence limits for the mean; and r<sup>2</sup>, variance or shape parameter. . . . .</p>	43
<p>8. Survey data for eggs of walleye pollock treated as random samples from a negative binomial distribution (NB). Statistics shown for each of the 1981 surveys are: n, sample size; m, mean daily abundance (eggs/day/m<sup>2</sup>); se(m), standard error of the mean; CV, coefficient of variation for the mean; CL, confidence limits for the mean; and k, shape parameter. . . . .</p>	44

9. Statistics for mean daily abundance (eggs/day/m<sup>2</sup>) and coefficient of variation (in parentheses) under the simple random sampling (SRS), delta (DLN), and negative binomial (NB) models for the catch curve. 44

10. Summary of estimates for survey 2MF81 under the stratified random sampling model (STRS). Statistics shown for the hth stratum are: N<sub>h</sub>/AREA, relative stratum size; n<sub>h</sub>, sample size; m<sub>h</sub>, mean daily abundance (eggs/day/m<sup>2</sup>); se(m<sub>h</sub>), standard error of a stratum mean; Y<sub>h</sub>, total daily egg abundance; se(Y<sub>h</sub>), standard error of a stratum total; and CV, coefficient of variation for a stratum total. The estimate for stratified total daily egg abundance is given on the bottom line of the Table, along with standard error of the stratified total, coefficient of variation, and approximate confidence limits. . . . . 45

11. Summary of total daily abundance estimates (eggs X 10<sup>10</sup>/day/survey area) under the simple random sampling (SRS), delta (DLN), negative binomial (NB), and stratified random sampling (STRS) models for spatial integration. The julian date for the midpoint of a survey was obtained by a weighted mean of sampling dates. . . . . 46

12. Confidence interval statistics under the delta (DLN), simple random sampling (SRS), and the negative binomial (NB) models for the catch data from survey 2MF81. The coefficient of local variation was set to a constant 0% prior to the generation of simulated catches. The true mean was 123 eggs/day/m<sup>2</sup> for abundance surface A and was 136 for abundance surface B. . . . . 64

13. Best fitting parameter estimates to the modified mortality model. Statistics are shown for NPOP, seasonal egg production; Z, coefficient of daily mortality; MU, julian date of peak spawning; and SIGMA, standard deviation of the normal spawning function (days). The data for survey 2MF81 were partitioned into set A and B. Data set 1 consisted of the total abundance values determined of surveys 1MF81, set A of 2MF81, 3MF81, and 4MF81; data set 2 consisted of the corresponding values for set B of survey 2MF81 and the remaining three surveys. Residuals were either unweighted or weighted by the inverse of the standard deviations for the observed values of total stage abundances. . . . . 112

14. Seasonal egg production during the 1981 spawning season (eggs /survey area/spawning season) by the method of trapezoidal integration. Statistics shown for the gth survey are the julian date upon which the survey was centered and P<sub>g</sub>, the total daily egg abundance estimate. The integrated abundance values represent the product of the average total daily egg production from the gth and (g+1) surveys and the difference in days between the julian dates of these surveys. Seasonal egg abundance is the sum of integrated values. . . . . 122

15. Seasonal egg production during the 1981 spawning season (eggs/survey area/spawning season) by the cruise duration method. Statistics shown for the gth survey are the first and last day of sampling (julian date); survey duration; $P_g$ , total daily egg abundance; $se(P_g)$ , standard deviation for the total. Also shown for the interval of the spawning season between the gth and (g+1)th surveys are egg production, standard error, and coefficient of variation. The final line of the Table also gives P, seasonal egg production; $se(P)$ , standard deviation; and CV, coefficient of variation. . . . .	123
16. Summary of seasonal egg production and spawner biomass estimates for walleye pollock for the 1981 spawning season. . . . .	123
A.1. Intermediate values in the calculations of average hourly stage abundance for eggs of walleye pollock obtained at station G022A of survey 2MF81. . . . .	137
A.2. Intermediate values in the calculations of average hourly stage abundance for eggs of walleye pollock obtained at station G023A of survey 2MF81. . . . .	139
A.3. Intermediate values in the calculations of average hourly stage abundance for eggs of walleye pollock obtained at station G024A of survey 2MF81. . . . .	141
A.4. Intermediate values in the calculations of average hourly stage abundance for eggs of walleye pollock obtained at station G025A of survey 2MF81. . . . .	143
A.5. Intermediate values in the calculations of average hourly stage abundance for eggs of walleye pollock obtained at station G046A of survey 2MF81. . . . .	145
A.6. Intermediate values in the calculations of average hourly stage abundance for eggs of walleye pollock obtained at station G066A of survey 2MF81. . . . .	147
A.7. Intermediate values in the calculations of average hourly stage abundance for eggs of walleye pollock obtained at station G067A of survey 2MF81. . . . .	149
A.8. Intermediate values in the calculations of average hourly stage abundance for eggs of walleye pollock obtained at station G068A of survey 2MF81. . . . .	151
A.9. Intermediate values in the calculations of average hourly stage abundance for eggs of walleye pollock obtained at station G069A of survey 2MF81. . . . .	153

A.10. Intermediate values in the calculations of average hourly stage abundance for eggs of walleye pollock obtained at station G077A of survey 2MF81. . . . .	155
A.11. Intermediate values in the calculations of average hourly stage abundance for eggs of walleye pollock obtained at station G078A of survey 2MF81. . . . .	157
A.12. Intermediate values in the calculations of average hourly stage abundance for eggs of walleye pollock obtained at station G079A of survey 2MF81. . . . .	159
A.13. Intermediate values in the calculations of average hourly stage abundance for eggs of walleye pollock obtained at station G082A of survey 2MF81. . . . .	161
A.14. Intermediate values in the calculations of average hourly stage abundance for eggs of walleye pollock obtained at station G086A of survey 2MF81. . . . .	163
A.15. Intermediate values in the calculations of average hourly stage abundance for eggs of walleye pollock obtained at station G087A of survey 2MF81. . . . .	165
A.16. Intermediate values in the calculations of average hourly stage abundance for eggs of walleye pollock obtained at station G088A of survey 2MF81. . . . .	167
A.17. Intermediate values in the calculations of average hourly stage abundance for eggs of walleye pollock obtained at station G089A of survey 2MF81. . . . .	169
A.18. Intermediate values in the calculations of average hourly stage abundance for eggs of walleye pollock obtained at station G090A of survey 2MF81. . . . .	171
A.19. Intermediate values in the calculations of average hourly stage abundance for eggs of walleye pollock obtained at station G091A of survey 2MF81. . . . .	173

#### ACKNOWLEDGEMENTS

I would like to express appreciation to Dr. Gunderson, Dr. Stauffer, and Dr. Miller for the attention and the advice they have provided me during the course of this investigation. I would especially like to acknowledge Dr. Kendall for giving me both the opportunity and the responsibility to pursue these investigations, and to express my appreciation for his patience in its long gestation. I would also like to extend my thanks to the personnel of the NOAA R.V. Miller Freeman and to Dr. Ed Nunnallee and others of the Pelagic Resources Assessment Task. And I would not fail to mention my appreciation to the staff in the Recruitment Processes Task.







## Chapter 1. Introduction

The occurrence of very large concentrations of walleye pollock, Theragra chalcogramma, in Shelikof Strait, Alaska, was known to local fishermen but this resource had received little attention prior to the 1980's. This region has since become a significant fishing ground and, in order to better manage the harvest of this stock, annual assessments of stock size have become increasingly important. The spawning population in Shelikof Strait was first surveyed late in the 1980 spawning season by the National Marine Fisheries Service (Nelson and Nunnallee, 1985). During the 1981 spawning season a program involving hydroacoustic, trawl, and ichthyoplankton sampling was undertaken to obtain preliminary information on the spawning ecology of the population and to serve as an initial examination of the population dynamics of the resource.

Estimates of spawner biomass based on ichthyoplankton data can serve as an additional source of stock information that is independent of methods requiring commercial fishery data or hydroacoustic and trawl surveys. The central concern in this investigation was the definition of appropriate sampling and analytical methodologies that will permit the valid mathematical description of plankton collections from the Shelikof egg population. In this paper I attempt to estimate the magnitude of seasonal egg abundance, egg mortality, and spawner biomass from ichthyoplankton survey data. Since the magnitude and numerical stability of estimates are a product not only of the information contained in sample data, but also of the particular techniques that are employed to analyze the data, a number of methods were developed, applied to the 1981 survey data, and evaluated.

The reliable estimation of spawner biomass by ichthyoplankton survey is predicated on obtaining a reliable estimate of seasonal egg production, which itself is derived from a suitable extrapolation of data obtained from a series of plankton collections. The preferential adoption of certain sampling and analytical techniques for an ongoing program of assessments should be dictated by considerations of

precision and accuracy. Suitable procedures should yield seasonal production estimates that have a minimum range of uncertainty (precision) and are reliably indicative of the true population size at the time of sampling (accuracy).

The process of estimating seasonal egg production and spawner biomass from ichthyoplankton survey data involves a series of calculations which can be partitioned into four phases. First, a value for egg abundance at each sampling station is obtained from a standardization of each egg catch. Second, station abundances from each survey are integrated over space to yield an estimate of egg abundance within the survey area. Third, the survey estimates of total egg abundance are integrated over time to yield an estimate of seasonal egg abundance within the survey area. If egg mortality was significant, then seasonal egg abundance provides a conservative estimate of seasonal egg production. Finally, an estimate of spawner biomass is obtained from seasonal egg production, fecundity by length, adult length frequencies, and sex ratio data.

Table 1 summarizes the major thrust of calculations on a chapter by chapter basis, details the terminology and units of the more significant parameters, and indicates the chapters in which the estimated quantities were carried forward for further calculations.

Catch standardization procedures, providing both standardized catches and standardized stage abundances, are detailed in Chapter 2. These two standardizations differ in the time units implicitly defined by the calculations. The implied time unit is identified in Table 1 by quotation marks, and the value of the unit can be considered to be 1. Time was explicitly incorporated into other procedures, such as for the calculation of age frequency distributions on a catch by catch basis which are also described in Chapter 2.

Chapter 3 summarizes the estimation of egg abundance within the survey area on a survey by survey basis. Chapter 4 represents a

=====

Table 1. Sequence of analytical procedures and basic data units. Summarized for each chapter are the main parameters determined by computational procedures; basic units of the estimated parameters; and the chapters in which the estimated quantities are discussed and/or employed in further extrapolations.

=====

Chapter    major focus of estimation procedures  
               (principal form of data entering into calculations:  
                   data units)  
               [subsequent chapter requiring estimates of current chapter]

-----

- 2            catch standardizations  
               (standardized catch: eggs of all ages/"incubation period"  
                   /m<sup>2</sup>)  
               (standardized stage abundance: eggs of a developmental  
                   stage/"stage duration"/m<sup>2</sup>) [3,4,5]
- frequency distributions of developmental stages at a number  
               of selected sampling stations  
               (hourly stage abundance: eggs of a stage/hr of stage  
                   duration/m<sup>2</sup>)
- 3            estimation of mean, total, and variance for egg abundance [6]  
               (daily station abundance: eggs of stages 1-10/development  
                   time to the end of stage 10/m<sup>2</sup>)
- 4            computer simulation of field sampling -- an empirical  
               evaluation of the sampling design and the statistical methods  
               of Chapter 3  
               (daily station abundance: eggs of stages 1-21/development  
                   time to the end of stage 21/m<sup>2</sup>)
- 5            estimation by a new method of seasonal egg production and the  
               coefficient of daily egg mortality during the incubation  
               period [6]  
               (total stage abundance: eggs of a developmental stage  
                   /"duration of stage"/survey area)
- 6            estimation of seasonal egg abundance, comparison of  
               production estimates, and estimation of spawner biomass  
               (total egg production: eggs spawned/spawning season/survey  
                   area)
- =====

temporary digression in the stream of calculations, in that the utility  
of the statistical models of chapter 3 are evaluated with a view toward  
answering the question: Which approach, if any, provides the simplest,

clearest, and most numerically stable method as a long term procedure for subsequent annual assessments of walleye pollock spawning? Chapter 5 is also somewhat digressive from the foregoing stream of calculations, in that a new procedure is developed for the estimation of seasonal egg production and egg mortality, neither of which could be directly determined from the previous approaches.

The estimation of spawner biomass was performed in Chapter 6, using the total egg abundance estimates of Chapter 3 and the seasonal egg production estimate of Chapter 5. Analyses are concluded in Chapter 7 with a detailing of suggested improvements to survey design and analytical extrapolations from survey data.

Since this stream of calculations must ultimately be consistent with the biology of walleye pollock, it is perhaps useful to briefly summarize some of what is currently known about the distribution and life history of walleye pollock.

Walleye pollock inhabit all continental shelves and slopes in the northern Pacific Ocean and the Bering Sea, and are one of the most abundant fish species to be found there. In the Pacific Ocean, they range continuously from northern California, along the North American coast to the Gulf of Alaska, throughout the Aleutian chain, and on to the southern Sea of Japan.

The worldwide commercial catch of walleye pollock has ranged from 4000 to 6000 thousand mt during the 1970's and early 1980's, and mainly involved the fishing fleets of Japan, U.S.S.R., South Korea and North Korea (Bakkala et al., 1984). Catches declined in the late 1970's due to the implementations of U.S.-Japan bilateral agreements and the establishment of the 200 mile Fishery Conservation Zone. Pollock are processed into fillets, blocks, surimi, and fish meal; and ovaries are harvested for roe.

Fishing areas in the Gulf of Alaska have historically included

regions near the Shumagin Islands and to the south and southeast of Kodiak Island, with catches of approximately 9 thousand mt in the early 1970's, 40-80 thousand mt in the mid-1970's, 100-200 thousand mt in the late 1970's, and 150-170 thousand mt in the early 1980's (Bakkala et al., 1984). The fishery in Shelikof Strait began in the early 1980's and catches reached 74 thousand mt in 1982 (Bakkala et al., 1984).

Walleye pollock are semidemersal, forming schools near the bottom during the daylight hours and dispersing higher into the water column during the night (Salveson and Alton, 1976; Smith, 1981). Adults undergo extensive seasonal spawning migrations.

Spawning periods vary with latitude. Spawning occurs during the winter months of December through March in Asian waters (Bakkala et al., 1984). Spawning in the Sea of Japan occurs from January to May (Zver'kova, 1974). In Canadian waters, the spawning period is relatively brief and occurs early in the year, with peak spawning in late March to mid April (Thompson, 1981). The spawning period in the eastern Bering Sea extends from late February to mid June (Nishiyama and Haryu, 1981), peaking in April to mid May (Smith, 1981). In the Bering Sea, spawning begins along the outer shelf and slope early in the season and progresses toward the inner shelf and further northward by mid to late April (Nishiyama and Haryu, 1981; Traynor, 1986). During cold years, adults do not enter in large numbers into the shallower areas, and remain instead in the warmer regions of the outer shelf (Salveson and Alton, 1976). In the western Gulf of Alaska, the eggs of walleye pollock have been collected from October to June, but spawning occurs principally in the spring and peaks in late March to early April in Shelikof Strait (Dunn, et. al.<sup>1</sup>; Kim, 1987).

During the spawning season, adults are size-stratified with depth,

<sup>1</sup> Dunn J.R., A.W. Kendall, Jr. and R.D. Bates. 1984. Distribution and abundance patterns of eggs and larvae of walleye pollock (Theragra chalcogramma) in the western Gulf of Alaska. U.S. Dept. Commer., NWAFC Proc. Rep 84-10, 66 p.

with the older fish occurring lower in the water column than the 1 and 2 year olds. Adult aggregations spawn at the midwater depths of 70-100 m in the Bering Sea (Nishiyama et al., 1986), 70-150 m in Asian waters (Bakkala et al., 1984), and 170-320 m in Canadian waters (Thompson, 1981). Fertilization is external and adults provide no parental care. Eggs are spherical, nonadhesive, and pelagic. Egg diameter is approximately 1.5 mm, but egg size varies with geographic region and date of the spawning season.

While eggs are often found throughout the water column, most are found over a limited range of depths which vary by region. In the Bering Sea, eggs are predominately found between the surface and 30 m of depth, and larvae are most abundant at 30-40 m (Nishiyama and Haryu, 1981). In the Strait of Georgia, Canada, eggs are found in the midwater depths of 100-300 m and larval densities are thought to increase toward the surface (Thompson, 1981). Kim (1987) found that eggs in Shelikof Strait, AK, were most abundant from midwater to near bottom at depths of 160-280 m in areas of active spawning.

The duration of the incubation period is temperature dependent, and typically ranges from 2-3 weeks. The length of larvae at hatching is 3.5-4.5 mm and the yolk sac is absorbed by the time larvae reach 5.5-6.5 mm (Nishiyama et al., 1986). Yolk sac absorption requires 10 days at 10°C, 15 days at 6°C, and 25 days at 2°C (Hamai et al., 1971). Juveniles become demersal at 35-50 mm (Salveson and Alton, 1976). Juveniles range from 2-20 cm and adults range from 20-90 cm (Smith, 1981).

Walleye pollock mature at 3 years of age in the eastern Bering Sea (Hughes and Hirschhorn, 1979) and at 4 years in the Sea of Japan (Zver'kova, 1974). Lengths at first maturity for fish in the Gulf of Alaska are 29-32 cm for males and 30-35 cm for females (Hughes and Hirschhorn, 1979). Females become more numerous than males at larger sizes (Zver'kova, 1974; Hughes and Hirschhorn, 1979). The maximum age of adults is 13-15 years (Zver'kova, 1979; Smith, 1981).





## Chapter 2. Preliminary analysis of egg catches

### METHODS

#### Sampling design

Ichthyoplankton surveys were separated in time to encompass the anticipated spawning season, and sampling stations were separated in space to cover the projected spawning grounds in and near Shelikof Strait. This design was motivated by the lack of any prior distributional and ecological information for this population, and was also in accordance with standard survey designs for pelagic spawning populations (Kramer, et al., 1972; Smith and Richardson, 1977).

Four ichthyoplankton surveys were conducted aboard the NOAA R/V Miller Freeman. Station positions for each survey are depicted in Figures 1-4. Three echo integrator/adult midwater trawl surveys were also conducted aboard the R/V Miller Freeman in alternation with ichthyoplankton surveys (Nunnallee, pers. commun.). Acoustic tracklines are shown in Figures 5-7. Not all acoustic transects are depicted; returns for a small number of transects were considered erroneous and these transects were excluded from analysis. Table 2 summarizes the sequence of surveys, the number of ichthyoplankton stations or acceptable hydroacoustic transect lines, and survey dates.

Ichthyoplankton stations were roughly distributed in a centric systematic sampling design (Milne, 1959), with station spacing being 5-15 km transverse to the main axis of Shelikof Strait and 10-35 km along this axis. Station patterns were changed between surveys in response to logistical requirements and spacing between stations was only approximately regular. Eleven additional stations, G081A-G091A, were added during survey 2MF81 (Figure 2) following the completion of the first pass through the survey area in order to increase the uniformity of station spacing. These stations were occupied as the third hydroacoustic cruise retraced the survey area.

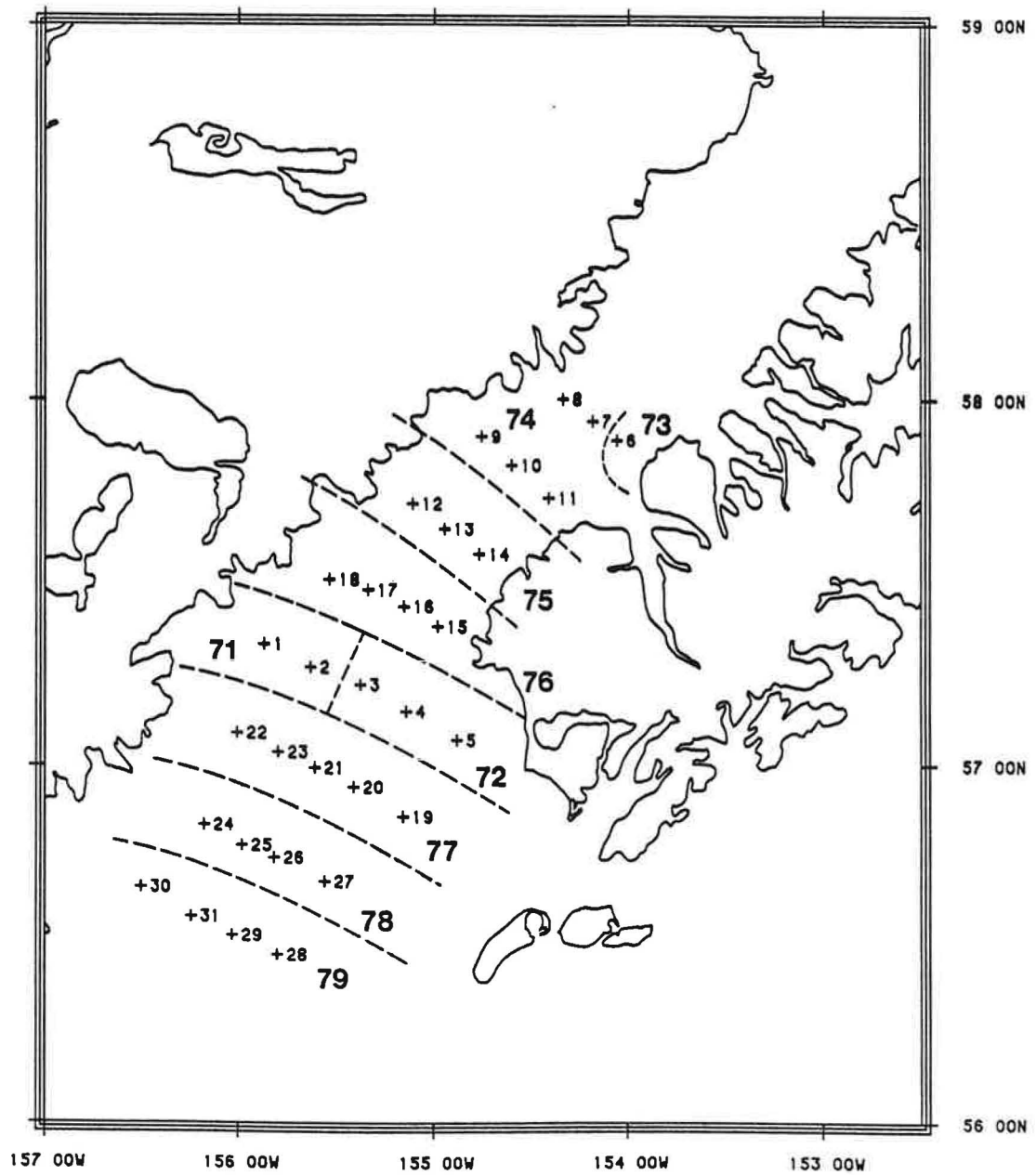


Figure 1. Ichthyoplankton stations and sampling dates for survey 1MF81 (March 11-20). The geographic position of a station is identified by a "+" and stations having the same julian date of sampling (bold number) are located between dashed lines.

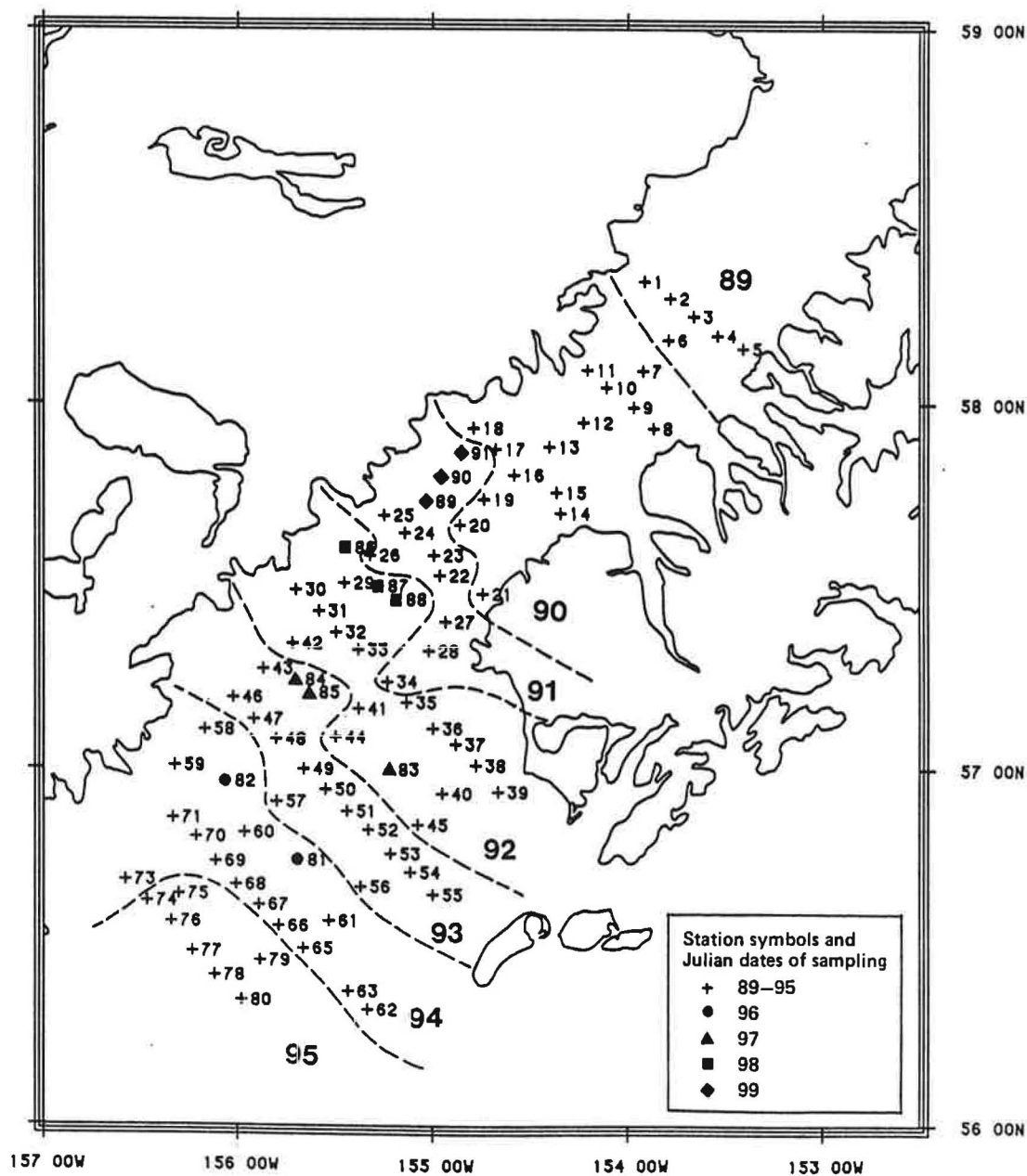


Figure 2. Ichthyoplankton stations and sampling dates for survey 2MF81 (March 29 - April 08). Stations G001A-G080A were occupied on the first pass through the survey area and stations G081A-G091A were occupied when the survey area was retraced during survey 3 of hydroacoustic cruise MF81-2. The geographic position of a station is identified by a "+" and stations having the same Julian date of sampling (bold number) are located between dashed lines.

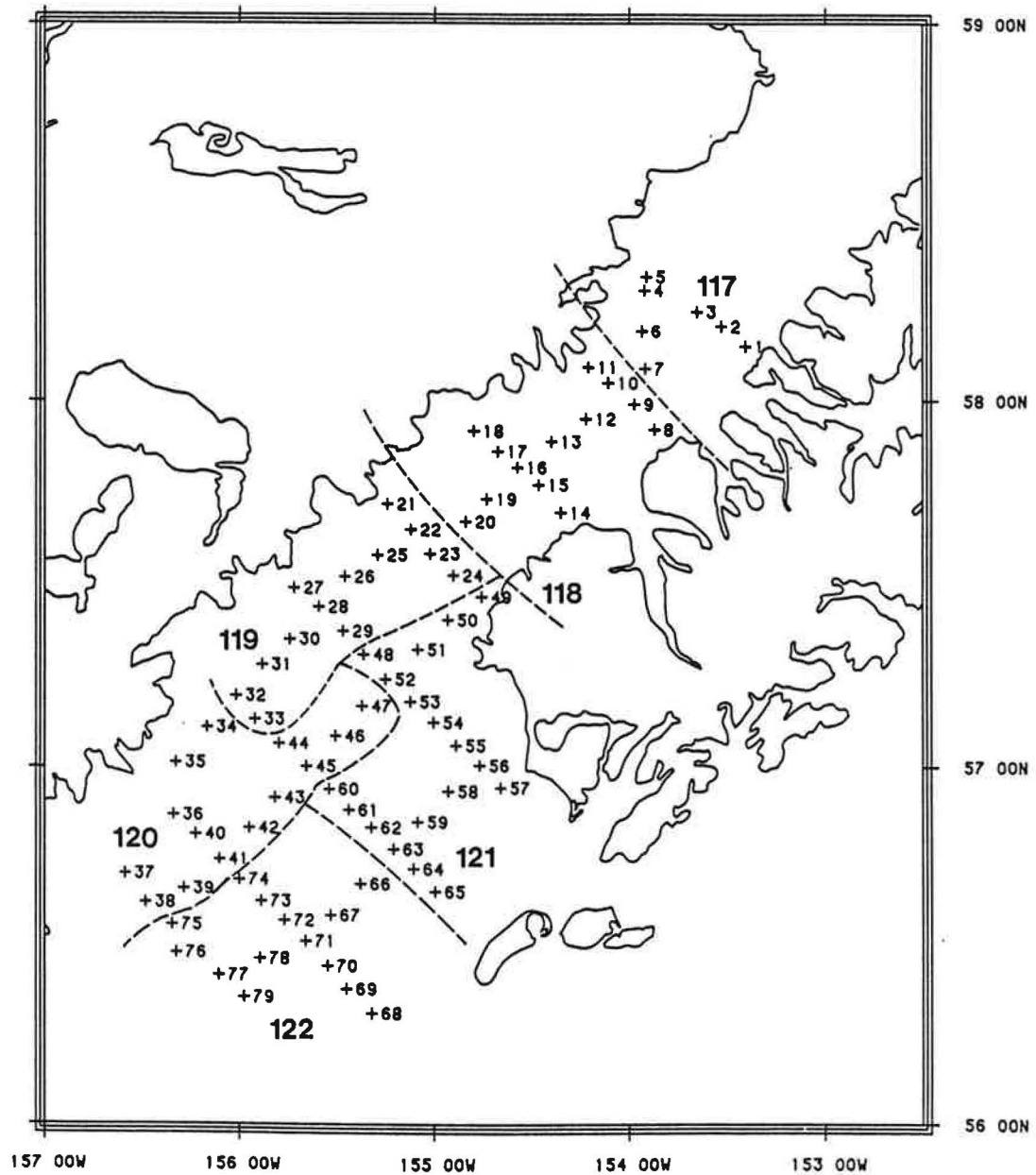


Figure 3. Ichthyoplankton stations and sampling dates for survey 3MF81 (April 26 - May 01). The geographic position of a station is identified by a "+" and stations having the same Julian date of sampling (bold number) are located between dashed lines.

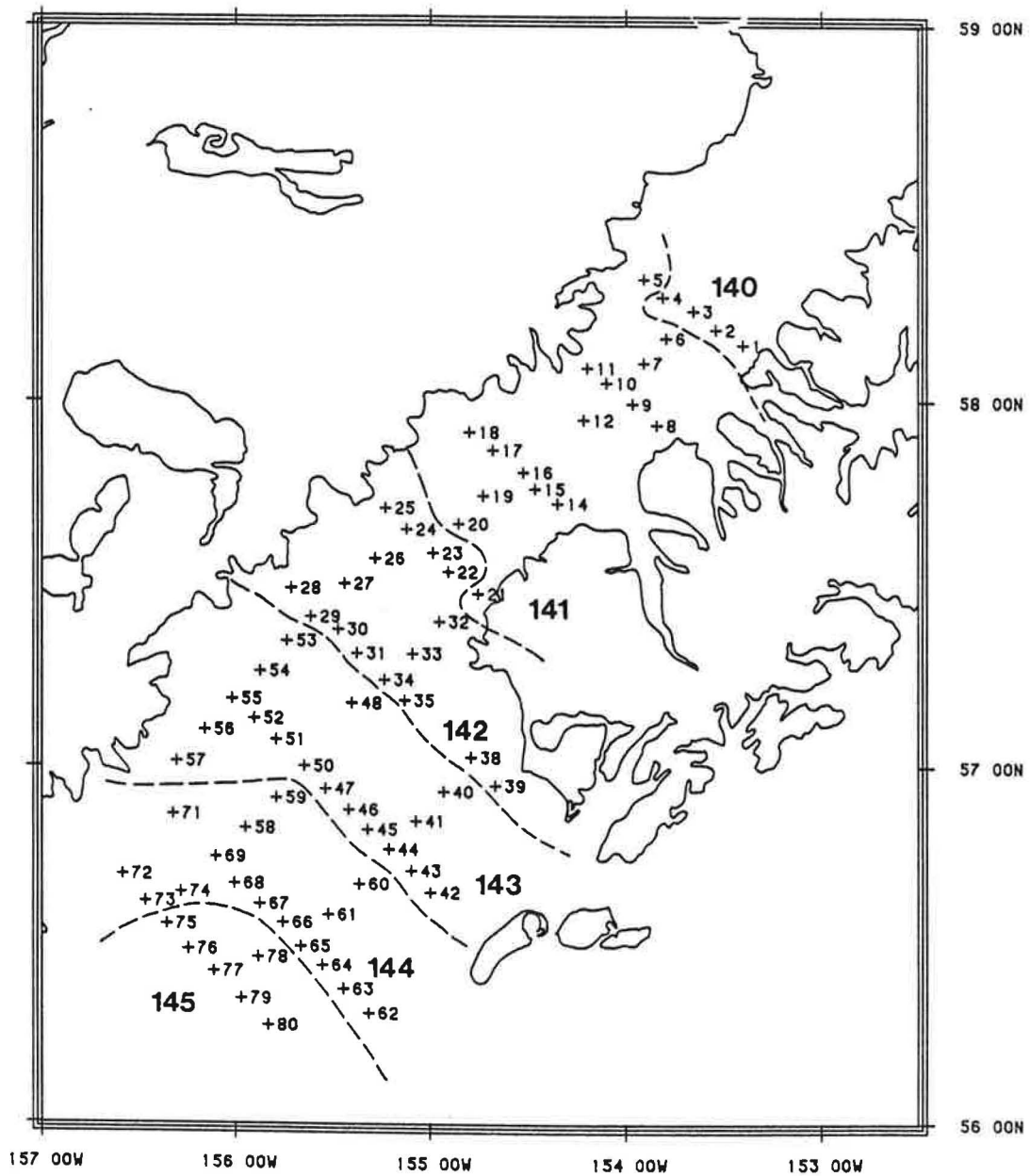


Figure 4. Ichthyoplankton stations and sampling dates for survey 4MF81 (May 19-24). The geographic position of a station is identified by a "+" and stations having the same Julian date of sampling (bold number) are located between dashed lines.

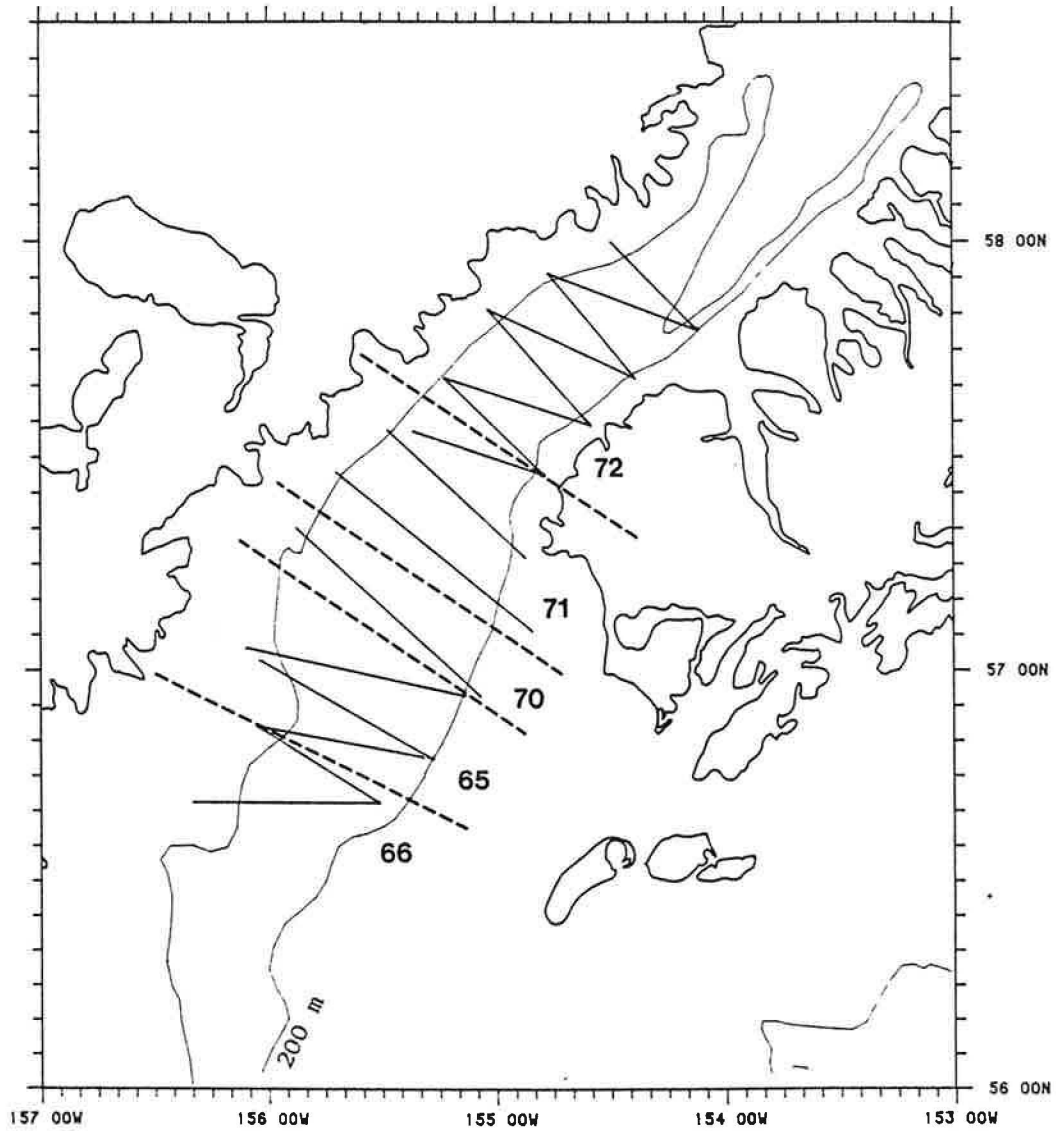


Figure 5. Hydroacoustic transect lines and sampling dates for cruise MF81-2, survey 1 (March 06-07 and 11-12). Transects are represented by solid lines and transects having the same Julian date of sampling (bold number) are located between dashed lines. The 200 m isobath is shown.

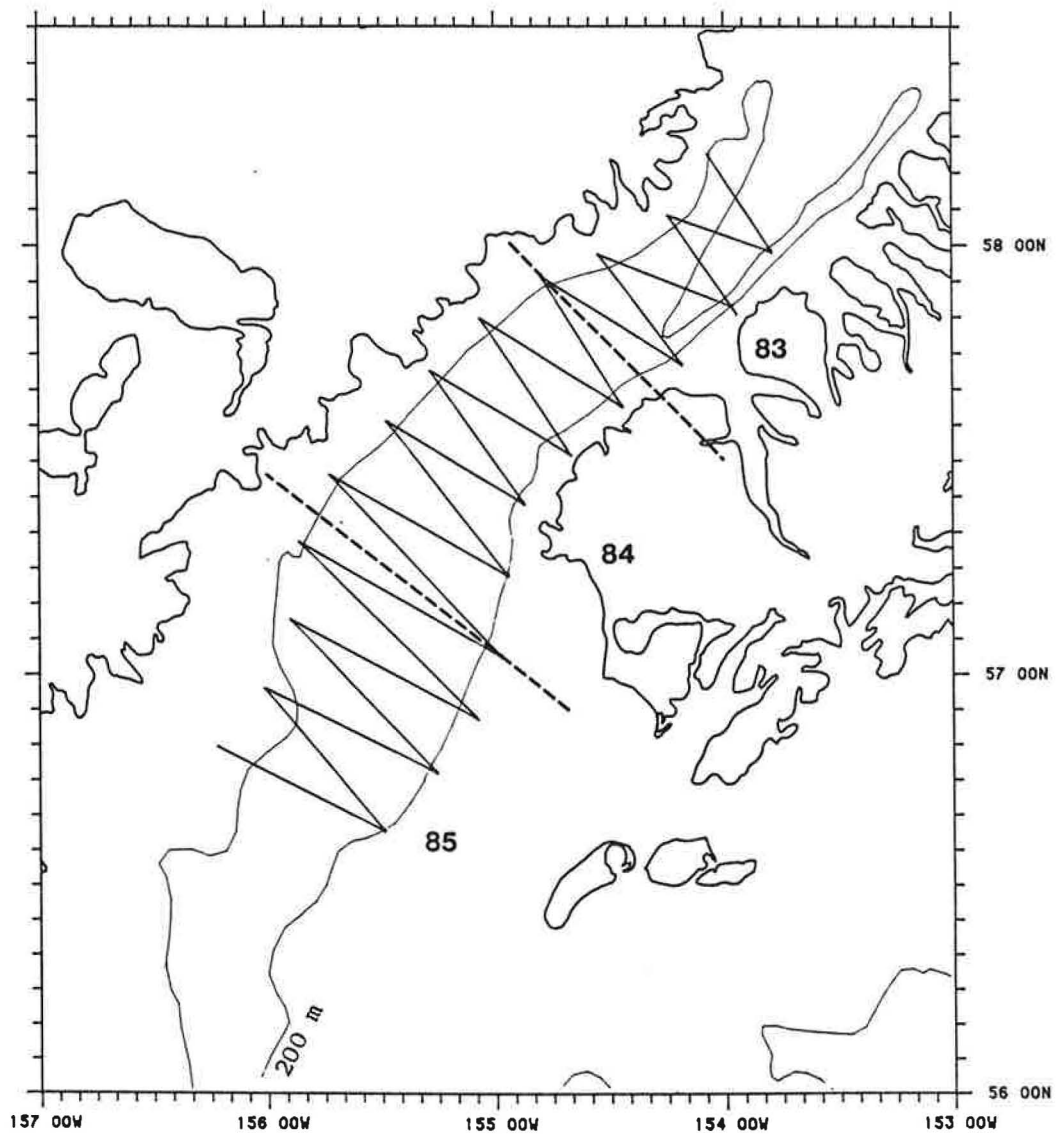


Figure 6. Hydroacoustic transect lines and sampling dates for cruise MF81-2, survey 2 (March 24-27). Transects are represented by solid lines and transects having the same Julian date of sampling (bold number) are located between dashed lines. The 200 m isobath is shown.

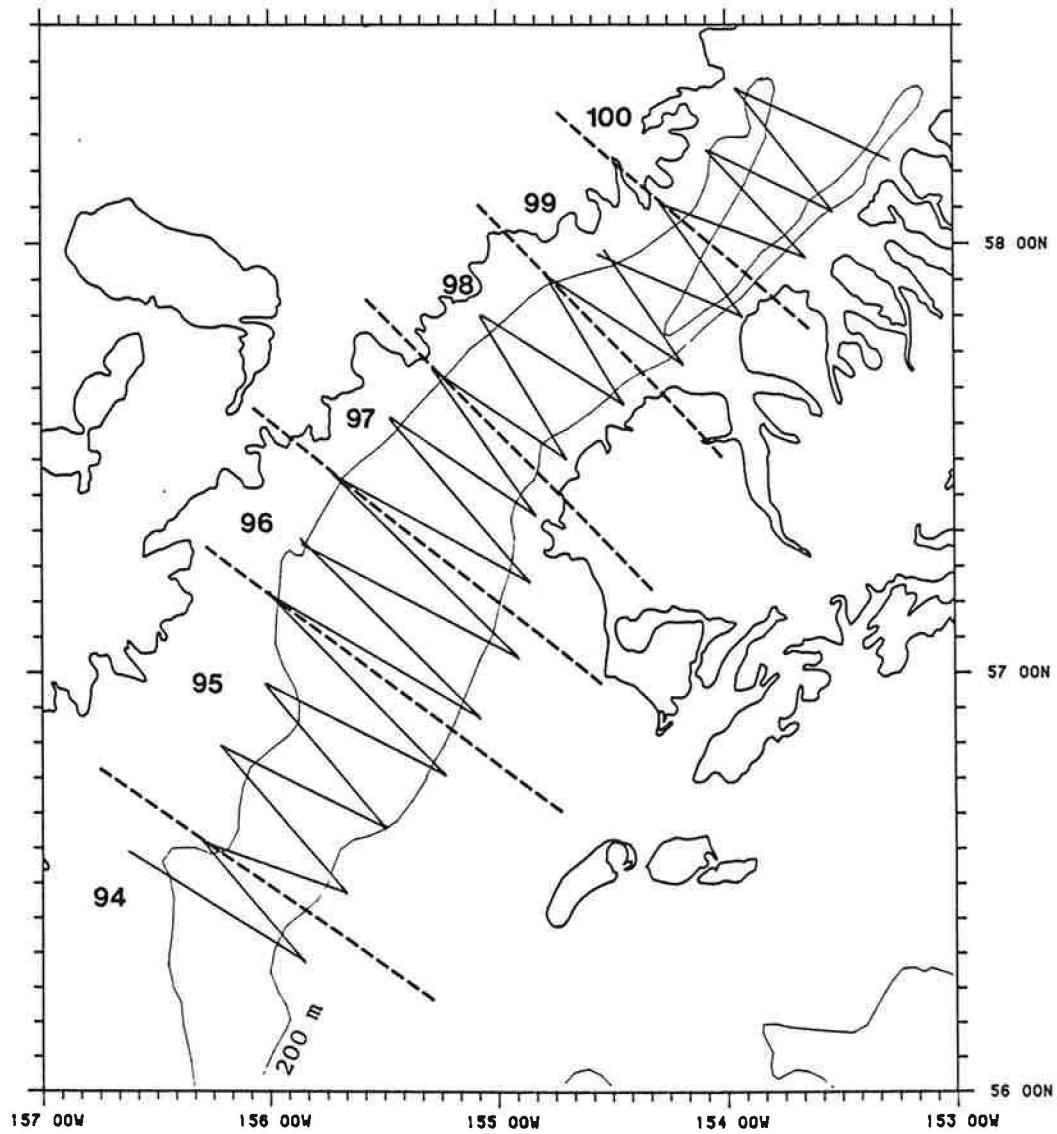


Figure 7. Hydroacoustic transect lines and sampling dates for cruise MF81-2, survey 3 (April 04-10). Transects are represented by solid lines and transects having the same Julian date of sampling (bold number) are located between dashed lines. The 200 m isobath is shown.

=====  
 Table 2. Summary of activity and timing for ichthyoplankton and hydroacoustic surveys. I denotes an ichthyoplankton survey and H denotes a hydroacoustic survey. At times, both ichthyoplankton and hydroacoustic sampling were conducted on the same dates.  
 =====

leg	survey designator	number of stations/ transects	survey dates (GMT)
H	MF81-2 #1	16	06-07MAR, 11-12MAR
I	1MF81	31	11-20MAR
H	MF81-2 #2	22	24-27MAR
I	2MF81	91	29MAR-08APR
H	MF81-2 #3	29	04-10APR
I	3MF81	79	26APR-01MAY
I	4MF81	75	19MAY-24MAY

=====

#### Field procedures

Ichthyoplankton stations were occupied as the ship arrived on station, regardless of whether this was during the day or night. Plankton samples were collected with paired 60 cm bongo samplers (Posgay and Marak, 1980) fitted with 505 um mesh nets and weighted with a 45 kg lead ball. A flowmeter was suspended in the center of the mouth of both nets to permit an estimate of the volume of seawater filtered. A time-depth recorder (bathymograph or BKG) was attached to the cable just above the bongo array. The BKG trace provided a permanent record of tow profile and permitted an estimate of the maximum depth attained during the tow. A wire angle indicator and stopwatch were used to monitor the progress of each tow. Ship's speed was adjusted to maintain a 45 degree wire angle. Tow configuration was double oblique, with deployment at a rate of 50 m of cable paid out per minute of tow and retrieval at 20 m/min. The bongo array was deployed to a target depth of 200 m or, if water depth was shallower, to approximately 5 m above the seabed. Temperature profiles were obtained by BT casts. Plankton samples were preserved in a 5% Formalin and seawater solution buffered with sodium borate. Net 1 samples were retained for analysis and net 2 samples were saved for use by scientists of the U.S.S.R. in an ongoing cooperative research program

Table 3. Developmental stages for eggs of walleye pollock, Theragra chalcogramma (Matarese, pers. commun.).

stage	morphological criterion
1	precell
2	2 cell
3	4 cell
4	8 cell
5	16 cell
6	early blastula
7	blastodermal cap
8	early germ ring
9	germ ring 1/4 circumference
10	germ ring 1/2 circumference
11	germ ring 3/4 circumference
12	blastopore almost closed
13	tail flush with yolk surface
14	tail bud thicker and more distinct
15	tail bud thick and begins to bulge out over yolk surface
16	tail tip has lifted off yolk surface
17	tail tip 5/8 around yolk
18	tail tip 3/4 around yolk
19	tail tip 7/8 around yolk
20	tail tip full circle around yolk
21	tail tip 9/8 around yolk
22	disintegrated - stage cannot be determined
23	cell stages 2-6 - specific stage cannot be determined
24	cell stages 8-12 - specific stage cannot be determined

(Kendall, 1981; Sherman, et al., 1983).

#### Laboratory procedures and incubation time equations

Ichthyoplankton samples were sorted and counted at the Polish Sorting Center, Szczecin, Poland. Egg identifications were performed and counts of walleye pollock eggs were verified under the direction of Ann Matarese of the NWAFC, Seattle, WA. The size of an egg catch was volumetrically estimated when eggs were extremely numerous.

A morphological scheme involving 21 developmental stages was established (Matarese, pers. commun.) to permit fast and accurate visual assignment of eggs to stages of development. Developmental

stages and their morphological criteria are summarized in Table 3. All walleye pollock eggs were assigned to developmental stages if eggs numbered less than 100 in the egg catch; larger catches were subsampled and approximately 100 eggs from each were staged. Eggs which were crushed or ruptured during collection could be identified only to a general range of age groups and stages 22-24 were used to accumulate these frequencies.

Sea temperatures at the 40 m depth were obtained from BT traces. It was assumed that eggs throughout the water column experienced this as ambient temperature. Seawater temperatures during survey 2MF81 approximated 5°C.

Although other mathematical functions may be equally or more suitable (Lasker, 1964; Zweifel and Lasker, 1976), a log-linear relationship between cumulative development time and incubation temperature (Haynes and Ignell<sup>2</sup>) was assumed in order to assign an age to a developmental stage. Twenty-one equations were developed, with one equation for each developmental stage, and these equations had the following form:

$$(eq. 2.1) \quad TIME_{ij} = \exp[SLOPE_i \cdot TEMP_j + YINTCP_i]$$

where

SLOPE<sub>i</sub> slope coefficient for the ith stage  
 TEMP<sub>j</sub> temperature (°C) at the jth station  
 YINTCP<sub>i</sub> Y intercept for the ith stage  
 TIME<sub>ij</sub> cumulative development time (hours) to the end of the ith stage at the ambient temperature for the jth station.

A laboratory determination of the approximate number of hours to the end of each developmental stage was made under a 5.0°C temperature regime (Matarese, pers. commun.). Slope coefficients were consistent with those listed in Table 7 of the preliminary data report of Haynes and Ignell. The Y intercept for each developmental stage was obtained by solving eq. 2.1 using the presumed slope coefficient and the cumulative development time to stage endpoint at a temperature of

<sup>2</sup> Haynes, E. and S. Ignell. 1981. Effect of temperature on rate of embryonic development of walleye pollock, Theragra chalcogramma. unpublished MS.

Table 4. Preliminary coefficients in the relationship between temperature and cumulative development time for the 21 developmental stages of walleye pollock eggs. Statistics are shown for cumulative development time to the stage endpoint at 5.0°C, stage duration at 5.0°C, fraction of the incubation period represented by the stage, and coefficients for the log-linear relationship between cumulative development time and temperature.

stage	stage endpoint (hours) <sub>1</sub>	stage duration (hours)	% of total	slope <sub>2</sub>	Y intercept <sub>3</sub>
1	5.0	5.0	1.3	-0.1	2.11
2	6.5	1.5	0.4	-0.1	2.37
3	9.0	2.5	0.7	-0.1	2.70
4	10.5	1.5	0.4	-0.1	2.85
5	13.5	3.0	0.8	-0.1	3.10
6	23.0	9.5	2.6	-0.1	3.64
7	52.0	29.0	7.8	-0.1	4.45
8	70.5	18.5	5.0	-0.1	4.76
9	82.5	12.0	3.2	-0.1	4.91
10	92.0	9.5	2.6	-0.1	5.02
11	100.0	8.0	2.2	-0.1	5.11
12	114.0	14.0	3.8	-0.1	5.24
13	130.5	16.5	4.5	-0.1	5.37
14	148.0	17.5	4.7	-0.1	5.50
15	166.5	18.5	5.0	-0.1	5.61
16	184.0	17.5	4.7	-0.1	5.71
17	196.0	12.0	3.2	-0.1	5.78
18	226.5	30.5	8.2	-0.1	5.92
19	262.5	36.0	9.7	-0.1	6.07
20	286.5	24.0	6.5	-0.1	6.16
21	370.5	84.0	22.7	-0.1	6.41

1 unpublished data (Matarese, pers. commun.)

2 slope coefficients interpolated from Table 7 in Haynes and Ignell (unpub. MS)

3 The y-intercept was obtained by solving eq. 2.1 using a constant temperature of 5°C and the data from columns 2 and 5.

5.0°C. Table 4 summarizes stage durations at 5.0°C and the coefficients of the log-linear equations. The relationships between temperature and development times are depicted in Figure 8. The incubation period for eggs of walleye pollock is approximately two weeks at 5°C.

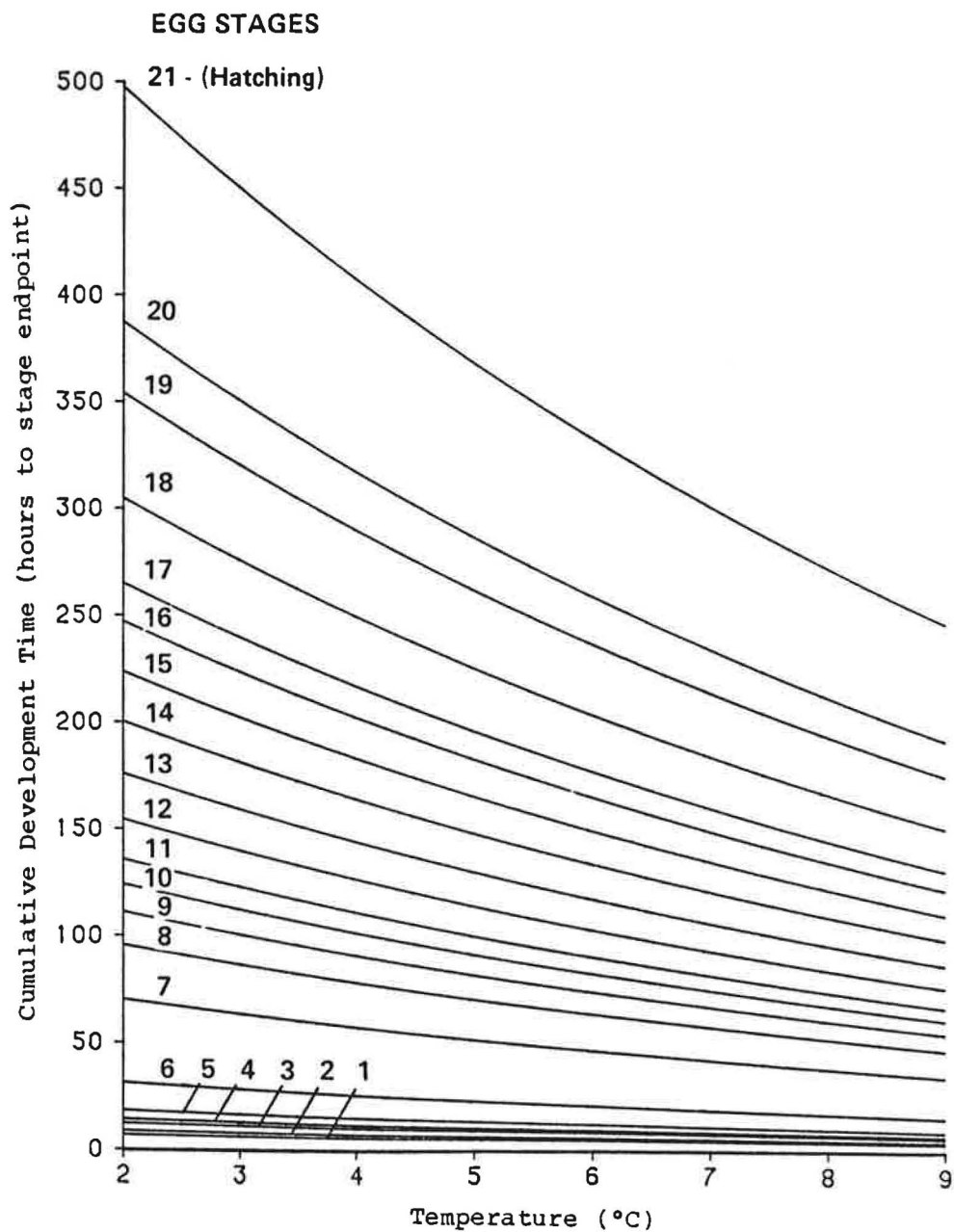


Figure 8. Preliminary relationships between incubation temperature (°C) and the cumulative development time (hours to stage endpoint) for the 21 developmental stages recognized for eggs of walleye pollock.

The duration of a developmental stage was calculated as the difference between cumulative development times for successive age groups:

$$(eq. 2.2) \quad STGDUR_{ij} = TIME_{ij} - TIME_{(i-1)j}$$

where

$STGDUR_{ij}$  duration (hours) of the  $i$ th stage at the  $j$ th station temperature.

The last term was equated to zero when estimating the duration of stage 1.

A stage midpoint, representing the cumulative development time to the approximate midpoint of a stage, was given by:

$$(eq. 2.3) \quad STGMID_{ij} = TIME_{(i-1)j} + \frac{STGDUR_{ij}}{2}$$

where

$STGMID_{ij}$  cumulative development time in hours to the midpoint of the  $i$ th stage at the  $j$ th station temperature.

#### Tow standardizations

Station egg abundance is usually expressed in terms of a standardized catch (Sette and Ahlstrom, 1948; Smith and Richardson, 1977). In its simplest form, standardized catch represents the product of the size of the egg catch and a standardization factor involving the sampling depth and the volume filtered:

$$(eq. 2.4) \quad AB_j = CATCH_j \frac{DEPTH_j}{VOL_j}$$

where

$CATCH_j$  egg catch from the  $j$ th bongo sample

$DEPTH_j$  maximum depth attained by the bongo array at the  $j$ th station (m)

$VOL_j$  volume filtered at the  $j$ th station ( $m^3$ )

$AB_j$  standardized catch for the  $j$ th station (eggs of all ages / $m^2$ ).

The maximum depth sampled at each station was estimated from tow profiles provided by a time-depth recorder. Volume filtered was determined from the cross-sectional area of the net mouth (60 cm diameter) times the estimated length of the double oblique tow path. Path length was calculated (Smith and Richardson, 1977) as:

$$(eq. 2.5) \quad PATH_j = \frac{REVS_j}{DOT_j} \text{ FACTOR } REVS_j$$

where

REVS<sub>j</sub> total flowmeter revolutions accumulated during the tow at the jth station  
 DOT<sub>j</sub> duration of the tow at the jth station (sec)  
 FACTOR calibration factor relating revs/sec to m/rev for the flowmeter in use  
 PATH<sub>j</sub> distance that the bongo array was towed at the jth station (m).

It was assumed that the net mouth achieved a complete frontal attack and had a 100% filtering efficiency. The rate with which revolutions accumulated on a flowmeter was assumed to be constant for the duration of the tow and given by the ratio REVS<sub>j</sub>/DOT<sub>j</sub>.

In addition to determining a standardized catch, it was also convenient to partition each egg catch into 21 developmental stages prior to performing the standardization of eq. 2.4. Unstandardized stage abundances were obtained by projecting stage frequencies from a subsample onto the corresponding egg catch:

$$(eq. 2.6) \quad FREQ_{ij} = \frac{STG_{ij}}{STAGED_j} \text{ CATCH}_j$$

where

STG<sub>ij</sub> stage frequency, the number of eggs in the ith stage for the jth sample (eggs/developmental stage/staged subsample)  
 STAGED<sub>j</sub> total number of eggs from the jth catch that were assigned to stages 1-21  
 CATCH<sub>j</sub> egg catch from the jth bongo sample  
 FREQ<sub>ij</sub> unstandardized stage abundance, the number of eggs assigned to the ith stage for the jth sample (eggs/stage/sample).

The egg frequencies for stages 22-24 were ignored since the proration of these frequencies over stages 1-21 would cause a number of analytical complications while contributing little to the characterization of the age structure for egg catches.

Standardized stage abundance was obtained by:

$$(eq. 2.7) \quad C_{ij} = FREQ_{ij} \frac{DEPTH_j}{VOL_j}$$

where

C<sub>ij</sub> standardized stage abundance for the ith stage at the jth station (eggs/stage/m<sup>2</sup>).

### Station abundance-age plots

Standardized stage abundances (eq. 2.7) summarize differing intervals of spawning and, in order to compare the abundance of one stage to that of another, these values were further standardized to similar durations:

$$(eq. 2.8) \quad AVGSTGAB_{ij} = \frac{C_{ij}}{STGDUR_{ij}}$$

where

$AVGSTGAB_{ij}$  hourly abundance for the  $i$ th stage at the  $j$ th station (eggs of a stage/hr of stage duration/m<sup>2</sup>).

Abundance-age plots were constructed for individual egg catches (Figure 9), with hourly stage abundances (eq. 2.8) plotted against the cumulative development time to the stage midpoint (eq. 2.3). The stage number serves as a label for the plotted point.

### Treatment of hydroacoustic data

Hydroacoustic survey data (Nunnallee, pers. commun.) were used to define the spatial distribution of adult fish concentrations. Midwater trawl sampling revealed the fish population to be greater than 95% walleye pollock by weight (Nelson and Nunnallee, 1985) and, therefore, echo integration data provided an almost pure measure of the relative abundance of walleye pollock adults over the sampled portions of the survey area. Echo returns from near surface to near bottom were integrated over 5 min intervals along a transect. These values were converted to three relative levels of abundance, plotted on charts, and contoured.

## RESULTS

### Egg age frequencies on a sample by sample basis

Preliminary information on the constancy of spawning with time in

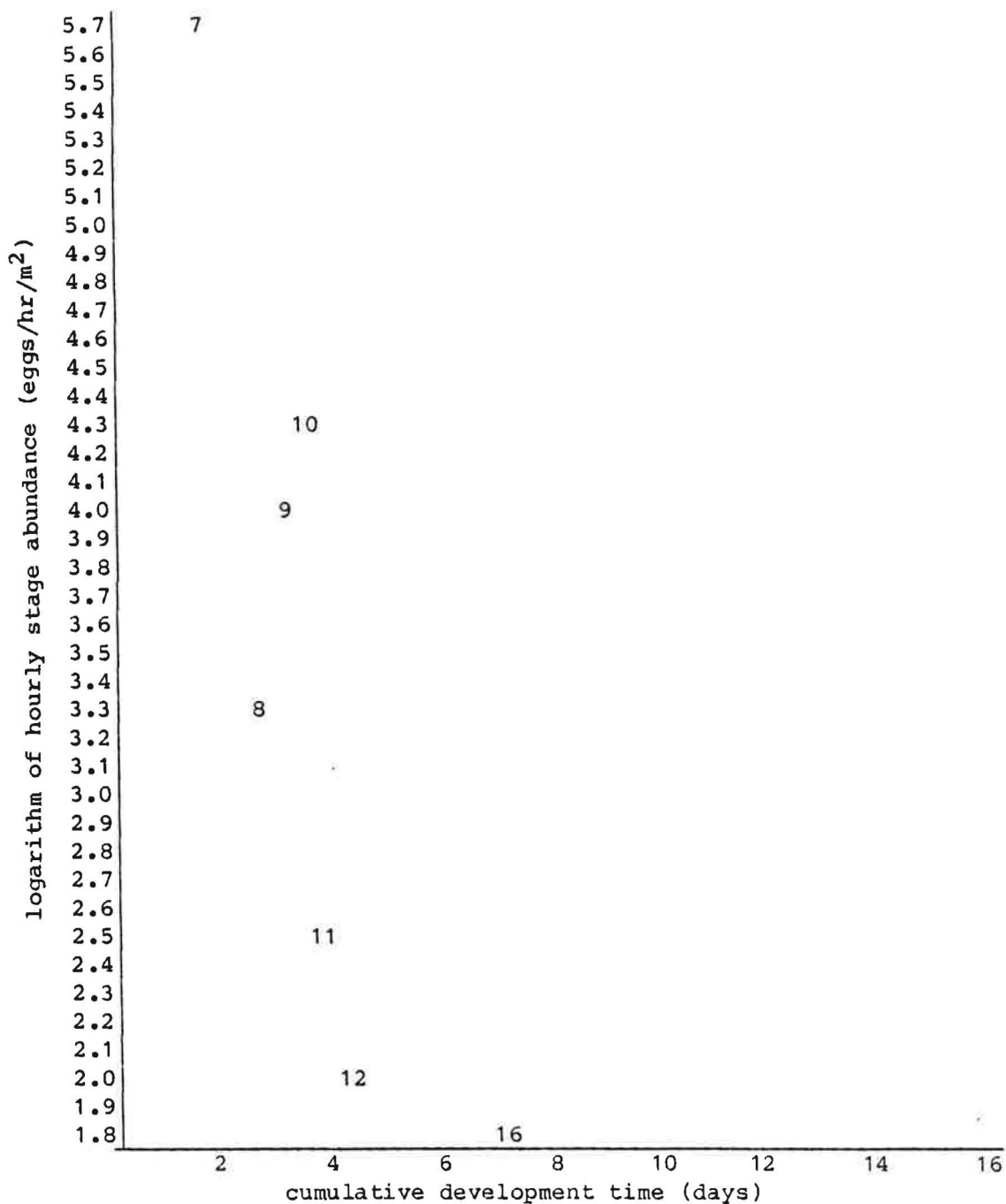


Figure 9. An example station abundance-age plot for the eggs of walleye pollock. The logarithms of hourly stage abundances are plotted against the cumulative development times to stage midpoints. A stage number identifies the plotted point for each developmental stage.

the vicinity of individual sampling stations was provided by station abundance-age plots. Abundance-age plots and tables of amplifying data are given for selected stations in Appendix A.

The station abundance-age plots for survey 2MF81 presented the clearest trends. Large egg catches were first observed at stations G022A-G025A (Appendix Figures A.1-A.4), and had standardized catches of 10512, 16770, 10455, and 2608 eggs/m<sup>2</sup> respectively. The patterns for the log-transformed hourly stage abundances were linear, steep, and negatively sloped. Egg ages ranged over approximately one-half of the incubation period, and older eggs were rarely found.

Stations G089A-G091A (Appendix Figures A.17-A.19) were added following the first pass through the survey area during cruise 2MF81 (Figure 2) and were occupied 8 days following the occupancy of stations G022A-G025A. These additional stations also had high catches, with standardized catches of 63657, 34563, and 28649 eggs/m<sup>2</sup> respectively. The patterns of the log-transformed hourly stage abundances again followed a linear trend, but with shallower slopes and more scatter along the trend. Eggs were found in almost all stages of development.

Stations G086A-G088A (Appendix Figures A.14-A.16) were located in the vicinity of stations G089A-G091A and also had relatively large standardized catches of 12766, 6948, and 5703 eggs/m<sup>2</sup> respectively. However, the log-transformed hourly stage abundances for these stations peaked toward the middle of the incubation period and values to either side of this peak fell off rapidly in magnitude. A similar pattern was found for stations G046A, G066A-G069A, G077A-G079A, and G082A (Appendix Figures A.5-A.13). These plots also show peak abundances at approximately one-half to two-thirds of the way through the incubation period, indicating that peak spawning occurred some 6 to 9 days prior to the time that each sampling station was occupied.

### Distribution of spawners

Hydroacoustic data revealed changes in the spatial distribution of adults as the spawning season progressed (Figures 10-12). A large, diffuse concentration of adults was first observed in the lower region of Shelikof Strait on julian days 65-66 and again on julian day 70 during hydroacoustic survey 1 (Figures 5 and 10). Smaller, scattered concentrations were detected further up the Strait about 6 days later during the same survey (julian days 71-72).

During the second hydroacoustic survey (julian days 84-85), adults were found concentrated along the position of the 200 m isobath off the Alaskan mainland from Portage Bay to Cape Ilktugitak (Figures 6 and 11). This area had first been occupied 20 days earlier during the first hydroacoustic survey (julian days 65-66). During these three weeks, the adults had apparently moved from the center of the Strait and had concentrated nearer to shore. Adults from the diffuse concentration in the lower region of the Strait had also shifted to this nearshore region, since only a remnant remained in the lower Strait when this area was resurveyed on julian day 85.

The third hydroacoustic survey (Figures 7 and 12) was carried out about 2 weeks after the second survey (julian days 98-99). Adults had further concentrated along the position of the 200 m isobath and were located from Cape Kekurnoi to Cape Ilktugitak.

### DISCUSSION

Simple trends in station abundance-age plots were difficult to discern. The plotted position for a developmental stage can potentially range over a wide interval as a result of the processes of sampling, staging, and plotting on a logarithmic scale. The number of eggs collected at a sampling station was a random event and, to a certain extent, so too were the numbers occurring in each stage of

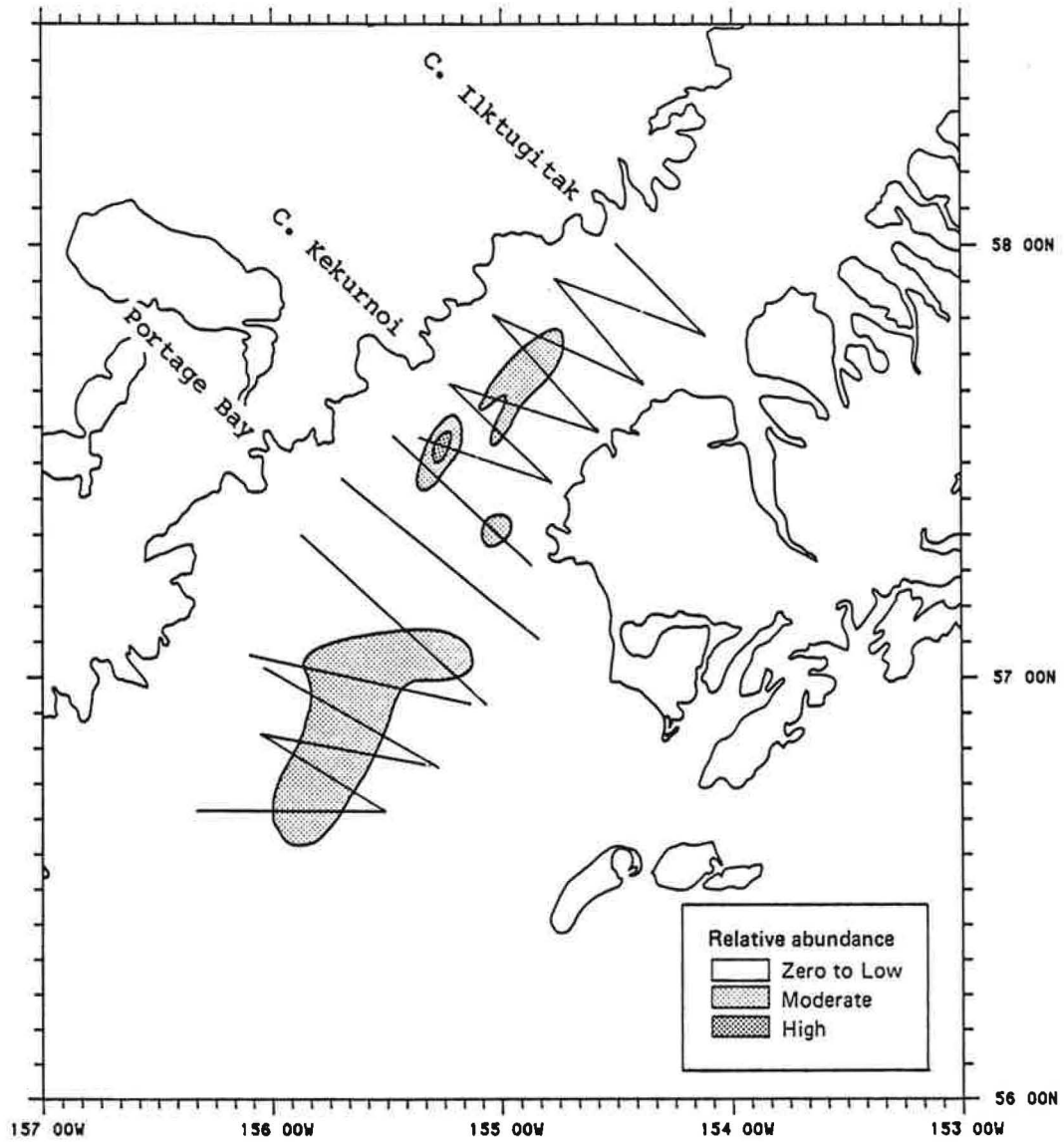


Figure 10. Distribution of adult walleye pollock as indicated by hydroacoustic echo-integration data, cruise MF81-2, survey 1 (March 06-07 and 11-12).

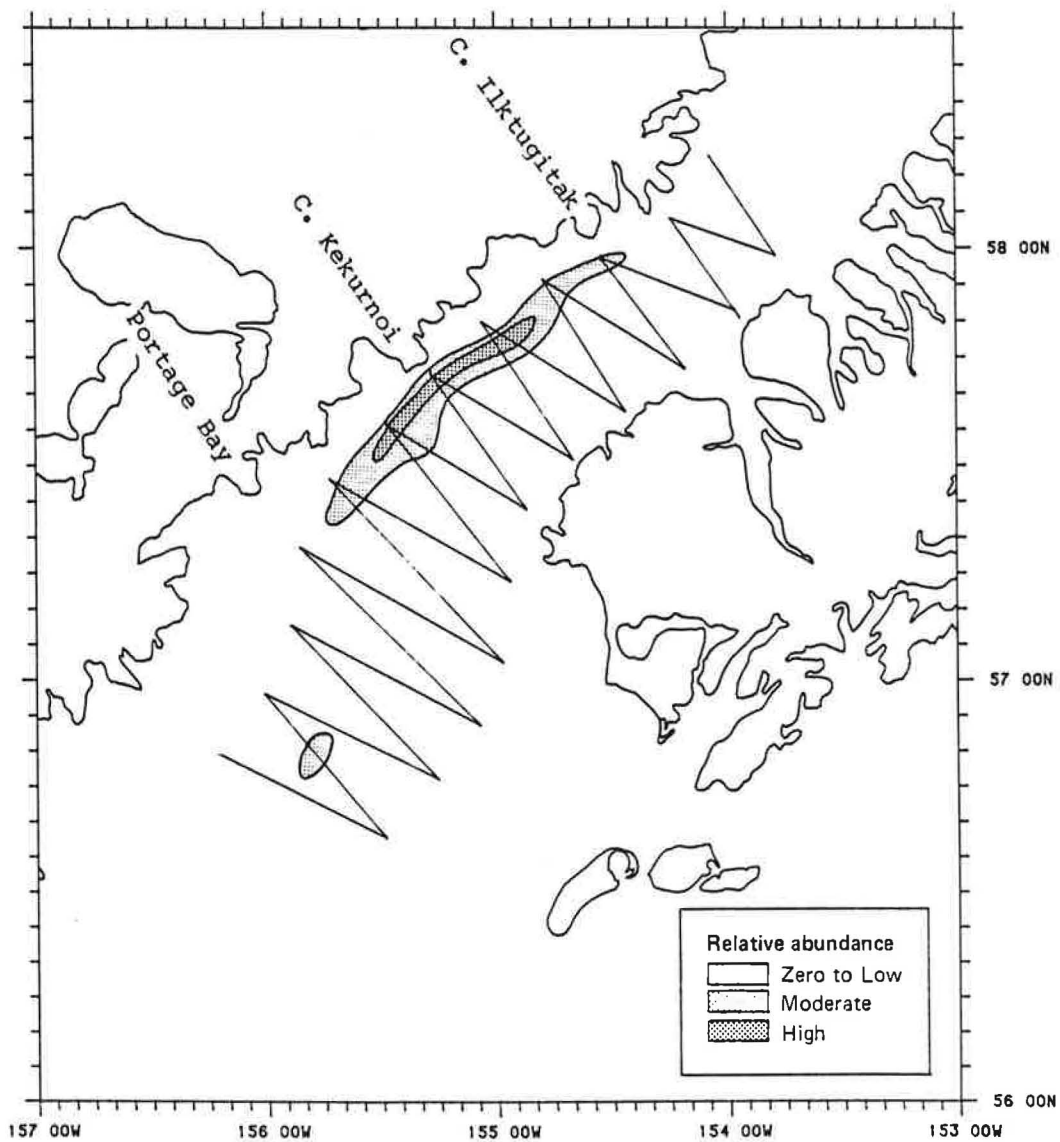


Figure 11. Distribution of adult walleye pollock as indicated by hydroacoustic echo-integration data, cruise MF81-2 survey 2 (March 24-27).

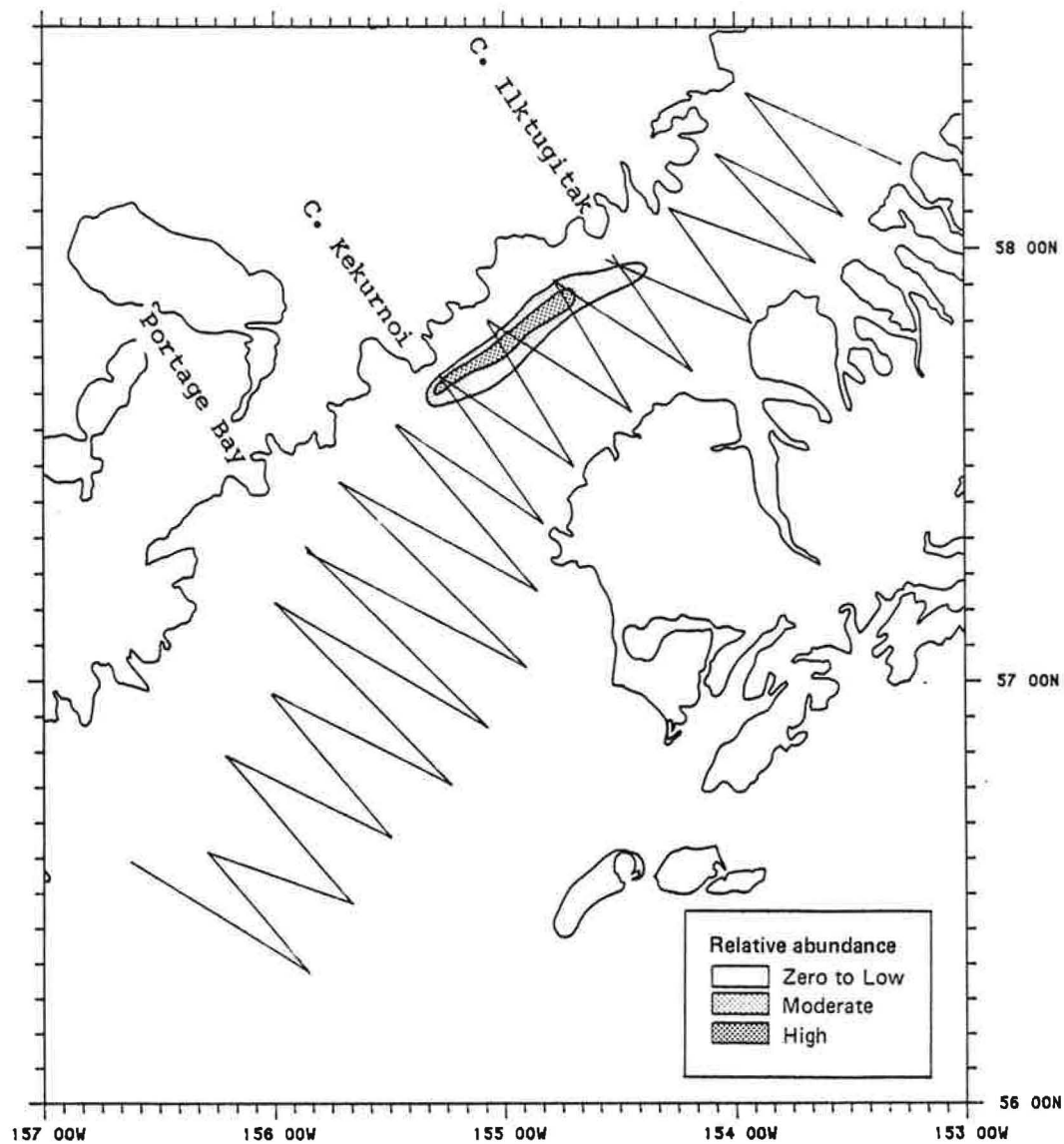


Figure 12. Distribution of adult walleye pollock as indicated by hydroacoustic echo-integration data, cruise MF81-2 survey 3 (April 04-10).

development. A stage frequency is fundamentally integer-valued since it reflects the collection of a whole number of animals, and this contributed to the stepped appearance of the plotted points on a real scale. The accuracy of stage abundance data was one or, at most, two significant digits, since approximately 100 or fewer eggs were classified into the 21 developmental stages recognized for walleye pollock eggs. The plots for cruise 2MF81 were least difficult to interpret, primarily because a large number of eggs were staged from each egg catch and because the variability of plotted values for the large egg catches was less apparent following the logarithmic transformation.

Judging by the slopes of the log-transformed hourly stage abundances (Appendix A), the general pattern of spawning near a sampling station typically began with a rapid onset and buildup in the level of spawning. Spawning may then either peak sharply or maintain a rough stability depending on the duration with which spawners lingered in the volume of seawater that was eventually sampled by the bongo array. A high level of spawning was often followed by a precipitous decline in spawning activity, apparently as the adults finished spawning or rapidly dispersed to new regions of the survey area. Typically only one pulse of spawning was evident in any abundance-age plot. The steep linear trend to either side of a peak seen in these log-linear plots indicates that changes in the level of spawning were strongly exponential in character and that spawning seldom persisted for much longer than a week in any given area.

#### Co-occurrence of eggs and adults within the survey area

A coherent pattern emerges for the spatial distribution of egg catches having similar age histories (Figure 13). Table 5 summarizes the general features of the spatial patterns of egg and adult concentrations.

Large concentrations of eggs were found near recent or

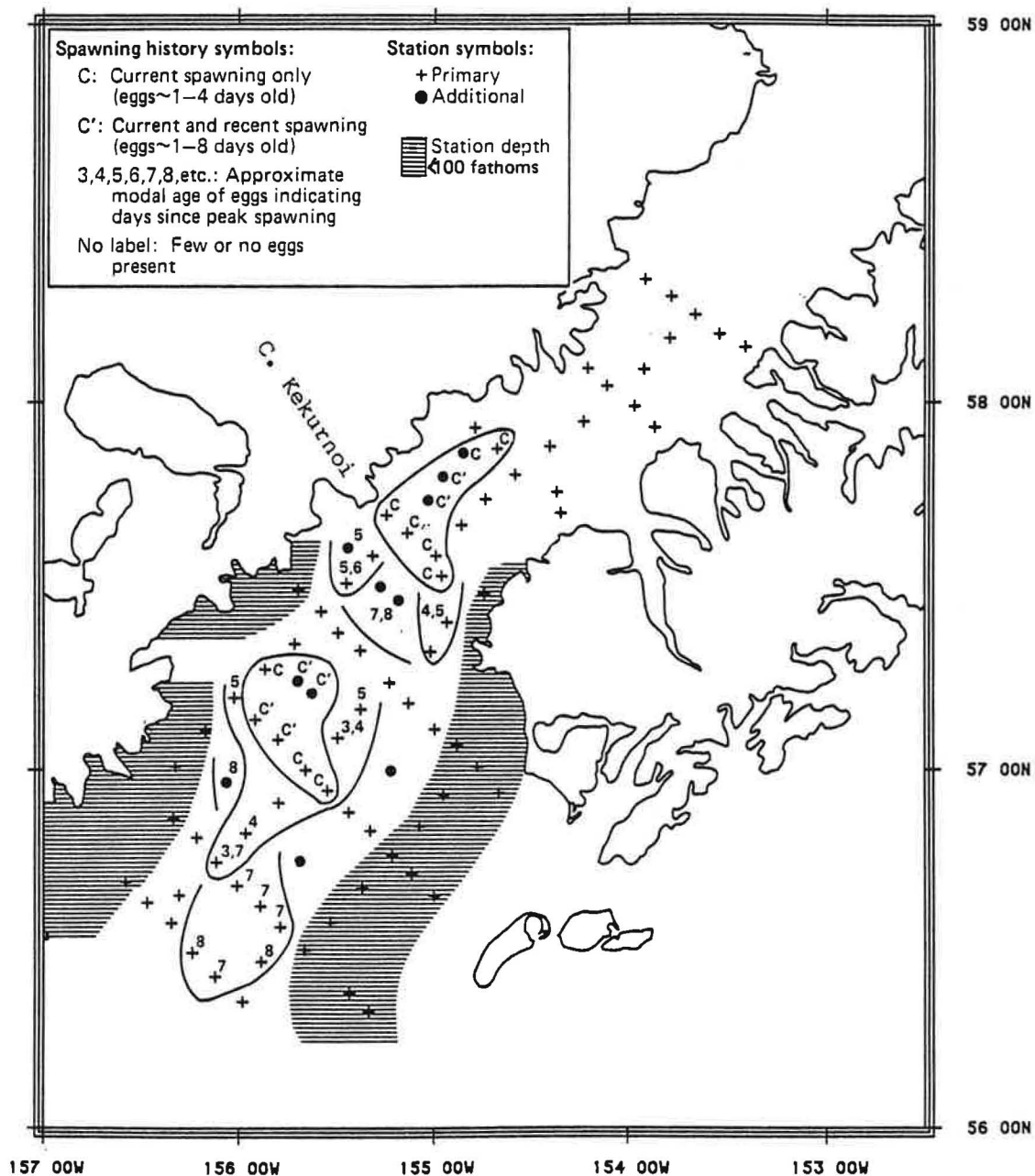


Figure 13. The recent history of spawning by walleye pollock as indicated by the dominant age groups of eggs from bongo catches, cruise 2MF81 (March 29 - April 08). Solid lines enclose stations with similar spawning histories.

Table 5. Summary of the distributional pattern of adults based on hydroacoustic survey data, and the pattern of egg ages on a station by station basis based on ichthyoplankton data from survey 2MF81.

chart notation in Figure 13	C	C'	4,5,6	7,8,9
relative size of egg catch	high	high	moderate	low
pattern of log-transformed hourly stage abundances	very steep negative slope	moderate negative slope	sharp peak	sharp peak
age of eggs at peak, indicating the days prior to sample collection when spawning intensity peaked	days 0-3	days 0-3	days 4-6	days 7-9
sampling location relative to contemporary concentrations of adults	in same general area	in same general area	down current and behind the migrating adults	further down current and further behind the migrating adults

contemporary concentrations of spawning adults. The largest egg catches were obtained in two regions of the survey area during cruise 2MF81 (stations labeled C). These catches also had a high proportion of eggs in the earlier developmental stages and few or none in the more advanced stages. A steep decline in stage abundances with age appears to indicate that spawning had recently begun and was currently in progress at the time these stations were occupied. This pattern suggests that spawners had rapidly formed-up in the region near these stations. Spawners subsequently migrated toward the nearshore region off Cape Kekurnoi.

Stations labeled C' in Figure 13 also had high catches but the corresponding station abundance-age plots showed less precipitous slopes, apparently indicating that significant spawning had been

occurring for some time prior to the time that sampling was conducted at these stations. Many collections of this type were obtained at stations that were occupied following the end of survey 2MF81 during the overlapping hydroacoustic survey 3 (stations G084A-G091A).

The geographic distances between the locations of spawners and maturing eggs increased as eggs were transported downcurrent away from the region of current spawning and as spawners moved further up the Strait during the course of the spawning season. To judge from the ages associated with peak abundances on the station abundance-age plots these older eggs were spawned about a week prior to the the time that stations were occupied. Older eggs predominated in catches for stations that were located the furthest to the southwest (Figure 13). Earlier, during the first and second hydroacoustic surveys, adults were found slightly to the northeast of these areas.

The rapidity with which spawners moved through Shelikof Strait was not anticipated when designing and conducting the ichthyoplankton surveys. The survey area was traversed twice during cruise 2MF81, occurring both immediately before and during the third hydroacoustic survey. The distribution of ichthyoplankton stations appears to have overemphasized the high egg abundance areas. Specifically, stations G022A-G025A of cruise 2MF81 may represent an initial sampling of the spawning concentration near Cape Kekurnoi (julian day 91), and this concentration may again have been sampled approximately one week later (julian day 99) during the subsequent retracing of the survey area when occupying stations G086A-G091A. Data from these additional stations were not employed in some analyses in order to improve the synopticity of the second ichthyoplankton survey.





### Chapter 3. The estimation of total daily egg abundance

#### INTRODUCTION

Sette and Ahlstrom (1948) referred to the process of estimating the total abundance of eggs within a survey area as spatial integration and introduced the method of polygonal station areas for this purpose. Station areas are constructed on charts by drawing perpendicular bisectors through lines connecting the positions of adjacent stations. The egg abundance in the vicinity of a station is then obtained as the product of an egg catch and a station area. In effect, this product represents the number of eggs to be found within a large polygonal column of seawater. Total egg abundance within the survey area is the sum of these products for all sampling stations.

Prior to the introduction of more rigorous statistical models, the method of contouring was also a common approach (Sette and Ahlstrom, 1948; Simpson, 1959). Both the polygonal area approach and the method of contouring are primarily graphical procedures enabling the characteristics of sample data to be extrapolated to the sampled egg population. However, neither of these approaches are capable of indicating the precision of the total egg abundance estimate.

Total egg abundance can also be estimated under a variety of other analytical frameworks. Four statistical models that have been used in prior ichthyoplankton studies are simple random sampling (SRS), the delta distribution (DLN), the negative binomial distribution (NB), and stratified random sampling (STRS).

Station abundance data can be treated as observations collected under a simple random sampling design (SRS) from a finite statistical population of sample units. A sample unit shall be defined as the volume occurring below a  $1 \text{ m}^2$  area of sea surface, and the total number of such  $\text{m}^2$  columns within the survey area defines the finite size of the statistical population. Mean egg abundance per sample unit and its apparent precision are obtained through estimators derived by the

method of moments.

It is commonly observed that a frequency distribution of egg catches has substantial positive skewness; that is, having many small catches but also having a very few, extremely large catches. A logarithmic transformation is frequently suggested as a means by which a positively-skewed catch distribution can be given a more normal appearance (Bagenal, 1955; Elliott, 1979). However, the log transformation cannot be applied directly to zero-valued catches. One approach to this problem is to ignore the frequency of zeros and to calculate approximate values for the parameters of the lognormal distribution from the positive data alone (Lockwood, et al., 1981). Thompson (1951) proposed that 1 be added to each observation prior to the logarithmic transformation, provided it can be assumed that the distribution of observed values is consistent with the lognormal model and where zeros actually represent small, positive quantities that were censored during the sampling process. However, the observed frequency of zeros in ichthyoplankton data usually differs markedly from the frequency expected under the lognormal model, often showing a pronounced bimodality of zeros and positive data.

A modified form of the lognormal distribution (Aitchison, 1955; Aitchison and Brown, 1957; Pennington, 1983), referred to as the delta distribution (DLN), has been used in a number of recent ichthyoplankton studies (Berrien, et al., 1981; Pennington and Berrien, 1984; Lough, et al., 1985). Under this model the conditional distribution of nonzero values is assumed to be lognormal. It is also assumed that the proportion of zero-valued sample units is positive and exactly known; it is therefore not a parameter in a statistical sense.

The negative binomial distribution (NB) is another statistical model suggested for the analysis of catch data (Elliott, 1979; Zweifel and Smith, 1981). The probability density function for a variate following a negative binomial distribution is completely specified by a mean,  $m$ , and a shape parameter,  $k$ . Both  $m$  and  $k$  may take a value from

zero to infinity. The negative binomial is a very flexible model in that the shape of the distribution approaches the lognormal family as  $k$  approaches zero and approaches the Poisson family as  $k$  approaches infinity. A number of estimators are available for this and other parameterizations of the distribution (Haldane, 1941; Fisher, 1941; Anscombe, 1950; Bliss and Fisher, 1953; Bissel, 1972a, 1972b).

Finally, a stratified random sampling (STRS) design (Cochran, 1977) is convenient for the analysis of some plankton survey data provided a suitable auxiliary variate is available to stratify the survey area into statistical subpopulations. Tanaka (1974) employed administrative districts (prefectures) as a basis for stratification. Data from the hydroacoustic surveys, which alternated with ichthyoplankton surveys during the 1981 sampling season in Shelikof Strait, provided a relative index to the abundance of spawners at locations throughout the survey area. It should be noted that egg abundances are treated as one statistical population under the former models (SRS, DLN, NB) but as a set of independent statistical subpopulations under the STRS model.

#### METHODS

The survey area was defined as the smallest area that included the positions of all sampling stations. This area was approximately that occupied during any of the last three egg surveys and was calculated as  $1.596 \times 10^{10} \text{ m}^2$ . The total number of sample units in the survey area was also  $1.596 \times 10^{10}$  since an egg catch was standardized to an element size of  $1 \text{ m}^2$  column of seawater. The survey area was poststratified into three regions based on the location of adult concentrations. The locations and sizes of strata and the boundaries to the survey area are depicted in Figure 14.

The inclusion of stations G084A-G091A of survey 2MF81 (Figure 2) in the calculation of total daily egg abundance was considered inappropriate. These stations were not considered synoptically

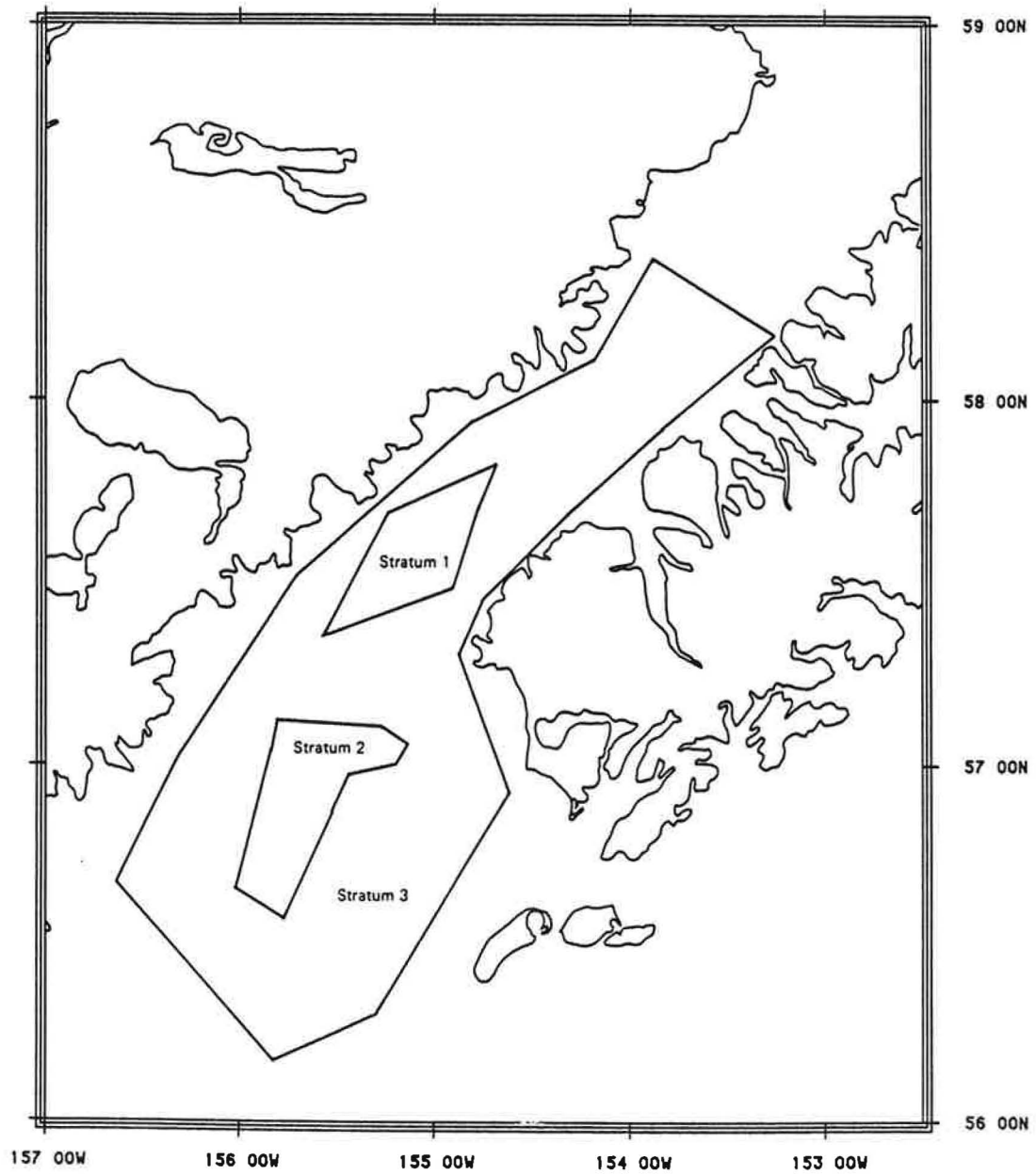


Figure 14. Geographic boundaries to the survey area and strata. The locations and sizes of strata roughly approximate the distribution of adults as indicated by hydroacoustic echo-integration data.

occupied with the other stations and were excluded in order to maintain the time dependent correlation between adult and egg distributional data. Only stations G001A-G083A were used in this analysis.

Since egg mortality may be significant over the extended incubation period of walleye pollock, egg data were restricted to the first ten developmental stages. Furthermore, as was indicated by the analysis of egg and adult co-occurrences, the correlation between the locations of eggs and spawners was strongest for eggs of early to intermediate age. The value of hydroacoustic data as an auxiliary variate defining the geographic extent of egg concentrations was considerably improved by restricting attention to only those eggs that were recently spawned.

Egg data were expressed as daily station abundances using 10 developmental stages:

$$(eq. 3.1) \quad A_j = \frac{\sum_{i=1}^{10} C_{ij}}{\frac{\text{day}}{24 \text{ hr}} \text{ PERIOD}_j}$$

where

- $C_{ij}$  standardized abundance of the  $i$ th stage at the  $j$ th station (eq. 2.7)  
 $\text{PERIOD}_j$  total development time (days) from fertilization to the end of stage 10 for the  $j$ th station  
 $A_j$  daily abundance at the  $j$ th station (eggs/day/m<sup>2</sup>).

The numerator represents the number of eggs of all ages through stage 10 within a unit volume of seawater in the vicinity of the  $j$ th sampling station. Average daily egg abundance was obtained through the division of this numerator by the period of time over which these eggs were spawned, a value which was obtained by evaluating eq. 2.1 with  $i=10$ . This time standardization of egg abundance data shifts the frame of reference from a stage basis to a time basis and is consistent with standard procedures (Sette and Ahlstrom, 1948; Taft, 1960; Smith and Richardson, 1977). Note, however, that egg mortality has been ignored. Consequently, while the integration of daily station abundances over the entire survey area will yield an estimate of the total daily egg

abundance, this abundance estimate will necessarily be a conservative estimate of the corresponding daily egg production for this portion of the spawning season.

Mean daily egg abundance was estimated for each of the four ichthyoplankton surveys using the following statistical models: simple random sampling (SRS), the delta distribution (DLN), the negative binomial distribution (NB), and stratified random sampling (STRS). It was necessary to assume that egg catches were obtained by a random sampling of the survey area in order to invoke these models.

Sample size was assumed to be large enough to permit the construction of symmetrical confidence intervals around the sample mean. Approximate confidence intervals were constructed with 2.0 as the value of Student's t statistic or the Z statistic. Satterthwaite's approximation for the effective degrees of freedom for a stratified population (Cochran, 1977) was not employed due to the high levels of skewness still remaining in the sample frequency distributions for strata, and the value of  $t=2.0$  was used for this model also. A value of  $t=2.0$  corresponds to 2 standard errors of the sample mean, or a 97.5% confidence interval for a normally distributed variate.

#### Estimators for simple random sampling (SRS)

Mean daily abundance (eggs/day/m<sup>2</sup>) was obtained by:

$$(eq. 3.2) \quad m = \frac{\sum_{j=1}^n A_j}{n}$$

where

$A_j$       daily station abundance based on data for eggs in developmental stages 1-10  
 $n$          sample size.

Sample variance of daily station abundances:

$$(eq. 3.3) \quad s^2(A) = \frac{\sum_{j=1}^n (A_j - m)^2}{n-1}$$

Standard error of the mean:

$$(eq. 3.4) \quad se(m) = [s^2(A)/n]^{1/2}$$

Upper and lower confidence limits for the mean:

$$(eq. 3.5) \quad CL(m) = m \pm t \, se(m)$$

where

t Student's t statistic, with t=2.0.

Estimators for the delta distribution (DLN), adapted from Aitchison and Brown (1957)

Natural logarithm of daily station abundance:

$$(eq. 3.6) \quad y_j = \ln(A_j)$$

where

A<sub>j</sub> daily station abundance.

Mean of log-transformed daily station abundances:

$$(eq. 3.7) \quad \bar{y} = \frac{\sum_{j=1}^p y_j}{p}$$

where

p number of nonzero daily station abundances.

Variance of log-transformed daily station abundances:

$$(eq. 3.8) \quad s^2(y) = \frac{\sum_{j=1}^p (y_j - \bar{y})^2}{p-1}$$

Mean daily abundance (eggs/day/m<sup>2</sup>):

$$(eq. 3.9) \quad m = \left(\frac{p}{n}\right) \exp(\bar{y}) G_p \left[ \frac{s^2(\bar{y})}{2} \right]$$

where

$n$  sample size  
 $G_p$  a bessel function given in Aitchison and Brown (1945, 1957).

The shape parameter for the delta distribution,  $r^2$ :

$$(eq. 3.10) \quad r^2 = \left(\frac{p}{n}\right) \exp(2\bar{y}) \left\{ G_p \left[ 2s^2(\bar{y}) \right] - \left(\frac{p-1}{n-1}\right) G_p \left[ \frac{p-2}{p-1} s^2(\bar{y}) \right] \right\}$$

Asymptotic variance of the mean:

$$(eq. 3.11) \quad S^2(m) = \frac{\exp(2m+r^2)}{n} \left(\frac{p}{n}\right) \left[ 1 - \frac{p}{n} + \frac{2r^2+r^4}{2} \right]$$

Standard error of the mean:

$$(eq. 3.12) \quad se(m) = [S^2(m)]^{1/2}$$

Upper and lower confidence limits for the mean:

$$(eq. 3.13) \quad CL(m) = m \pm Z_{\alpha} se(m)$$

where

$Z_{\alpha}$  standard normal or Z statistic, with  $Z_{\alpha} = 2.0$ .

Estimators for the negative binomial distribution (NB), adapted from Bissel (1972b)

Mean daily abundance (eggs/day/m<sup>2</sup>):

$$(eq. 3.14) \quad m = \frac{\sum_{j=1}^n A_j}{n}$$

where

$A_j$  daily station abundance  
 $n$  sample size.

The shape parameter for the negative binomial was obtained from an iterative solution of:

$$(eq. 3.15) \quad 0 = n \ln\left(\frac{k}{m+k}\right) + \sum_{j=1}^n \sum_{j'=1}^{A_j} (k+j'-1)^{-1}$$

Asymptotic variance of the mean:

$$(eq. 3.16) \quad S^2(m) = \frac{\left[ \frac{m+m^2}{k} \right]}{n}$$

Standard error of the mean:

$$(eq. 3.17) \quad se(m) = \left[ S^2(m) \right]^{1/2}$$

Upper and lower confidence limits for the mean:

$$(eq. 3.18) \quad CL(m) = m \pm Z_{\alpha} se(m)$$

where

$Z_{\alpha}$  standard normal or Z statistic, with  $Z_{\alpha} = 2.0$ .

#### Total daily egg abundance under the models SRS, DLN, and NB

Estimates of total daily egg abundance within the survey area were calculated from each estimate of the mean under the SRS, DLN, and NB models as:

$$(eq. 3.19) \quad P_g = \text{AREA } m_g$$

where

AREA size of the survey area ( $1.596 \times 10^{10} \text{ m}^2$ )  
 $m_g$  mean daily abundance (eggs/day/m<sup>2</sup>) for the gth survey, estimated under either the SRS, DLN, or NB models  
 $P_g$  total daily egg abundance for the gth survey (eggs/day/survey area).

#### Estimators for stratified random sampling (STRS), adapted from Cochran (1977)

Stratum mean:

$$(eq. 3.20) \quad m_h = \frac{\sum_{j=1}^{n_h} A_{jh}}{n_h}$$

where

$A_{jh}$  daily station abundance for the  $j$ th station from the  $h$ th stratum  
 $n_h$  sample size for the  $h$ th stratum.

Stratum total:

$$(eq. 3.21) \quad Y_h = N_h \bar{m}_h$$

where

$N_h$  stratum size, the number of sample units in the  $h$ th stratum.

Stratified total, the total daily abundance for the  $g$ th survey:

$$(eq. 3.22) \quad P_g = \sum_{h=1}^H Y_h$$

where

$H$  number of strata comprising the survey area.

Variance of observations from the  $h$ th stratum:

$$(eq. 3.23) \quad s^2(A_h) = \frac{\sum_{j=1}^{n_h} (A_{jh} - \bar{m}_h)^2}{n_h - 1}$$

Variance of a stratum total:

$$(eq. 3.24) \quad s^2(Y_h) = \sum_{h=1}^H N_h^2 \frac{(N_h - n_h)}{N_h} \frac{s^2(A_h)}{n_h}$$

Variance of the stratified total for the  $g$ th survey:

$$(eq. 3.25) \quad s^2(P_g) = \sum_{h=1}^H s^2(Y_h)$$

Upper and lower confidence limits to the estimate of total daily egg abundance for the  $g$ th survey:

$$(eq. 3.26) \quad CL(P_g) = Y_h \pm t \left[ s^2(P_g) \right]^{1/2}$$

where

$t$  Student's  $t$  statistic, with  $t=2.0$ .

## RESULTS

Table 6. Survey data for eggs of walleye pollock treated as samples from a simple random sampling design (SRS). Statistics shown for each of the 1981 surveys are: n, sample size; m, mean daily abundance (eggs/day/m<sup>2</sup>); se(m), standard error of the mean; CV, coefficient of variation for the mean; and CL, confidence limits for the mean.

survey	n	m	se(m)	CV	CL
1MF81	31	2.37	1.39	59%	0.0 - 5.2
2MF81	81	167.	69.2	41%	29. - 305.
3MF81	79	11.1	1.35	12%	8.4 - 13.8
4MF81	75	1.19	0.217	18%	0.8 - 1.6

Estimates for mean daily egg abundance (m) under the assumption of a simple random sampling design (SRS) are given for each survey in Table 6. Parameter estimates for the delta distributions (DLN) are given in Table 7, and Table 8 gives the statistics for the negative binomial distributions (NB).

Estimates of mean daily egg abundance and associated coefficients of variation are summarized in Table 9 for the SRS, DLN, and NB models for the catch curve. Estimates of mean egg density were roughly

Table 7. Survey data for eggs of walleye pollock treated as random samples from a delta distribution (DLN). Statistics shown for each of the 1981 surveys are: n, the number of positive and zero-valued catches, and p, the number of positive catches; p/n, the fraction of the sample units within the survey area having positive egg abundances; m, mean daily abundance (eggs/day/m<sup>2</sup>); se(m), standard error of the mean; CV, coefficient of variation for the mean; CL, confidence limits for the mean; and r<sup>2</sup>, variance or shape parameter.

survey	n	p	p/n	m	se(m)	CV	CL	r <sup>2</sup>
1MF81	31	25	81%	2.09	0.406	19%	1.28- 2.90	15.1
2MF81	81	72	89%	204.	52.4	26%	99. -309.	6.6 X10 <sup>6</sup>
3MF81	79	75	95%	40.5	2.43	6%	35.6 - 45.4	8.7 X10 <sup>3</sup>
4MF81	75	67	89%	4.53	0.314	7%	3.90- 5.16	45.0

Table 8. Survey data for eggs of walleye pollock treated as random samples from a negative binomial distribution (NB). Statistics shown for each of the 1981 surveys are: n, sample size; m, mean daily abundance (eggs/day/m<sup>2</sup>); se(m), standard error of the mean; CV, coefficient of variation for the mean; CL, confidence limits for the mean; and k, shape parameter.

survey	n	m	se(m)	CV	CL	k
1MF81	31	2.37	0.425	18%	1.52- 3.22	1.1
2MF81	81	167.	18.6	11%	130. -204.	0.20
3MF81	79	11.1	1.25	11%	8.6 - 13.6	0.97
4MF81	75	1.19	0.137	12%	0.92- 1.46	105.

similar across all models on a survey by survey basis. Coefficients of variation on a survey by survey basis were largest under the SRS model and smallest under the DLN and NB models, as anticipated for positively skewed catch distributions. Cruise 2MF81 provided virtually all the information defining the seasonal magnitude of spawning while the remaining surveys served largely to delimit the duration of the spawning season.

Hydroacoustic data were suitable for a poststratification of the survey area near the time of peak spawning. Statistics under the STRS model for survey 2MF81 are given in Table 10. The largest egg catches were found in stratum 1. Although stratum 1 comprised only 7% of the survey area, it accounted for 76% of the estimated total daily egg abundance by virtue of a high value for mean daily abundance (1701

Table 9. Statistics for mean daily abundance (eggs/day/m<sup>2</sup>) and coefficients of variation (in parentheses) under the simple random sampling (SRS), delta (DLN), and negative binomial (NB) models for the catch curve.

survey	SRS	DLN	NB
1MF81	2.37 (59%)	2.09 (19%)	2.37 (18%)
2MF81	167. (41%)	204. (26%)	167. (11%)
3MF81	11.1 (12%)	40.5 ( 6%)	11.1 (11%)
4MF81	1.19 (18%)	4.53 ( 7%)	1.19 (12%)

Table 10. Summary of estimates for survey 2MF81 under the stratified random sampling model (STRS). Statistics shown for the hth stratum are:  $N_h/\text{AREA}$ , relative stratum size;  $n_h$ , sample size;  $m_h$ , mean daily abundance (eggs/day/m<sup>2</sup>);  $se(m_h)$ , standard error of a stratum mean;  $Y_h$ , total daily egg abundance;  $se(Y_h)$ , standard error of a stratum total; and CV, coefficient of variation for a stratum total. The estimate for stratified total daily egg abundance is given on the bottom line of the Table, along with standard error of the stratified total, coefficient of variation, and approximate confidence limits.

h	$N_h/\text{AREA}$	$n_h$	$m_h$	$se(m_h)$	$Y_h$ X 10 <sup>10</sup>	$se(Y_h)$ X 10 <sup>10</sup>	CV	CL X 10 <sup>10</sup>
1	7%	6	1701.	690.	181.	73.4	41%	
2	9%	9	270.	113.	39.0	16.3	42%	
3	84%	66	13.7	5.3	18.5	7.09	39%	
	-----	---			-----			
	100%	81			239.	75.5	32%	88.-390.

eggs/day/m<sup>2</sup>). The sample mean for stratum 3 was two orders of magnitude less than that of stratum 1 but, because stratum 3 comprised 84% of the survey area, it was responsible for 8% of the estimated total daily production. The relative precision of stratum means was roughly the same for all strata (CV=40%). The CV for the stratified total was only 32% because, while the bulk of the eggs were found in stratum 1, stratum 3 represented the bulk of the sample units defining the survey area and also had the lowest standard error for the stratum mean (5.3 eggs/day/m<sup>2</sup>).

#### DISCUSSION

Estimates of total daily egg abundance are summarized in Table 11 for the four models for spatial integration. In general, the highest estimates on a survey by survey basis were obtained under the DLN model and the lowest estimates were obtained under the STRS model. The estimates of total daily egg abundance were identical for the SRS and NB models because the estimators for the mean were identical (eqs. 3.2 and 3.14).

The disparity between estimates can be readily accounted for by an

Table 11. Summary of total daily abundance estimates (eggs X  $10^{10}$ /day /survey area) under the simple random sampling (SRS), delta (DLN), negative binomial (NB), and stratified random sampling (STRS) models for spatial integration. The julian date for the midpoint of a survey was obtained by a weighted mean of sampling dates.

survey	julian date	SRS	DLN	NB	STRS
1MF81	74.8	3.78	3.34	3.78	
2MF81	90.1	267.	326.	267.	239.
3MF81	118.3	17.7	64.6	17.7	
4MF81	141.1	1.90	7.23	1.90	

examination of the appropriate equations. The mean of the DLN model is, in part, a function of sample variance for the log-transformed data. It was assumed when this model was invoked that the transformed data were normally distributed. If the transformed data display any residual skewness, however, the sample variance estimate would be inflated and the backtransformed mean would consequently have an upward bias.

Differences between the estimated totals under the STRS and the SRS and NB models can also be accounted for by examination of the appropriate formulae. The pattern of totals on a survey by survey basis under the SRS and NB models was identical to that found for means (Table 9) since a total was obtained merely as the product of a mean (eqs. 3.2 or 3.14) and a constant size for the survey area (eq. 3.19). This calculation, in effect, expanded each daily station abundance,  $A_j$ , by a scalar constant, this constant being the quotient of the number of sample units in the statistical population, AREA, and sample size,  $n$ . The effect of this multiplier was to represent each egg catch as the average abundance for a large fraction of sample units within the survey area. For example, each catch from the total of 81 collections would be weighted  $1.9 \times 10^8$  when sampling from a survey area of  $1.596 \times 10^{10} \text{ m}^2$ .

In the estimation of the stratified total on the other hand,

catches were weighted by stratum weights,  $N_h/n_h$ , which differ between strata. Stratum weights were  $1.77 \times 10^8$ ,  $1.61 \times 10^8$ , and  $2.04 \times 10^8$  for stratum 1, 2, and 3 respectively. The definition of stratum 1 as 7% of the total survey area and the occurrence of 6 collections in this stratum caused these individual catches to be weighted 10% less than would occur under a constant weighting scheme. Similarly, stratum 2 comprised 9% of the survey area and accounted for 9 collections, resulting in a 18% reduction in the effective weight for these catches. In effect, changes in catch weights, brought about by the poststratification of the egg population into three statistical subpopulations of sample units, reduced the importance of high catches and strengthened the impact of low catches in the estimation of total daily egg abundance.

The allocation of samples within strata was not optimal for the minimum-variance estimation of total daily egg abundance under a STRS design. Stratum 1 had the highest standard error, yet sample size was only 7% of the total effort. The high sample heterogeneity in stratum 1 resulted from the high variability in spawning levels over small distances. While most catches were very large, stratum 1 also included a few samples having only a few eggs. As a mathematical procedure, the optimal allocation of sampling stations to strata is a function of the number of strata, stratum sizes, anticipated stratum variances, and the number of sampling stations that can be occupied during a survey. The values for these parameters were not known prior to the execution of the 1981 surveys since these surveys represent the first time that the egg population had ever been sampled.

The estimates under the SRS model (Tables 6 and 11) were deemed the most reliable, based on a subsequent examination of the stability of estimates under the SRS, DLN, and NB models, and were subsequently employed in the estimation of seasonal egg production and spawner biomass.







## Chapter 4. Simulations of field sampling

### INTRODUCTION

Estimates of mean daily egg abundance and associated measures of precision have been obtained for the 1981 spawning season under a variety of common models for catch data (SRS, DLN, NB, and STRS). Comparisons between the models in the previous chapter revealed that estimates of the mean differed relatively little on a survey by survey basis and that variance estimates were generally smallest under the skewed models DLN and NB. However, estimates were expected to show similarities because the same catch data were used in all formulae and some of the formulae were similar if not computationally identical. In addition, the reliability of parameter estimates has yet to be determined. For example, can the mean truly be known with greater precision by employing the DLN or NB models, as the magnitudes of the foregoing variance estimates have indicated?

The validity of parameter estimates depends ultimately on the validity of the assumptions made in order to invoke these models. It is useful to examine these models more thoroughly before standards are proposed for future assessments based on the results of the 1981 egg surveys. This chapter will address the following questions: How should the locations of sampling stations be distributed over the survey area? What is the most convenient and reliable model for estimating the mean and total egg abundance within a survey area? What method provides a truly minimum variance for an estimated mean?

Sampling and analytical standards must be established on the basis of limited field experience. If evaluations are to be based on actual field data, then many years of egg surveys would be required before the appropriateness of any of these models could be examined. However, it was not necessary to wait for the accumulation of field data. The suitability of these models to the present analytical problem could be evaluated by a computer simulation of field sampling, and the 1981 survey data were quite useful for this purpose.

The distribution and abundance of eggs were simulated by a 3-dimensional abundance surface that was constructed from egg catch data. Simulated egg catches were generated from this model according to either a random or systematic sampling design. In addition, this geometric interpretation of the spatial pattern of abundance permitted the determination of the "true" mean daily egg abundance for the simulated egg population. With this portrayal of population structure and sampling methodology, the numerical stability of parameter estimates and associated errors could then be evaluated as if replicate surveys had been undertaken. The statistical model to be preferred for the summary of catch data should provide estimates for mean egg abundance that are the least variable and biased, and should also lead to confidence intervals which include the true mean at a rate consistent with theoretical expectation.

The STRS model was not examined in the sampling simulations. A number of problems must be resolved before a realistic simulation of this design can be developed. For example, a systematic procedure is needed for varying the number, sizes, and locations of strata. Also, a systematic concentration of sampling effort in areas of high egg abundance is required since data from these strata are critical for the minimum variance estimation of the size of the simulated egg population.

#### METHODS

##### General characteristics of egg catch distributions

The statistical characteristics of a catch curve are determined by the scale of distance over which sampling is conducted. Distance scales can be categorized as global, intermediate, and local. When sampling is conducted over a global scale of distances, most catches will usually be found to contain relatively few eggs, and only a few catches, which happened to be obtained near spawning centers, will be extremely large. Under these circumstances, mean catch size will be

greater than the modal catch size.

If sampling is conducted over an intermediate scale of distances, each catch from a series of tows will often contain approximately the same number of animals. Given a rough stability in catch sizes at this scale, the size of a potential catch can be anticipated by the size of catches at nearby sampling locations. That is, large catches are found near the geographic position of other relatively large catches, and small catches tend to occur with other small catches. Since catch size is in large part a function of geographic position, changes in the magnitude of egg catches will occur with a directional displacement of a proposed sampling station to another location within an intermediate region. Catches may tend to decline regularly, to hold constant, or to increase regularly when sampling along an arbitrary transect line. It was assumed for the purpose of simulations that a planar surface adequately models the trend in catches over a limited geographic region.

Finally, the size of a catch is a random event over a local scale of distances. It was assumed that a catch in the vicinity of a sampling station was a random selection from a normal distribution of potential catches. Mean catch size at a simulated sampling station was modeled by the status of the planar surface at the geographic coordinates of the station. It was also assumed that catch variability was not constant throughout an immediate region, but was instead a function of this local mean catch size. That is, consistently small catches will be found in regions of few eggs, but regions of high egg abundance can yield extremely large as well as extremely small catches.

Formulae were developed for the global, intermediate, and local scales of distance and patterns of egg abundance on the basis of these reoccurring patterns.

### Construction of an egg abundance surface

A global region was defined by the geographic extent of the survey area, and intermediate regions were formed by partitioning the global region into a set of contiguous triangles (Figure 15). Intermediate regions were constructed such that no region overlapped another region and that no portion of the survey area remained unincorporated into a triangular region.

The vertices of these triangles represent the geographic positions of sampling stations. Station coordinates were converted from a system of latitudes and longitudes to a 2-dimensional position on the global plane. This conversion involved a series of transformations through a number of coordinate systems, and the essence of this process can be quickly summarized. A global plane was constructed tangent to a spherical Earth at a selected position within the survey area. The geographic position of each sampling station was transformed to a 3-dimensional system of Cartesian coordinates and then orthogonally mapped to the global plane. The transferral of points from the surface of a sphere to positions on a nearby plane resulted in little distortion to distances and areas because the overall dimensions of the survey area were not too extensive relative to the size of the Earth. Finally, a 2-dimensional Cartesian system was then imposed on this global plane. These axes were formed by projecting the north-south axis of the Earth onto the global plane and establishing another axis on the global plane orthogonal to the first axis; these axes were designated the Y and X axis respectively. The origins of both axes were located at the point of tangency between the spherical Earth and the global plane. The coordinates of the remapped sampling stations were expressed in terms of meters from the origin to be consistent with the units for egg abundances (eggs/day/m<sup>2</sup>).

The pattern of egg abundances over an intermediate scale of distance was modeled by a prismatic solid (Figure 16). The geographic

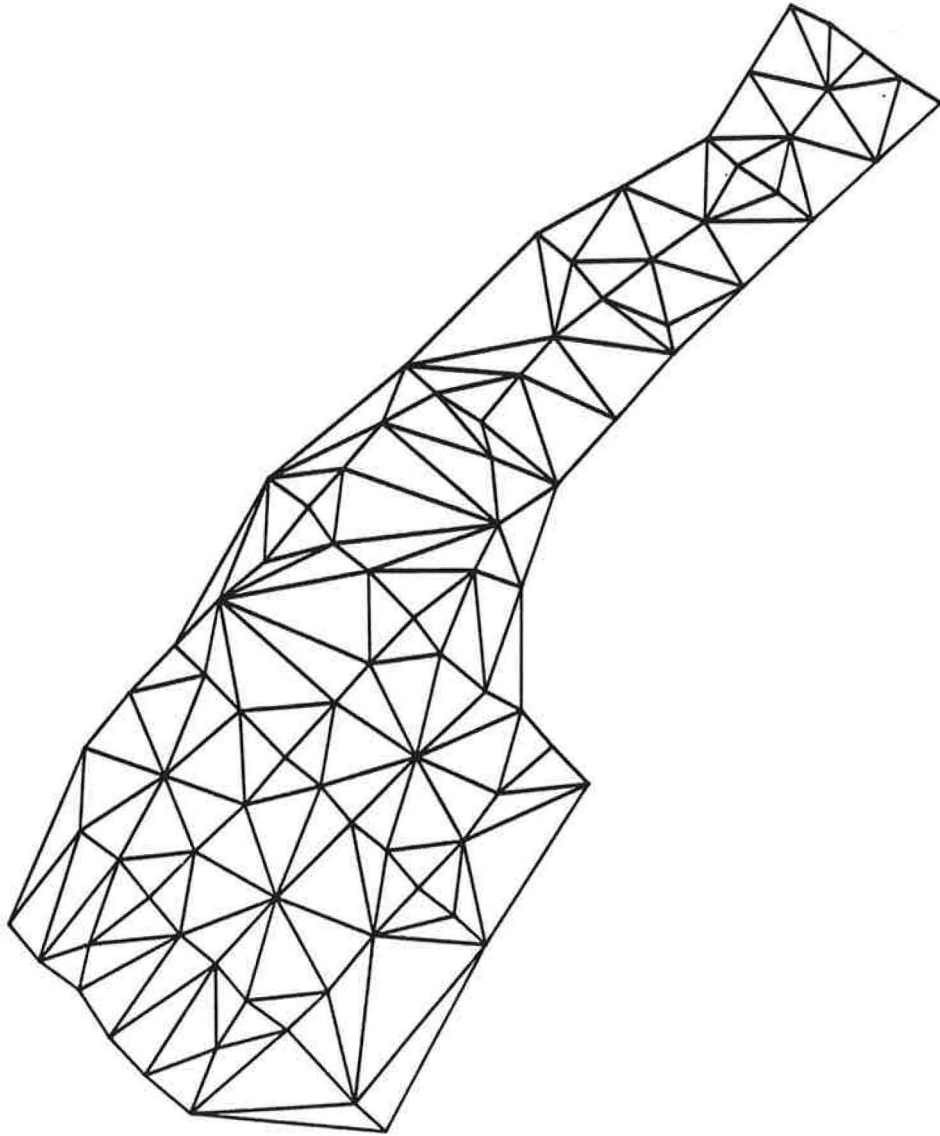


Figure 15. Global region A and intermediate regions of the survey area. Intermediate regions were constructed from position and egg abundance data from stations G001A-G083A of survey 2MF81.

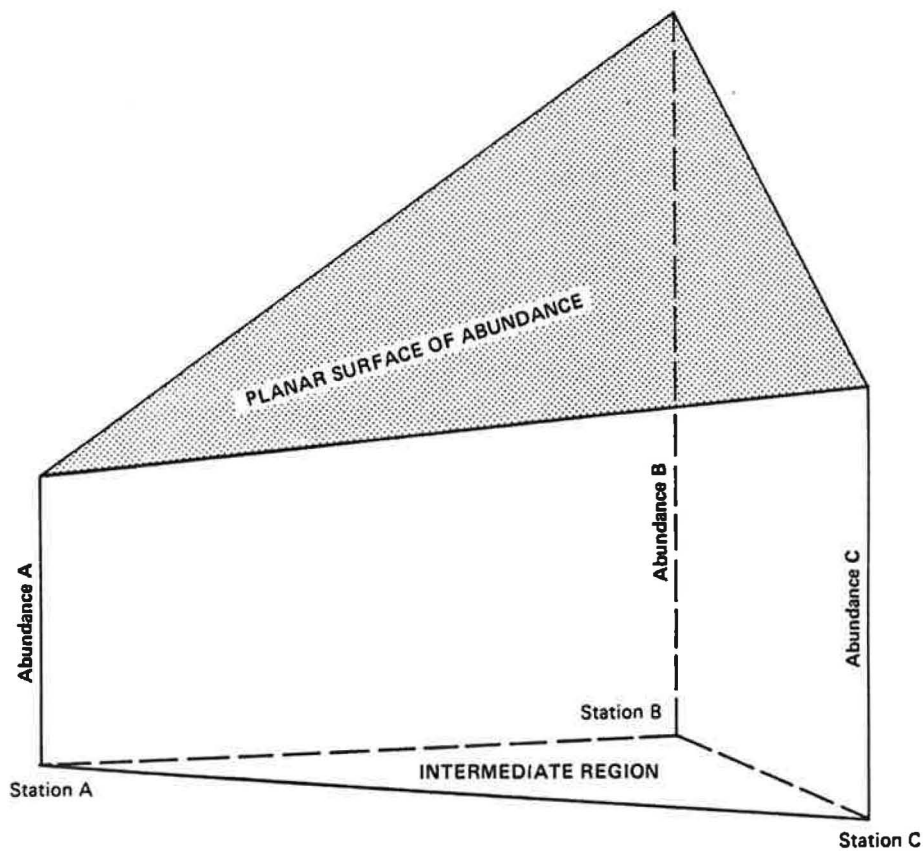


Figure 16. Wire diagram in the form of a prismatic solid depicting the pattern of egg abundances for an intermediate region. An intermediate region was defined by the positions of 3 adjacent sampling stations. The planar surface of abundance models the on-average continuity in egg abundances within the geographic limits of an intermediate region, and the volume of the prismatic solid represents total egg abundance within the region.

area defining an intermediate region is depicted as the triangular face forming the base of the solid. It will be recalled that the geographic extent of an intermediate region was determined by the locations of three adjacent sampling stations. Similarly, the pattern of egg abundances within the intermediate region was determined by the size of egg catches at these stations and the assumed planar trend in abundances. Each egg catch in Figure 16 is depicted as a height rising vertically from the prismatic base and the trend in abundance is depicted as a plane supported by these three heights.

Egg data were expressed as daily station abundances using 21 developmental stages:

$$(eq. 4.1) \quad A_j = \frac{\sum_{i=1}^{21} C_{ij}}{\frac{\text{day}}{24 \text{ hr}} \text{ PERIOD}_j}$$

where

$C_{ij}$  abundance of the  $i$ th stage at the  $j$ th station (eq. 2.7)  
 $\text{PERIOD}_j$  total development time from fertilization to the end of stage 21 at the  $j$ th station  
 $A_j$  daily station abundance (eggs/day/m<sup>2</sup>).

The numerator represents the abundance of eggs, irrespective of age, in a unit volume of seawater in the vicinity of the  $j$ th sampling station. Division by the period of time over which these eggs were spawned gives the average number of eggs spawned per day prior to the time of sample collection. PERIOD was obtained by evaluating eq. 2.1 with  $i=21$ . Egg mortality was ignored in this analysis. The focus of attention here is on the suitability of the catch curve models and the number of eggs actually spawned is not of immediate concern.

A local mean catch for any location within an intermediate region can be determined from the coordinates of a simulated sampling station and the assumed planar trend for the region:

$$(eq. 4.2) \quad ZMEAN = \frac{A X + B Y + D}{C}$$

where  
 X,Y coordinates of the simulated position within an intermediate region (meters from the origin of the global region)  
 A,B,C,D coefficients to the planar equation of abundance for an intermediate region  
 ZMEAN simulated local mean catch, the average number of eggs that may be captured per sample unit at the coordinates (X,Y).

A set of planar coefficients was determined from egg catch and position data for each intermediate region of the global surface.

Simulated global patterns of egg abundances were constructed from sets of prismatic solids (Figures 17 and 18). Total egg abundance for a global region was determined by summing the volumes of prismatic solids for all the intermediate regions defining a global region. The volume of each solid was determined by a double integration of eq. 4.2 between the geographic limits of the X and Y coordinates for the corresponding region. Mean egg abundance for a simulated egg population was determined by dividing total egg abundance by the size of the survey area.

Data from survey 2MF81 were chosen to define the spatial pattern of egg abundances to be used in simulations. The motivations for employing these data were twofold. Data collected by sampling at or near the time of peak spawning provided the most information as to the magnitude of seasonal egg production and, consequently, the behavior of analytical procedures using data collected near this point of the spawning season was of critical importance. Also, the dispersion and skewness of catch data were greatest near the time of peak spawning and, for this reason, the estimates of mean daily egg abundance were determined with the least precision.

Two quasi-synoptic sets of reference stations and egg catches were used to construct abundance surfaces A and B (Figures 17 and 18 respectively). Stations G001A-G083A represented the first sampling of the egg population during survey 2MF81, and these stations, designated

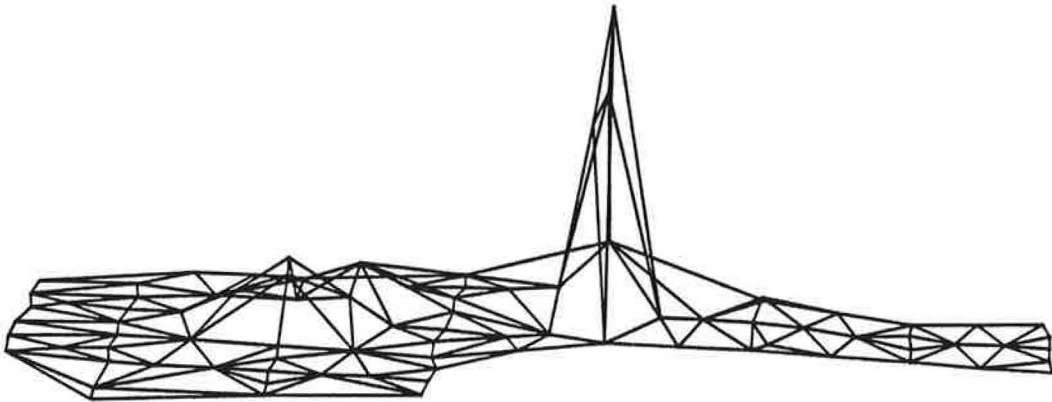


Figure 17. Global abundance surface A. This wire diagram was constructed from position and egg abundance data for stations G001A-G083A of survey 2MF81, with stations G084A-G091A excluded.

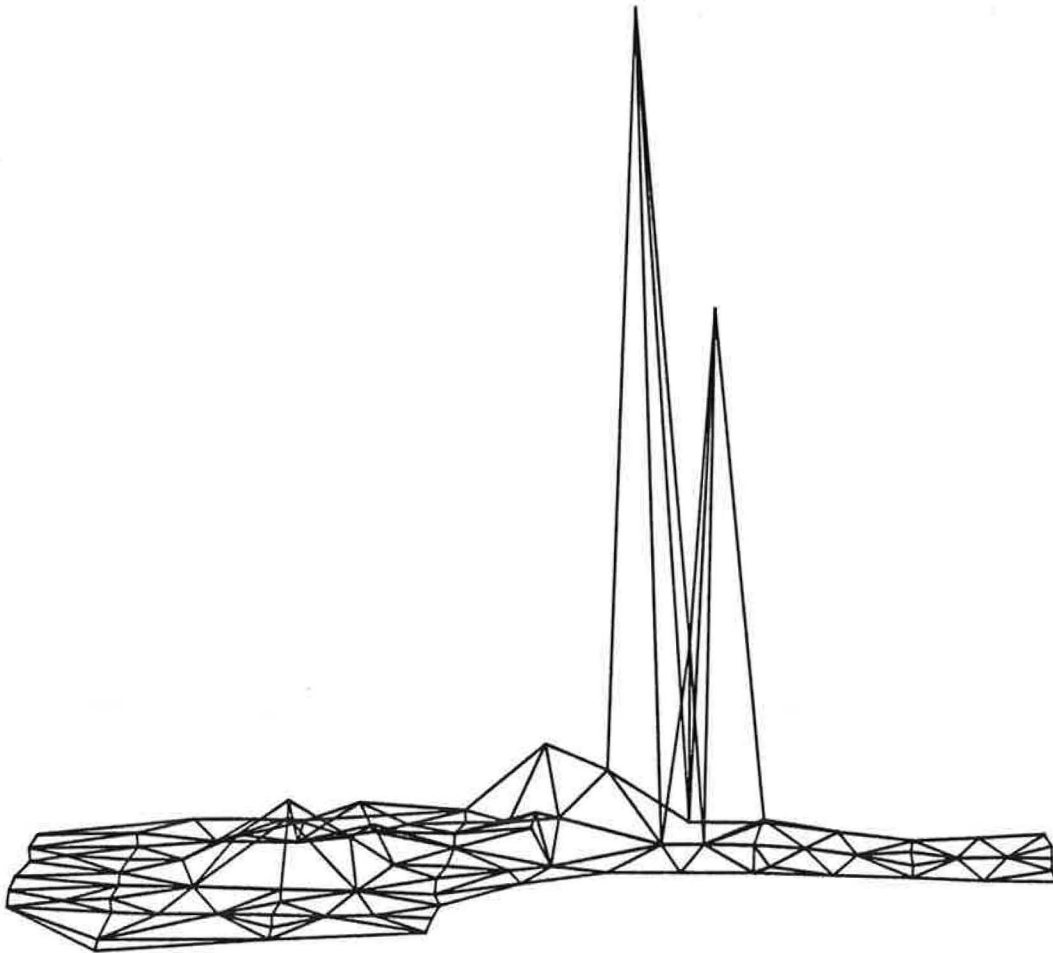


Figure 18. Global abundance surface B. This wire diagram was constructed from position and egg abundance data for stations G001A-G091A, less stations G022A-G024A, of survey 2MF81.

set A, were used to construct abundance surface A. Stations G084A-G091A were occupied as the survey area was retraced during sampling operations, and the catch data from these stations have been interpreted as a resampling of the egg population. It was assumed in the case of set A that data for the excluded stations G084A-G091A were overrepresentative of the true frequency of larger egg catches.

Set B was composed of stations G001A-G091A, less the stations G021A-G024A. It was assumed for the purpose of simulation that spawners had moved from the vicinity of these latter stations to areas nearer the geographic position of stations previously excluded under set A and that egg abundances had not measurably changed in outlying areas. Set B modeled the egg population approximately one week after the survey area was first occupied.

Additional reference stations with zero-valued abundances were also defined for each data set in order to extend the abundance surface to the perimeter of the survey area.

#### Simulation of an egg catch

The planar trend in egg catches over an intermediate scale of distances is not a completely realistic model of egg catches at a more local scale. In order to examine the impact of local catch behavior on the estimation of global mean abundance, it was assumed that the sizes of potential catches were normally distributed around the mean egg catch for a simulated sampling station and that the coefficient of variation for catches was constant throughout the survey area.

With the local mean and coefficient of relative variability both known, the former by eq. 4.2 and the latter as a given scalar value, the magnitude of a simulated egg catch could be randomly generated for a simulated sampling station from:

$$(eq. 4.3) \quad ZCATCH = ZMEAN + ZNORM (ZMEAN CV)$$

where  
 ZMEAN simulated local mean catch at the coordinates (X,Y)  
 ZNORM standard normal deviate, randomly generated using the IMSL routine GGNML  
 CV constant coefficient of local variation, indicating the relative variability of egg catches at all potential sampling stations within the survey area  
 ZCATCH simulated catch for the coordinates (X,Y).

This equation will now be explained in greater detail.

A low coefficient for local variability indicates that an egg catch provides a great deal of information as to the magnitude of catches in the immediate vicinity of a sampling station, while a high coefficient implies that simulated catches can vary at random over a wide range of values. For example, a CV of 0.5 implies a standard deviation equal to half the magnitude of the mean. Since two standard deviations to either side of the mean approximately defines the length of a 97.5% confidence interval for a population following a normal distribution, this coefficient indicates that most potential catches in the vicinity of a sampling station can range in size from approximately zero to double the size of the local mean egg catch. In contrast, a 0% coefficient of local variation indicates that every simulated catch that might be generated for a simulated sampling station will contain the same number of eggs, and catches at nearby sampling stations differ only in accordance with the planar trend in egg abundances for this region of the survey area.

The operation of eq. 4.2 can be made clearer by an examination of the three transformations involved. The coefficient of local variation, CV, was a constant supplied to the simulation model and was limited to a value between 0 and 1. Since CV is defined as the ratio of one standard deviation to the mean, it represents a fixed level of relative variability in potential catches around each local mean. Relative catch variability was converted to absolute catch variability by multiplying CV by ZMEAN. This product represents one standard deviation around the value for a local mean, ZMEAN.

A randomly generated value from the standard normal distribution, ZNORM, was then scaled by the derived estimate of local absolute catch variability, (ZMEAN CV). This randomly generated adjustment, ZNORM (ZMEAN CV), was then added to a simulated local mean, ZMEAN, to yield a simulated catch, ZCATCH. Each adjustment had an equal chance of being either positive or negative since the standard normal distribution is symmetrical and has an expected value of zero. Since the potential catches for a sampling station were assumed to be normally distributed, each adjustment had a 63% probability of occurring within one standard deviation to either side of zero and a 97.5% probability of occurring within two standard deviations to either side of zero. A simulated catch was set to zero on the rare occasion that a negative value for ZCATCH was generated by an extremely negative value for ZNORM.

#### Survey simulation

Both random and gridded (regular or systematic) distributions of sampling stations were modeled. The number of stations occupied during survey 2MF81, n=89, was assumed to approximate the average sample size attainable under normal survey operations. Accordingly, the number of simulated stations generated for each sampling experiment was set to n=90 for the random sampling design. The coordinates for each simulated station were obtained by first making two calls to a random number generator, a Burrough's FORTRAN intrinsic function, followed by rescaling to a position within the survey area.

The gridded design was not as easy to simulate. During the 1981 surveys the distances between stations of the survey grid were greater along the axis of Shelikof Strait than transverse to it. A grid template was constructed with interstation distances of 12 km along and 4.5 km transverse to the main axis of the Strait, and this specification permitted approximately n=85 simulated stations per sampling experiment. Each generation of a gridded station pattern was preceded by a random positioning of the first station within the survey area.

Statistical summary of catch data from simulated egg surveys

One hundred simulated surveys were generated for each selected combination of abundance surface A or B; a 0%, 25%, or 50% coefficient of local variation; and a random or a gridded sampling design. Estimates of mean daily egg abundance and variance of the mean were determined for each simulated survey under the catch curve models SRS, DLN, and NB. Confidence intervals were constructed under the assumptions that simulated egg catches were statistically independent of one another and that each set of simulated survey data was representative of the true frequencies of eggs per sample unit in the simulated populations.

Statistics employed in the comparison of confidence intervals

Four aspects of confidence intervals were selected to evaluate the catch distribution models: average length of confidence intervals, variability in confidence interval lengths, root mean squared error, and the rate of containment of the true mean by confidence intervals constructed for the simulated surveys.

Minimum variance is an important criterion for assessing the suitability of a statistical model, and the average length of confidence intervals provided a graphic portrayal of this characteristic:

$$(eq. 4.4) \quad AVGLEN = \frac{\sum_{q=1}^Q (CLHI_q - CLLO_q)}{Q}$$

where

Q                    number of simulated surveys generated from a global abundance surface (Q=100)  
 CLHI<sub>q</sub>            upper confidence interval limit for the qth simulated survey  
 CLLO<sub>q</sub>            lower confidence interval limit for the qth simulated survey  
 AVGLEN            average length of 97.5% confidence intervals under the current statistical model and data set.

The numerical stability of variance estimates is reflected in the variability of confidence interval lengths. Thus, the model which generated confidence intervals with the least variability in length may also be expected to provide, on average, the most reproducible estimate of the precision of the estimated mean:

$$(eq. 4.5) \quad S^2(CILEN) = \frac{\sum_{q=1}^Q [(CLHI_q - CLLO_q) - AVGLEN]^2}{(Q - 1)}$$

where

$S^2(CILEN)$  sample variance for the length of confidence intervals.

Root mean squared error is a measure of the variability in the estimated mean relative to the true mean egg abundance. The statistical model with the lowest root mean squared error can be expected to provide an estimate of mean daily egg abundance that is the least biased and the least variable:

$$(eq. 4.6) \quad RMSE = \left[ \frac{\sum_{q=1}^Q (m - MTRUE)^2}{Q} \right]^{1/2}$$

where

$m$  sample mean for the  $q$ th simulated survey under the current statistical model

$MTRUE$  true mean density for the appropriate abundance surface

$RMSE$  root mean squared error.

Containment rate represents the frequency with which confidence intervals include the true mean. Confidence intervals should include the true mean in 97.5 out of 100 cases if the assumptions of representative sampling, model appropriateness, and normality in the sampling distribution of means at the given sample size were adequately met.

## RESULTS

Appendix Figures B.1-B.18 depict the estimated mean and 97.5% confidence interval for each simulated survey generated from either global surface A or B. The vertical line in each Figure indicates the

magnitude of the true global mean for the corresponding abundance surface. Appendix Figures B.1-B.6 were derived under a random sampling design and a 0% coefficient of local variation; Appendix Figures B.7-B.18 were derived under a gridded sampling design and a 0%, 25%, or 50% coefficient of local variation.

Negative lower limits to confidence intervals were obtained for some models. Although only nonnegative ranges have meaning in the description of animal abundances, no distinction is made by the models between positive and negative values. The SRS model yielded negative lower limits with approximately a 1% frequency when sampling from abundance surface A and with a 25-30% frequency when sampling from abundance surface B. The confidence intervals for the DLN model had negative limits when sampling was at random from surface B or when the coefficient of local variation was set as high as 50%; but in both of these cases the frequency was less than 10%. No negative lower limits were produced by any other permutation of abundance surface, coefficient of local variation, and sampling design.

The estimates of central tendency for abundance surface B under the random sampling design ranged over one order of magnitude, specifically 26-360 eggs/day/m<sup>2</sup> for the SRS and NB models and 26-291 for the DLN model. Under a systematic sampling of abundance surface B, however, estimated means ranged only from 2-3 times the lowest value, specifically 79-263 for the SRS and NB models and 110-182 for the DLN model. A 0% coefficient of local variation was used in generating the simulated catches by which these ranges were derived; the ranges were greater for larger values of this coefficient.

Statistics derived from the means and confidence intervals under the DLN, SRS, and NB models are summarized in Table 12 for simulated surveys constrained to a 0% coefficient of local variation.

The statistical model which seemed the most appropriate depended on the data set available. No model was consistently superior in

=====  
 Table 12. Confidence interval statistics under the delta (DLN), simple random sampling (SRS), and the negative binomial (NB) models for catch data from survey 2MF81. The coefficient of local variation was set to a constant 0% prior to the generation of simulated catches. The true mean was 123 eggs/day/m<sup>2</sup> for abundance surface A and was 136 for abundance surface B.  
 =====

model:	DLN	SRS	NB
-----			
random sampling --			
average confidence interval length / standard deviation:			
abundance surface A	212/139	156/ 50	52/ 17
abundance surface B	163/ 97	233/142	58/ 29
root mean squared error:			
abundance surface A	76	39	39
abundance surface B	57	66	66
rate of containment:			
abundance surface A	89	93	49
abundance surface B	71	74	30
grid sampling, with data treated as if obtained under a random sampling design --			
average confidence interval length / standard deviation:			
abundance surface A	195/ 28	169/ 25	55/ 5
abundance surface B	157/ 41	254/ 86	60/ 16
root mean squared error:			
abundance surface A	30	12	12
abundance surface B	27	36	36
rate of containment:			
abundance surface A	100	100	99
abundance surface B	100	99	64

=====  
 providing estimates of the mean with the least variability and bias. Regardless of whether sampling of the abundance surfaces was systematic or random, minimum RMSE for set A was achieved under the SRS and NB models and minimum RMSE for set B was achieved under the DLN model; the SRS and NB models behaved identically since the computational formulae for mean egg abundance were identical (eqs. 3.2 and 3.14).  
 =====

The NB model had the narrowest confidence intervals for all

models. For the DLN and SRS models, the model with the smallest average length for confidence intervals varied with the global pattern of abundance. The average length was smallest for the SRS model when sampling from surface A and was smallest for the DLN model when sampling from surface B.

The systematic sampling design was superior to the random sampling design in estimating the mean. Regardless of the model employed to summarize the catch curve, RMSE was reduced by about half when sampling was systematic throughout the survey area rather than at random. Thus, the gridded sampling design appeared to provide greater numerical stability in an estimate of mean egg abundance.

Model for model, the average length of confidence intervals was approximately equal for both random and grid sampling. However, the variability in interval length under a gridded sampling design was approximately half that found under the random sampling design. Thus, an estimate of confidence interval length appeared to be more numerically stable under the gridded sampling design.

Containment rates were substantially larger under the gridded sampling design than the random sampling design. Under the random sampling design, the rates of containment for the SRS and DLN models were 70-90% for either abundance surface, instead of the 97.5% that was expected. In contrast, containment rates under a gridded sampling design approached or reached 100%, regardless of whether sampling was from abundance surfaces A or B. Confidence intervals were therefore excessively large since the accuracy of an estimated mean was greater than would be implied by the calculated 97.5% probability of containment. The NB model had containment rates approaching only 30-50% under a random sampling design and 65-100% under a gridded design.

The higher rates of containment under the gridded design persisted as the coefficient of local variation was increased to 25% and 50% in

simulations. Containment rates for surface B under a gridded sampling design and a 50% coefficient of local variation were 95% for the SRS model, 97% for the DLN model, and 47% for the NB model. These rates were only slightly lower than those produced under the gridded design and a 0% coefficient of local variation; specifically, 99% for the SRS model, 100% for the DLN model, and 64% for the NB model (Table 12). In contrast, when sampling was indeed at random, as assumed when the catch curve models were invoked, and the coefficient for local catch variability was set to 0%, the containment rates were 74% for the SRS model, 71% under the DLN model, and 30% under the NB model (Table 12). The effects of the 25% and 50% coefficient of local variability are illustrated for the systematic sampling of surface B in Appendix Figures B.9-B.10 for the DLN model, Appendix Figures B.13-B.14 for the SRS model, and Appendix Figures B.17-B.18 for the NB model.

#### DISCUSSION

The purpose for constructing the abundance surfaces should be clearly recognized. The validation of earlier estimates for egg abundance in Shelikof Strait was not a goal since actual distributions and abundance levels throughout the survey area were known only to a limited extent. Nor was it intended that the two abundance surfaces represent identical magnitudes of egg abundance. Instead, surfaces A and B (Figures 17 and 18) represented two plausible patterns for the distribution and abundance of eggs within the survey area near the time of peak spawning, insofar as the available data indicated. The intent was to investigate how reliably the catch curve models SRS, DLN, and NB defined the simulated egg populations.

A mathematical model was required to describe both the abundance and the spatial distribution of eggs within the survey area. The complexity of the model that was developed was necessitated by the complexity of both the abundance pattern and the sampling design. Narrow aspects of the sampling experiment could have been modeled by a simple statistical model in the interest of a quick assessment.

However, such a simplification would have been done at the risk of ignoring potentially pivotal components in the analytical problem. For example, such classical models as the normal, lognormal, or negative binomial distributions do not adequately model the egg population nor the sampling experiment; and consequently, these models should not be used to generate simulated catches. A minimally realistic model for egg abundances must accommodate the contagious, rather than independent, distribution of eggs over space. Moreover, the sampling component of the model must accommodate a random sampling design, to be consistent with the statistical theory underlying the catch curve models, and a systematic (gridded) sampling design, to be consistent with actual survey practices.

Only qualitative comparisons were of interest in this analysis and comparisons were limited to the magnitude and variability of means and confidence interval lengths. Specific results were dependent on the spatial pattern of egg abundances and on the sample size used when sampling the idealized egg populations. In addition, the specific results for the gridded sampling design were dependent on interstation distances and the orientation of the grid template. A consistent oversampling or undersampling of egg concentrations could arise from differing specifications of global abundance pattern, sample size, interstation distances, or grid orientation.

Two abundance surfaces were constructed in an attempt to realistically simulate the distribution of eggs and the heterogeneity of egg catches to be expected when sampling near the time of peak spawning. Some of the highest egg catches occurred at stations G084A-G091A, but these stations are specifically excluded from set A in order to provide a more representative and synoptic description of egg abundances. Since the standardized catches at these excluded stations were often extremely large ( $>25,000$  eggs of all ages/m<sup>2</sup>), the range of catches obtainable under most simulations was smaller than might have otherwise have been generated. Thus abundance surface A may conservatively model the heterogeneity of egg catches obtainable near

the time of peak spawning. On the other hand, abundance surface B included these catches while excluding the relatively large catches from stations G022A-G025A; and future sampling may reveal that this model for egg catches may approach the greatest degree of heterogeneity to be expected from sampling the Shelikof egg population.

#### Confidence intervals for the NB model

The confidence intervals for the NB model were entirely too small, indicating that the maximum likelihood estimator for the variance of the mean (eq. 3.16) was inappropriate for the sample size available. Statistical theory for the construction of maximum likelihood estimators relies on the large sample behavior of the sampled variate and, therefore, the catch data must be truly representative of the sampled population, and not merely assumed to be representative, in order to safely invoke these estimators. No universal guideline can be given as to how many observations are sufficient to be considered as a "large" sample size, but 30 or more is generally considered adequate for most statistical models (Elliott, 1979). However, these simulations have demonstrated that a sample size of 90 was too small for the normality assumption to be valid. An asymmetrical confidence interval is needed to adequately characterize the probable magnitude of the true mean on the basis of a single survey.

In addition to the dependence on large sample size, the NB model is also extremely flexible in the shape of catch curves that can be accommodated, and is therefore more sensitive to small changes in the information provided by catch data. Lognormal models, on the other hand, assume that the distribution of logarithmically transformed data at least approximates a normal curve, and all deviations from this assumed shape will then contribute to the variance of the estimated mean. There is no such constraining shape under the NB model. Sample frequency distributions ranging from a lognormal ( $k = 0$ ) to a completely random distribution ( $k$  very large) can all be approximated by the NB distribution. Therefore, although the NB is much more

flexible in the range of catch curves that can be modeled and therefore appears to be useful under a variety of data sets, this model is also demanding in its requirements for data. When sample size is small and the true distribution of abundances is highly skewed, the frequencies of extremely large egg catches will seldom approximate true proportions, and the frequencies in this upper region of a catch curve is critical to obtaining reliable estimates of both the mean and dispersion.

Small sample approximations to the NB model were not simulated. Normality-promoting transformations of the catch data are based on the presumed value for the shape parameter  $k$  (Anscombe, 1948; Elliott, 1979) and are very inefficient when  $k$  is less than 2.0 (Anscombe, 1949). The estimated value of  $k$  for survey 2MF81 was 0.2 (Table 8).

#### Low containment rates and a random sampling design

The low containment rates that occurred under the random sampling design were a result of a small sample size and the assumption of normality for the sampling distribution of sample means. An estimate of the mean is a random variable since it is constructed from  $n$  independent, identically distributed, random observations from the population of potential egg catches. One version of the Central Limit Theorem of statistics states that, for a sufficiently large sample size, the sampling distribution for all means of size  $n$  will conform to a normal distribution regardless of the normality or lack of normality in the original distribution of the sampled variate. Under this circumstance the assumption of normality can be invoked for the construction of a symmetrical confidence interval around an estimated mean.

The number of samples necessary to confidently invoke the assumption of normality depends upon the skewness of the distribution of the sampled variate. Few observations are required for distributions having a near-normal shape and a very large sample size

is necessary for an extremely skewed distribution. When  $n$  is less than "sufficiently large", the sampling distribution for all possible estimates of the mean will display an intermediate degree of skewness between that of the original distribution of the sampled variate and the normal distribution, and this skewness will become more and more pronounced with an increasingly smaller sample size.

One consequence of the residual skewness in the sampling distribution of sample means, as a result of an insufficiently large sample size, is that the dispersion of the statistical population will often be underestimated under a random sampling design. With an "insufficiently large" sample size, most randomly obtained catches will still cluster around the modal catch size and extremely few egg catches, if any, will be very large. With the true frequency of very large catches therefore underreported, the estimate of dispersion will be biased downward from the true value. As sample size increases, the expected value for the variance of the mean will, on average, increase toward the true value. However, until the sample size becomes "sufficiently large", the assumption of normality is inappropriate for the construction of confidence intervals and asymmetrical confidence intervals are again required in order that the true mean be included with the probability expected.

#### High containment rates and a systematic sampling design

When using statistical models based on random sampling theory to summarize egg catch data, it might be thought desirable that sampling be conducted at random coordinates within the survey area in order not to bias the estimation procedure in some undesirable manner. Indeed, it was assumed that a random sampling design was implemented when invoking the catch curve models SRS, DLN, and NB. In the simulations of field sampling, however, RMSE and the variability of confidence interval lengths were smallest and containment rates were largest under the systematic, rather than the random, sampling design. Moreover, the frequency with which confidence intervals contained the true mean was

equal to or greater than the frequency expected. These results can best be explained by relating the spatial distribution of potential catches within the survey area to the theoretical catch curve, which shall be defined as the hypothetical curve representing the frequency distribution of potential catches for all possible sample units defining the survey area.

Sample units can be characterized as to abundance and location. Each sample unit contains a fixed number of eggs since a survey is considered to represent a synoptic and therefore static view of egg abundances throughout the survey area. Each sample unit is also associated with a unique set of geographic coordinates.

In contrast to Figure 16, in which both the magnitude and physical locations of potential catches are emphasized, a frequency distribution of egg catches emphasizes only the catch component of collections and provides no information as to geographic position. Position information is usually of no interest in the construction of a frequency distribution.

In Figure 19 a hypothetical frequency distribution is constructed for the intermediate region of Figure 16. A region will typically contain a very large number of sample units. For example, the 1981 ichthyoplankton surveys sampled an area of approximately  $10^{10}$  m<sup>2</sup>, with each m<sup>2</sup> column representing a sample unit. If the survey area was partitioned into 100 intermediate regions of equal size, then each region would be composed of 100 million sample units. However, for ease of illustration, the region of Figure 16 is considered to be composed of very few sample units.

Each possible egg catch for the intermediate region of Figure 16 is represented by X's in the frequency distribution in Figure 19. The lowest catch, which was associated with station A of Figure 16, is located to the far left of the frequency distribution and the highest catch, which was associated with station B, is located to the far

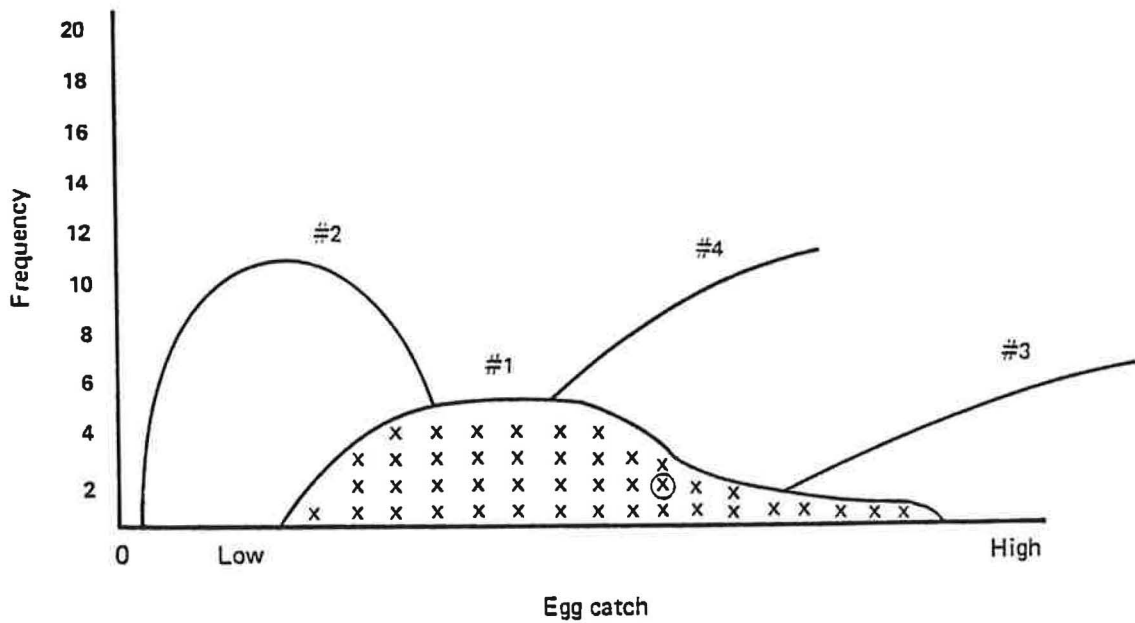


Figure 19. Hypothetical frequency distributions of potential egg catches from several intermediate regions of the survey area. The distributions for these hypothetical regions are indicated by the numbers 1, 2, 3, and 4. All potential catches for region 1 are indicated by X's. For each region, egg abundances are relatively homogeneous in magnitude and range over only a portion of the total range of abundances for the entire survey area. A single collection is taken from each region out of all the potential sample units available for that region. For intermediate region 1 this particular sample unit is indicated by the encircled X.

right. All catches for the remaining potential sample units are distributed between these delimiting extremes, but the tallying of frequencies for catches follows no particular sequence over the geographic extent of the intermediate region. In other words, there is no way of relating an X with the geographic position of a sample unit once the potential catch has been tallied. The fact that all sample units for the intermediate region are tallied before proceeding to the tallying of another region is sufficient to allow the consequences of a systematic sampling of an unacknowledged trend in egg abundances to be illustrated.

Any number of sample units may be taken from an intermediate region during the course of a synoptic survey, but typically only one collection is taken and the catch is subsequently extrapolated to the entire region. The encircled X in Figure 19 represents the magnitude of one such catch obtained at a hypothetical sampling station.

Figure 20 illustrates a geography-based interpretation of the frequency distribution of all potential catches for a survey area. The distribution is partitioned into clusters of sample units in such a way that the geographic association between sample units from each intermediate region is preserved. The construction of this theoretical distribution would proceed in the following way. The survey area is partitioned into a number of separate and contiguous intermediate regions. Starting with one arbitrarily selected region, the potential egg catch for each sample unit is added to the developing frequency distribution, and all potential catches are tallied before proceeding to a subsequent region of the survey area. This process is repeated until all intermediate regions are accounted for. Again, one collection is taken from each region and the magnitude for this sample unit is indicated in Figure 20 by an X in each region of the theoretical catch curve.

A visual examination of Figure 20 leads to several observations and conclusions. It should be apparent that the range of catch

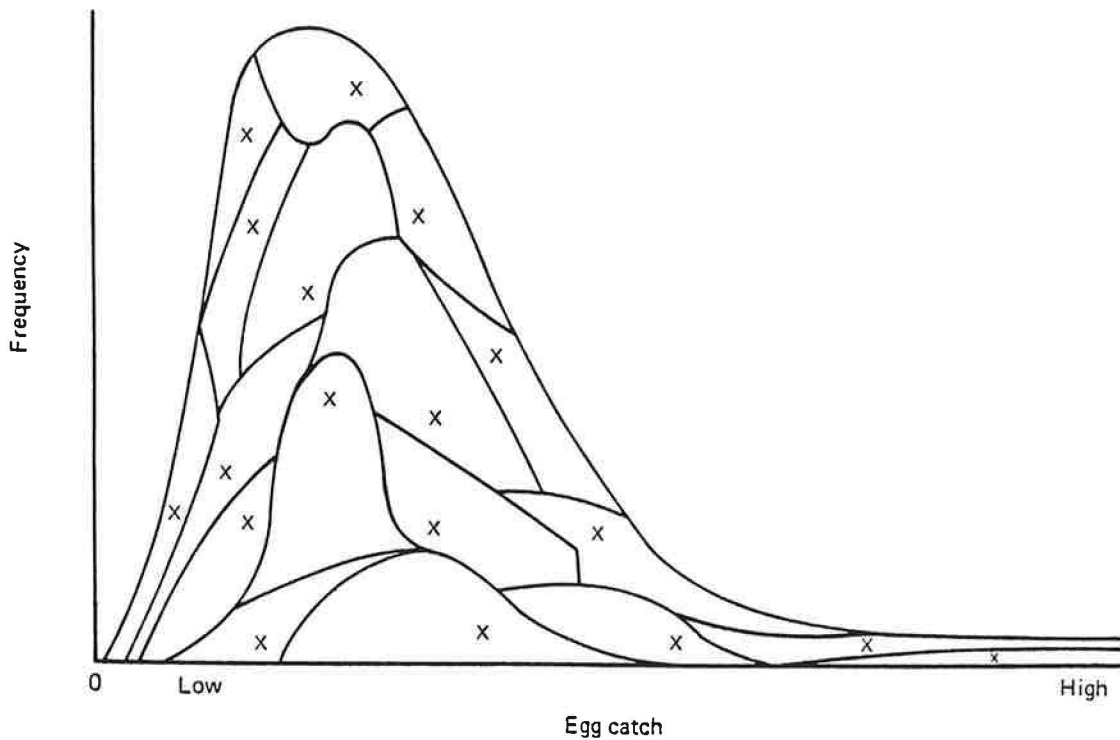


Figure 20. Hypothetical frequency distribution of potential egg catches from all intermediate regions of the survey area. A single collection is systematically taken from each region and the magnitudes are indicated by X's. If a sample frequency distribution was constructed using all collections from every region of the survey area, this distribution would provide a good approximation to the true distribution of egg abundances. A random sampling design would often fail to sample regions having relatively high egg abundances because these regions are so uncommon. However, a systematic sampling throughout the survey area of the systematic trend in egg abundances is often much more successful in obtaining egg abundances in their true proportions.

magnitudes for all the potential samples of a region is substantially smaller than the range of catch magnitudes for the entire survey area. Furthermore, this range varies with region. The range of potential catches is relatively small for most regions; and while a few regions have a wide range of potential catches, the size of most of these catches are all relatively large. As a consequence, it can be seen in Figure 20 that a systematic distribution of sampling effort throughout the survey area often results in a sample frequency distribution that provides a good approximation to the shape of the theoretical catch curve. Each subrange for the theoretical curve is represented in approximately its true proportion by the corresponding frequencies of sampled catches. And since the shape of the theoretical distribution is more reliably determined by this systematic sampling design, all statistical characteristics of the theoretical catch curve would also be determined with greater numerical stability. Finally, since the systematic placement of sampling stations is seen to be more important than increasing the number of randomly placed stations, this proportional sampling of the egg population could conceivably be obtained by almost any feasible sample size.

The characteristics of the sampled population can be known with substantially greater precision under a systematic sampling design even though the relative variability of catches at a sampling site may be high. The fact that all catches from the intermediate region of Figure 16 all cluster around approximately the same catch size in Figure 19 indicates that this intermediate region is highly homogeneous in egg abundances and that the coefficient of variation for this region would not be large. However, should the coefficient of variation be sizeable for this and all other regions of the survey area, then the frequency distribution for each region (Figure 20) would take on a much flatter shape and cover a larger range of catch sizes than is depicted here. Still, the systematic distribution of sampling stations throughout the survey area would yield a sample frequency distribution that closely resembled the theoretical catch curve in the relevant statistical properties. This is true because the range of potential catches for

any particular region is still smaller than the range for the entire survey area and is often substantially smaller. Since low abundances are often found with other low abundances, an egg collection made in a region of this type will have essentially no chance of being large. And although a small catch may be obtained in a region of generally high abundances, more often than not the collection will contain a large number of eggs. Thus, even though the local variability of catches is large, a systematic distribution of sampling stations would still tend to obtain catches in their true proportions relative to that obtainable under a random sampling design.

In contrast to the results obtained by systematic sampling, a random sampling scheme would guarantee a heavy sampling of sample units with catches approximating the modal catch size. This is true because small catches are the most numerous and therefore the most probable when selecting sample units at random. Furthermore, a random sampling scheme would fail to ensure that the long tail of the theoretical catch distribution be sampled in its true proportions unless sample size was "sufficiently large".

#### Modeling the spatial trend in egg abundances

Increases in the accuracy and precision of estimates for both the mean and total egg abundance for a survey area come about through recognition of the inherent structure in the analytical problem. The catch curve models only summarize a narrow aspect of the statistical information contained in egg data, such as the central tendency and dispersion of egg catches in a sample frequency distribution. It should be clearly recognized that these are characteristics of a catch curve per se and not the probabilistic behavior of individual samples.

It is usually desired that sampling be conducted in such a way that observations may be considered independent of one another. When samples are independent, the statistical information provided by a single sample provides absolutely no information about realization in

any other potential sample. In reality, the size of an egg catch is not independent of the size of catches at nearby stations, but instead partakes of what might be likened to an on-average continuity in egg abundances over space. The spatial component of egg abundance data is inappropriately ignored when attention is concentrated solely on the characteristics of the catch curve. The success of the grid design over the random sampling design indicates that additional information is contained in sample data for the definition of population structure that is not being utilized by the catch curve models. This behavior is a manifestation of the fact that animals typically do not occur at random throughout their environment.

The information provided by an egg catch can be partitioned into two components:

$$(eq. 4.7) \quad ZCATCH = SIGNAL + NOISE$$

where

SIGNAL	systematic trend in egg abundances over space
NOISE	random component to egg abundances at a location
ZCATCH	observed catch at a sampling station.

The signal is treated as having a value of zero when the catch is truly a random variable, and the catch frequency distribution can be characterized, under the assumption of random sampling, by the first and second sample moments without loss of information if nothing else were known about the true distribution of egg abundances.

It is often noted that the catch curves for sample data are positively skewed. Since this prior knowledge consistently appears valid, the various lognormal and negative binomial models should allow the variance of the mean to be reduced relative to the variance under a simple random sampling design. However, the magnitude of the shape parameter for these skewed models must be well estimated in order to safely invoke these variance estimators for the mean. The shape parameter is often not well estimated when the sampled population exhibits a high degree of heterogeneity in catch sizes or when sample size is small. Large catches are extremely rare and are often not well represented in the sample data, but these data are highly important in

determining the magnitude of the shape parameter. Since sample data are then only minimally representative of the egg population (and the spatial trend in abundances was ignored), these models of the random error component may often be less useful than one would hope.

The STRS model provides a convenient means to anticipate the specification of a spatial trend in egg abundances. Eq. 4.7 now becomes:

$$(eq. 4.8) \quad ZCATCH_h = SIGNAL + NOISE_h$$

where

SIGNAL zero, again indicating no systematic trend  
 NOISE<sub>h</sub> random component for the hth statistical subpopulation within the survey area, again characterizable as to the first and second sample moments  
 ZCATCH<sub>h</sub> observed catch size at a sampling station from the hth stratum.

Assume now that a catch can be partitioned into a trend over space and a random fluctuation. If the mean abundance could be anticipated for a region prior to sampling, this information can be entered into the individual catch equation by equating SIGNAL to a particular value for mean egg density on a stratum by stratum basis:

$$(eq. 4.9) \quad ZCATCH_h = SIGNAL_h + NOISE_h$$

where

SIGNAL<sub>h</sub> the anticipated constant defining average daily egg abundance for the hth statistical subpopulation.

The expected value of the noise component now represents a small positive or negative adjustment to the anticipated average, and the variance of the noise component is again greater than zero.

A more realistic portrayal of abundance pattern and systematic sampling design would appear to be available through the techniques developed in the field of geostatistics (Agterberg, 1974; Ripley, 1981). The trend of eq. 4.9 need not be defined simply as a constant. For example, the characterization of the spatial trend could be represented by a continuous polynomial of higher order in the two variables for position:

$$(eq. 4.10) \quad ZCATCH(X,Y) = TREND(X,Y) + NOISE$$

where

TREND(X,Y) status of the spatial trend in abundance at the coordinates (X,Y)

ZCATCH(X,Y) observed catch at any geographical coordinate (X,Y).

The behavior of the random error may be assumed to conform to some probabilistic law, but the trend component is of greater interest. The trend function describes the systematic pattern in animal abundance over the survey area, and one mathematical form of this function might be:

$$(eq. 4.11) \quad T(X,Y) = a + bX + cY + dX^2 + eXY + fY^2$$

where

a,b,c,d, coefficients to a complete quadratic surface in two dimensions.  
e,f

The distinction between the trend and the error component is somewhat arbitrary and will usually have to be defined by experience since, in a sense, two pieces of unknown information are desired from each egg catch: the status of the trend at the geographic coordinates of the sampling station and the current realization of a completely random event. Because of this ambiguity between the trend and error components for each egg catch, it will be necessary in practice to adopt a consistent mathematical model for the characterization of the trend. This is completely analogous to the common practice in linear regression methodology of first hypothesizing a linear relationship between a predictor and a variable based on the consistent empirical behavior of these factors and then deriving the coefficients defining this relationship.

Although higher order expressions in the two predictive variables of position can be hypothesized and fitted to a data set, the quadratic equation (eq. 4.11) is probably sufficient to accommodate a concentration of animals without fitting an expression too exactly to an available set of survey data at the cost of an inappropriately small error term. Multiple concentrations of eggs within a survey area could be accommodated by fitting a quadratic trend separately to each concentration. When station coordinates are expressed in meters, the integration of the volume beneath these fitted trend surfaces would

provide the estimate of total egg abundance. Error terms might also be projected to the total as the estimate of precision for the mean or the total.

Trend fitting is likely to result in a considerably smaller variance estimate for a total but the implementation of this procedure is beyond the scope of this thesis. If the error term is not of critical interest and a point estimate for total daily egg abundance is all that is desired, then a relatively stable estimate can be obtained very simply. The first requirement of this approach relates to sample collection: the density of sampling effort should vary over the survey area. Stations should be more closely spaced in regions of high egg concentrations and more widely spaced in regions of low egg concentrations. Since the upper limb of the theoretical catch distribution is critical to the stable estimation of mean egg abundance, the concentration of sampling stations in areas of high abundance would cause this region of the catch curve to be more thoroughly determined. However, catches must now be weighted to reduce the impact of this systematic oversampling of a few regions:

$$(eq. 4.12) \quad TOTAL = \sum_{j=1}^n POLYAREA_j A_j$$

where

n	sample size
POLYAREA <sub>j</sub>	polygonal area for the jth station by the Sette and Ahlstrom method (1948)
A <sub>j</sub>	daily station abundance for the jth station (eq. 2.9)
TOTAL	total daily egg abundance for the survey area.

Polygonal station weights will be smallest for closely spaced stations and largest for the widely dispersed stations. The importance of any one station on the magnitude of the total would be indicated by the relative size of each product in eq. 4.12, and these terms should be examined to verify the adequacy of the sampling design. A few data points should not account for a large percentage of the estimated total.

A weighted variance may also be calculated, but this estimate is likely to be excessive since sampling is systematic rather than at

random and since the trend in egg abundances is ignored. In fact, all variance estimates are likely to be excessive without a rigorous definition of the spatial trend incorporated into the analytical procedure, for otherwise this information on the systematic variation in catches is consigned to the "catchall" noise component.





## Chapter 5. A new approach to the estimation of seasonal egg production and egg mortality

### INTRODUCTION

It has long been recognized that a cohort can be severely reduced in numbers from the time of spawning, when tremendous numbers of eggs are released, to the time that juveniles are recruited to the fishable stock. Commonly, the magnitude of this recruitment is thought to show great variation from one year to the next. Sources of mortality during the early life history stages of pelagic spawners have been attributed to predation, to a mismatch in the timing of yolk sac absorption with the blooming of prey populations, to the transport of spawning products away from environments more suitable for survival, or to a combination of these or other factors (Sette, 1943; Bakun, 1985).

Mortality may significantly affect the estimation of total egg production, and this would then adversely affect the subsequent estimation of either spawner biomass or future stock sizes from ichthyoplankton data. Strategies which have been adopted to contend with this factor include: 1. ignore the problem and qualify abundance estimates, either implicitly or explicitly, as approximate (Sette, 1943; Ahlstrom, 1948; Sette and Ahlstrom, 1948; Ahlstrom and Ball, 1954; Cushing, 1957; Taft, 1960; Saville, 1964; Ciechomski and Capezzani, 1973; Tanaka, 1974; Richardson, 1981; Mason, et al., 1984), 2. restrict data to the fraction of eggs most recently spawned (Simpson, 1959; Harding and Talbot, 1973; Lockwood, et al., 1981; Sundby and Solemdal, 1984), and 3. estimate egg mortality and then adjust sample data prior to any estimation of egg production in order to compensate for the reduction in numbers of the more mature eggs (Berrien, et al., 1981; Pennington and Berrien, 1984).

The decision to use total counts irrespective of age is an analytical simplification which should lead to conservative estimates since the older eggs represent the remnants of a considerable number of eggs that had originally been spawned. Alternatively, constraining the

analysis to just those eggs recently spawned should reduce the impact of mortality on production estimates, but this could also require that a substantial portion of the data be ignored. A large fraction of the walleye pollock eggs collected during a survey can be greater than one week old since the incubation period lasts for at least two weeks at sea temperatures commonly encountered. It was desired that the potentially large contribution to production estimates represented by the older eggs should not be dismissed outright, and that an estimation procedure be developed that would be capable of employing all the data collected.

#### The pattern of mortality with age

The exponential model is commonly used as the analytical framework for the estimation of mortality. This model has had three basic parameterizations based on assumptions regarding the pattern of mortality with age (Marr, 1956; May, 1974; Hewitt and Methot, 1982; Lo, 1986). Typically, the rate of mortality is considered to be constant for the range of ages to be found in sample data. Alternatively, a decreasing rate of mortality is appropriate should mechanisms, such as decreasing predation rates or increasing prey densities, operate to reduce egg and larval mortalities as the animals age. Finally, laboratory experiments (Hamai, et al., 1971) have pointed to the transition from yolk sac to free feeding modes of nutrition as a potentially significant time for the survival of larvae in nature. Similar observations made earlier this century have lead to the concept of a critical period, the hypothesis that there is perhaps a period in the early life history of pelagic spawners during which mortality can be so pronounced as to significantly affect the recruitment of a yearclass to the adult stock. Skepticism has been voiced as to the success with which field data are capable of revealing such a period of catastrophic mortality, whether for pelagic spawners in general (Marr, 1956) or for the yolk sac stage in particular (May, 1974). There does not appear to be any evidence to support consideration of either a catastrophic or a decreasing rate of mortality during the incubation

period of walleye pollock and a constant rate of egg mortality was assumed.

A reasonable assumption concerning the character of mortality in a natural population holds that a constant percentage of the animals representing a cohort is regularly removed from the population as the animals age. Thus, if it were possible to follow the decline of a recently spawned cohort, the conventional model would suggest a declining pattern of abundance given by:

$$\text{(eq. 5.1) } NSUBT = NZERO \exp(-Zt)$$

where

NZERO	initial numerical abundance of a cohort within the survey area
NSUBT	numerical abundance of the cohort at some age following spawning
Z	seasonal mortality coefficient associated with the basic time unit (e.g., hour, day, etc.)
t	current age of the cohort.

The mortality coefficient,  $Z$ , applies to the entire egg population regardless of when the animals were spawned during the spawning season or where the animals occurred within the survey area. Mortality in this sense represents a time and space averaged approximation to the consequences of events occurring at more local scales.

#### Conventional approaches to the aggregation of stage abundance data

Sette (1943) conducted a pioneering study concerning the population dynamics of the early life stages of Atlantic mackerel (*Scomber scombrus*). He assumed that each age group was sampled in proportion to its true abundance both within the survey area and over the spawning season, and that the relative decline observed in a series of summed stage abundances provided a measure of the seasonal mortality rate. However, the data from the 1981 Shelikof surveys were not suitable for use with this seasonal approach because the assumption that sampling was representative over the duration of the spawning season and the extent of the survey area could not be assured. Only survey 2MF81 occurred during significant levels of spawning and

accounted for 96.2% of all the eggs collected (320,673 out of 333,458). Had all data been aggregated according to Sette's seasonal approach, the estimated mortality coefficient would not differ substantially from that obtained for this survey alone.

As an alternative approach, the abundances of a consecutive series of cohorts can approximate the decline of a single cohort if the spawning rate can be assumed to be constant. Under this circumstance, a single cruise may be suitable for the estimation of seasonal mortality (Hewitt and Methot, 1982; Hewitt and Brewer, 1983). Again, the data from the 1981 Shelikof surveys were not suitable for use with this cruise approach because the rate of spawning was not constant for a duration of time approximating the incubation period. This point can be made clearer by a simple illustration. Suppose the duration of the incubation period was one-fourth the duration of the spawning season, a scenario which approximates that occurring with the Shelikof population. Suppose further, for the sake of simplicity, that the spawning curve increases linearly from the time that spawning begins for the season to the time that spawning peaks. If a survey was conducted at the time of peak spawning, to take just one instance, then recently spawned eggs would occur at approximately twice the initial level of production as compared to those eggs which were just nearing the point of hatching. The cruise approach is only appropriate if initial abundances are of approximately equal size for all consecutive cohorts.

The estimation of a seasonal mortality coefficient for the Shelikof egg population is apparently more complex than usually encountered in ichthyoplankton studies. A closer examination of the conventional mortality model is required since many more factors must now be considered. These factors necessarily include a brief spawning season, an egg production rate that changes substantially as the season progresses, an incubation period that has a relatively long duration, stage durations that are dissimilar in length and are temperature dependent, varying precision in the estimates for total stage

abundances, and a confounding of the estimated age distribution for eggs in the survey area by the spawning histories at a few pivotal sampling locations. The mortality equation (eq. 5.1) was modified to accommodate these factors and a graphical representation was developed to provide a suitable framework for the depiction of the relationships between mathematical terms.

#### Generalization of the cohort concept

It was necessary to generalize the usual definition of a cohort somewhat in order to accommodate the classification of eggs into developmental stages comprised of dissimilar intervals of age. The underlying interval of spawning which defines a cohort is usually understood and not made explicit in most analytical problems. For example, a cohort of adults is usually viewed as a natural grouping of animals, all of which originated from the same spawning season. The term yearclass, a synonym for cohort in this context, makes this temporal frame of reference clearer. A comparison of the abundance of one yearclass with that of another is relatively straightforward since both yearclasses were spawned over similar intervals of time. However, the developmental stages for eggs of walleye pollock were not of equal duration. Stages were defined by easily recognizable morphological features and these features marked specific, but nonperiodic, intervals in the progress of development. The derived mortality model will explicitly accommodate stage durations that are of nonconstant size.

A further divergence from the usual definition of a cohort was necessary. A cohort of adults typically implies a focus on a unique set of animals and this set is composed of fewer and fewer individuals as the animals age. However, since the developmental stages for the eggs of walleye pollock were not of equal duration and therefore delineate differing intervals of spawning, the focus is no longer on a specific set of animals, but on a particular interval of the spawning season during which spawning had occurred. While the idea of a cohort as a grouping of animals which were spawned over an arbitrary interval

of the spawning season is not a familiar approach, it arises naturally from a morphological definition of age.

The constant exponential mortality model and the nonconstant production curve

Figure 21 depicts the time-dependent relationship between initial egg production and egg abundance with the passage of time. The age axis extends toward the right of the page. This axis is arbitrarily partitioned into a number of successive age groups beginning with the egg stage or incubation period, proceeding to the yolk sac and free feeding larval stages, and leading subsequently to juvenile and adult age groups. The axis extending toward the upper right corner of the Figure (or, if you will, extending back into the page) is another time scale, but representing in this case an annual cycle of spawning. It will be assumed for the purposes of illustration that the bulk of spawning occurs over an interval of 60 days and the incubation period has a constant duration of 15 days. Both the seasonal unit and the age unit have the same unit length (e.g., one day). The remaining axis, extending toward the top of the Figure, represents initial production or subsequent abundance on a unit time basis for any combination of spawning date and age. The range of the abundance axis can be arbitrarily scaled to any convenient height.

The three shaded areas in Figure 21 depict the seasonal abundance of eggs at certain arbitrarily-selected ages. These curves will hereafter be referred to as seasonal abundance curves or simply as abundance curves. Abundance curves are shown at fertilization, at the transition between the egg and yolk sac stages, and at the transition between yolk sac and free feeding larval stages. Many more than these three abundance curves can be constructed just as easily. The totality of abundance curves from fertilization through mature adult existence forms a 3-dimensional surface, and this surface of seasonal abundance curves will be referred to as the abundance surface.

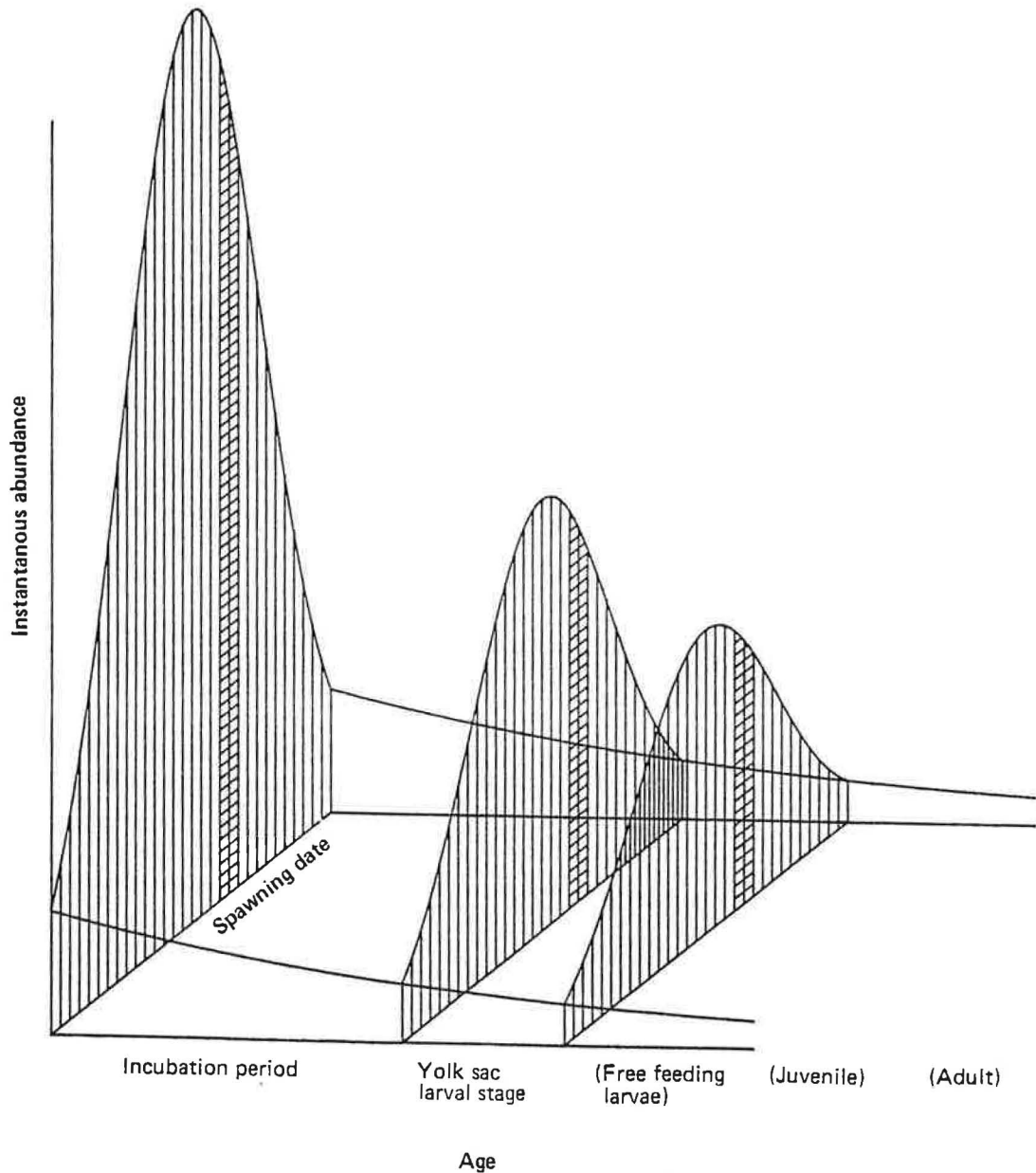


Figure 21. The relationship between spawning date, age, and egg abundance within the survey area is shown by this 3-dimensional depiction. The normal curve was assumed to illustrate the seasonal spawning curve, and mortality with age was modeled by a constant exponential decline in egg abundances. Two additional curves for seasonal egg abundance as a function of spawning date and age are shown at the ages associated with hatching and yolk sac absorption. The decline of an egg cohort is depicted by the crosshatched areas on the abundance curves. The totality of all abundance curves from spawning to mature adult forms a 3-dimensional surface which was termed the abundance surface.

The magnitude of seasonal egg production is represented by the abundance curve to the far left of the Figure. Spawning intensity within the survey area increases from the time considered to be the onset of spawning, rises to some maximum, and declines thereafter until the effective cessation of spawning. The magnitude of seasonal egg production can be determined by an integration of the area beneath the entire spawning curve. A normal curve was chosen to illustrate the changing levels of spawning, but the spawning function for a population need not conform to this representation. The bulk of seasonal egg production is represented by the area of the normal curve occurring within two standard deviations to either side of the date of peak spawning; egg production associated with intervals beyond these limits are truncated in the Figure.

The demarcation from one life stage to the next need not occur at a constant age for the entire spawning season as depicted by these abundance curves. In reality, stage durations are progressively reduced over the course of the spawning season because development is more rapid at higher temperatures and the temperature of seawater increases in Shelikof Strait as the spawning season progresses. If temperature substantially influences the rate of development, then a seasonal abundance curve might better be depicted as a curvilinear surface that only approximately parallels the abundance curve representing egg production. A constant temperature regime was assumed in order to simplify the depiction of the abundance surface.

An abundance curve is a useful analytical abstraction for illustrating the shape of the abundance surface. But it can only be constructed after the parameters of the modified mortality model are estimated. Each such curve represents the seasonal abundance for eggs that have all attained the same instant of age. However, such a determination of population size cannot be made from sample data, for this would require that counts be made over the course of the entire spawning season of those eggs which had reached the same exact age.

Earlier, an egg cohort was defined as those animals which were spawned within the survey area over a specifiable interval of the spawning season, with the duration of this interval being of varying and somewhat arbitrary length. In Figure 21, the area beneath the spawning curve is partitioned into constant intervals over the course of the spawning season. The crosshatched area beneath the spawning curve represents the initial numerical size of a hypothetical cohort. The number of eggs remaining after two periods of mortality are depicted by crosshatching on the remaining two abundance curves.

The initial size of a cohort is a function, in part, of the interval of the spawning season over which spawning occurred. Since the duration of spawning can be defined as any convenient length, it can also be reduced as an abstraction to a single moment of the spawning season. This abstraction of an age group will be termed an instantaneous cohort. The abundance of an instantaneous cohort can be associated with a single point on the abundance surface as a function of the date of spawning and an age at or subsequent to spawning. This focus on the instant is in keeping with the continuous nature of the spawning and mortality functions as mathematical expressions.

#### The determination of a date of sampling for a survey

A date of sampling for a survey was required in order to relate the survey to a specific moment of the spawning season, and the observed trend in stage abundances could then be related to the abundance surface. It was assumed that the age distribution developed for the eggs collected during a survey was representative of the underlying age structure of the entire egg population at this instant.

The time of sampling (TOS) for a survey was calculated as a weighted average of station sampling dates:

$$(eq. 5.2) \quad TOS = \frac{\sum_{j=1}^n \sum_{i=1}^{21} STAJUL_j C_{ij}}{\sum_{j=1}^n \sum_{i=1}^{21} C_{ij}}$$

where

STAJUL<sub>j</sub>      date and time that the jth station was occupied (local  
                  julian date)  
C<sub>ij</sub>            standardized stage abundance for the ith stage from the  
                  jth sample (eq. 2.7)  
TOS            time of sampling for a cruise, the local julian date around  
                  which the survey was centered.

A time of sampling defines the date during a survey around which most eggs were collected.

The representation of age and spawning date for an instantaneous cohort and for a series of successive cohorts

Figure 22 depicts the mathematical terms of eq. 5.1. Again, the axes are spawning date, abundance, and age. Two planes are emphasized. The seasonal spawning plane represents the seasonal production of eggs within the survey area. A constant spawning rate was assumed for this depiction. The sampling plane represents the abundance of a series of developmental stages at a specific moment of the spawning season, and the construction of this plane will now be developed in greater detail.

Two lines are shown across the middle of the spawning date-age plane which allow the age of an egg to be related to the date that the egg was spawned. The heavy horizontal line represents the age history of an instantaneous cohort. In particular, this instantaneous cohort had originally been spawned at the instant upon which the survey was centered (TOS). The subsequent age trajectory for this cohort is shown from the moment of spawning to just after the moment of hatching. The heavy slanted line just below the horizontal age trajectory is termed a time transfer line. It also allows the age of an egg to be related to the date of spawning. In this case, however, the line does not represent the age history of a single cohort, but rather it represents a "snapshot" of ages for a series of instantaneous cohorts at the time

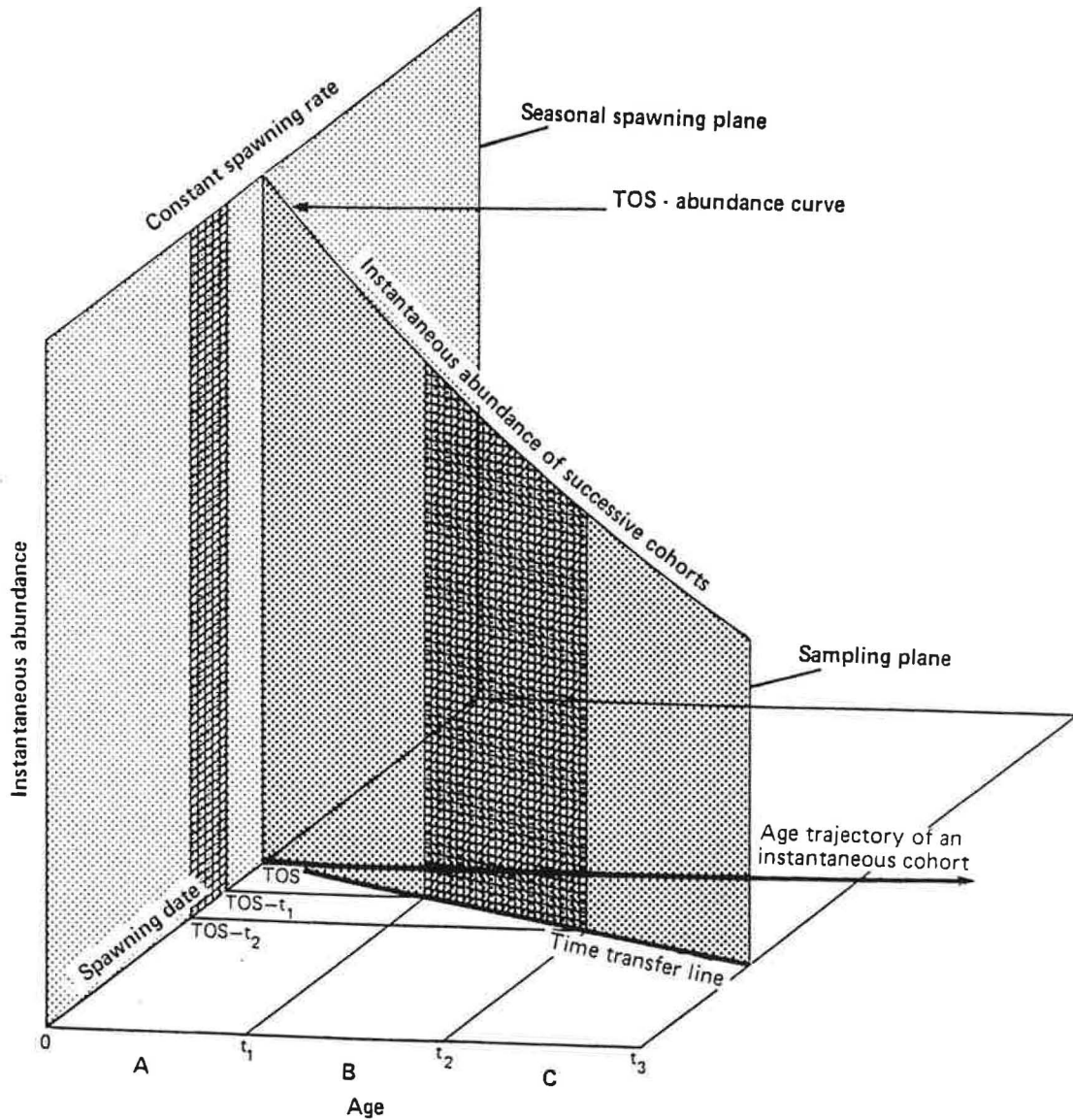


Figure 22. A constant rate of spawning and a constant exponential decline in egg abundance with age are depicted. An egg survey was assumed to center on a specific date of the spawning season (TOS = the time of sampling). The ages of eggs in plankton collections range throughout the entire incubation period, from age 0 to age  $t_3$ . A time transfer line relates the age of an egg to the date of spawning. The age axis was partitioned into 3 hypothetical age groups, denoted A, B, and C. The initial abundance of cohort B is depicted on the seasonal spawning plane and the subsequent abundance of this cohort at the time the survey was conducted is depicted on the sampling plane. The TOS-abundance curve represents the trend in egg abundances with age as of a specific date (TOS) of the spawning season.

the survey was conducted. These instantaneous cohorts were each spawned during successive instants of the spawning season.

The time transfer line relates the age of an egg to the date of spawning with respect to the time of sampling (TOS) for the survey. Given the age of an egg, say  $t_1$ , the date of spawning can be obtained by tracing back to the time transfer line, turning  $90^\circ$ , and continuing on to the spawning date axis. The complete range of ages for all eggs captured during a survey spans the cumulative development time from spawning, age 0, to hatching, age  $t_3$ , a period of approximately two weeks for walleye pollock. The corresponding interval of the spawning season during which all these eggs had originally been spawned ranges from the time that the survey was conducted, julian day TOS, to a point some two weeks prior to sampling operations, julian day  $TOS-t_3$ .

A sampling plane is formed by the projection of a time transfer line up to the 3-dimensional abundance surface, the dimensions of which are yet to be determined. The sampling plane cuts through the 3-dimensional model at a  $45^\circ$  angle to the axes of age and spawning date. The curve formed by the intersection of the sampling plane with the abundance surface will be termed a TOS-abundance curve. The areas of the sampling plane beneath the TOS-abundance curve represent the abundances of egg cohorts with respect to the time of sampling (TOS) for the survey.

The intersection of the sampling plane with the seasonal spawning plane partitions the seasonal spawning curve in Figure 22 into two areas. The rectangular area of the seasonal spawning plane which precedes this intersection represents a historical magnitude of egg production spawned prior to the time the hypothetical survey was conducted. The rectangular area beyond the TOS-abundance curve represents future egg production not yet spawned at the time of the survey.

In order to illustrate the relationship between the initial size

of an egg cohort and subsequent abundances of that cohort, the age axis was partitioned at ages  $t_1$ ,  $t_2$ , and  $t_3$  into hypothetical age groups A, B, and C respectively. The ages of eggs collected during a survey range from those recently spawned, such as those eggs of hypothetical age group A, to those which have completed incubation and are about to hatch, as are the older eggs of hypothetical age group C.

The abundances of cohort B is emphasized by the two crosshatched areas, one at fertilization on the spawning plane and the other over a subsequent range of ages on the sampling plane. The crosshatched area on the spawning plane between the dates  $TOS-t_2$  and  $TOS-t_1$  represents the initial number of eggs constituting the cohort. The magnitude of this initial abundance is the product of the constant rate of production and the duration of the spawning season defining the cohort.

Survivorship is represented by the crosshatched area on the sampling plane. These eggs were originally spawned over an interval of the spawning season which equaled in duration the range of ages defining the cohort,  $t_2-t_1$ . At the time that sampling was conducted, the oldest eggs of this cohort had survived a period of mortality equaling  $t_2$  in duration and the youngest had survived for a period of only  $t_1$  in duration.

The hypothetical cohorts A, B, and C together comprise all developmental stages of the incubation period. Only cohort B was accentuated in this depiction, but the abundance of each of the three cohorts are represented by successive areas under the TOS-abundance curve between the ages of fertilization and hatching.

#### The constant exponential mortality model and the normal production curve

Figures 23-26 depict the abundance surface under the assumptions of a normal spawning curve and a constant exponential mortality function at four moments of the spawning season. The discussion of

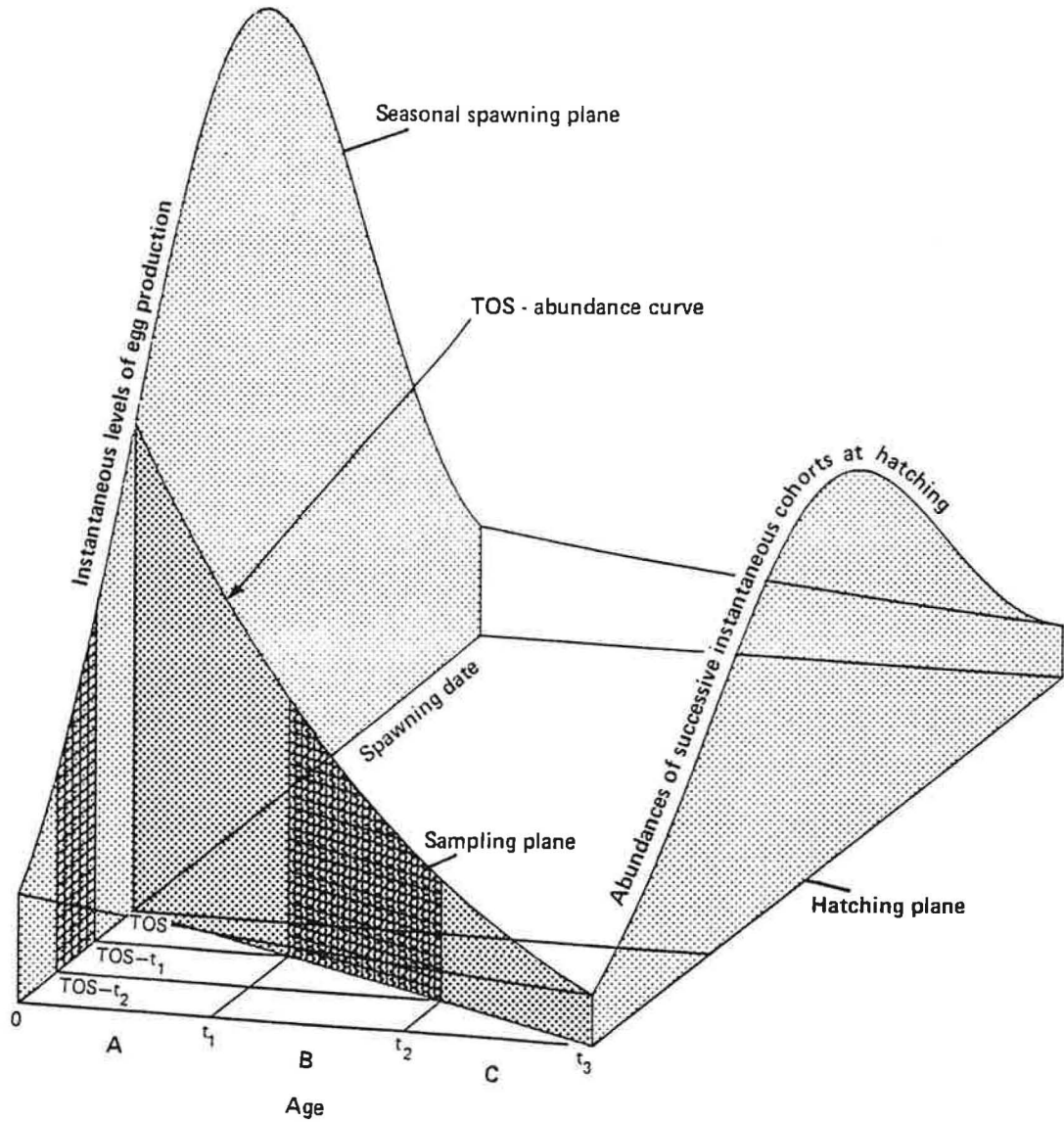


Figure 23. A normal spawning curve and a constant exponential decline in egg abundances are depicted. The time of sampling (TOS) for a hypothetical egg survey was positioned 15 days prior to the date of peak spawning. The age axis was partitioned into 3 hypothetical age groups, denoted A, B, and C. The initial abundance of cohort B is depicted on the seasonal spawning plane and the subsequent abundance of this cohort at the time the survey was conducted is depicted on the sampling plane. The TOS-abundance curve indicates the trend in egg abundances with increasing age.

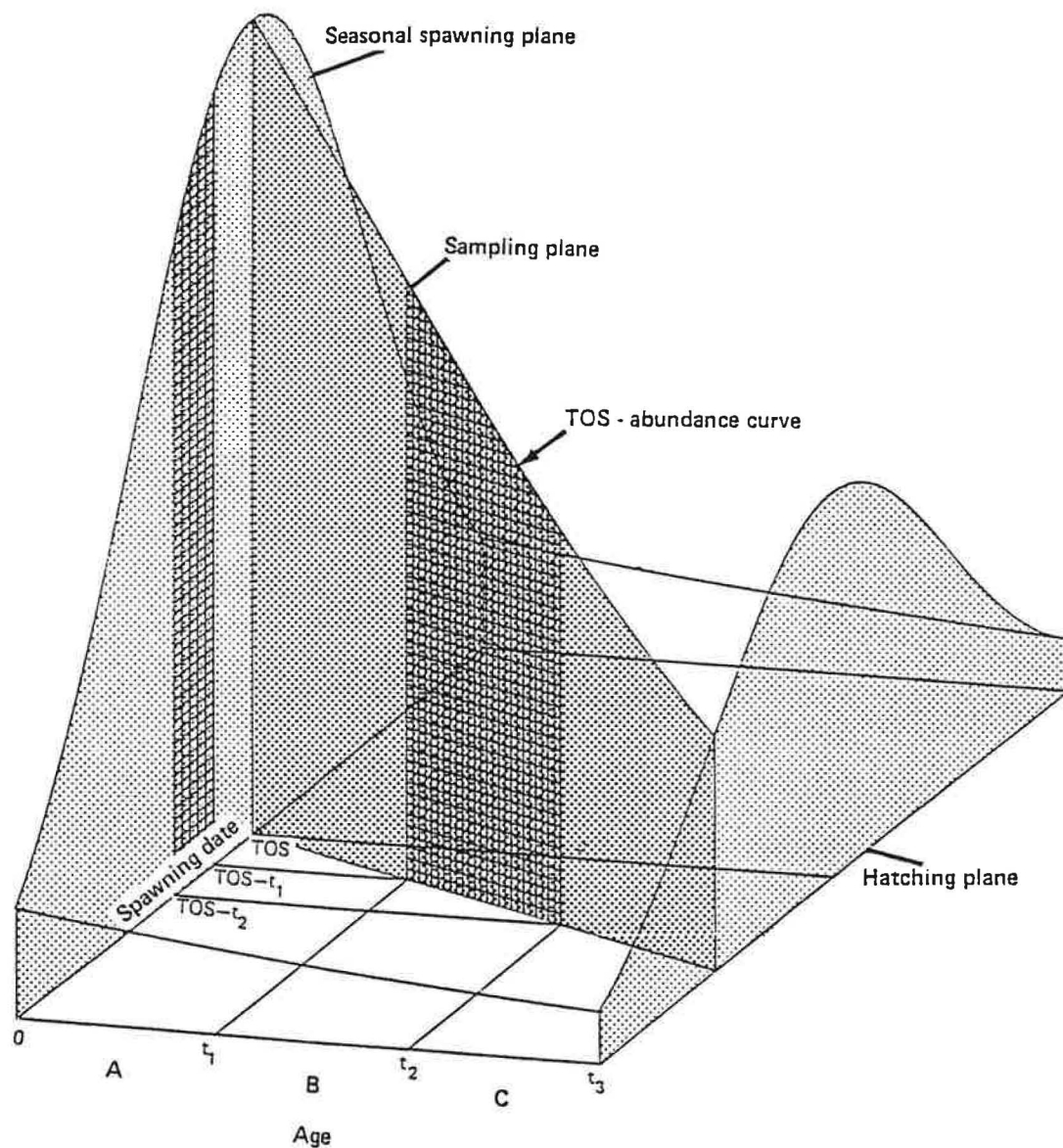


Figure 24. A normal spawning curve and a constant exponential decline in egg abundances are depicted. The time of sampling (TOS) for a hypothetical egg survey was positioned at the date of peak spawning. The age axis was partitioned into 3 hypothetical age groups, denoted A, B, and C. The initial abundance of cohort B is depicted on the seasonal spawning plane and the subsequent abundance of this cohort at the time the survey was conducted is depicted on the sampling plane. The TOS-abundance curve indicates the trend in egg abundances with increasing age.

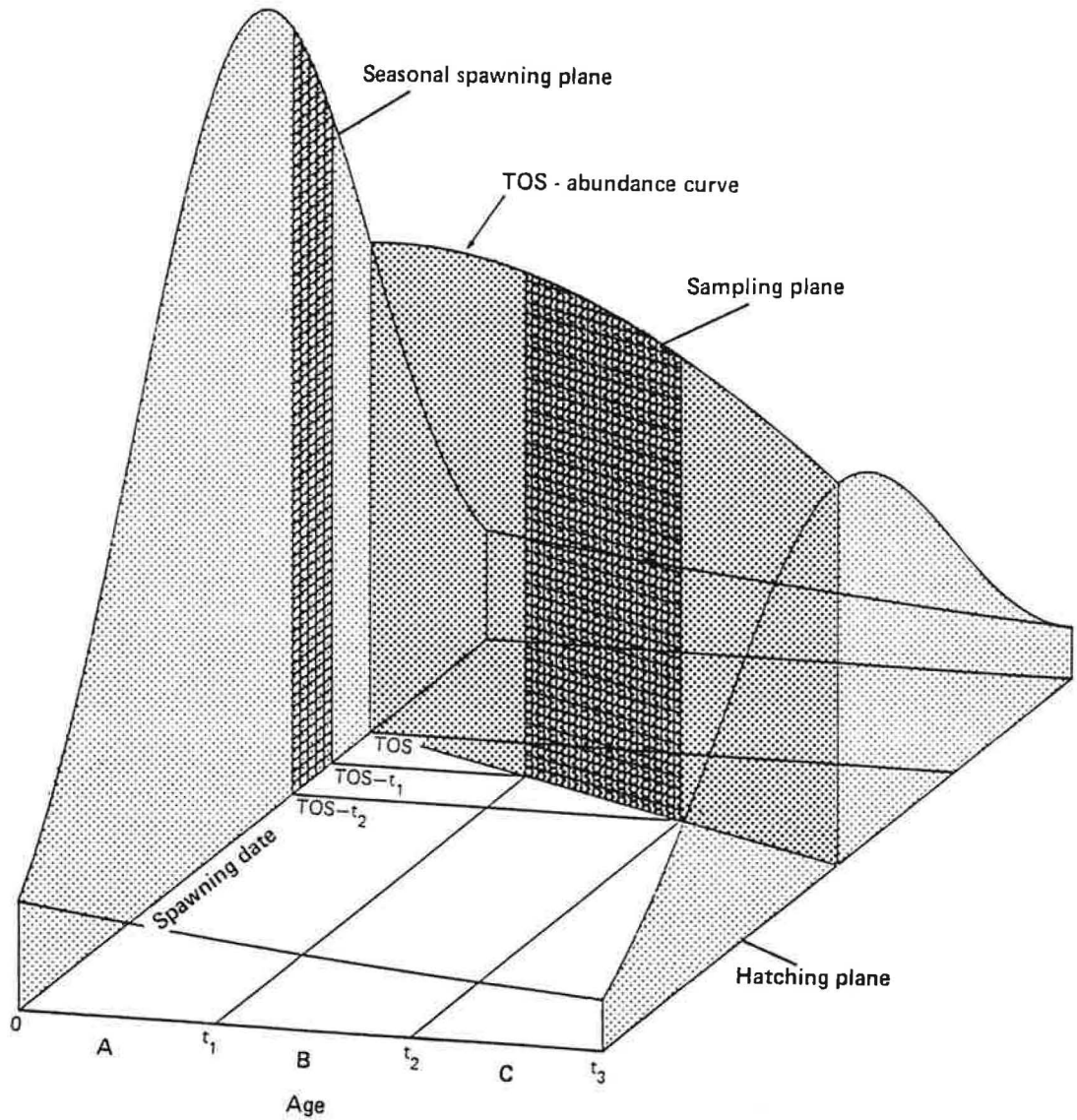


Figure 25. A normal spawning curve and a constant exponential decline in egg abundances are depicted. The time of sampling (TOS) for a hypothetical survey was positioned 15 days subsequent to the date of peak spawning. The age axis was partitioned into 3 hypothetical age groups, denoted A, B, and C. The initial abundance of cohort B is depicted on the seasonal spawning plane and the subsequent abundance of this cohort at the time the survey was conducted is depicted on the sampling plane. The TOS-abundance curve indicates the trend in egg abundances with increasing age.

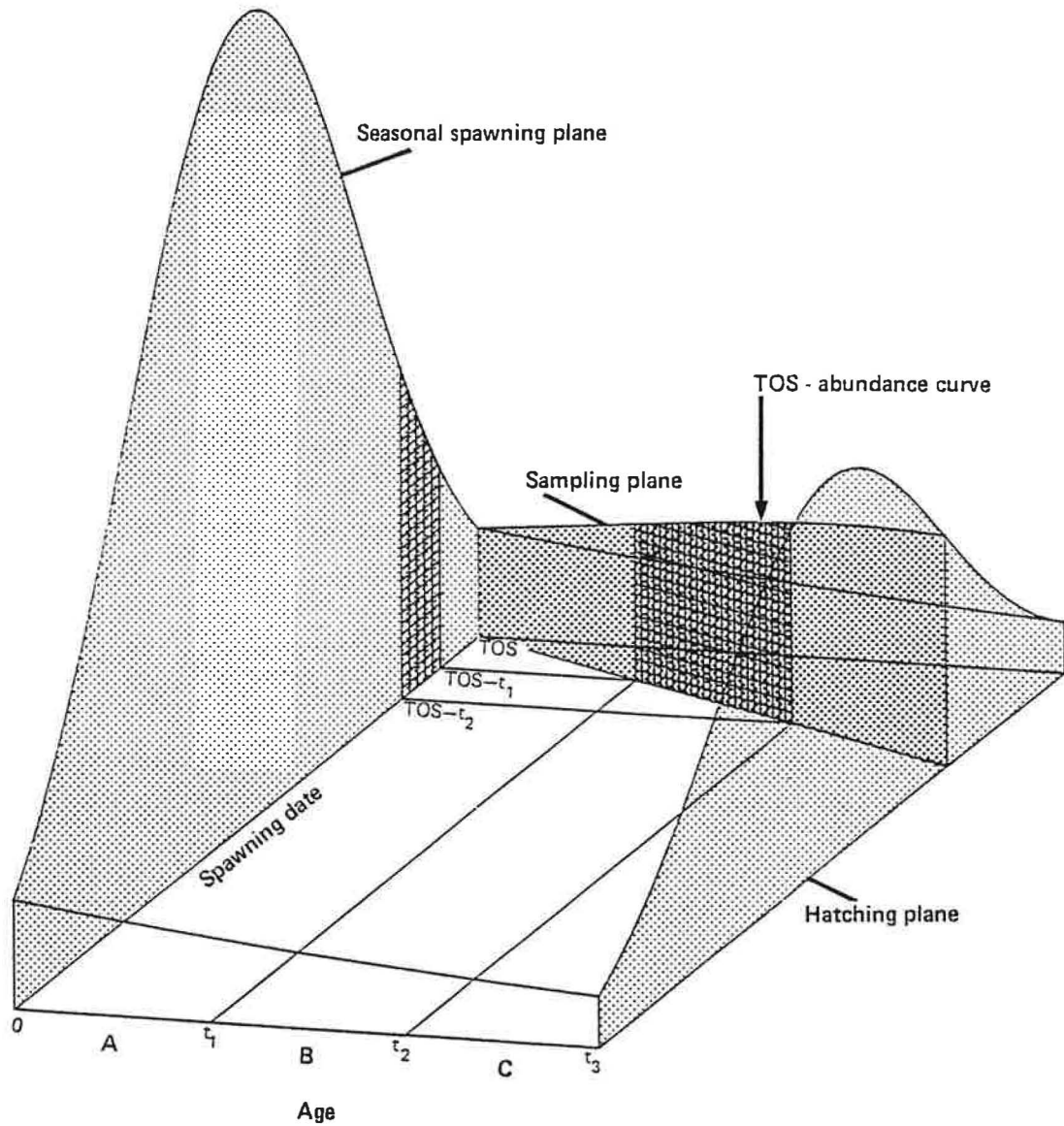


Figure 26. A normal spawning curve and a constant exponential decline in egg abundances are depicted. The time of sampling (TOS) for a hypothetical survey was positioned 30 days subsequent to the date of peak spawning. The age axis was partitioned into 3 hypothetical age groups, denoted A, B, and C. The initial abundance of cohort B is depicted on the seasonal spawning plane and the subsequent abundance of this cohort at the time the survey was conducted is depicted on the sampling plane. The TOS-abundance curve indicates the trend in egg abundances with increasing age.

these Figures will be brief since only the shape of the spawning curve has changed. In these latter Figures, the instantaneous level of egg production can be seen to vary over the course of the spawning season. Moreover, the relative numerical dominance between the three hypothetical age groups can be seen to change over the course of the spawning season.

In order to demonstrate more clearly the changing relative dominance of consecutive cohorts given a nonconstant spawning function, the viewing perspective is shifted in Figure 27 to a more revealing angle. In effect, the abundance surface was rotated approximately  $90^\circ$  from that of the previous depictions, such that now the hatching plane is in the foreground and the seasonal spawning plane is in the background. Sampling planes for five hypothetical surveys are depicted at a series of sampling dates along the spawning date axis. The intersections of these planes with the abundance surface forms five TOS-abundance curves. The area beneath each curve is partitioned into 15 stages having identical stage durations. The oldest age group is depicted at the far left of each sampling plane and the youngest occurs at the far right. The number of age groups that may be depicted is arbitrary but, since the age axis was defined as 15 days in duration, these age groups depict the more familiar conception of egg cohorts as arising from daily intervals of spawning.

What should be apparent in the depiction is that during any particular survey, the older eggs were spawned at quite different levels of initial production than were the younger eggs, and the relative differences in abundances is dependent on the moment of the spawning season during which sampling was conducted. The slopes of the TOS-abundance curves can be seen to follow a complex pattern of changes when production rates are not constant for the duration of the incubation period. If the conventional mortality function (eq. 5.1) had been used for the estimation of seasonal egg mortality, then sampling conducted prior to peak spawning would overestimate the seasonal mortality coefficient and sampling conducted subsequent to

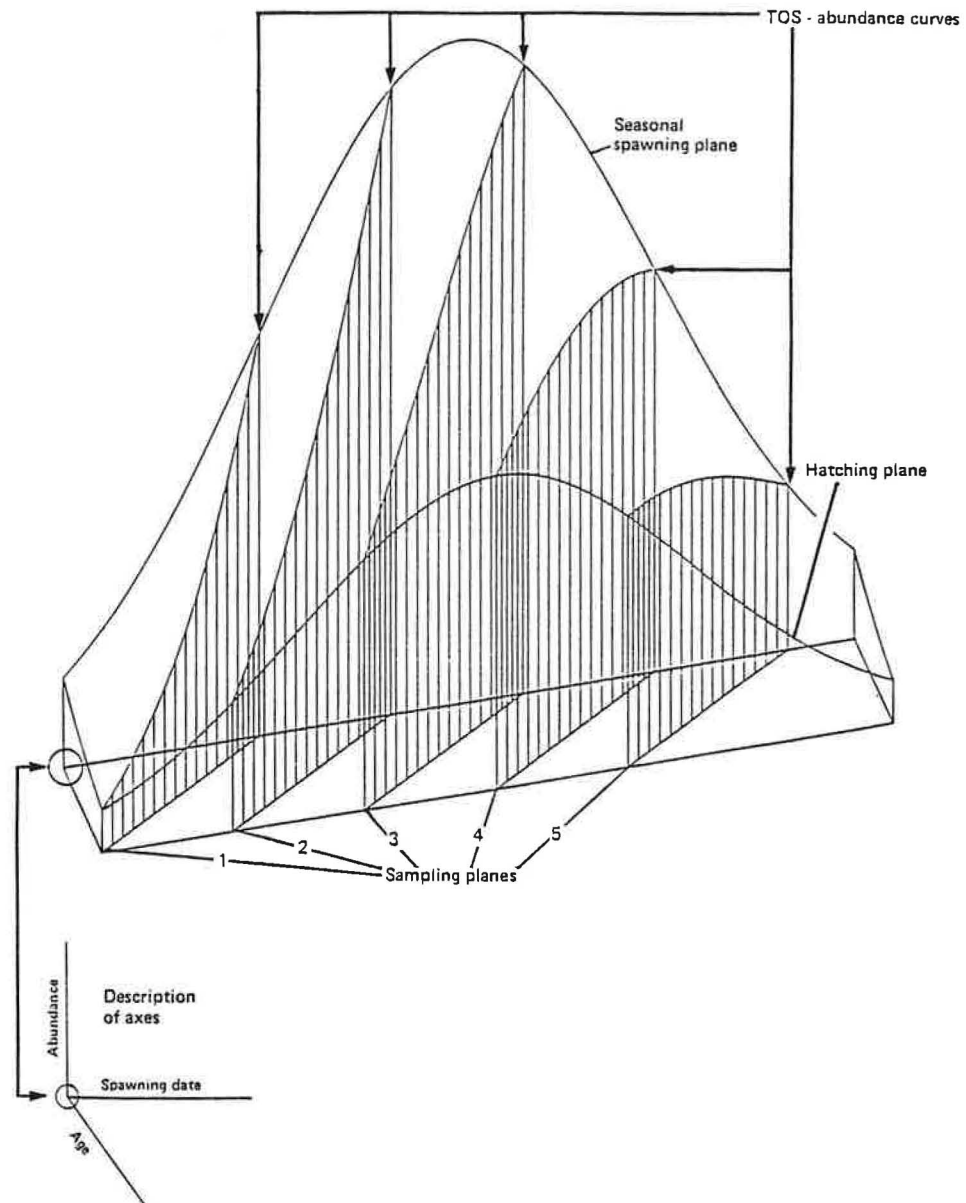


Figure 27. The 3-dimensional model for spawning date, age, and egg abundance was rotated approximately  $90^\circ$  to clearly illustrate the shapes of TOS-abundance curves and sampling planes at five moments of the spawning season. The spawning plane is in the background and the hatching plane is in the foreground. The shape of a TOS-abundance curve can be seen to be a complex function of spawning date and age. The estimation of egg mortality is not a simple function of the abundances of a series of successive egg cohorts when the rate of egg production is not constant.

peak spawning would underestimate it (Hewitt and Methot, 1982). If the 1981 survey data had been analyzed on a cruise by cruise basis under the assumption of a constant spawning rate, the resulting pattern of stage abundances would be similar to those seen on these sampling planes. The egg abundances simulated by sampling planes 1 and 2 show sharply decreasing abundances with age. On the other hand, planes 4 and 5 appear to indicate increasing abundance with age. Since a cohort can only decrease in numbers with the passage of time, the abundances for a succession of cohorts clearly do not simulate the decline in abundance of a cohort in a simple manner.

#### Incorporating a nonconstant production function into the mortality model

Nonconstant production levels were accommodated by adapting the mortality equation to the apparent pattern of biological events. A number of simplifying assumptions were necessary in order to develop a suitable mathematical procedure. It was again assumed that the normal curve was an adequate model for the seasonal spawning curve and that egg mortality could be approximated by a constant exponential curve. It was further assumed that surveys were completed in a fraction of the time required for egg incubation, such that the relative pattern in total stage abundances was not obscured by a protracted program of sampling and that each survey could be centered at a single moment of the spawning season. Total abundance estimates for the various stages were assumed to be independent of one another and also were assumed to be representative of true abundances within the survey area.

Estimates were desired for the magnitude of seasonal egg production and the apparent rate of seasonal mortality during the incubation period. The date of peak spawning and a parameter related to the duration of the spawning season were also estimated. Data required in the modified mortality model were the time of sampling for each survey, an estimate of total stage abundance and an expression of the precision of this total for each developmental stage, the average

sea temperature at the time of each survey, and a series of coefficients relating temperature to cumulative development time for the developmental stages employed in the analysis.

#### Derivation of the objective function

Rather than give initial and subsequent abundances in terms of a total number of eggs, as was done in eq. 5.1, abundances were instead defined as the product of a spawning rate and a duration of spawning:

$$(eq. 5.3) \quad NT (T_2 - T_1) = NO (T_2 - T_1) \exp(-Zt)$$

where

NO	average egg production per unit interval of the spawning season
T <sub>1</sub>	initial date of spawning for eggs of a cohort (julian date)
T <sub>2</sub>	final date of spawning for eggs of a cohort (julian date)
NT	average abundance per unit spawning interval following t days of mortality.

The quantity  $(T_2 - T_1)$  defines the period of time during which a cohort of eggs was spawned. The initial size of a cohort, NZERO in eq. 5.1, is now represented by the product of NO, the average rate of egg production, and the duration of the spawning season during which this rate was applicable. Similarly, the abundance of a cohort at some age subsequent to spawning, NSUBT in eq. 5.1, is now represented by the product of NT, the average survivorship for a unit interval of age, and the duration of spawning that defined the cohort. This explicit acknowledgement of the time elements in abundance data -- T for spawning date and t for age -- allows the flexibility needed for enriching the conventional mortality equation to suit the present analytical problem.

The initial abundance of a cohort, NZERO, had been defined as constant for all developmental stages, but can now be redefined as a varying function of time. The normal curve was selected to model the seasonal spawning function. An unscaled instantaneous height of the normal curve is given for a particular date of the spawning season by:

$$(eq. 5.4) \quad NPOINT = \frac{1}{SIGMA \sqrt{2 PI}} \exp \left[ \frac{-(BD-MU)^2}{2 SIGMA^2} \right]$$

where

SIGMA      one standard deviation in the normal production function  
 (days)  
 BD          julian date of spawning for an instantaneous cohort  
 MU          julian date of peak spawning  
 NPOINT     instantaneous height of the normal curve.

A nonconstant duration of spawning was accomodated by an integration of the normal density function between appropriate dates of the spawning season:

$$(eq. 5.5) \quad NFRAC = \int_{T_2}^{T_1} NPOINT \, dT$$

where

NFRAC      fraction of the area under a normal curve between the julian dates  $T_1$  and  $T_2$ .

Since an integrated value of the normal density function has a value between 0 and 1, multiplying this fraction by the numerical value for seasonal egg production gives the numerical abundance of a cohort spawned over a specifiable interval of the spawning season:

$$(eq. 5.6) \quad AB_{init} = NPOP \int_{T_2}^{T_1} NPOINT \, dT$$

where

NPOP          seasonal egg production  
 $AB_{init}$       initial abundance of an egg cohort.

The initial abundance of a cohort can be limited to a few animals spawned over a few moments of the spawning season or expanded to the total seasonal production. For example, the abundance of an entire yearclass is represented by expanding the range of spawning dates to encompass the entire annual cycle of spawning.

The "birthdate" parameter BD of eq. 5.4 can be expressed as a function of two knowable quantities, these being age and time of sampling for a survey:

$$(eq. 5.7) \quad BD = TOS - t$$

where

TOS            julian date of sampling assigned to the gth survey  
t                age of an animal from a cohort (days).

Replacing BD in eq 5.4 with eq. 5.7 gives the necessary form of the normal curve as:

$$(eq. 5.8) \quad NPOINT = \frac{1}{SIGMA \sqrt{2 PI}} \exp \left[ \frac{-(TOS-t-MU)^2}{2 SIGMA^2} \right]$$

NPOINT is now a function of the estimatable parameters MU and SIGMA and the quantities TOS and t obtainable from sample data. Having replaced spawning date with age in the normal density function, it was also necessary to modify eqs. 5.5 and 5.6 from an integration over an interval of the spawning season to an integration over a range of ages:

$$(eq. 5.9) \quad AB_{init} = NPOP \int_b^a NPOINT \, dt$$

where

a                cumulative development time to beginning of a stage (days)  
b                cumulative development time to end of a stage (days).

The values a and b could be replaced in this equation with the equation by which they were derived (eq. 2.1) if it were desired that stage durations be made an explicit function of temperature.

With the initial abundance of a cohort expressed as a function of age, the abundance at some age subsequent to spawning was obtained by continuously reducing the initial size of a cohort by means of the constant exponential mortality function,  $\exp(-Zt)$ :

$$(eq. 5.10) \quad AB_{pred} = NPOP \int_b^a NPOINT \exp(-Zt) \, dt$$

where

Z                coefficient of daily mortality  
AB<sub>pred</sub>        predicted total stage abundance (number of eggs of an age group within the survey area).

The modified mortality model in its complete form, with the scalar NPOP brought inside the integral, is:

(eq. 5.11)

$$AB_{\text{pred}} = \int_b^a \frac{1}{\text{SIGMA} \sqrt{2 \text{PI}}} \exp \left[ -\frac{(\text{TOS}-t-\text{MU})^2}{2 \text{SIGMA}^2} \right] \text{NPOP} \exp(-Zt) dt$$

where

a	cumulative development time to beginning of stage (days)
b	cumulative development time to end of stage (days)
SIGMA	standard deviation of the normal spawning function (days)
TOS	date of sampling assigned to the gth survey (julian date)
t	egg age (days)
MU	date of peak spawning (julian date)
NPOP	seasonal egg production (eggs/survey area/spawning season)
Z	coefficient of daily mortality
AB <sub>pred</sub>	predicted total stage abundance (number of eggs of an age group within the survey area).

The size of an instantaneous cohort at an age subsequent to spawning can be obtained by evaluating the integrand, and the initial size of this cohort can be obtained by removing the constant exponential mortality term before evaluating the integrand.

## METHODS

### Fitting data to the objective function

Up to this point the development of the modified mortality model has been a mechanistic formulation of the relevant factors. However, the fitting of data from the 1981 egg surveys to the model required a number of modifications and standardizations. These additional procedures were not explicitly required by the model, but were instead the consequence of the fitting procedure that was selected and the quality of the sample data available for analysis. Having specified the objective function (eq. 5.11), it was also necessary to select a fitting procedure, select an error norm, calculate an observed total abundance for each developmental stage of each survey, standardize abundances to a unit interval of spawning, weight the residual differences between observed and predicted abundances, and restrict parameter values should the observed data conform only weakly to the objective function.

Bestfitting parameter estimates were obtained by brute computational force using a self-directing search procedure called the simplex method (Spendley, et. al., 1962; Kowalik and Osborne, 1968). Beginning with trial values for the parameters of the objective function, the simplex procedure repeatedly examines and modifies these values in such a way that a local minimum in the error function is attained up to a specifiable level of precision in the parameters. The sum of squared differences between observed and predicted values of the objective function is commonly used in curve fitting and was selected as a basis for the error criterion defining an optimum fit.

Each iteration of the simplex method involved a number of preliminary calculations. Since the equation for the normal curve cannot be integrated exactly by elementary functions, an iterative procedure was required for the numerical integration of eq. 5.11. To accomplish this, each predicted value for total stage abundance was calculated by first evaluating the integrand at a number of ages over the duration of the developmental stage. Ages began and ended with the cumulative development time to the onset and cessation of the stage, and intervening ages were spaced no greater than one-tenth day apart. The resulting series of instantaneous ages and abundances were then integrated by the method of trapezoids. This process was repeated for each developmental stage of each survey in order to obtain a predicted total abundance to correspond to each observed total abundance. The resulting values were then employed in the next iteration of the simplex algorithm.

Data from all four egg surveys were employed in the fitting procedure and the second survey was again interpreted as a double sampling of the areas of high egg concentrations. As was done earlier in Chapter 4, the data from survey 2MF81 were partitioned into two quasi-synoptic sets of sampling stations. Data set A included stations G001A-G083A and data set B included stations G001A-G091A less stations G021A-G024A. As was discussed in Chapter 2, the egg catches for stations G084A-G091A overrepresent the frequency of very large catches

within the survey area. Set B models the egg population at a subsequent date of the spawning season. This partitioning of the data is considered more representative of the egg population at the time survey 2MF81 was conducted and it also allows the stability of parameter estimates to be assessed. Specifically, the parameter estimates should not differ dramatically between the two data sets if they are considered equally representative of the egg population.

An observed value for the total abundance of a developmental stage was obtained by first calculating the mean abundance for the stage and then multiplying the mean by the size of the survey area:

$$(eq. 5.12) \quad AB_{ob} = AREA \frac{\sum_{j=1}^n C_{ij}}{n}$$

where

AREA	size of the survey area ( $1.596 \times 10^{10} \text{ m}^2$ )
n	sample size
$C_{ij}$	standardized stage abundance for the <i>i</i> th stage at the <i>j</i> th sampling station from eq. 2.7 (eggs/stage/ $\text{m}^2$ )
$AB_{ob}$	observed total stage abundance for the <i>i</i> th stage (eggs/stage/survey area).

As has been pointed out earlier, this procedure represents an implicit area-weighting of each egg catch by the constant  $AREA/n$ . It must be assumed here that sample size and sampling design led to an adequate representation of true abundances on a stage by stage basis.

Each pair of observed and predicted total stage abundance estimates must be standardized to constant intervals of spawning if each pair was to have equal importance in the fitting procedure. On average, differences between observed and predicted values were relatively small for short duration stages and relatively large for long duration stages. Unless this tendency is countered, the observed abundances for longer duration stages can heavily influence the magnitudes of bestfitting parameter estimates. The effect on the error function of varying stage durations was accommodated by standardizing the total stage abundances to a unit interval of the spawning season by means of a division with the corresponding stage duration:

$$(eq. 5.13) \quad ABUND_{pred} = \frac{AB_{pred}}{STGDUR_i}$$

where

STGDUR<sub>i</sub>      stage duration for the i<sup>th</sup> stage at the average temperature during the survey (eq. 2.2)

ABUND<sub>pred</sub>    predicted total stage abundance per unit time interval.

Both the observed and predicted abundances were standardized to unit duration prior to the calculation of residual differences.

The total abundance for a developmental stage, ABUND<sub>ob</sub>, cannot be known exactly; instead, each value was determined from sample data and was subject to some level of uncertainty. Since the precision of estimates varied substantially in absolute terms, the information provided by each of these observations was not of equivalent quality and some acknowledgement of the stochastic behavior of the data was required. Because catch heterogeneity was greatest at the time of peak spawning, the variability of total stage abundances near this time was also greatest as compared to periods of little or no spawning activity. In addition, the younger stages also had lower levels of precision, regardless of the date that a survey was conducted, since catch heterogeneity was greater for the younger stages than for the older stages. Accordingly, residuals were weighted by the corresponding standard deviation for the estimate of total abundance for each stage:

$$(eq. 5.14) \quad TERM1 = \frac{(ABUND_{pred} - ABUND_{ob})^2}{STDDEV}$$

where

ABUND<sub>pred</sub>    total abundance predicted by the objective function using current parameter estimates

ABUND<sub>ob</sub>      total abundance observed from sample data

STDDEV       standard deviation for an observed value of total stage abundance

TERM1        squared difference error term.

The compound error function included this and two additional error components which will now be described.

Although the sense of the problem would require it, the modified mortality model is not constrained to provide positive values for parameters if sample data conform only weakly to the behavior specified by the objective function. For example, when the quality of data is

very poor, the global minimum in the error function may suggest inadmissible values for the mortality coefficient, apparently indicating an increase in abundance for a cohort at ages subsequent to spawning. A "penalty" was added to the error function by changing the sign and exponentiating the trial mortality coefficient during each update of the compound error function. Trial values with the correct sign would thus produce an exponentiated value near zero and have little or no effect on the compound error function, while those with the wrong sign would "explode" the penalty term. The nonnegative constraint for the daily mortality coefficient was:

$$(eq. 5.15) \quad TERM2 = \exp(-Z)$$

where

TERM2           penalty for trial values of the mortality coefficient having a negative sign.

Observed stage abundances were the largest and the most variable for surveys conducted near the time of peak spawning. Since the first term of the error criterion minimizes the squared differences between observed and predicted abundances, it is possible for a few data points of this type to exercise substantial control over the eventual fit obtained for model parameters. For example, these data may be so inconsistent with the trend modeled by eq. 5.11 that the mortality coefficient may be forced to either a very small or a very large value, and as a result the predicted abundances for the remaining data points may either be substantially overestimated or approach zero. In order to prevent the occurrence of this effect, a predicted abundance was constrained to rarely be less than the corresponding observed abundance by exponentiating the difference:

$$(eq. 5.16) \quad TERM3 = \exp \left[ -(ABUND_{pred} - ABUND_{ob}) \right]$$

where

TERM3           penalty for trial values of predicted total stage abundances that were substantially smaller than the observed values.

This term would serve little purpose if the estimates for total stage abundances followed a consistent trend as defined by eq. 5.11.

Although it is a biasing procedure, a constraint having this kind of effect becomes necessary if there is much scatter in the observed

values for total stage abundances.

A local minimum was sought for a compound error function composed of the three foregoing error terms:

$$(eq. 5.17) \quad ERR = \sum_{g=1}^G \sum_{i=7}^{20} [TERM1 + TERM2 + TERM3]$$

where

G                    number of surveys conducted during the spawning season  
ERR                  the compound error term.

Not all of the stage data were suitable for usage in the modified mortality model. The eggs of both the very youngest and the very oldest stages were not well represented in the catch data and, as is commonly done (eg., Sette and Ahlstrom, 1948), were ignored. Only stages 7-20 were employed in calculations.

#### The depiction of residuals

A residual represents the difference between an observed total stage abundance and the corresponding predicted value using bestfitting parameter estimates in the modified mortality model (eq. 5.11). Both observed and predicted abundances represent areas of a sampling plane between two limiting ages, but this means of graphically showing residuals would unduly clutter the depiction of a TOS-abundance curve. Instead, residuals were shown as line segments either above or below a TOS-abundance curve parallelling the abundance axis (Figure 28).

The essential equivalence of these representations can be made clearer by considering the graphical depiction of both areas and line segments. A predicted total abundance for an age group corresponds to an area beneath the TOS-abundance curve between the beginning and ending ages of the stage. An area under a complex curve can be equivalently expressed as the product of the average height and the length of the base. Thus a predicted total stage abundance can also be represented as a rectangular area, with stage duration forming the base and average instantaneous abundance forming the height. The corresponding observed value for total stage abundance can also be

viewed as a rectangular area. The length of the base again represents the duration of the stage, and the observed abundance per unit time represents the height. Thus, both predicted and observed values can be thought of as rectangular areas with each having a base of the same duration. Residual differences then correspond to differences in average, or rectangular, height.

Each line segment representing a residual was positioned at the age and spawning date corresponding to the intersection of a predicted average instantaneous height,  $AVGAB_i$ , for a stage with the TOS-abundance curve. These coordinates were dependent on the shape of the fitted abundance surface and were obtained by rearranging the integrand of eq. 5.11 as a quadratic in the variable  $t$ :

$$(eq. 5.18) \\ 0 = (TOS - \mu)^2 + 2\sigma^2 \ln \left[ \frac{AVGAB_i \sigma 2\pi}{NPOP} \right] + 2(-TOS + \mu + \sigma^2 Z)t + t^2$$

where

$AVGAB_i$  average instantaneous height, obtained by dividing the predicted total abundance for a stage by the stage duration in terms of hours.

The bestfitting estimates for the parameters  $NPOP$ ,  $Z$ ,  $\mu$ , and  $\sigma$  were inserted into eq. 5.18 along with estimates of average instantaneous height, and the appropriate roots were found by the quadratic formula.

## RESULTS

The modified mortality model was employed on data from the four 1981 ichthyoplankton surveys to estimate seasonal egg production and mortality during the incubation period. A total of 56 datapoints was provided by the four ichthyoplankton surveys. Bestfitting parameters were obtained both using weighted and unweighted residuals.

Station temperatures were equated to 5.0°C. Since the bulk of seasonal egg production appears to have been spawned closest to the time that survey 2MF81 was conducted, this analytical simplification had little impact on parameter estimates for the current data. The

temperatures that were obtained at all stations occupied during this survey approximated 5°C, and the pattern of temperature with depth was more or less isothermal throughout the survey area.

Bestfitting parameter estimates are shown in Table 13. The estimates derived for the unweighted data were unreliable. The best fit for data set 2 was obtained by reducing the standard deviation for the normal spawning function, SIGMA, to 3 days, indicating an improbable duration of the spawning season of about two weeks. The best fit for data set 1 was obtained by inflating the estimates for both seasonal egg production and the coefficient of daily mortality.

The best fitting abundance surfaces produced by the weighting of residuals are shown (Figure 28) for data sets 1 and 2. Each plot summarizes the shape of the bestfitting abundance surface, the fitted TOS-abundance curve for each survey, and the pattern of residuals. The abundance surface was truncated at upper and lower limits of age and julian date of spawning. The normal spawning function is shown between dates located at a distance of three standard deviations from the date of peak spawning. The age axis is shown extending from spawning to

=====  
 Table 13. Best fitting parameter estimates to the modified mortality model. Statistics are shown for NPOP, seasonal egg production; Z, coefficient of daily mortality; MU, julian date of peak spawning; and SIGMA, standard deviation of the normal spawning function (days). The data for survey 2MF81 were partitioned into set A and B. Data set 1 consisted of the total abundance values determined for of surveys 1MF81, set A of 2MF81, 3MF81, and 4MF81; data set 2 consisted of the corresponding values for set B of survey 2MF81 and the remaining three surveys. Residuals were either unweighted or weighted by the inverse of the standard deviations for the observed values of total stage abundances.  
 =====

data set	residuals weighted	NPOP X 10 <sup>12</sup>	Z	MU	SIGMA
1	YES	264.	.44	97.9	11.2
1	NO	412.	.56	98.5	7.3
2	YES	250.	.21	96.4	10.2
2	NO	137.	.29	92.9	3.1

=====

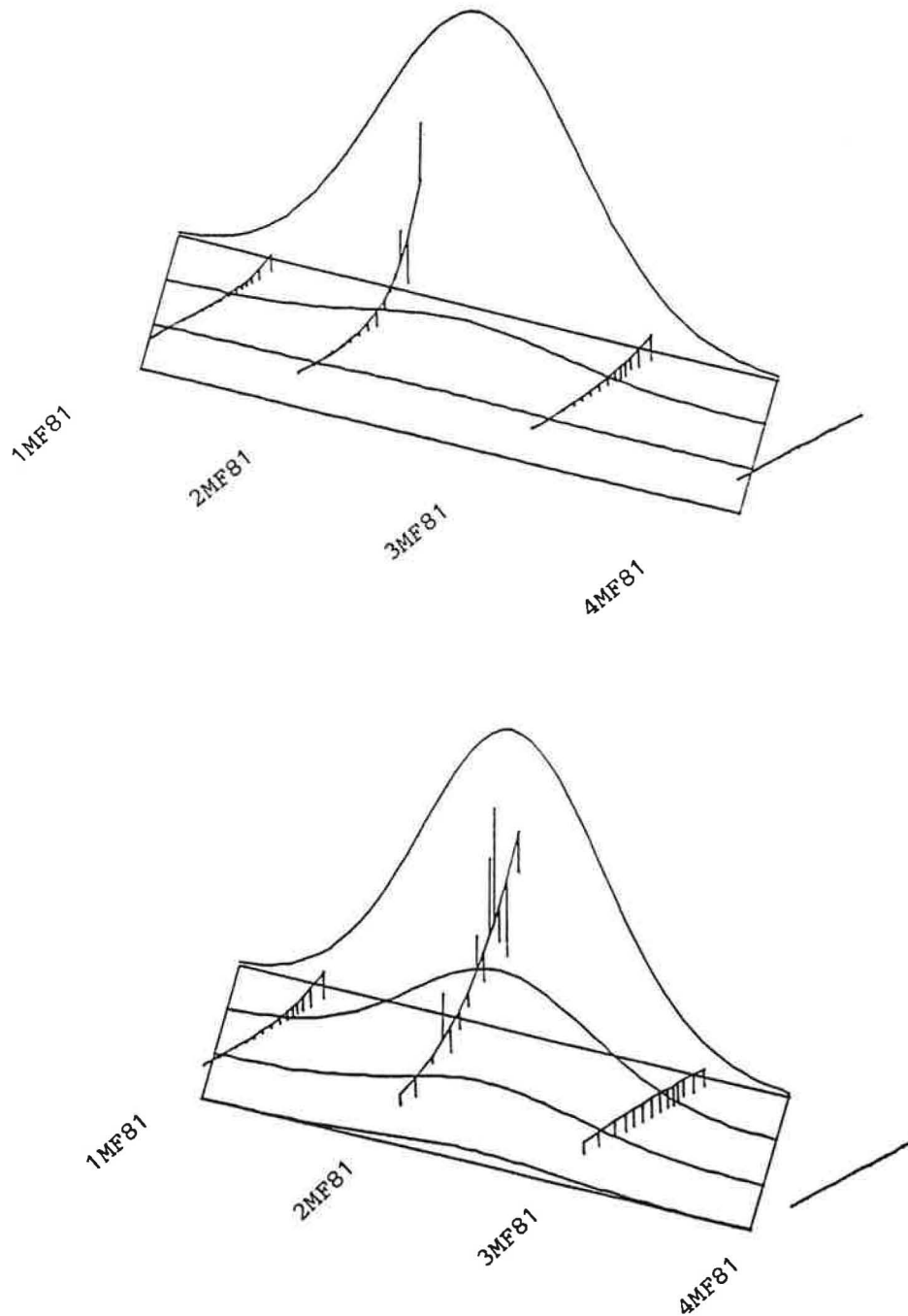


Figure 28. The best fitting abundance surfaces for the 1981 egg surveys. Only developmental stages 7 through 20 were used and residuals were weighted. Stage abundance data were from surveys 1MF81, 2MF81 (set A), 3MF81, and 4MF81 (top) and from surveys 1MF81, 2MF81 (set B), 3MF81, and 4MF81 (bottom).

hatching for the 5°C temperature regime. The shape of the bestfitting abundance surface is indicated by abundance curves at 0, 5, 10, and 15 days of age. Fitted TOS-abundance curves are shown from left to right for the surveys 1MF81, 2MF81, 3MF81, and 4MF81 respectively.

#### DISCUSSION

A number of problems can be recognized in this implementation of the modified mortality model that were directly related to limitations in sampling methodology and the determination of the observed values for total stage abundances.

Data from survey 2MF81 provided most of the information as to the magnitude of NPOP, seasonal egg production; of MU, the date of peak spawning; and of Z, the coefficient of daily mortality. This was as expected since this survey was conducted closest to the time of peak spawning and accounted for the 96.2% of all the eggs collected. The best fitting estimates for all parameters, including SIGMA, were obtained by minimizing residuals based partly or entirely on this survey.

Surveys 1MF81, 3MF81, and 4MF81 were conducted either long before or long after the main period of spawning activity. The data from these surveys influenced the magnitude of SIGMA but provided little information for the estimation of the other parameters.

The estimates for total stage abundances for survey 2MF81 were so variable that, without the weighting of residuals, the first few stages exercised almost exclusive influence on the magnitude, and sometimes even the sign, of fitted parameter values. Inspection of the TOS-abundance curves in Figure 28 reveals that the youngest stages for survey 2MF81 were the most variable of all estimated stage abundances.

The magnitudes of the estimates for SIGMA were also a function of the variability in the data from survey 2MF81. Best fitting estimates

of SIGMA were larger than would be suggested by the data from surveys 1MF81, 3MF81, and 4MF81 alone. The influence of survey 2MF81 can be inferred in the case of the unweighted residuals since the estimates for SIGMA were only 3.1 and 7.3 days (Table 13). The weighting of residuals reduced the importance of data obtained near peak spawning and, as a result, the data for survey 2MF81 did not exercise as great an influence on the magnitude of SIGMA, as is indicated by the more consistent and admissible estimates of 10.2 and 11.2 days.

The influence of survey 2MF81 can also be seen in the residuals for the other surveys (Figure 28). The residuals for 2MF81 were reduced by inflating the residuals for the off-peak surveys. The downward direction to residuals indicates a consistent overestimation of predicted total stage abundances. This suggests that an estimate of the duration of the spawning season was inflated as the fitting procedure attempted to accommodate the high variability in the stage abundance data for survey 2MF81. If the data from the off-peak surveys are considered to be truly representative of stage abundances at these dates of the spawning season, then the magnitude of SIGMA was smaller than indicated by the best fitting parameter estimates.

This consistent behavior in the directions of residuals was in part promoted by TERM3 of the compound error function in that a penalty was exacted if a predicted abundance was less than the corresponding observed abundance. However, this penalty does not account for the fact that all the residuals for these off-peak surveys were directed downward, and the operation of another systematic factor is indicated.

The large differences between the estimates of the daily mortality coefficient for the 1981 spawning season provided the most dramatic evidence of the inadequacies of the sample data, and thereby in sampling procedures. Regardless of whether residuals were weighted or unweighted, the mortality coefficients were largest for data set 1 and smallest for data set 2 (Table 13). This systematic behavior indicates that the two sets of data are not equally representative of

the age structure for walleye pollock eggs within the survey area. A closer examination of the formula for an observed total stage abundance, eq. 5.12, reveals that an observed abundance can be largely determined by a few samples which happened to be allocated to regions of the survey area and periods of the spawning season that had high egg concentrations; all further samples gathered during the quasi-synoptic surveys may have little influence on the magnitudes of the observed stage abundances.

The data set dependent behavior in the magnitudes of parameter estimates leads to the conclusion that the abundance estimates were not independent on a stage by stage basis, contrary to the assumed behavior, but were instead correlated with each other as a result of a factor that was not accounted for. The magnitude of the mortality coefficient was essentially dictated by the patterns of recent spawning by adults in the areas of a very few, very large egg collections. The local history of spawning in the vicinity of these few pivotal sampling stations determined the overall trend in the magnitudes of mean abundances. In the case of the upper plot of Figure 28, stations G022A-G024A of survey 2MF81 had the largest catches of all the egg data. Since spawning had recently begun in the vicinity of these stations (Appendix Figures A.1-A.3) and these data strongly influenced the magnitudes of total stage abundances, a large coefficient for daily mortality was generated to account for the apparently rapid decline in abundance with age. A much lower level of apparent mortality was obtained by using data set B (the lower plot of Figure 28). The catches at stations G089A-G091A of survey 2MF81 comprised the bulk of all eggs collected and the apparent history of spawning at these stations suggested that spawning had continued at a high level for a relatively long period of time (Appendix Figures A.17-A.19).

The apparent pattern of egg mortality is inextricably confounded by local spawning patterns if a few pivotal collections represent the bulk of the egg catches. As discussed in Chapter 4, the overriding influence of a few, very large, egg catches can be diminished if

sampling effort is increased in the areas of high egg abundance and proportionally less effort is allocated to areas of little apparent abundance.





## Chapter 6. Estimation of seasonal egg production and spawner biomass

### INTRODUCTION

Four general approaches have been used for the temporal integration of total daily egg abundance estimates. Data have been fitted to a parabola (English, 1963), fitted to an area beneath a normal curve (Saville, 1964), summed by trapezoidal integration (Simpson, 1959; Lockwood, et al., 1981), and summed by the method of cruise durations (Sette and Ahlstrom, 1948). English (1963) had only modest success fitting data to a parabola and did not attempt an estimate of total seasonal abundance. The normal distribution is an intuitively appealing candidate to describe the seasonal spawning curve, but Saville (1964) seems to be the only one who has attempted its use. Richardson (1981) employed both trapezoidal integration and the cruise duration method, and found that an estimate of seasonal egg production by the former method to be half as large as that of the latter. While both the method of trapezoids and the method of cruise durations are graphical approaches at heart, the interpretation of the latter as a stratified or a systematic sampling scheme has garnered increased attention (Taft, 1960; Pennington and Berrien, 1984) as it provides an analytical structure for the estimation of variance of the seasonal estimate.

There are perhaps two general approaches that have been of use in relating the abundance of spawning products to the size of the spawning stock. A measure of instantaneous egg abundance at some point during the spawning season may be estimated and converted to spawner biomass by appropriate biological factors (Parker, 1980; Picquelle and Hewitt, 1983, 1984; Hewitt, 1985; Picquelle and Stauffer, 1985). Alternatively, seasonal egg production may be estimated by integrating egg catches over the survey area (spatial integration) and the spawning season (seasonal integration), and the estimate for seasonal egg production is then converted to spawner biomass by appropriate biological factors (Saville, 1964, 1981). The 1981 egg surveys were designed such that

analytical models of the double integration type would be appropriate.

#### METHODS

Seasonal egg production was estimated under the modified mortality model of Chapter 5, and seasonal egg abundance was estimated by both the trapezoidal integration and the cruise duration methods using the total daily abundance estimates of Chapter 3. The seasonal egg abundance estimates by these latter two methods were not adjusted for egg mortality and were instead treated as conservative estimates of seasonal production, as is commonly done as an approximation (Sette, 1943; Ahlstrom, 1948; Sette and Ahlstrom, 1948; Ahlstrom and Ball, 1954; Cushing, 1957; Taft, 1960; Saville, 1964; Ciechomski and Capezzani, 1973; Tanaka, 1974; Richardson, 1981; Mason, et al., 1984).

#### Integrations over the spawning season

Estimates of total daily egg abundance were first associated with a date of the spawning season before performing seasonal integrations. Cruise midpoints were obtained as weighted averages of the local dates of sampling for each survey (eq. 5.2). Since most eggs were in an early stage of development, these dates corresponded to the dates that most eggs were captured during each survey.

Trapezoidal integration involves the summing of two or more trapezoidal areas, where each area represents the product of total daily egg abundance and an interval of the spawning season. To calculate the area of a trapezoid, the estimates of total daily egg abundance for the  $g$ th and the  $(g+1)$ th cruise were averaged and then multiplied by the intervening number of days between survey midpoints. These  $G-1$  determinations were then summed to form the seasonal egg production estimate:

$$(eq. 6.1) \quad P = \sum_{g=1}^{G-1} \left[ \frac{P_{g+1} + P_g}{2} (TOS_{g+1} - TOS_g) \right]$$

where

$P_g$  total daily egg abundance determined for the gth survey  
 TOS time of sampling, weighted mean local date of sampling  
 for a survey  
 G number of surveys conducted during the spawning season  
 P seasonal egg production.

Seasonal egg production was calculated from estimates of total daily egg abundance obtained under the SRS model for each survey (Table 11).

Under the cruise duration method, the estimate of total daily egg abundance is multiplied by an interval of the spawning season,  $CRUISEDUR_g$ . This interval was calculated as follows: 1. calculate the interval of time between occupancy of the first and last station of the gth cruise, 2. calculate one half the number of days intervening between the beginning of the gth cruise and the ending of the preceding (g-1)th cruise, 3. calculate one half the number of days between the ending of the gth cruise and the beginning of the following (g+1)th cruise, and 4. sum items 1, 2, and 3 for the gth cruise. The cruise duration for the first (or last) survey was obtained by doubling the following (or preceding) half period. Finally, seasonal egg production was calculated as:

$$(eq. 6.2) \quad P = \sum_{g=1}^G P_g \quad CRUISEDUR_g$$

where

$CRUISEDUR_g$  duration in days of the gth survey.

Seasonal egg production was calculated from estimates of total daily egg abundance obtained under the SRS model for each survey (Table 11).

The precision of the seasonal estimate for the cruise duration method was obtained by partitioning the spawning season into consecutive intervals and treating the estimate of total daily egg abundance during each of these periods as a randomly selected element from a finite population of such daily levels of total abundance. The variance for the estimate of total daily abundance for the gth survey was calculated as:

$$(eq. 6.3) \quad s^2(P_g) = AREA^2 \quad s^2(m_g)$$

where

AREA size of the survey area ( $1.596 \times 10^{10} \text{ m}^2$ )  
 $s^2(m_g)$  variance of the mean for the gth survey (eq. 3.2)  
 $s^2(P_g)$  variance for total daily egg abundance for the gth survey.

Estimates of the standard error of the mean for each survey were obtained from Table 6. The variance estimate for each total daily egg abundance was then extrapolated to the corresponding time stratum, and the square root of the sum of these values formed the standard error for the seasonal egg production estimate:

$$(eq. 6.4) \quad se(P) = \left[ \sum_{g=1}^G CRUISEDUR_g^2 s^2(P_g) \right]^{1/2}$$

where

se(P) standard error for seasonal egg production.

#### Estimation of spawner biomass

The numerical abundance of females was calculated from estimates of seasonal egg production and fecundity per average female:

$$(eq. 6.5) \quad NUM = P / F$$

where

F fecundity (eggs/catch-weighted female)  
 NUM numerical abundance of female spawners

Estimates of seasonal egg production were available from the method of cruise durations, trapezoidal integration, and the modified mortality equation. Fecundity per average female was calculated from a length-fecundity relationship for the Shelikof population (Miller, et al., 1986) and the length frequency distribution of animals captured in trawls conducted during the hydroacoustic surveys (Nunnallee, pers. commun.):

$$(eq. 6.6) \quad F = \sum_{l=1}^L F_l LFREQ_l$$

where

L maximum length for trawl-caught fish (cm)  
 $F_l$  fecundity of a female in the lth length class  
 $LFREQ_l$  percent of adults in the lth length class based on catches by research trawls.

The length frequency of adults was assumed to approximate the length frequency of females.

Biomass of spawners was estimated from numerical abundance of females, sex ratio, and a weight-length relationship for the Shelikof population (Miller, et al., 1986):

$$(eq. 6.7) \quad B = \frac{NUM}{SR} WT \quad FACTOR$$

where

SR            sex ratio, ratio of the number of females to adults.  
 WT            weight per average fish (g)  
 FACTOR       conversion factor (mt =  $10^6$  g)  
 B             biomass (mt).

The ratio of females to males was assumed to be 1:1, giving a sex ratio of 0.5. The length-weight relationship was assumed to be approximately similar for both sexes and the weight per average fish was calculated in the same manner as that for fecundity (eq. 6.6).

#### RESULTS

Table 14 summarizes seasonal egg production estimates obtained under the method of trapezoids and Table 15 summarizes those obtained under the cruise duration method. Estimates of seasonal egg production

=====  
 Table 14. Seasonal egg production during the 1981 spawning season (eggs/survey area/spawning season) by the method of trapezoidal integration. Statistics shown for the gth survey are the julian date upon which the survey was centered and  $P_g$ , the total daily egg abundance estimate. The integrated abundance values represent the product of the average total daily egg production from the gth and (g+1) surveys and the difference in days between the julian dates of these surveys. Seasonal egg abundance is the sum of integrated values.  
 =====

survey	julian date	$P(g)$ $\times 10^{10}$	integrated abundance $\times 10^{12}$
1MF81	74.8	4.	20.7
2MF81	90.1	267.	40.2
3MF81	118.3	18.	2.3
4MF81	141.1	2.	63.2

=====

Table 15. Seasonal egg production during the 1981 spawning season (eggs/survey area/spawning season) by the cruise duration method. Statistics shown for the gth survey are the first and last day of sampling (julian date); survey duration;  $P_g$ , total daily egg abundance;  $se(P_g)$ , standard deviation for the total. Also shown for the interval of the spawning season between the gth and (g+1)th surveys are egg production, standard error, and coefficient of variation. The final line of the Table also gives P, seasonal egg production;  $se(P)$ , standard deviation; and CV, coefficient of variation.

survey	julian date of survey (begin)(end)		survey duration (days)	$P_g$ $\times 10^{10}$	$se(P_g)$ $\times 10^{10}$	P $\times 10^{12}$	$se(P)$ $\times 10^{12}$	CV
1MF81	71	80	18.0	4.	2.22	0.72	0.40	56%
2MF81	89	97	22.5	267.	110.	60.1	25.	42%
3MF81	117	122	24.0	18.	2.15	4.3	0.52	12%
4MF81	140	145	23.0	2.	.35	0.46	0.08	17%
						65.6	26.	40%

varied by a factor of 4, ranging from a low of  $63 \times 10^{12}$  eggs by the method of trapezoidal integration to a high of  $264 \times 10^{12}$  eggs by the modified mortality equation (Table 16).

Table 16. Summary of seasonal egg production and spawner biomass estimates for walleye pollock during the 1981 spawning season.

method	seasonal egg production (eggs $\times 10^{12}$ )	spawner biomass (million mt)
trapezoidal integration (Simpson, 1959)	63.	.29
cruise duration method (Sette & Ahlstrom, 1948)	66.	.31 (40% CV)
modified mortality equation	264.	1.23
echo-integration (Nelson & Nunnallee, 1984)		3.8 (33% CV)

The estimate for fecundity was  $1.27 \times 10^5$  eggs/average female and the estimate for weight was 296.8 g/average adult. The estimates of spawner biomass ranged from 0.29 million metric tons based on the method of trapezoidal integration to 1.23 million mt based on the modified mortality equation. The total biomass of adult fish for the 1981 spawning season by echo integration was 3.77 million mt (Nelson and Nunnallee, 1985), which was 3-13 times greater than the ichthyoplankton-based estimates.

#### DISCUSSION

Representative samples of egg concentrations may not have been obtained if the sampling gear failed to sample the entire water column, and therefore production estimates may have been systematically reduced. The optimal target depth for double oblique sampling had not been firmly established at the time the 1981 ichthyoplankton surveys were conducted. Walleye pollock eggs in the Bering Sea are neustonic (Nishiyama and Haryu, 1981). Eggs in the Gulf of Alaska were initially thought to be within the upper 200 m; prior data on the vertical distribution of eggs around Kodiak Island (Kendall, et al.<sup>3</sup>) were not inconsistent with the hypothesis that eggs have a homogeneous distribution throughout the water column. Since bottom depths over much of Shelikof Strait range between 200-250 m, a 200 m target depth would then be sufficient to collect the bulk of the eggs to be found under such a distributional pattern. Subsequent experience has revealed that the depth distributions for eggs in the areas of maximum egg concentrations are principally from midwater to off bottom (Kim, 1987).

The seasonal egg production estimate produced by the method of trapezoids was similar to that obtained by means of the cruise duration method. However, Richardson (1981) found that the estimate by the

<sup>3</sup> Kendall, A.W., Jr., J.R. Dunn, and R.J. Wolotira, Jr. 1980. Zooplankton, including ichthyoplankton and decapod larvae, of the Kodiak Shelf. U.S. Dept. Commer., NWAF C Proc. Rep. 80-3, 393 p.

method of trapezoids to be half that obtained by the cruise duration method. Estimates of seasonal egg production can be either similar or differ markedly solely due to computational reasons. From a graphical point of view, similar portions of the seasonal spawning curve were evaluated by both methods and both exclude areas under the spawning curve that the other includes. Potential differences between the two methods can be minimized if cruise midpoints are equally spaced over the spawning season and if surveys are conducted in nearly equal intervals of time. In this case, an endpoint between intervals under the cruise duration method would be identical to a point corresponding to half the interval of a trapezoid. The 1981 estimates given by trapezoidal integration and the cruise duration method were nearly identical because surveys were fairly evenly spaced in time and because relatively little egg production was found during surveys other than survey 2MF81.

Both of these last two methods of temporal integration seem almost certain to lead to conservative estimates, assuming that estimates of daily egg production are not too different from true values. The method of trapezoids will underestimate seasonal egg production whenever sampling is not undertaken at or near the time of peak spawning. Errors under the cruise duration method arise not only from the failure to sample near the time of peak spawning, but also by the assignment of inappropriately long or short durations to estimates of daily egg production.

Seasonal egg production was largest for the modified mortality model, as anticipated, due to the projection of total daily stage abundances back to the seasonal production curve. However, the trend in stage abundances was not found to be exclusively a function of egg mortality. Instead, the trend for the 1981 surveys was confounded by local spawning patterns at a few pivotal sampling stations.





## Chapter 7. Recommendations for survey design and analysis of future sampling efforts

The principle objectives of the 1981 hydroacoustic/trawl and ichthyoplankton surveys were the detection of spawning activity, the qualitative description of the pattern of egg and adult distributions, and preliminary assessments of population sizes. The estimation of population parameters was properly relegated to a secondary objective due to the exploratory nature of this initial sampling program. The estimation of these parameters is, however, intended to assume a higher priority as the necessary sampling and analytical requirements are determined. These examinations represent the first attempt at specifying the necessary sampling procedures and the analytical models required to accomplish this end.

The 1981 surveys in Shelikof Strait have contributed substantially to the qualitative understanding of the spatial and temporal patterns of abundance for the walleye pollock egg population. As an outgrowth of these preliminary assessments, a number of improvements to sampling technique and statistical analyses can be recognized and these suggested improvements should contribute substantially to the quality of biological information to be derived from ichthyoplankton surveys.

The search for spawning grounds, as indicated by the presence or absence of eggs in plankton collections, is most efficiently implemented by a regular distribution of stations throughout the survey area. Such a distribution of stations, however, is not an efficient means of making a quantitative description of the abundance of spawning products. Given the high heterogeneity in egg catches that was observed near the time of peak spawning and given the operational limits to the number of samples that can be taken, the qualitative goal of defining the location and spatial extent of spawning activity may be incompatible with the quantitative goal of estimating seasonal egg production and spawner biomass.

The systematic distribution of sampling effort over the survey

area was a useful means of locating concentrations of spawning. As a consequence of this design, however, few samples were allocated toward defining the egg abundance gradient in areas of extremely high and rapidly changing abundance levels. It is now recognized that the definition of this gradient on a stage by stage basis is an essential requirement for the estimation of total stage abundance, seasonal production, and seasonal mortality.

By far the most significant step toward improvements in the reliability of estimation procedures involves the concentration of sampling effort in areas of moderate to high egg abundance. Representative estimates of mean daily stage abundances can only be achieved within the present level of survey resources if sampling is concentrated in the regions for which egg abundance is greatest. As a rule of thumb, perhaps approximately one-half to two-thirds of available sampling effort should be allocated to these regions. Simply increasing sampling effort will be considerably less effective. The confounding of mortality estimation by local spawning events should also be reduced by a greater intensity of sampling where the animals occur in greatest numbers.

Several methods for the estimation of seasonal egg production from estimates of total stage abundance have been considered. If possible, a number of rapid surveys should be conducted near the expected time of peak spawning. It is far more critical to define the magnitude of peak spawning than the duration of the spawning season. When the spawning peak is confined to a limited period of time, it can be easily missed. Sampling of off-peak spawning adds little to the definition of the magnitude of seasonal egg production unless a number of assumptions are permitted concerning the shape of the spawning function and the placement of the surveys with respect to the date of peak spawning. Furthermore, estimation of spawning duration may be inferred from sources other than ichthyoplankton data, such as ovary maturation data and records of the historical duration of spawning activity.

The bulk of spawners appear to migrate up Shelikof Strait through regions of greatest bathymetric depth and are channeled towards a constricted region off Cape Kekurnoi within about two or three weeks of crossing the sill to the southwest of the Chirikof Islands (Kim, 1987). Egg surveys should proceed in the opposite direction down the Strait, from the northeast to the southwest, in order to avoid resampling the recently released eggs from these highly mobile concentrations of spawners.

Results of these analyses indicate that the precision and accuracy of seasonal production estimates can be substantially improved, without increased cost, by an informed definition of trends in abundance over the area and duration of spawning. The fitting of catch data on a stage by stage basis to a model incorporating both spatial and random components is probably the most important analytical step yet required for the minimum variance estimation of egg abundance within the survey area. These data can then be more successfully employed in mortality estimation.







## Literature Cited

- Agterberg, F.P. 1974. Geomathematics: Mathematical Background and Geo-Science Applications. Elsevier Scientific Publ. Co., New York, N.Y., 596 p.
- Ahlstrom, E.H. 1948. A record of pilchard eggs and larvae collected during surveys made in 1939 to 1941. U.S. Fish Wildlife Svc., Spec. Sci. Rep. No. 54., 82 p.
- Ahlstrom, E.H. and O.P. Ball. 1954. Description of eggs and larvae of jack mackerel (Trachurus symmetricus) and distribution and abundance of larvae in 1950 and 1951. Fish. Bull., U.S. 56:207-245.
- Aitchison, J. 1955. On the distribution of a positive random variable having a discrete probability mass at the origin. J. Am. Stat. Assoc. 50:901-908.
- Aitchison, J. and J.A.C. Brown. 1957. The Lognormal Distribution: with Special Reference to its Uses in Economics. Cambridge Univ. Press, 176 p.
- Anscombe, F.J. 1948. The transformation of Poisson, binomial and negative-binomial data. Biometrika 35:246-254.
- Anscombe, F.J. 1949. The statistical analysis of insect counts based on the negative binomial distribution. Biometrics 5:165-173.
- Anscombe, F.J. 1950. Sampling theory of the negative binomial and logarithmic series distributions. Biometrics 37:358-382.
- Bagenal, M. 1955. A note on the relations of certain parameters following a logarithmic transformation. J. Mar. Biol. Assoc. U.K. 34:289-296.
- Bakkala, R., T. Maeda and G. McFarlane. 1984. Distribution and stock structure of pollock (Theragra chalcogramma) in the North Pacific Ocean. p. 3-20. IN: D.H. Ito (editor), Proceedings of the Workshop on Walleye Pollock and its Ecosystem in the Eastern Bering Sea. U.S. Dept. Commer., NOAA Tech. Memo. NMFS F/NWC-62.
- Bakun, A. 1985. Comparative studies and the recruitment problem: searching for generalizations. Calif. Coop. Oceanic Fish. Invest. Rep. 26:30-40.
- Berrien, P.L., N.A. Naplin and M.R. Pennington. 1981. Atlantic mackerel, Scomber scombrus, egg production and spawning population estimates for 1977 in the Gulf of Maine, Georges Bank, and Middle Atlantic Bight. Rapp. P.-v. Reun. Cons. int. Explor. Mer 178:279-288.
- Bissel, A.F. 1972a. A negative binomial model with varying element sizes. Biometrika 59:435-441.

- Bissel, A.F. 1972b. Another negative binomial model with varying element sizes. *Biometrika* 59:691-693.
- Bliss, C.I. and R.A. Fisher. 1953. Fitting the negative binomial distribution to biological data and note on the efficient fitting of the negative binomial. *Biometrics* 9:176-200.
- Ciechomski, J.D. and D.A. Capezzani. 1973. Studies on the evaluation of the spawning stocks of the Argentinean anchovy, Engraulis anchoita, on the basis of egg surveys. *Rapp. P.-v. Reun. Cons. int. Explor. Mer* 164:293-301.
- Cochran, W.G. 1977. *Sampling Techniques*. John Wiley & Sons, New York, N.Y., 428 p.
- Cushing, D.H. 1957. The number of pilchards in the Channel. *Fish. Invest.*, London. Ser 2. 21:1-27.
- Elliott, J.M. 1979. Some Methods for the Statistical Analysis of Samples of Benthic Invertebrates. Freshwater Biological Association, Scientific Publ. No. 25., 160 p.
- English, T.S. 1963. A theoretical model for estimating the abundance of planktonic fish eggs. *Rapp. P.-v. Reun. Cons. int. Explor. Mer* 155:174-182.
- Fisher, R.A. 1941. The negative binomial distribution. *Annals of Eugenics* 11(part 2):182-187.
- Haldane, J.B.S. 1941. The fitting of binomial distributions. *Annals of Eugenics* 11(part 2):179-181.
- Hamai, I., K. Kyushin and T. Kinoshita. 1971. Effect of temperature on the body form and mortality in the developmental and early larval stages of the Alaska pollack, Theragra chalcogramma (Pallas). *Bull. Fac. Fish., Hokkaido Univ.* 22:11-29.
- Harding, D. and J.W. Talbot. 1973. Recent studies on the eggs and larvae of the plaice (Pleuronectes platessa L.) in the Southern Bight. *Rapp. P.-v. Reun. Cons. int. Explor. Mer* 164:261-269.
- Hewitt, R.P. 1985. The 1984 spawning biomass of the northern anchovy. *Calif. Coop. Oceanic Fish. Invest. Rep.* 26:17-25.
- Hewitt, R.P. and G.D. Brewer. 1983. Nearshore production of young anchovy. *Calif. Coop. Oceanic Fish. Invest. Rep.* 24:235-244.
- Hewitt, R.P. and R.D. Methot, Jr. 1982. Distribution and mortality of northern anchovy larvae in 1978 and 1979. *Calif. Coop. Oceanic Fish. Invest. Rep.* 23:226-245.

- Hughes, S.E. and G. Hirschhorn. 1979. Biology of walleye pollock, Theragra chalcogramma, in the western Gulf of Alaska, 1973-1975. Fish. Bull., U.S. 77:263-274.
- IMSL. 1984. IMSL User's Manual: Problem Solving Software System for Mathematical and Statistical FORTRAN Programming. International Mathematical and Statistical Libraries, Houston, Texas.
- Kendall, A.W., Jr. 1981. Early life history of Eastern North Pacific fishes in relation to fishery investigations. Wash. Sea Grant Tech. Rep. 81-3, 7 p.
- Kim, S. 1987. Spawning behavior and early life history of walleye pollock, Theragra chalcogramma, in Shelikof Strait, Gulf of Alaska, in relation to oceanographic factors. Ph. D. Dissertation, Univ. of Washington, Seattle, 221 p.
- Kramer, D., M.J. Kalin, E.G. Stevens, J.R. Thrailkill and J.R. Zweifel. 1972. Collecting and processing data on fish eggs and larvae in the California Current region. NOAA Tech. Rep. NMFS CIRC-370, 38 p.
- Kowalik, J. and M.R. Osborne. 1968. Methods for Unconstrained Optimization Problems. American Elsevier Publ. Co., New York, N.Y., 148 p.
- Lasker, R. 1964. An experimental study of the effect of temperature on the incubation time, development, and growth of Pacific sardine embryos and larvae. Copeia 2:399-405.
- Lo, N.C.H. 1986. Modeling life-stage-specific instantaneous mortality rates, an application to northern anchovy, Engraulis mordax, egg and larvae. Fish. Bull., U.S. 84:395-407.
- Lockwood, S.L., J.H. Nichols and W.A. Dawson. 1981. The estimation of a mackerel (Scomber scombrus L.) spawning stock size by plankton survey. J. Plankton Res. 3:217-233.
- Lough, R.G., G.R. Bolz, M. Pennington and M.D. Grosslein. 1985. Larval abundance and mortality of Atlantic herring (Clupea harengus L.) spawned in the Georges Bank and Nantucket Shoals areas, 1971-78 seasons, in relation to spawning stock size. J. Northw. Atl. Fish. Sci. 6:21-35.
- Marr, J.C. 1956. The "critical period" in the early life history of marine fishes. J. Cons. 21:160-170.
- Mason, J.C., A.C. Phillips and O.D. Kennedy. 1984. Estimating the spawning stocks of Pacific hake (Merluccius productus) and walleye pollock (Theragra chalcogramma) in the Strait of Georgia, B.C. from their released egg production. Can. Tech. Rep. Fish. Aquat. Sci. No. 1289, 51 p.

- May, R.C. 1974. Larval mortality in marine fishes and the critical period concept. p 3-19. In: J.H.S. Blaxter (editor), *The Early Life History of Fish*. Springer-Verlag, New York, N.Y.
- Miller, B.S., D.R. Gunderson, D. Glass, D.B. Powell and B.A. Megrey. 1986. Fecundity of walleye pollock (*Theragra chalcogramma*) from the Shelikof Strait, Gulf of Alaska. Univ. Washington, School of Fisheries, Fish. Res. Inst. Final Rep. FRI-UW-8608, 40 p.
- Milne, A. 1959. The centric systematic area-sample treated as a random sample. *Biometrics* 15:270-297.
- Nelson, M.O. and E.P. Nunnallee. 1985. Acoustic-midwater trawl surveys of spawning walleye pollock in the Shelikof Strait region, 1980-81 and 1983-84. p. 179-206. In: R.L. Major (editor), *Condition of Groundfish Resources of the Gulf of Alaska Region*. U.S. Dept. Commer., NOAA Tech. Memo. NMFS F/NWC-80.
- Nishiyama, T. and T. Haryu. 1981. Distribution of walleye pollock eggs in the uppermost layer of the southeastern Bering Sea. p. 993-1012. In: D.H. Hood and J.A. Calder (editors), *The Eastern Bering Sea Shelf: Oceanography and Resources, Vol II*. Univ. of Wash. Press, Seattle.
- Nishiyama, T., K. Hirano and T. Haryu. 1986. The early life history and feeding habits of larval walleye pollock *Theragra chalcogramma* (Pallas) in the southeast Bering Sea. p. 177-227. In: *Symposium on Biology, Stock Assessment, and Management of Pollock, Pacific cod, and Hake in the North Pacific Region*. Int. North. Pac. Fish. Comm., Bull. No. 45.
- Parker, K. 1980. A direct method for estimating northern anchovy, *Engraulis mordax*, spawning biomass. *Fish. Bull.*, U.S. 78:541-544.
- Pennington, M. 1983. Efficient estimators of abundance, for fish and plankton surveys. *Biometrics* 39:281-286.
- Pennington, M. and P. Berrien. 1984. Measuring the precision of estimates of total egg production based on plankton surveys. *J. Plankton. Res.* 6:869-879.
- Picquelle, S.J. and R.P. Hewitt. 1983. The northern anchovy spawning biomass for the 1982-1983 California fishing season. *Calif. Coop. Oceanic Fish. Invest. Rep.* 24:16-28.
- Picquelle, S.J. and R.P. Hewitt. 1984. The 1983 spawning biomass of the northern anchovy. *Calif. Coop. Oceanic Fish. Invest. Rep.* 25:16-27.

- Picquelle, S. and G. Stauffer. 1985. Parameter estimation for an Egg Production Method of northern anchovy biomass assessment. p 7-15. In: R. Lasker (editor), An egg production method for estimating spawning biomass of pelagic fish: Application to the northern anchovy, Engraulis mordax. U.S. Dept. Commer., NOAA Tech. Rep. NMFS 36.
- Posgay, J.A. and R.R. Marak. 1980. The MARMAP bongo zooplankton samplers. J. Northw. Atl. Fish. Sci. 1:91-99.
- Richardson, S.L. 1981. Spawning biomass and early life of northern anchovy, Engraulis mordax, in the northern subpopulation off Oregon and Washington. Fish. Bull., U.S. 78:855-876.
- Ripley, B.D. 1981. Spatial statistics. John Wiley & Sons, New York, N.Y., 252 p.
- Salveson, S.J. and M.S. Alton. 1976. Pollock (Family Gadidae). p. 369-381. In: W.T. Pereyra, J.E. Reeves and R. Bakkala (editors), Demersal fish and Shellfish Resources of the Eastern Bering Sea in the Baseline Year 1975. U.S. Dept. Commer., Proc. Rep.
- Saville, A. 1964. Estimation of the abundance of a fish stock from egg and larval surveys. Rapp. P.-v. Reun. Cons. int. Explor. Mer 155:164-170.
- Saville, A. 1981. The estimation of spawning stock size from fish egg and larval surveys. Rapp. P.-v. Reun. Cons. int. Explor. Mer 178:268-278.
- Sette, O.E. 1943. Biology of the Atlantic mackerel (Scomber scombrus) of North America. Part 1: Early life history, including growth, drift, and mortality of the egg and larval populations. Fish. Bull., U.S. 38:149-237.
- Sette, O.E. and E.H. Ahlstrom. 1948. Estimations of abundance of the eggs of the Pacific pilchard (Sardinops caerulea) off southern California during 1940 and 1941. J. Mar. Res. 7:511-542.
- Sherman, K., R. Lasker, W. Richards and A.W. Kendall, Jr. 1983. Ichthyoplankton and fish recruitment studies in large marine ecosystems. Mar. Fish. Rev. 45:1-25.
- Simpson, A.C. 1959. The spawning of the plaice (Pleuronectes platessa) in the North Sea. Fish. Invest., London. Ser 2, 22(7):1-111.
- Smith, G.B. 1981. The biology of walleye pollock. p. 527-551. In: D.W. Hood and J.A. Calder (editors), The Eastern Bering Sea Shelf: Oceanography and Resources, Vol I. U.S. Dept. Commer., Nat. Ocean. Atmos. Admin., Office Mar. Poll. Assess.

Smith, P.E. and R.P. Hewitt. 1985. Sea survey design and analysis for an egg production method of anchovy biomass. p 17-26. In: R. Lasker (editor), An egg production method for estimating spawning biomass of pelagic fish: Application to the northern anchovy, Engraulis mordax, U.S. Dept. Commer., NOAA Tech. Rep. NMFS 36.

Smith, P.E. and S.L. Richardson. 1977. Standard techniques for pelagic fish egg and larva surveys. FAO Fish. Tech. Paper No. 175, 100 p.

Spendley, W., G.R. Hext and F.R. Himsforth. 1962. Sequential application of simplex designs in optimization and evolutionary operation. Technometrics 4:441-461.

Sundby, S. and P. Solemdal. 1984. The egg production of Arcto-Norwegian cod (Gadus morhua L.) in the Lofoten area estimated by egg surveys. p. 113-135. In: O.R. Godo and S. Tilseth (editors), The proceedings of the Soviet-Norwegian symposium on reproduction and recruitment of Arctic cod, Leningrad, 26-30 September, 1983, Institute of Mar. Res., Bergen, Norway.

Taft, B.A. 1960. A statistical study of the estimation of abundance of sardine (Sardinops caerulea) eggs. Limnology and Oceanography 5:245-264.

Tanaka, S. 1974. Significance of egg and larval surveys in the studies of population dynamics of fish. p. 151-157. In: J.H.S. Blaxter (editor), The Early Life History of Fish, Springer-Verlag, New York, N.Y.

Thompson, H.R. 1951. Truncated lognormal distributions: I. solution by moments. Biometrika 38:414-422.

Thompson, J.M. 1981. Preliminary report on the population biology and fishery of walleye pollock (Theragra chalcogramma) off the Pacific coast of Canada. Can. Tech. Rep. Fish. Aquatic Sci., No. 1031, 103 p.

Traynor, J.J. 1986. Midwater abundance of walleye pollock in the eastern Bering Sea, 1979 and 1982. p. 121-135. In: Symposium of Biology, Stock Assessment, and Management of Pollock, Pacific Cod, and Hake in the North Pacific Region, Int. North Pac. Comm., Bull. No. 45.

Zver'kova, L.M. 1974. Maturation, fecundity and spawning grounds of the walleye pollock (Theragra chalcogramma) in the northeast of the Sea of Japan. J. Ichthyol. 17:219-231.

Zweifel, J.R. and R. Lasker. 1976. Prehatch and posthatch growth of fishes - a general model. Fish. Bull., U.S. 74:609-621.

Zweifel, J.R. and P.E. Smith. 1981. Estimates of abundance and mortality of larval anchovies (1951-75): application of a new method. Rapp. P.-v. Reun. Cons. int. Explor. Mer 178:248-259.





Appendix A. Age distributions for eggs of walleye pollock, Theragra chalcogramma, on a catch by catch basis

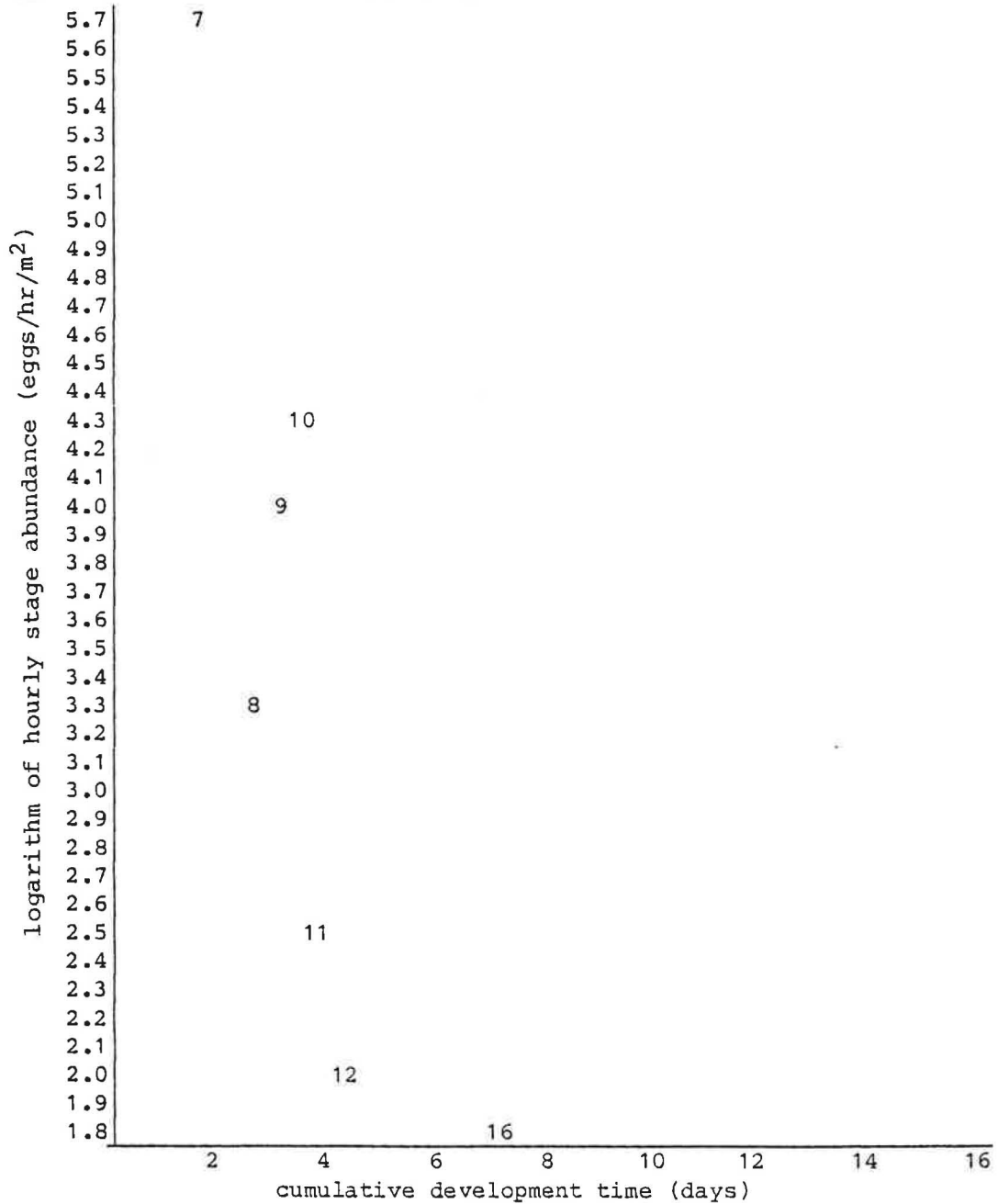
Station abundance-age plots were constructed with the logarithm of hourly stage abundance (eq. 2.8) on the ordinate and age on the abscissa. Abundances were calculated to the nearest tenth of a log cycle and plotted against the cumulative development time to the corresponding stage midpoint (eq. 2.3) expressed in days. The range of the ordinate is shown only between the highest and lowest values for the observed log hourly stage abundances. The plotted position for a developmental stage was identified by the stage number. No label was plotted for an age group if no eggs were found for that group in the staged subsample.

Amplifying data given above a station age plot include: cruise identifier; station identifier; nominal station temperature; local julian day and time of sampling; number of eggs from the subsample of each catch that were assigned to stages 1-21; catch (number of eggs in the sample); and standardized catch.

A table of amplifying data occurs on the page following each station abundance-age plot. The additional data on a stage by stage basis are cumulative development time in hours at the station temperature for stage midpoint and endpoint; stage duration in hours; stage frequency for the subsample; stage abundance (eggs/m<sup>2</sup>); stage abundance per hour of stage duration; and natural logarithm of hourly abundance. Any difference between this last tabulated value and the ordinate value of the plotted label is due to rounding of the former.



survey	station	temp	julian	local	staged(21)	catch	#/m <sup>2</sup>
2MF81	G022A	4.9	91	1047	100	15123	10512.1



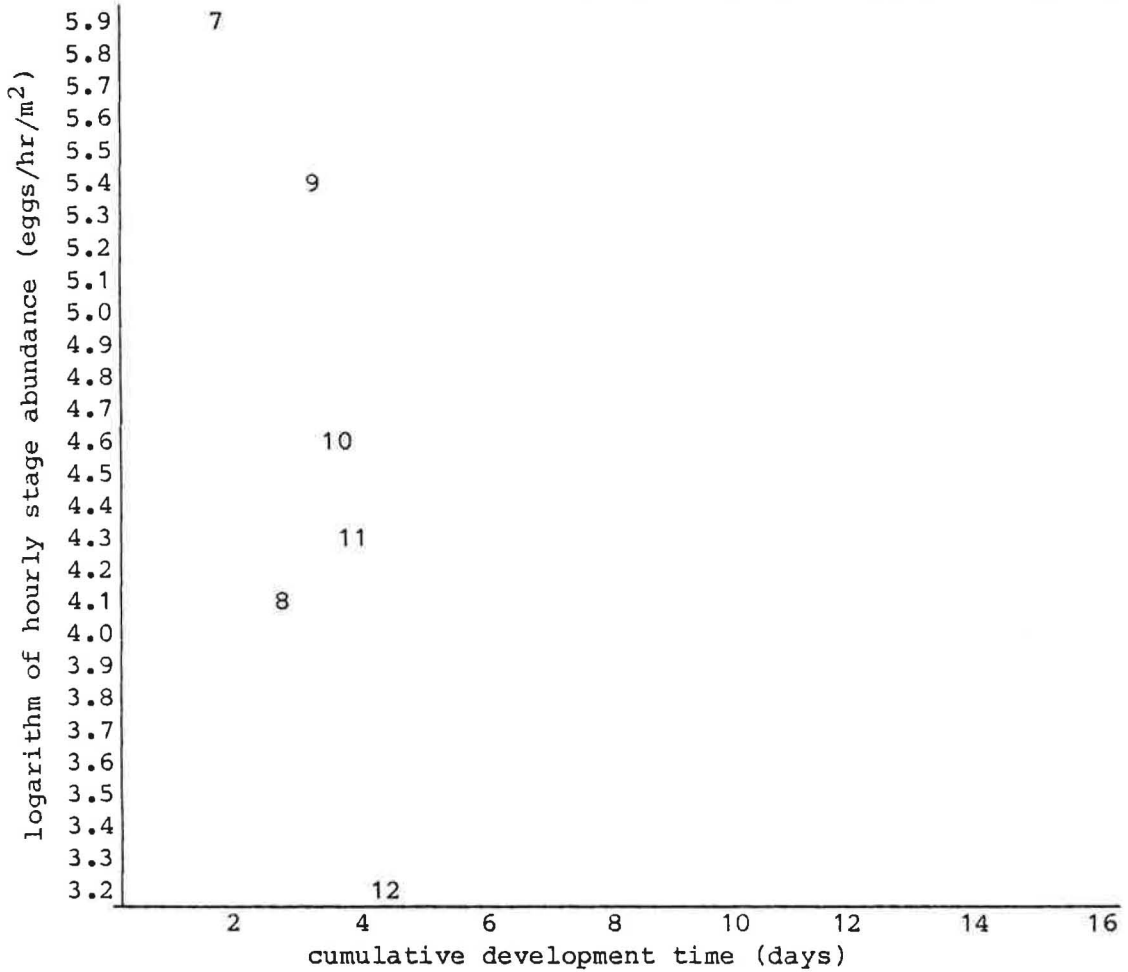
Appendix Figure A.1. Station abundance-age plot for eggs of walleye pollock obtained at station G022A of survey 2MF81. The logarithms of hourly stage abundances are plotted against the cumulative development times to stage midpoints. Each stage is identified by a stage number. See Appendix Table A.1 for intermediate values in the computations.

=====  
 Appendix Table A.1. Intermediate values in the calculations of average hourly stage abundance for eggs of walleye pollock obtained at station G022A of survey 2MF81.  
 =====

stage	mid	end	length	n staged	#/m <sup>2</sup>	#/hr/m <sup>2</sup>	ln(#/hr/m <sup>2</sup> )
1	2.5	5.1	5.1	0	0.0	0.0	0.0
2	5.8	6.6	1.5	0	0.0	0.0	0.0
3	7.8	9.1	2.6	0	0.0	0.0	0.0
4	9.9	10.6	1.5	0	0.0	0.0	0.0
5	12.1	13.6	3.0	0	0.0	0.0	0.0
6	18.5	23.3	9.7	0	0.0	0.0	0.0
7	37.9	52.5	29.1	79	8304.6	285.2	5.7
8	62.0	71.5	19.1	5	525.6	27.6	3.3
9	77.3	83.1	11.6	6	630.7	54.5	4.0
10	87.9	92.8	9.7	7	735.8	76.2	4.3
11	97.1	101.5	8.7	1	105.1	12.0	2.5
12	108.5	115.6	14.1	1	105.1	7.5	2.0
13	123.6	131.6	16.0	0	0.0	0.0	0.0
14	140.8	149.9	18.3	0	0.0	0.0	0.0
15	158.6	167.3	17.4	0	0.0	0.0	0.0
16	176.1	184.9	17.6	1	105.1	6.0	1.8
17	191.6	198.3	13.4	0	0.0	0.0	0.0
18	213.2	228.1	29.8	0	0.0	0.0	0.0
19	246.6	265.1	36.9	0	0.0	0.0	0.0
20	277.6	290.0	25.0	0	0.0	0.0	0.0
21	331.2	372.4	82.4	0	0.0	0.0	0.0

=====

survey	station	temp	julian	local	staged(21)	catch	#/m <sup>2</sup>
2MF81	G023A	4.9	91	1205	100	27148	16769.6



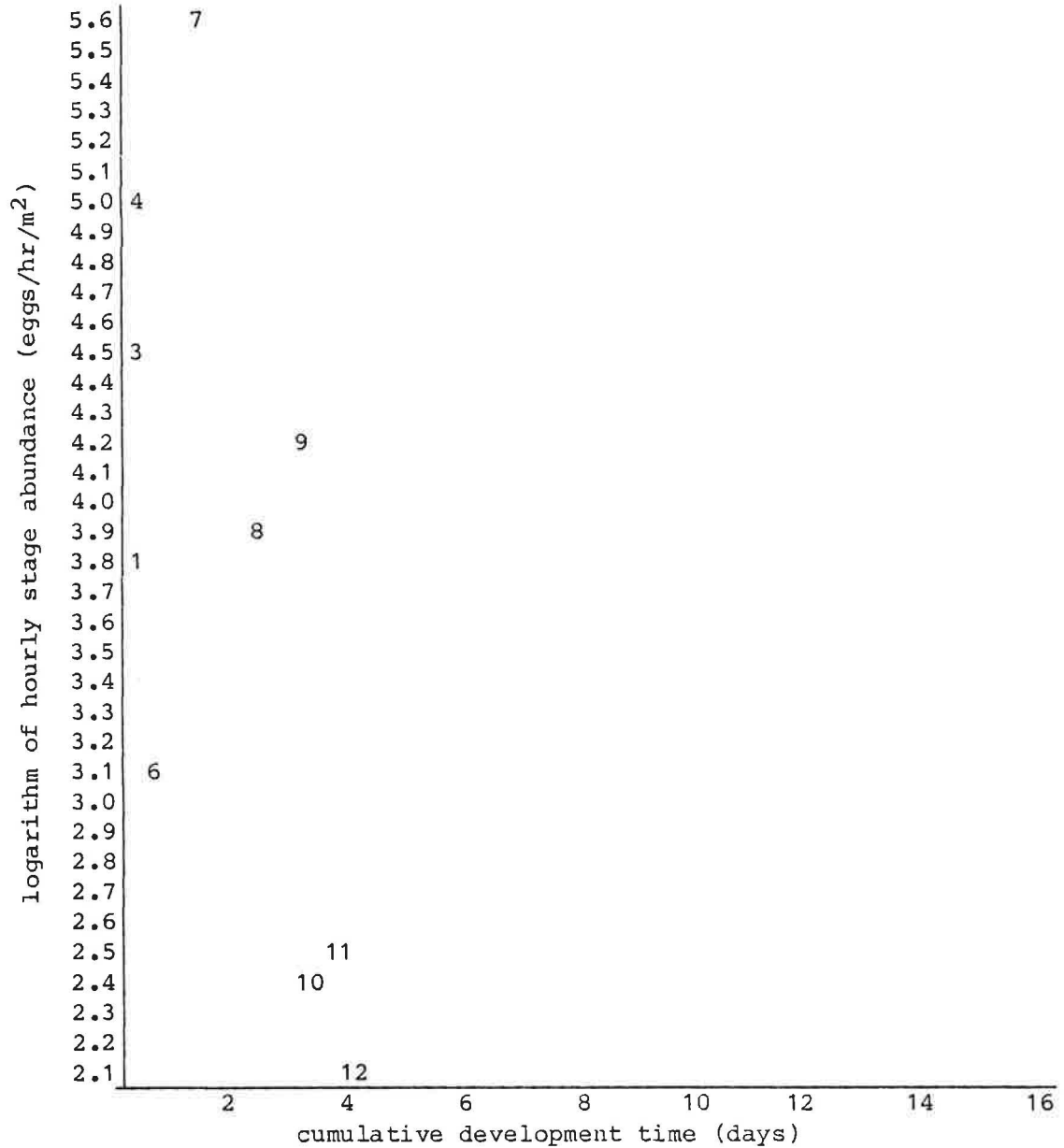
Appendix Figure A.2. Station abundance-age plot for eggs of walleye pollock obtained at station G023A of survey 2MF81. The logarithms of hourly stage abundances are plotted against the cumulative development times to stage midpoints. Each stage is identified by a stage number. See Appendix Table A.2 for intermediate values in the computations.

=====  
 Appendix Table A.2. Intermediate values in the calculations of average hourly stage abundance for eggs of walleye pollock, Theragra chalcogramma, from the bongo sample obtained at station G023A of survey 2MF81.  
 =====

stage	mid	end	length	n staged	#/m <sup>2</sup>	#/hr/m <sup>2</sup>	ln(#/hr/m <sup>2</sup> )
1	2.5	5.1	5.1	0	0.0	0.0	0.0
2	5.8	6.6	1.5	0	0.0	0.0	0.0
3	7.8	9.1	2.6	0	0.0	0.0	0.0
4	9.9	10.6	1.5	0	0.0	0.0	0.0
5	12.1	13.6	3.0	0	0.0	0.0	0.0
6	18.5	23.3	9.7	0	0.0	0.0	0.0
7	37.9	52.5	29.1	66	11067.9	380.1	5.9
8	62.0	71.5	19.1	7	1173.9	61.6	4.1
9	77.3	83.1	11.6	15	2515.4	217.3	5.4
10	87.9	92.8	9.7	6	1006.2	104.1	4.6
11	97.1	101.5	8.7	4	670.8	76.8	4.3
12	108.5	115.6	14.1	2	335.4	23.8	3.2
13	123.6	131.6	16.0	0	0.0	0.0	0.0
14	140.8	149.9	18.3	0	0.0	0.0	0.0
15	158.6	167.3	17.4	0	0.0	0.0	0.0
16	176.1	184.9	17.6	0	0.0	0.0	0.0
17	191.6	198.3	13.4	0	0.0	0.0	0.0
18	213.2	228.1	29.8	0	0.0	0.0	0.0
19	246.6	265.1	36.9	0	0.0	0.0	0.0
20	277.6	290.0	25.0	0	0.0	0.0	0.0
21	331.2	372.4	82.4	0	0.0	0.0	0.0

=====

survey	station	temp	julain	local	staged(21)	catch	#/m <sup>2</sup>
2MF81	G024A	5.3	91	1335	99	17812	10455.1



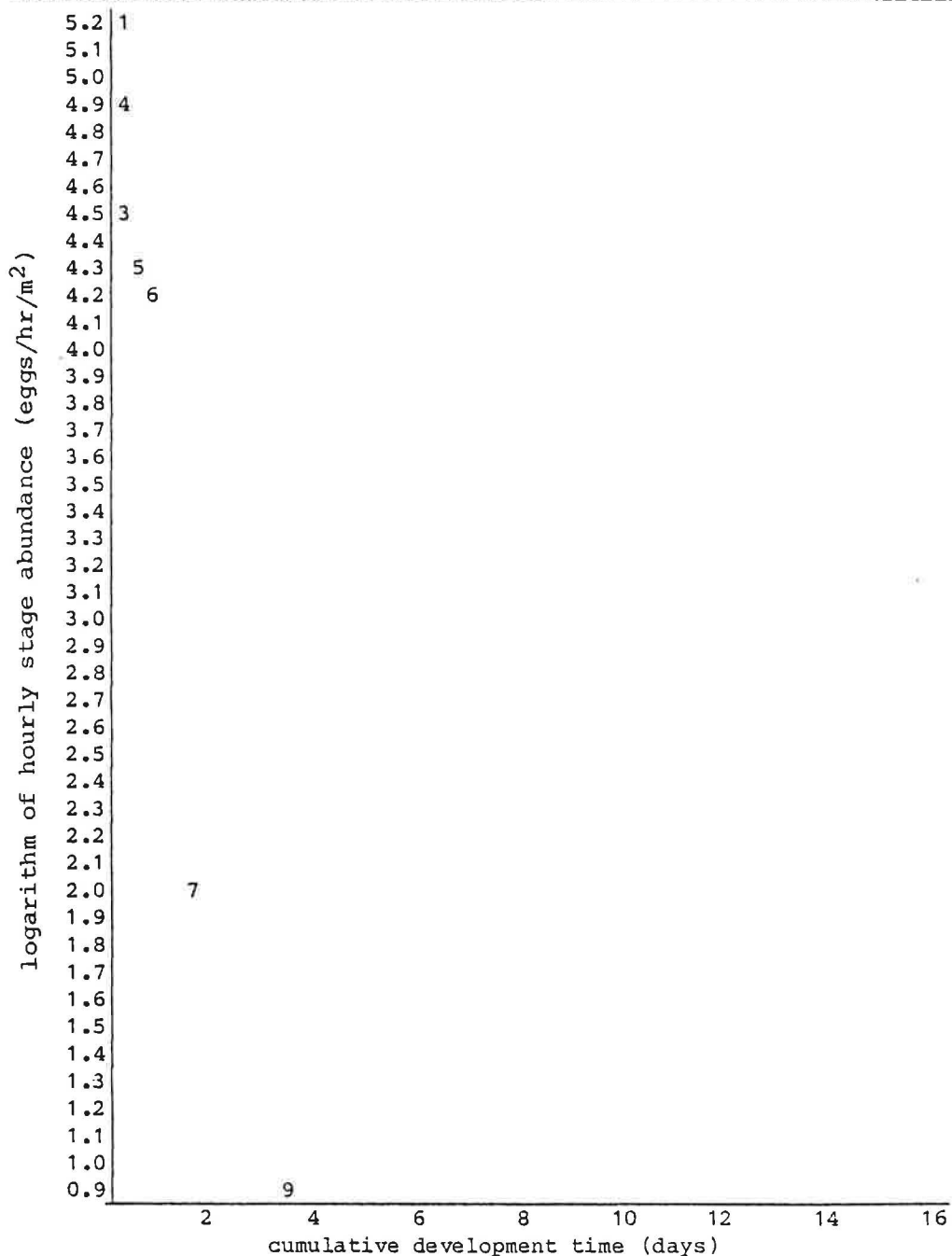
Appendix Figure A.3. Station abundance-age plot for eggs of walleye pollock obtained at station G024A of survey 2MF81. The logarithms of hourly stage abundances are plotted against the cumulative development times to stage midpoints. Each stage is identified by a stage number. See Appendix Table A.3 for intermediate values in the computations.

=====  
 Appendix Table A.3. Intermediate values in the calculations of average hourly stage abundance for eggs of walleye pollock obtained at station G024A of survey 2MF81.  
 =====

stage	mid	end	length	n staged	#/m <sup>2</sup>	#/hr/m <sup>2</sup>	ln(#/hr/m <sup>2</sup> )
1	2.4	4.9	4.9	2	211.2	43.5	3.8
2	5.6	6.3	1.4	0	0.0	0.0	0.0
3	7.5	8.8	2.5	2	211.2	85.8	4.5
4	9.5	10.2	1.4	2	211.2	149.0	5.0
5	11.6	13.1	2.9	0	0.0	0.0	0.0
6	17.7	22.4	9.4	2	211.2	22.6	3.1
7	36.4	50.4	28.0	72	7603.7	271.8	5.6
8	59.6	68.7	18.3	9	950.5	51.9	3.9
9	74.3	79.8	11.1	7	739.2	66.5	4.2
10	84.5	89.1	9.3	1	105.6	11.4	2.4
11	93.3	97.5	8.4	1	105.6	12.6	2.5
12	104.3	111.1	13.5	1	105.6	7.8	2.1
13	118.8	126.5	15.4	0	0.0	0.0	0.0
14	135.2	144.0	17.6	0	0.0	0.0	0.0
15	152.4	160.8	16.7	0	0.0	0.0	0.0
16	169.2	177.7	16.9	0	0.0	0.0	0.0
17	184.1	190.6	12.9	0	0.0	0.0	0.0
18	204.9	219.2	28.6	0	0.0	0.0	0.0
19	236.9	254.7	35.5	0	0.0	0.0	0.0
20	266.7	278.7	24.0	0	0.0	0.0	0.0
21	318.2	357.8	79.1	0	0.0	0.0	0.0

=====

survey	station	temp	julian	local	staged(21)	catch	#/m <sup>2</sup>
2MF81	G025A	4.4	91	1450	88	4076	2607.5

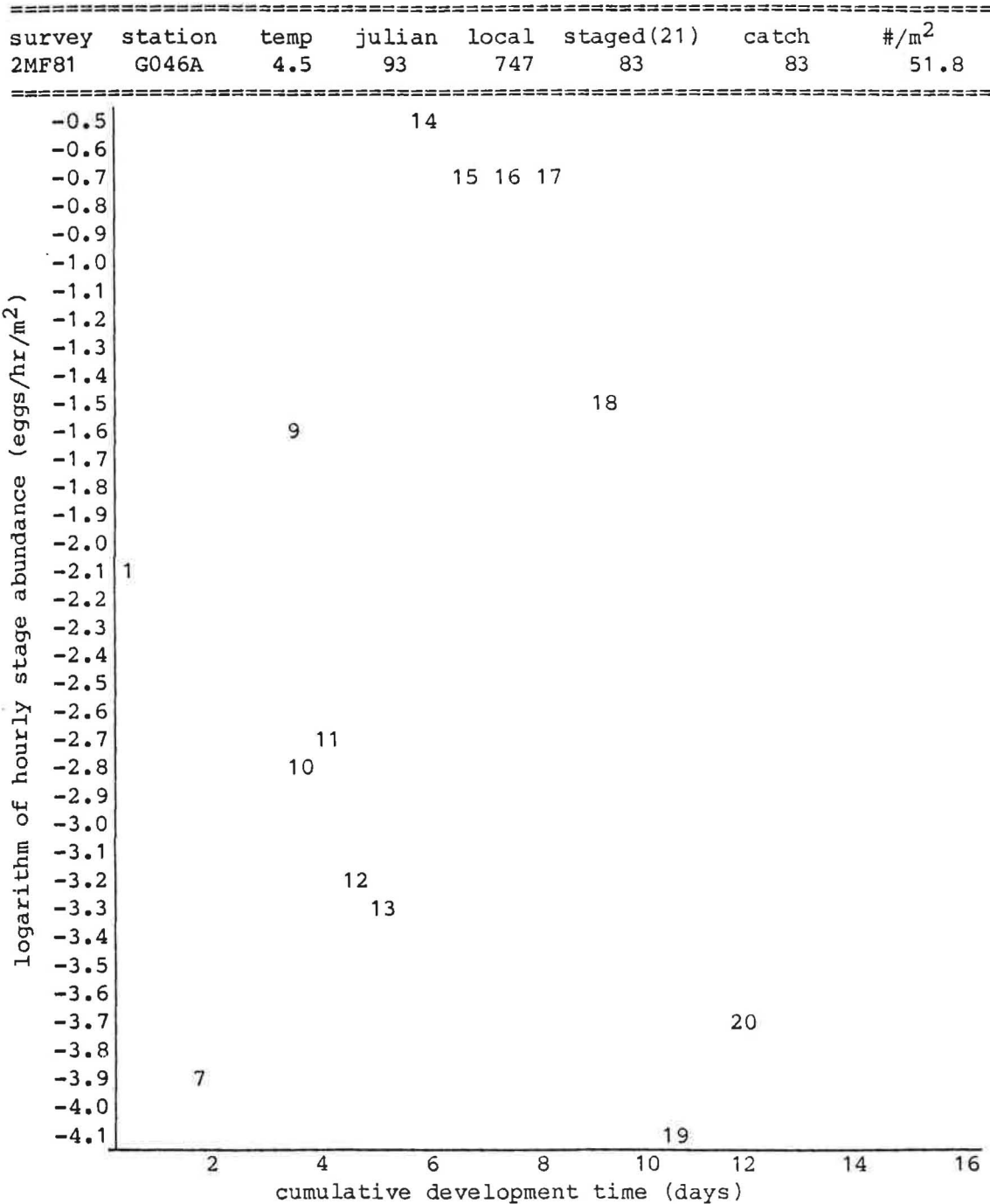


Appendix Figure A.4. Station abundance-age plot for eggs of walleye pollock obtained at station G025A of survey 2MF81. The logarithms of hourly stage abundances are plotted against the cumulative development times to stage midpoints. Each stage is identified by a stage number. See Appendix Table A.4 for intermediate values in the computations.

=====  
 Appendix Table A.4. Intermediate values in the calculations of average hourly stage abundance for eggs of walleye pollock obtained at station G025A of survey 2MF81.  
 =====

stage	mid	end	length	n staged	#/m <sup>2</sup>	#/hr/m <sup>2</sup>	ln(#/hr/m <sup>2</sup> )
1	2.7	5.3	5.3	32	948.2	178.5	5.2
2	6.1	6.9	1.6	0	0.0	0.0	0.0
3	8.2	9.6	2.7	8	237.0	88.0	4.5
4	10.4	11.1	1.6	7	207.4	133.7	4.9
5	12.7	14.3	3.2	8	237.0	75.0	4.3
6	19.4	24.5	10.2	24	711.1	69.5	4.2
7	39.8	55.1	30.6	8	237.0	7.7	2.0
8	65.2	75.2	20.0	0	0.0	0.0	0.0
9	81.3	87.4	12.2	1	29.6	2.4	0.9
10	92.4	97.5	10.2	0	0.0	0.0	0.0
11	102.1	106.7	9.2	0	0.0	0.0	0.0
12	114.1	121.5	14.8	0	0.0	0.0	0.0
13	129.9	138.4	16.9	0	0.0	0.0	0.0
14	148.0	157.6	19.2	0	0.0	0.0	0.0
15	166.8	175.9	18.3	0	0.0	0.0	0.0
16	185.2	194.4	18.5	0	0.0	0.0	0.0
17	201.5	208.5	14.1	0	0.0	0.0	0.0
18	224.2	239.8	31.3	0	0.0	0.0	0.0
19	259.3	278.7	38.8	0	0.0	0.0	0.0
20	291.8	304.9	26.2	0	0.0	0.0	0.0
21	348.2	391.5	86.6	0	0.0	0.0	0.0

=====

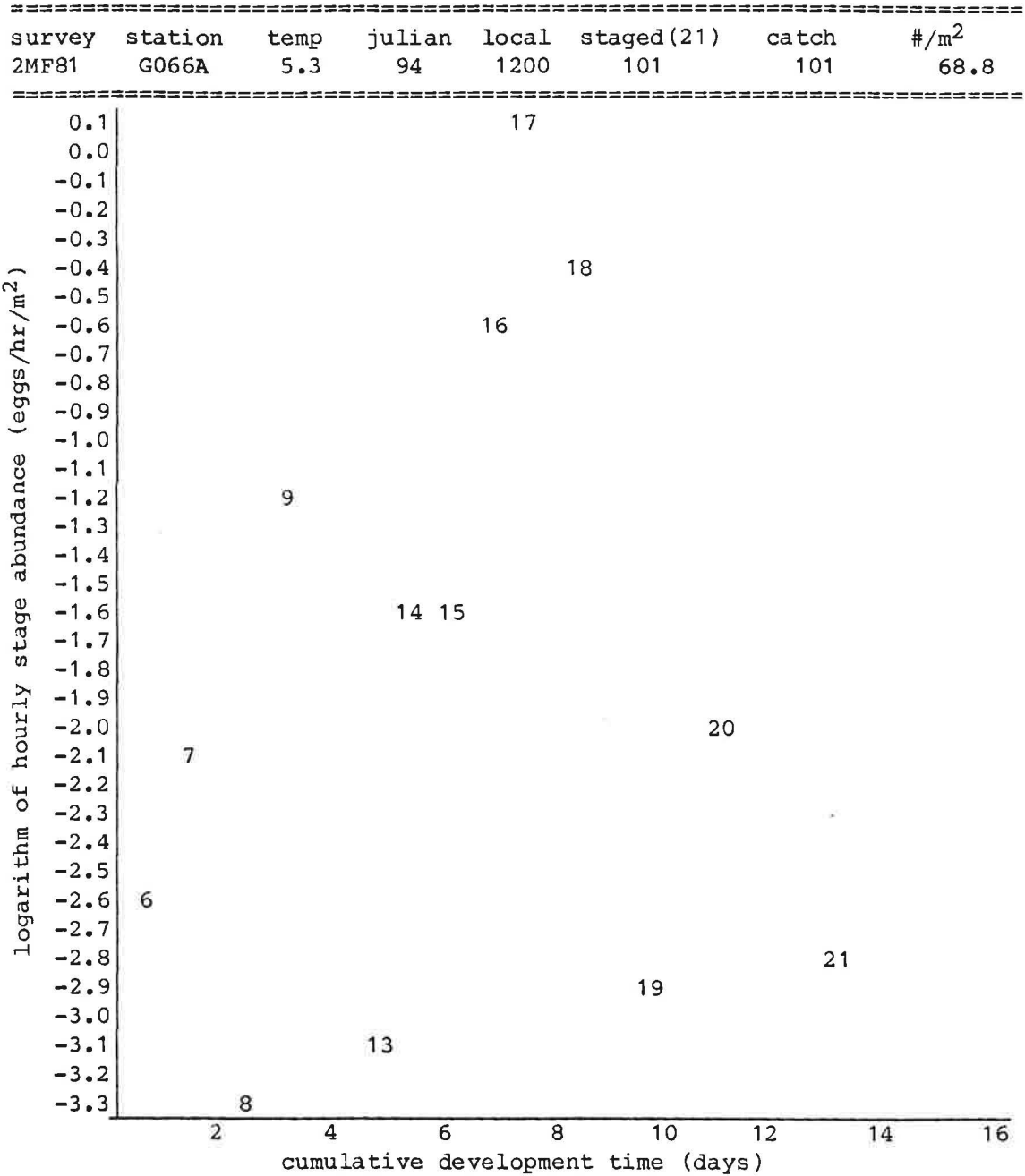


Appendix Figure A.5. Station abundance-age plot for eggs of walleye pollock obtained at station G046A of survey 2MF81. The logarithms of hourly stage abundances are plotted against the cumulative development times to stage midpoints. Each stage is identified by a stage number. See Appendix Table A.5 for intermediate values in the computations.

=====  
 Appendix Table A.5. Intermediate values in the calculations of average hourly stage abundance for eggs of walleye pollock obtained at station G046A of survey 2MF81.  
 =====

stage	mid	end	length	n staged	#/m <sup>2</sup>	#/hr/m <sup>2</sup>	ln(#/hr/m <sup>2</sup> )
1	2.6	5.3	5.3	1	0.6	0.1	-2.1
2	6.0	6.8	1.6	0	0.0	0.0	0.0
3	8.2	9.5	2.7	0	0.0	0.0	0.0
4	10.3	11.0	1.5	0	0.0	0.0	0.0
5	12.6	14.2	3.1	0	0.0	0.0	0.0
6	19.2	24.3	10.1	0	0.0	0.0	0.0
7	39.4	54.6	30.3	1	0.6	0.0	-3.9
8	64.5	74.4	19.8	0	0.0	0.0	0.0
9	80.5	86.5	12.0	4	2.5	0.2	-1.6
10	91.5	96.5	10.1	1	0.6	0.1	-2.8
11	101.1	105.6	9.1	1	0.6	0.1	-2.7
12	113.0	120.3	14.7	1	0.6	0.0	-3.2
13	128.7	137.0	16.7	1	0.6	0.0	-3.3
14	146.5	156.0	19.0	19	11.9	0.6	-0.5
15	165.1	174.2	18.1	15	9.4	0.5	-0.7
16	183.3	192.5	18.3	15	9.4	0.5	-0.7
17	199.5	206.4	14.0	11	6.9	0.5	-0.7
18	221.9	237.5	31.0	11	6.9	0.2	-1.5
19	256.7	275.9	38.4	1	0.6	0.0	-4.1
20	288.9	301.9	26.0	1	0.6	0.0	-3.7
21	344.7	387.6	85.7	0	0.0	0.0	0.0

=====

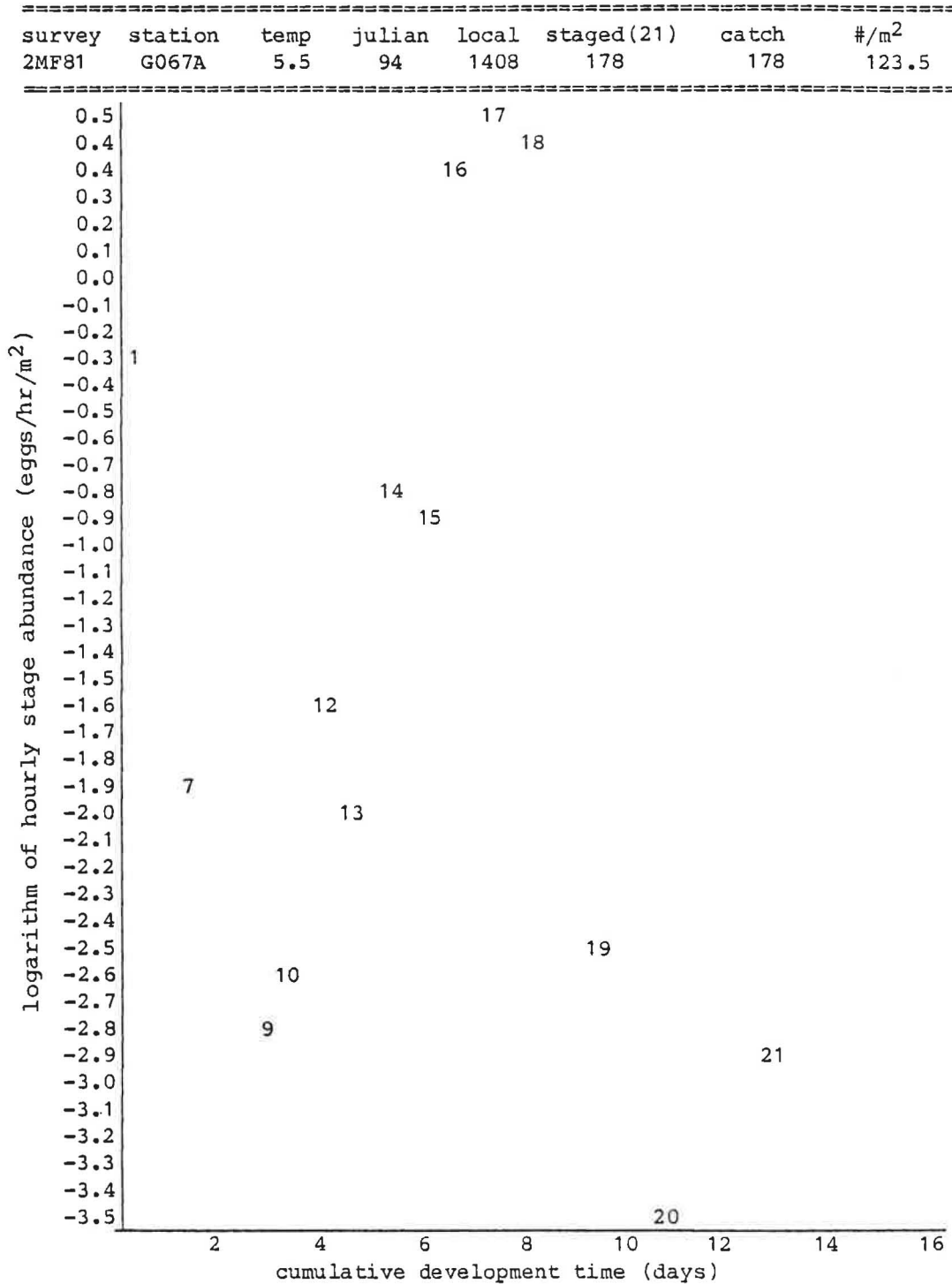


Appendix Figure A.6. Station abundance-age plot for eggs of walleye pollock obtained at station G066A of survey 2MF81. The logarithms of hourly stage abundances are plotted against the cumulative development times to stage midpoints. Each stage is identified by a stage number. See Appendix Table A.6 for intermediate values in the computations.

=====  
 Appendix Table A.6. Intermediate values in the calculations of average hourly stage abundance for eggs of walleye pollock obtained at station G066A of survey 2MF81.  
 =====

stage	mid	end	length	n staged	#/m <sup>2</sup>	#/hr/m <sup>2</sup>	ln(#/hr/m <sup>2</sup> )
1	2.4	4.9	4.9	0	0.0	0.0	0.0
2	5.6	6.3	1.4	0	0.0	0.0	0.0
3	7.5	8.8	2.5	0	0.0	0.0	0.0
4	9.5	10.2	1.4	0	0.0	0.0	0.0
5	11.6	13.1	2.9	0	0.0	0.0	0.0
6	17.7	22.4	9.4	1	0.7	0.1	-2.6
7	36.4	50.4	28.0	5	3.4	0.1	-2.1
8	59.6	68.7	18.3	1	0.7	0.0	-3.3
9	74.3	79.8	11.1	5	3.4	0.3	-1.2
10	84.5	89.1	9.3	0	0.0	0.0	0.0
11	93.3	97.5	8.4	0	0.0	0.0	0.0
12	104.3	111.1	13.5	0	0.0	0.0	0.0
13	118.8	126.5	15.4	1	0.7	0.0	-3.1
14	135.2	144.0	17.6	5	3.4	0.2	-1.6
15	152.4	160.8	16.7	5	3.4	0.2	-1.6
16	169.2	177.7	16.9	13	8.9	0.5	-0.6
17	184.1	190.6	12.9	21	14.3	1.1	0.1
18	204.9	219.2	28.6	29	19.8	0.7	-0.4
19	236.9	254.7	35.5	3	2.0	0.1	-2.9
20	266.7	278.7	24.0	5	3.4	0.1	-2.0
21	318.2	357.8	79.1	7	4.8	0.1	-2.8

=====



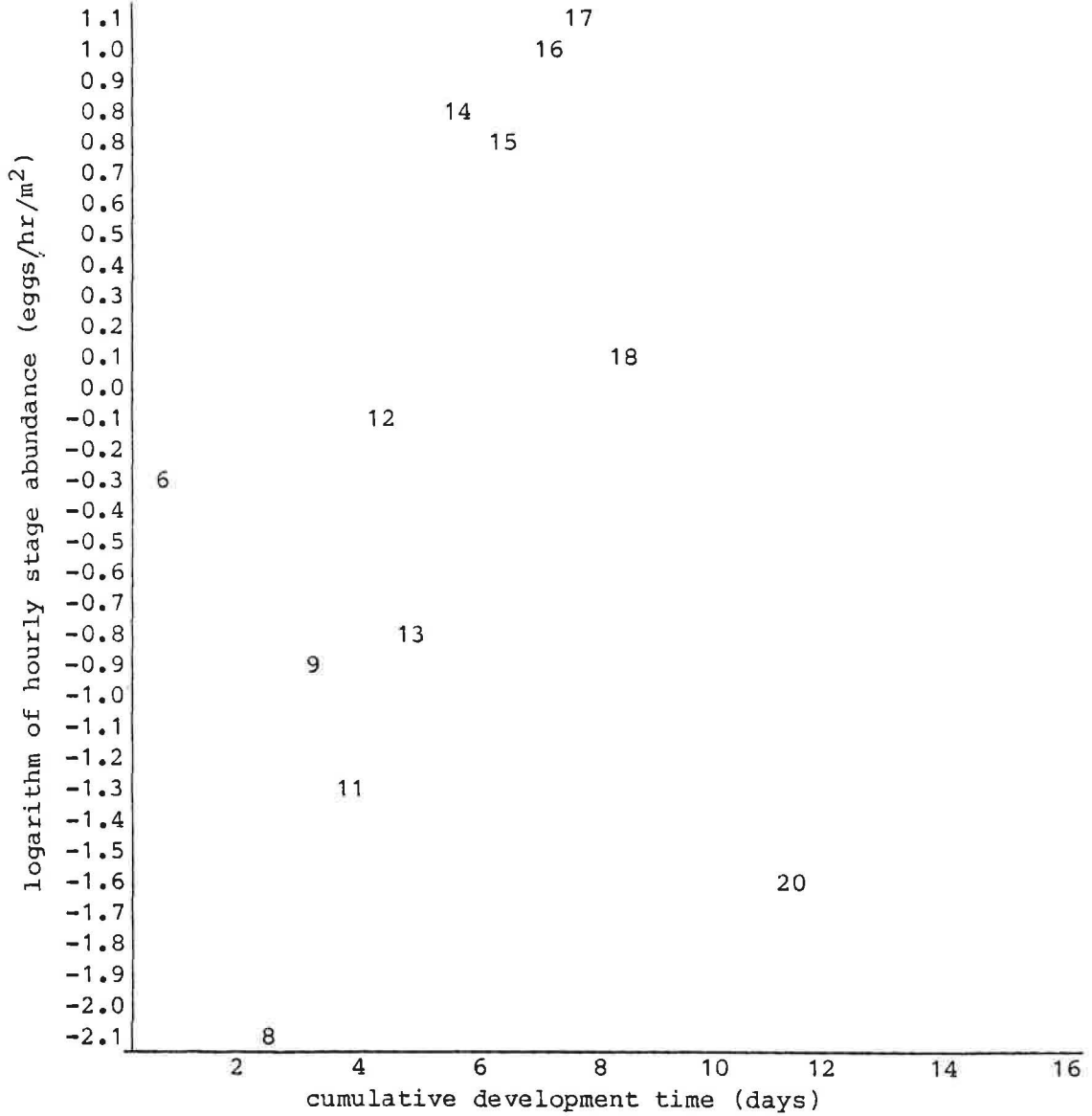
Appendix Figure A.7. Station abundance-age plot for eggs of walleye pollock obtained at station G067A of survey 2MF81. The logarithms of hourly stage abundances are plotted against the cumulative development times to stage midpoints. Each stage is identified by a stage number. See Appendix Table A.7 for intermediate values in the computations.

=====  
 Appendix Table A.7. Intermediate values in the calculations of average hourly stage abundance for eggs of walleye pollock obtained at station G067A of survey 2MF81.  
 =====

stage	mid	end	length	n staged	#/m <sup>2</sup>	#/hr/m <sup>2</sup>	ln(#/hr/m <sup>2</sup> )
1	2.4	4.8	4.8	5	3.5	0.7	-0.3
2	5.5	6.2	1.4	0	0.0	0.0	0.0
3	7.4	8.6	2.4	0	0.0	0.0	0.0
4	9.3	10.0	1.4	0	0.0	0.0	0.0
5	11.4	12.8	2.8	0	0.0	0.0	0.0
6	17.4	22.0	9.2	0	0.0	0.0	0.0
7	35.7	49.4	27.4	6	4.2	0.2	-1.9
8	58.4	67.4	18.0	0	0.0	0.0	0.0
9	72.8	78.3	10.9	1	0.7	0.1	-2.8
10	82.8	87.4	9.1	1	0.7	0.1	-2.6
11	91.5	95.6	8.2	0	0.0	0.0	0.0
12	102.2	108.9	13.3	4	2.8	0.2	-1.6
13	116.4	124.0	15.1	3	2.1	0.1	-2.0
14	132.6	141.2	17.2	11	7.6	0.4	-0.8
15	149.4	157.6	16.4	10	6.9	0.4	-0.9
16	165.9	174.2	16.6	35	24.3	1.5	0.4
17	180.5	186.8	12.6	29	20.1	1.6	0.5
18	200.8	214.9	28.1	62	43.0	1.5	0.4
19	232.2	249.6	34.8	4	2.8	0.1	-2.5
20	261.4	273.1	23.5	1	0.7	0.0	-3.5
21	311.9	350.7	77.6	6	4.2	0.1	-2.9

=====

survey	station	temp	julian	local	staged(21)	catch	#/m <sup>2</sup>
2MF81	G068A	5.1	94	1524	100	354	238.6

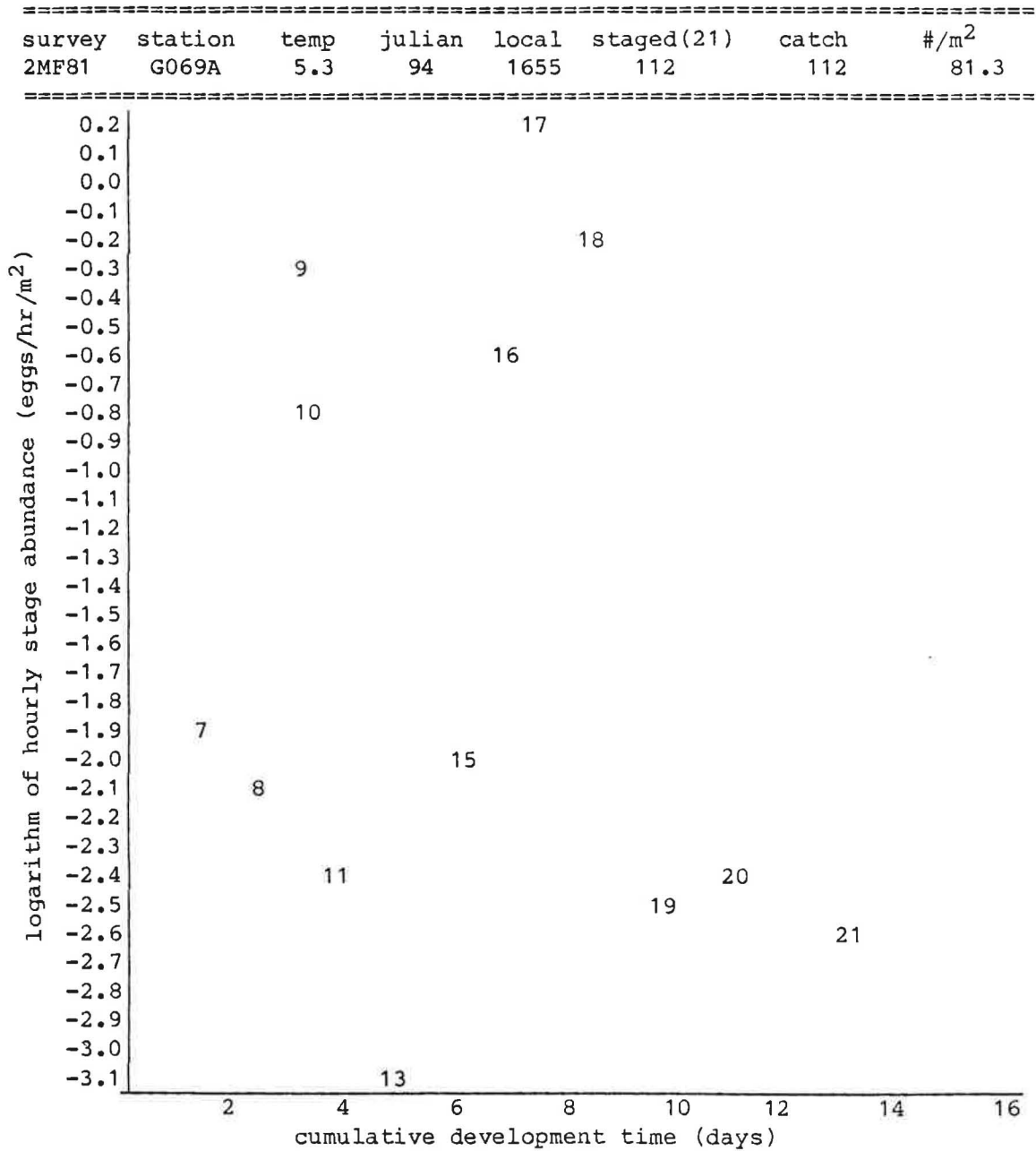


Appendix Figure A.8. Station abundance-age plot for eggs of walleye pollock obtained at station G068A of survey 2MF81. The logarithms of hourly stage abundances are plotted against the cumulative development times to stage midpoints. Each stage is identified by a stage number. See Appendix Table A.8 for intermediate values in the computations.

=====  
 Appendix Table A.8. Intermediate values in the calculations of average hourly stage abundance for eggs of walleye pollock obtained at station G068A of survey 2MF81.  
 =====

stage	mid	end	length	n staged	#/m <sup>2</sup>	#/hr/m <sup>2</sup>	ln(#/hr/m <sup>2</sup> )
1	2.5	5.0	5.0	0	0.0	0.0	0.0
2	5.7	6.4	1.5	0	0.0	0.0	0.0
3	7.7	8.9	2.5	0	0.0	0.0	0.0
4	9.7	10.4	1.4	0	0.0	0.0	0.0
5	11.9	13.3	2.9	0	0.0	0.0	0.0
6	18.1	22.9	9.5	3	7.2	0.8	-0.3
7	37.1	51.4	28.5	0	0.0	0.0	0.0
8	60.8	70.1	18.7	1	2.4	0.1	-2.1
9	75.8	81.5	11.3	2	4.8	0.4	-0.9
10	86.2	90.9	9.5	0	0.0	0.0	0.0
11	95.2	99.5	8.6	1	2.4	0.3	-1.3
12	106.4	113.3	13.8	5	11.9	0.9	-0.1
13	121.2	129.0	15.7	3	7.2	0.5	-0.8
14	138.0	146.9	17.9	17	40.6	2.3	0.8
15	155.5	164.0	17.1	16	38.2	2.2	0.8
16	172.6	181.3	17.3	20	47.7	2.8	1.0
17	187.8	194.4	13.1	17	40.6	3.1	1.1
18	209.0	223.6	29.2	13	31.0	1.1	0.1
19	241.7	259.8	36.2	0	0.0	0.0	0.0
20	272.1	284.3	24.5	2	4.8	0.2	-1.6
21	324.7	365.0	80.7	0	0.0	0.0	0.0

=====

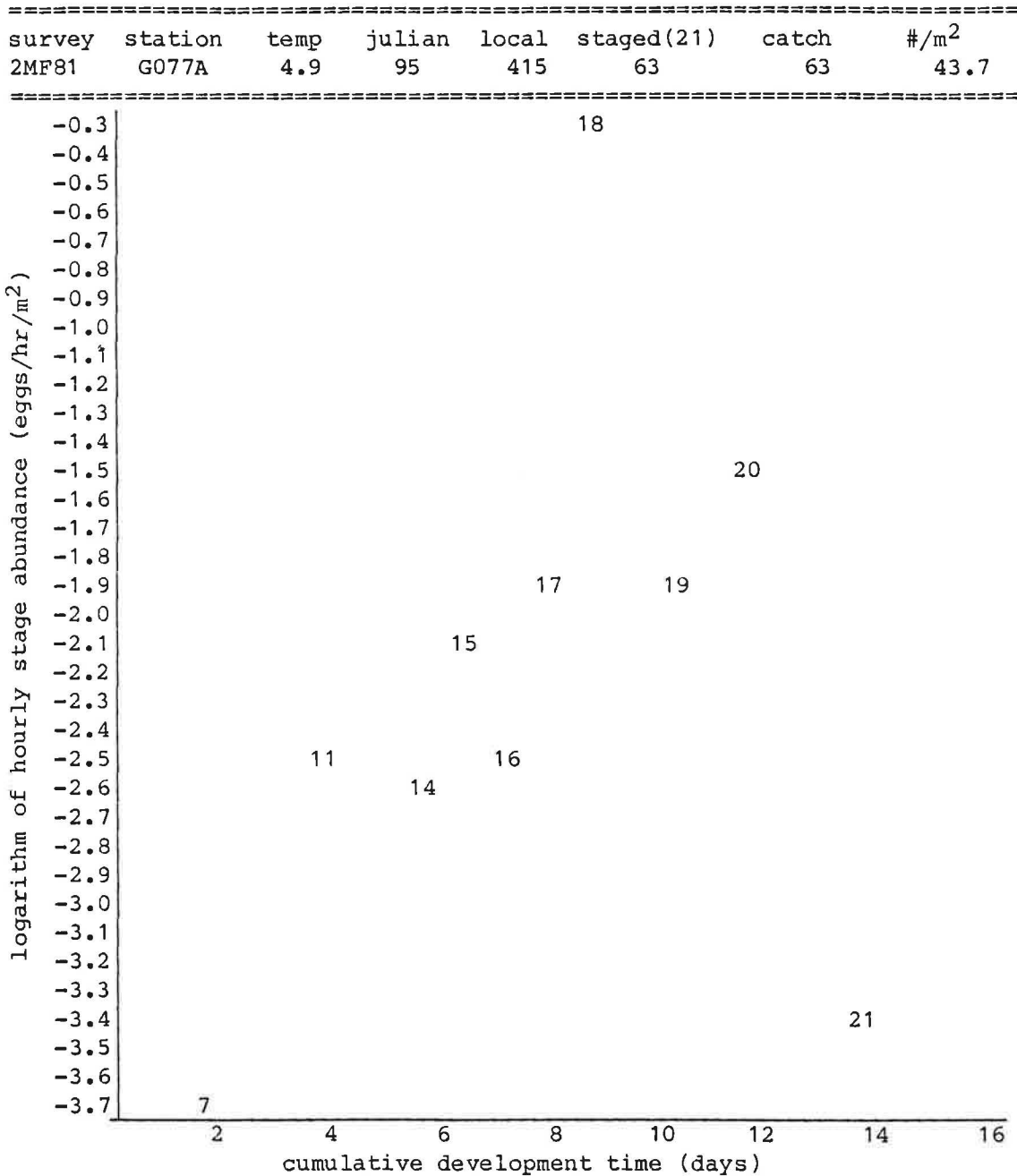


Appendix Figure A.9. Station abundance-age plot for eggs of walleye pollock obtained at station G069A of survey 2MF81. The logarithms of hourly stage abundances are plotted against the cumulative development times to stage midpoints. Each stage is identified by a stage number. See Appendix Table A.9 for intermediate values in the computations.

=====  
 Appendix Table A.9. Intermediate values in the calculations of average hourly stage abundance for eggs of walleye pollock obtained at station G069A of survey 2MF81.  
 =====

stage	mid	end	length	n staged	#/m <sup>2</sup>	#/hr/m <sup>2</sup>	ln(#/hr/m <sup>2</sup> )
1	2.4	4.9	4.9	0	0.0	0.0	0.0
2	5.6	6.3	1.4	0	0.0	0.0	0.0
3	7.5	8.8	2.5	0	0.0	0.0	0.0
4	9.5	10.2	1.4	0	0.0	0.0	0.0
5	11.6	13.1	2.9	0	0.0	0.0	0.0
6	17.7	22.4	9.4	0	0.0	0.0	0.0
7	36.4	50.4	28.0	6	4.4	0.2	-1.9
8	59.6	68.7	18.3	3	2.2	0.1	-2.1
9	74.3	79.8	11.1	11	8.0	0.7	-0.3
10	84.5	89.1	9.3	6	4.4	0.5	-0.8
11	93.3	97.5	8.4	1	0.7	0.1	-2.4
12	104.3	111.1	13.5	0	0.0	0.0	0.0
13	118.8	126.5	15.4	1	0.7	0.0	-3.1
14	135.2	144.0	17.6	0	0.0	0.0	0.0
15	152.4	160.8	16.7	3	2.2	0.1	-2.0
16	169.2	177.7	16.9	13	9.4	0.6	-0.6
17	184.1	190.6	12.9	21	15.2	1.2	0.2
18	204.9	219.2	28.6	32	23.2	0.8	-0.2
19	236.9	254.7	35.5	4	2.9	0.1	-2.5
20	266.7	278.7	24.0	3	2.2	0.1	-2.4
21	318.2	357.8	79.1	8	5.8	0.1	-2.6

=====



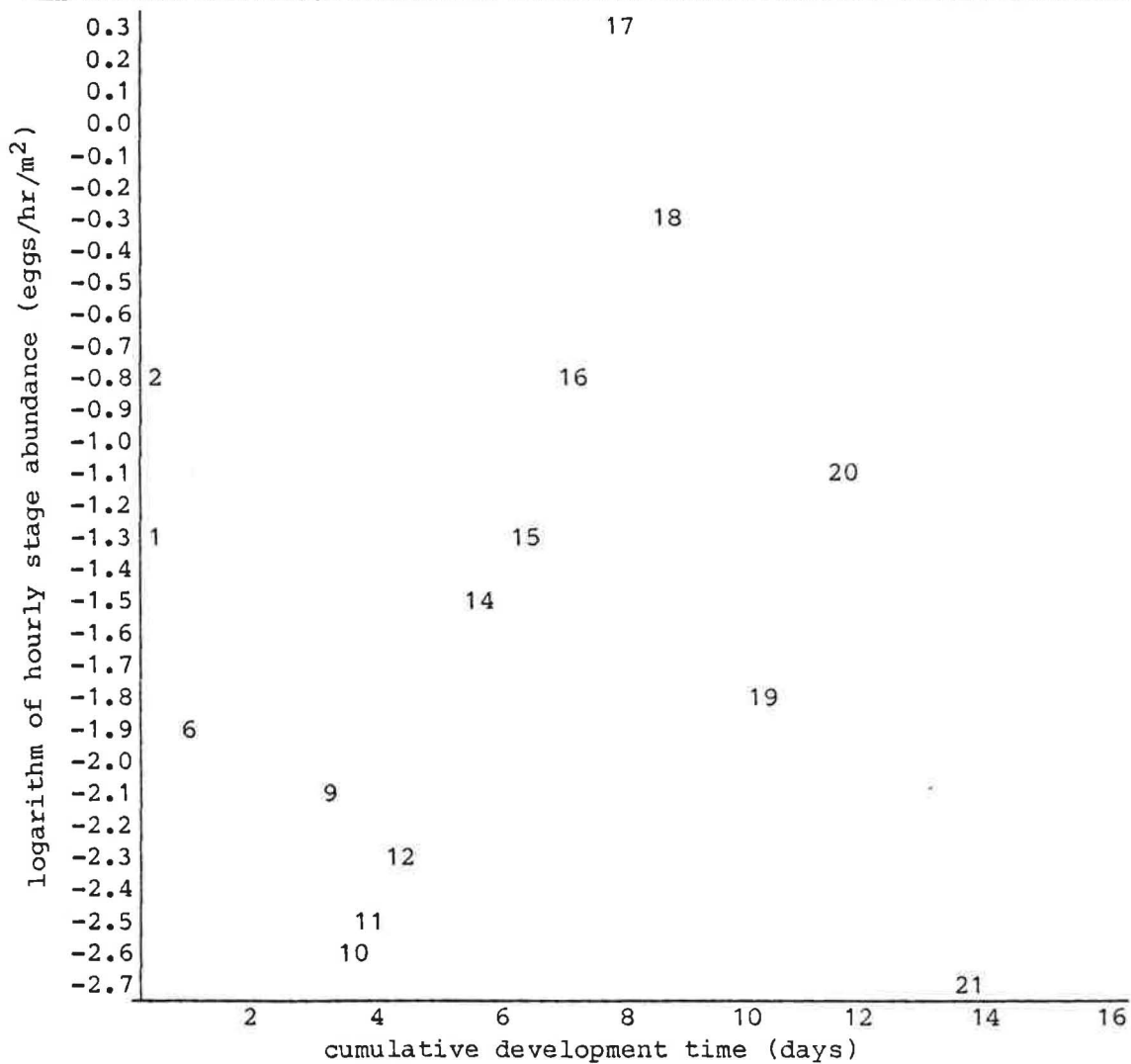
Appendix Figure A.10. Station abundance-age plot for eggs of walleye pollock obtained at station G077A of survey 2MF81. The logarithms of hourly stage abundances are plotted against the cumulative development times to stage midpoints. Each stage is identified by a stage number. See Appendix Table A.10 for intermediate values in the computations.

=====  
 Appendix Table A.10. Intermediate values in the calculations of  
 average hourly stage abundance for eggs of walleye pollock obtained at  
 station G077A of survey 2MF81.  
 =====

stage	mid	end	length	n staged	#/m <sup>2</sup>	#/hr/m <sup>2</sup>	ln(#/hr/m <sup>2</sup> )
1	2.5	5.1	5.1	0	0.0	0.0	0.0
2	5.8	6.6	1.5	0	0.0	0.0	0.0
3	7.8	9.1	2.6	0	0.0	0.0	0.0
4	9.9	10.6	1.5	0	0.0	0.0	0.0
5	12.1	13.6	3.0	0	0.0	0.0	0.0
6	18.5	23.3	9.7	0	0.0	0.0	0.0
7	37.9	52.5	29.1	1	0.7	0.0	-3.7
8	62.0	71.5	19.1	0	0.0	0.0	0.0
9	77.3	83.1	11.6	0	0.0	0.0	0.0
10	87.9	92.8	9.7	0	0.0	0.0	0.0
11	97.1	101.5	8.7	1	0.7	0.1	-2.5
12	108.5	115.6	14.1	0	0.0	0.0	0.0
13	123.6	131.6	16.0	0	0.0	0.0	0.0
14	140.8	149.9	18.3	2	1.4	0.1	-2.6
15	158.6	167.3	17.4	3	2.1	0.1	-2.1
16	176.1	184.9	17.6	2	1.4	0.1	-2.5
17	191.6	198.3	13.4	3	2.1	0.2	-1.9
18	213.2	228.1	29.8	31	21.5	0.7	-0.3
19	246.6	265.1	36.9	8	5.6	0.2	-1.9
20	277.6	290.0	25.0	8	5.6	0.2	-1.5
21	331.2	372.4	82.4	4	2.8	0.0	-3.4

=====

survey	station	temp	julian	local	staged(21)	catch	#/m <sup>2</sup>
2MF81	G078A	4.9	95	534	120	121	84.8



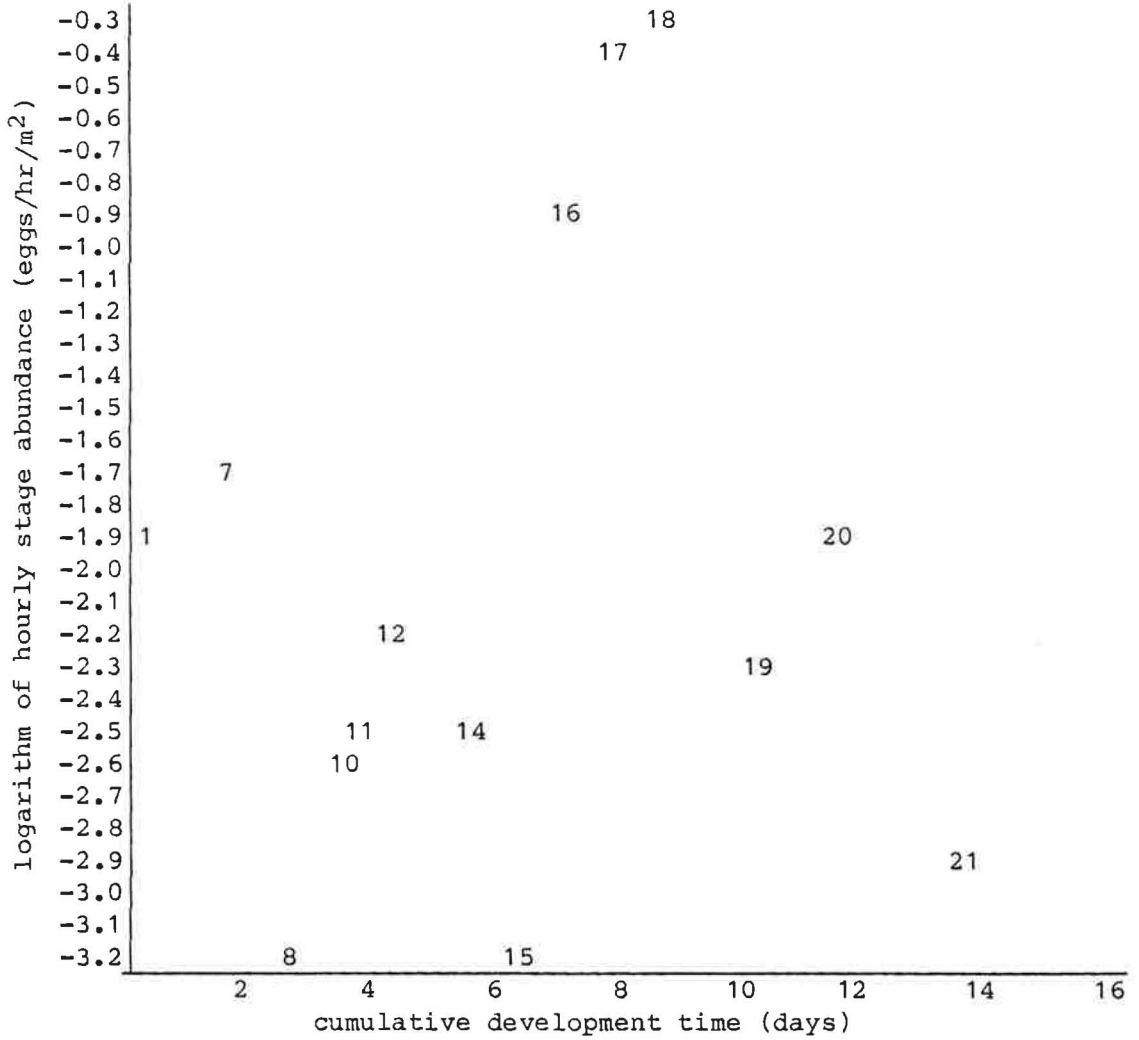
Appendix Figure A.11. Station abundance-age plot for eggs of walleye pollock obtained at station G078A of survey 2MF81. The logarithms of hourly stage abundances are plotted against the cumulative development times to stage midpoints. Each stage is identified by a stage number. See Appendix Table A.11 for intermediate values in the computations.

=====  
 Appendix Table A.11. Intermediate values in the calculations of  
 average hourly stage abundance for eggs of walleye pollock obtained at  
 station G078A of survey 2MF81.  
 =====

stage	mid	end	length	n staged	#/m <sup>2</sup>	#/hr/m <sup>2</sup>	ln(#/hr/m <sup>2</sup> )
1	2.5	5.1	5.1	2	1.4	0.3	-1.3
2	5.8	6.6	1.5	1	0.7	0.5	-0.8
3	7.8	9.1	2.6	0	0.0	0.0	0.0
4	9.9	10.6	1.5	0	0.0	0.0	0.0
5	12.1	13.6	3.0	0	0.0	0.0	0.0
6	18.5	23.3	9.7	2	1.4	0.1	-1.9
7	37.9	52.5	29.1	0	0.0	0.0	0.0
8	62.0	71.5	19.1	0	0.0	0.0	0.0
9	77.3	83.1	11.6	2	1.4	0.1	-2.1
10	87.9	92.8	9.7	1	0.7	0.1	-2.6
11	97.1	101.5	8.7	1	0.7	0.1	-2.5
12	108.5	115.6	14.1	2	1.4	0.1	-2.3
13	123.6	131.6	16.0	0	0.0	0.0	0.0
14	140.8	149.9	18.3	6	4.2	0.2	-1.5
15	158.6	167.3	17.4	7	4.9	0.3	-1.3
16	176.1	184.9	17.6	11	7.8	0.4	-0.8
17	191.6	198.3	13.4	26	18.4	1.4	0.3
18	213.2	228.1	29.8	30	21.2	0.7	-0.3
19	246.6	265.1	36.9	9	6.4	0.2	-1.8
20	277.6	290.0	25.0	12	8.5	0.3	-1.1
21	331.2	372.4	82.4	8	5.7	0.1	-2.7

=====

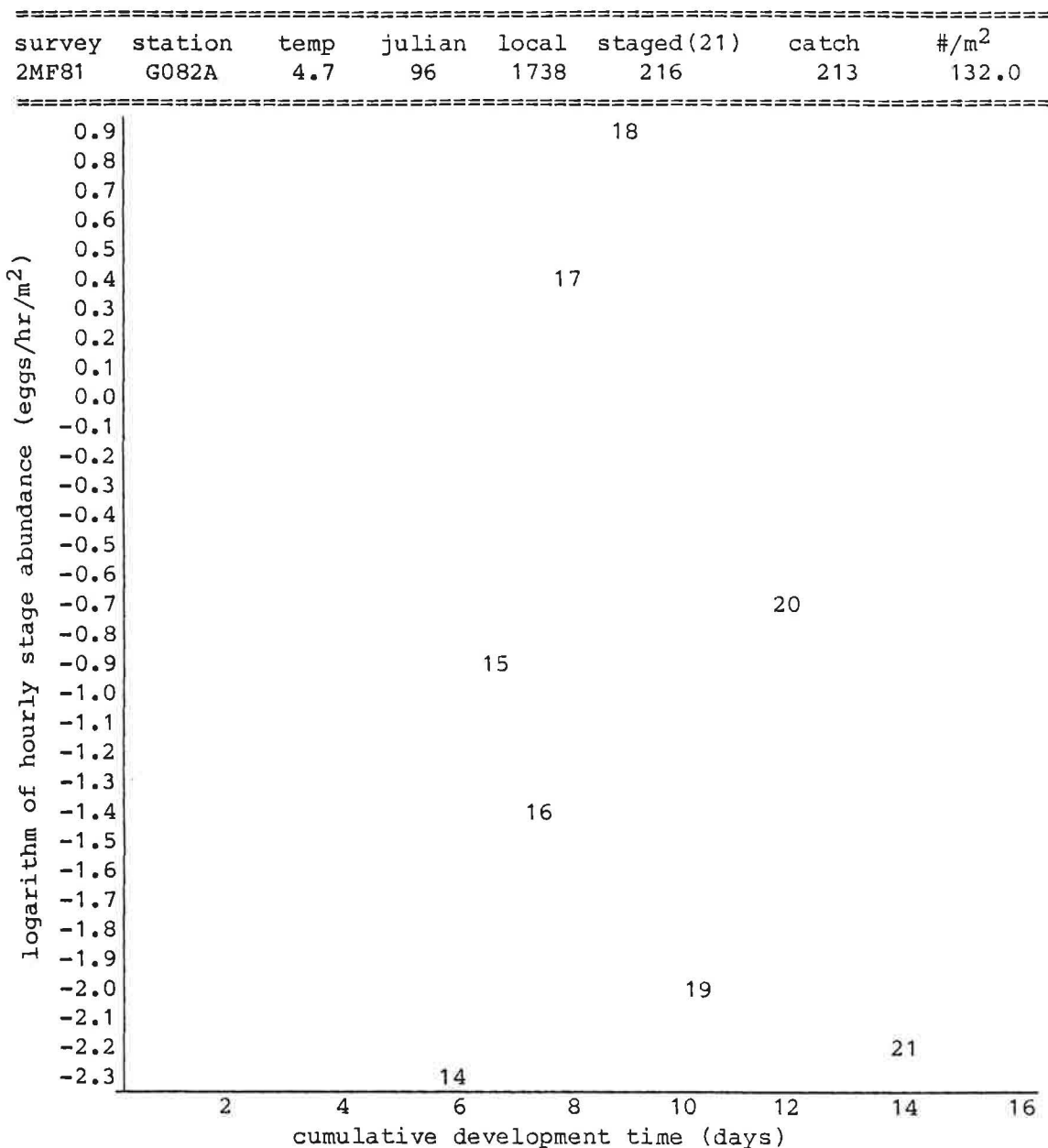
survey	station	temp	julian	local	staged(21)	catch	#/m <sup>2</sup>
2MF81	G079A	4.9	95	708	83	83	61.8



Appendix Figure A.12. Station abundance-age plot for eggs of walleye pollock obtained at station G079A of survey 2MF81. The logarithms of hourly stage abundances are plotted against the cumulative development times to stage midpoints. Each stage is identified by a stage number. See Appendix Table A.12 for intermediate values in the computations.

Appendix Table A.12. Intermediate values in the calculations of average hourly stage abundance for eggs of walleye pollock obtained at station G079A of survey 2MF81.

stage	mid	end	length	n staged	#/m <sup>2</sup>	#/hr/m <sup>2</sup>	ln(#/hr/m <sup>2</sup> )
1	2.5	5.1	5.1	1	0.7	0.1	-1.9
2	5.8	6.6	1.5	0	0.0	0.0	0.0
3	7.8	9.1	2.6	0	0.0	0.0	0.0
4	9.9	10.6	1.5	0	0.0	0.0	0.0
5	12.1	13.6	3.0	0	0.0	0.0	0.0
6	18.5	23.3	9.7	0	0.0	0.0	0.0
7	37.9	52.5	29.1	7	5.2	0.2	-1.7
8	62.0	71.5	19.1	1	0.7	0.0	-3.2
9	77.3	83.1	11.6	0	0.0	0.0	0.0
10	87.9	92.8	9.7	1	0.7	0.1	-2.6
11	97.1	101.5	8.7	1	0.7	0.1	-2.5
12	108.5	115.6	14.1	2	1.5	0.1	-2.2
13	123.6	131.6	16.0	0	0.0	0.0	0.0
14	140.8	149.9	18.3	2	1.5	0.1	-2.5
15	158.6	167.3	17.4	1	0.7	0.0	-3.2
16	176.1	184.9	17.6	10	7.4	0.4	-0.9
17	191.6	198.3	13.4	12	8.9	0.7	-0.4
18	213.2	228.1	29.8	29	21.6	0.7	-0.3
19	246.6	265.1	36.9	5	3.7	0.1	-2.3
20	277.6	290.0	25.0	5	3.7	0.1	-1.9
21	331.2	372.4	82.4	6	4.5	0.1	-2.9



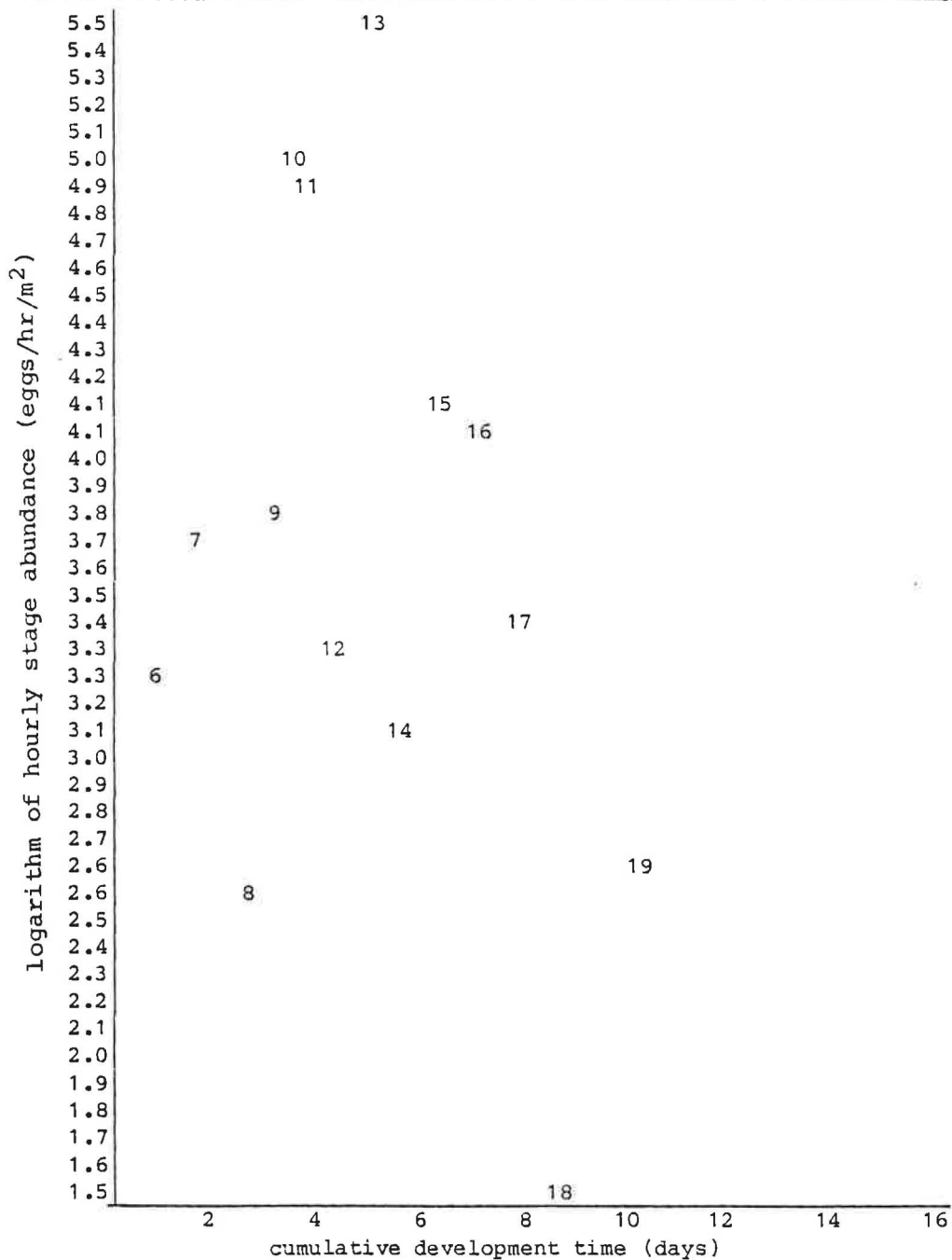
Appendix Figure A.13. Station abundance-age plot for eggs of walleye pollock obtained at station G082A of survey 2MF81. The logarithms of hourly stage abundances are plotted against the cumulative development times to stage midpoints. Each stage is identified by a stage number. See Appendix Table A.13 for intermediate values in the computations.

=====  
 Appendix Table A.13. Intermediate values in the calculations of  
 average hourly stage abundance for eggs of walleye pollock obtained at  
 station G082A of survey 2MF81.  
 =====

stage	mid	end	length	n staged	#/m <sup>2</sup>	#/hr/m <sup>2</sup>	ln(#/hr/m <sup>2</sup> )
1	2.6	5.2	5.2	0	0.0	0.0	0.0
2	5.9	6.7	1.5	0	0.0	0.0	0.0
3	8.0	9.3	2.6	0	0.0	0.0	0.0
4	10.1	10.8	1.5	0	0.0	0.0	0.0
5	12.3	13.9	3.1	0	0.0	0.0	0.0
6	18.8	23.8	9.9	0	0.0	0.0	0.0
7	38.7	53.5	29.7	0	0.0	0.0	0.0
8	63.2	73.0	19.4	0	0.0	0.0	0.0
9	78.9	84.8	11.8	0	0.0	0.0	0.0
10	89.7	94.6	9.9	0	0.0	0.0	0.0
11	99.1	103.5	8.9	0	0.0	0.0	0.0
12	110.7	117.9	14.4	0	0.0	0.0	0.0
13	126.1	134.3	16.4	0	0.0	0.0	0.0
14	143.6	152.9	18.6	3	1.8	0.1	-2.3
15	161.8	170.7	17.8	12	7.3	0.4	-0.9
16	179.7	188.7	18.0	7	4.3	0.2	-1.4
17	195.5	202.4	13.7	32	19.6	1.4	0.4
18	217.6	232.8	30.4	119	72.7	2.4	0.9
19	251.6	270.4	37.7	8	4.9	0.1	-2.0
20	283.2	295.9	25.5	20	12.2	0.5	-0.7
21	337.9	379.9	84.0	15	9.2	0.1	-2.2

=====

survey	station	temp	julian	local	staged(21)	catch	#/m <sup>2</sup>
2MF81	G086A	4.9	98	916	99	18469	12766.4



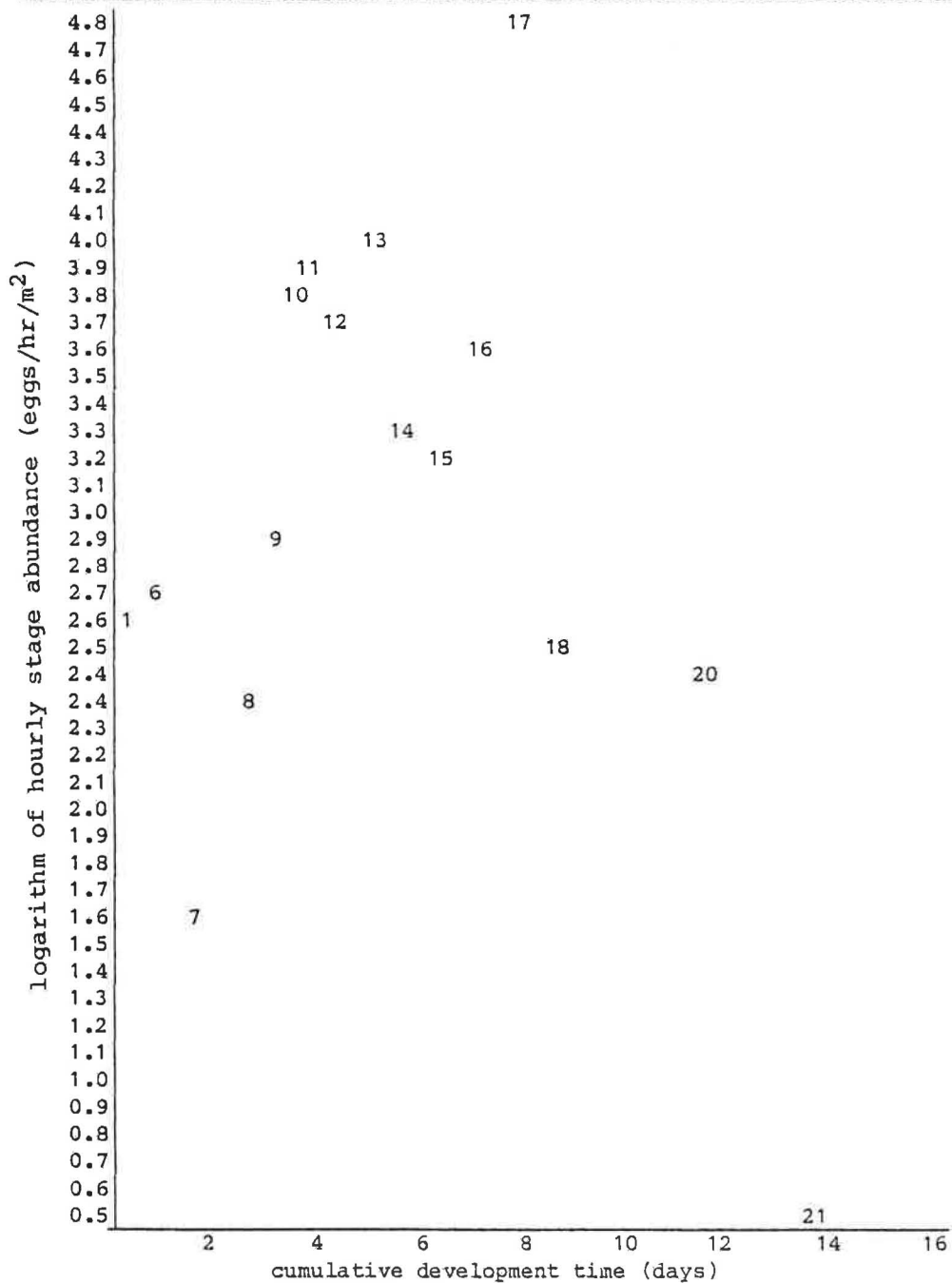
Appendix Figure A.14. Station abundance-age plot for eggs of walleye pollock obtained at station G086A of survey 2MF81. The logarithms of hourly stage abundances are plotted against the cumulative development times to stage midpoints. Each stage is identified by a stage number. See Appendix Table A.14 for intermediate values in the computations.

=====  
 Appendix Table A.14. Intermediate values in the calculations of  
 average hourly stage abundance for eggs of walleye pollock obtained at  
 station G086A of survey 2MF81.  
 =====

stage	mid	end	length	n staged	#/m <sup>2</sup>	#/hr/m <sup>2</sup>	ln(#/hr/m <sup>2</sup> )
1	2.5	5.1	5.1	0	0.0	0.0	0.0
2	5.8	6.6	1.5	0	0.0	0.0	0.0
3	7.8	9.1	2.6	0	0.0	0.0	0.0
4	9.9	10.6	1.5	0	0.0	0.0	0.0
5	12.1	13.6	3.0	0	0.0	0.0	0.0
6	18.5	23.3	9.7	2	257.9	26.5	3.3
7	37.9	52.5	29.1	9	1160.6	39.9	3.7
8	62.0	71.5	19.1	2	257.9	13.5	2.6
9	77.3	83.1	11.6	4	515.8	44.6	3.8
10	87.9	92.8	9.7	11	1418.5	146.8	5.0
11	97.1	101.5	8.7	9	1160.6	132.9	4.9
12	108.5	115.6	14.1	3	386.9	27.5	3.3
13	123.6	131.6	16.0	32	4126.5	257.2	5.5
14	140.8	149.9	18.3	3	386.9	21.2	3.1
15	158.6	167.3	17.4	8	1031.6	59.2	4.1
16	176.1	184.9	17.6	8	1031.6	58.6	4.1
17	191.6	198.3	13.4	3	386.9	28.9	3.4
18	213.2	228.1	29.8	1	129.0	4.3	1.5
19	246.6	265.1	36.9	4	515.8	14.0	2.6
20	277.6	290.0	25.0	0	0.0	0.0	0.0
21	331.2	372.4	82.4	0	0.0	0.0	0.0

=====

survey	station	temp	julian	local	staged(21)	catch	#/m <sup>2</sup>
2MF81	G087A	4.9	98	1039	100	10310	6948.3

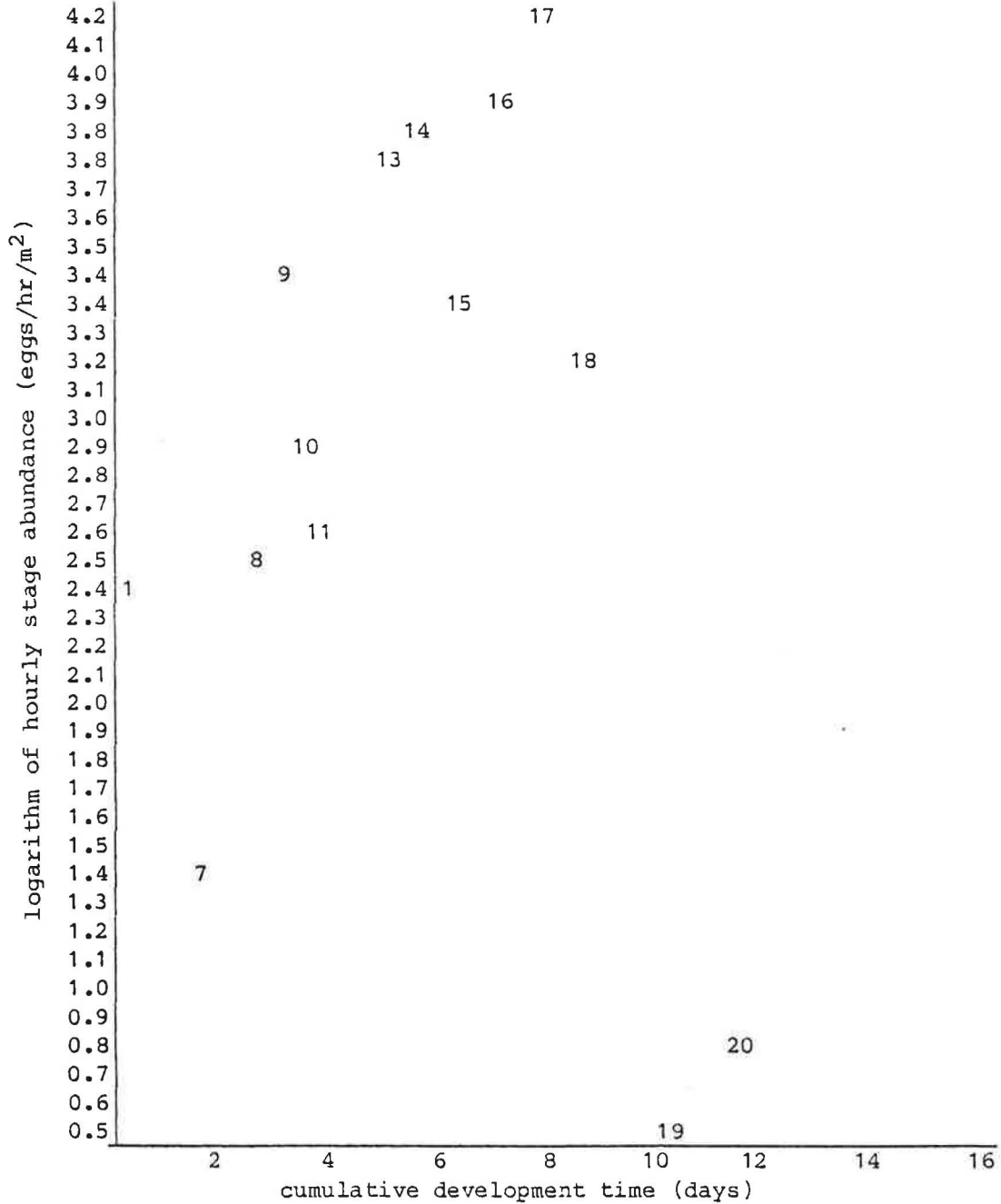


Appendix Figure A.15. Station abundance-age plot for eggs of walleye pollock obtained at station G087A of survey 2MF81. The logarithms of hourly stage abundances are plotted against the cumulative development times to stage midpoints. Each stage is identified by a stage number. See Appendix Table A.15 for intermediate values in the computations.

Appendix Table A.15. Intermediate values in the calculations of average hourly stage abundance for eggs of walleye pollock obtained at station G087A of survey 2MF81.

stage	mid	end	length	n staged	#/m <sup>2</sup>	#/hr/m <sup>2</sup>	ln(#/hr/m <sup>2</sup> )
1	2.5	5.1	5.1	1	69.5	13.8	2.6
2	5.8	6.6	1.5	0	0.0	0.0	0.0
3	7.8	9.1	2.6	0	0.0	0.0	0.0
4	9.9	10.6	1.5	0	0.0	0.0	0.0
5	12.1	13.6	3.0	0	0.0	0.0	0.0
6	18.5	23.3	9.7	2	139.0	14.3	2.7
7	37.9	52.5	29.1	2	139.0	4.8	1.6
8	62.0	71.5	19.1	3	208.4	10.9	2.4
9	77.3	83.1	11.6	3	208.4	18.0	2.9
10	87.9	92.8	9.7	6	416.9	43.1	3.8
11	97.1	101.5	8.7	6	416.9	47.7	3.9
12	108.5	115.6	14.1	8	555.9	39.5	3.7
13	123.6	131.6	16.0	13	903.3	56.3	4.0
14	140.8	149.9	18.3	7	486.4	26.6	3.3
15	158.6	167.3	17.4	6	416.9	23.9	3.2
16	176.1	184.9	17.6	9	625.3	35.5	3.6
17	191.6	198.3	13.4	23	1598.1	119.2	4.8
18	213.2	228.1	29.8	5	347.4	11.7	2.5
19	246.6	265.1	36.9	0	0.0	0.0	0.0
20	277.6	290.0	25.0	4	277.9	11.1	2.4
21	331.2	372.4	82.4	2	139.0	1.7	0.5

survey	station	temp	julian	local	staged(21)	catch	#/m <sup>2</sup>
2MF81	G088A	4.9	98	1147	98	8211	5703.3

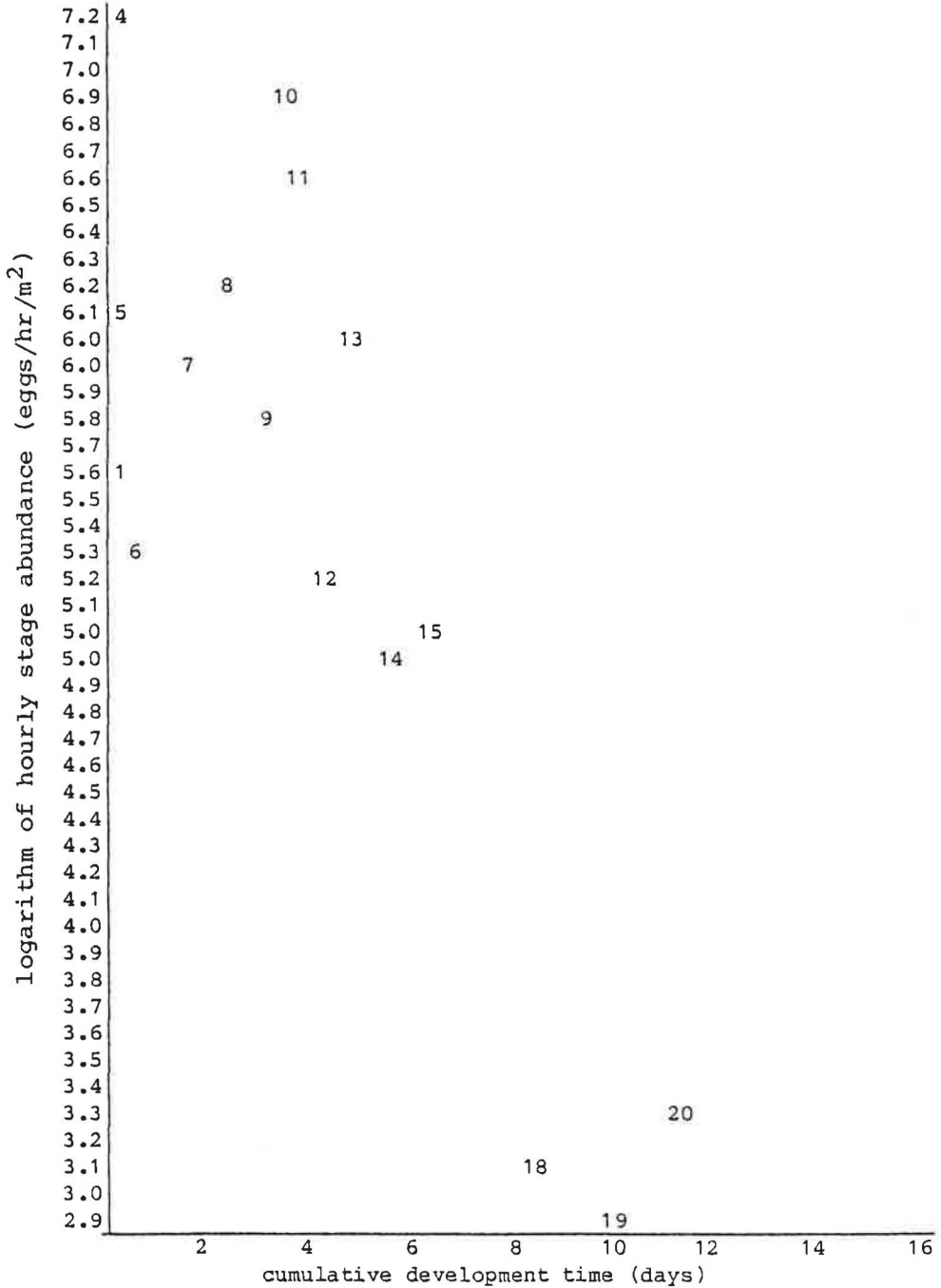


Appendix Figure A.16. Station abundance-age plot for eggs of walleye pollock obtained at station G088A of survey 2MF81. The logarithms of hourly stage abundances are plotted against the cumulative development times to stage midpoints. Each stage is identified by a stage number. See Appendix Table A.16 for intermediate values in the computations.

Appendix Table A.16. Intermediate values in the calculations of average hourly stage abundance for eggs of walleye pollock obtained at station G088A of survey 2MF81.

stage	mid	end	length	n staged	#/M <sup>2</sup>	#/hr/m <sup>2</sup>	ln(#/hr/m <sup>2</sup> )
1	2.5	5.1	5.1	1	58.2	11.5	2.4
2	5.8	6.6	1.5	0	0.0	0.0	0.0
3	7.8	9.1	2.6	0	0.0	0.0	0.0
4	9.9	10.6	1.5	0	0.0	0.0	0.0
5	12.1	13.6	3.0	0	0.0	0.0	0.0
6	18.5	23.3	9.7	0	0.0	0.0	0.0
7	37.9	52.5	29.1	2	116.4	4.0	1.4
8	62.0	71.5	19.1	4	232.8	12.2	2.5
9	77.3	83.1	11.6	6	349.2	30.2	3.4
10	87.9	92.8	9.7	3	174.6	18.1	2.9
11	97.1	101.5	8.7	2	116.4	13.3	2.6
12	108.5	115.6	14.1	0	0.0	0.0	0.0
13	123.6	131.6	16.0	12	698.4	43.5	3.8
14	140.8	149.9	18.3	14	814.8	44.6	3.8
15	158.6	167.3	17.4	9	523.8	30.0	3.4
16	176.1	184.9	17.6	15	873.0	49.6	3.9
17	191.6	198.3	13.4	15	873.0	65.1	4.2
18	213.2	228.1	29.8	13	756.6	25.4	3.2
19	246.6	265.1	36.9	1	58.2	1.6	0.5
20	277.6	290.0	25.0	1	58.2	2.3	0.8
21	331.2	372.4	82.4	0	0.0	0.0	0.0

survey	station	temp	julian	local	staged(21)	catch	#/m <sup>2</sup>
2MF81	G089A	5.1	99	1154	98	83932	63656.7



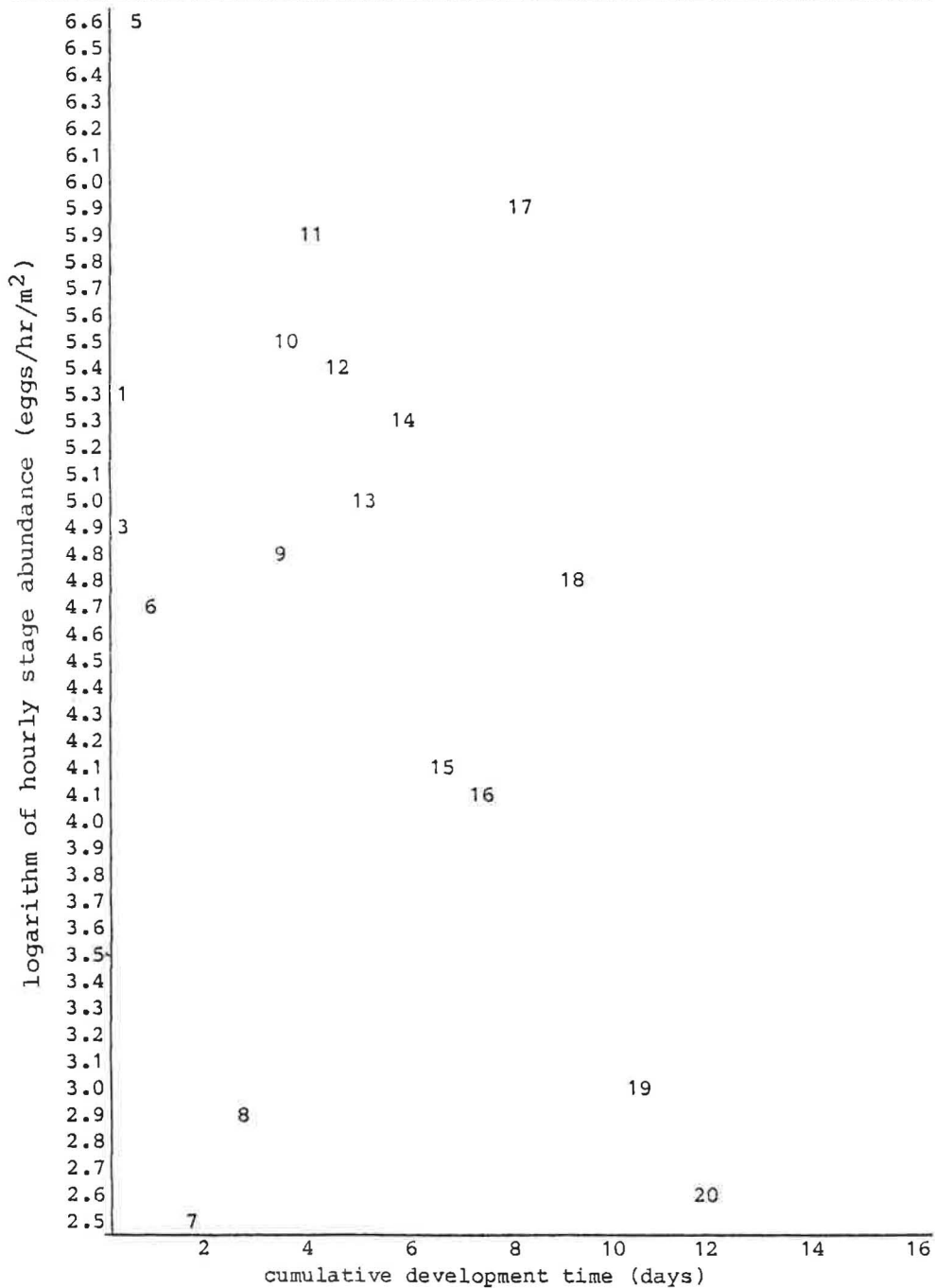
Appendix Figure A.17. Station abundance-age plot for eggs of walleye pollock obtained at station G089A of survey 2MF81. The logarithms of hourly stage abundances are plotted against the cumulative development times to stage midpoints. Each stage is identified by a stage number. See Appendix Table A.17 for intermediate values in the computations.

=====  
 Appendix Table A.17. Intermediate values in the calculations of  
 average hourly stage abundance for eggs of walleye pollock obtained at  
 station G089A of survey 2MF81.  
 =====

stage	mid	end	length	n staged	#/m <sup>2</sup>	#/hr/m <sup>2</sup>	ln(#/hr/m <sup>2</sup> )
1	2.5	5.0	5.0	2	1299.1	262.3	5.6
2	5.7	6.4	1.5	0	0.0	0.0	0.0
3	7.7	8.9	2.5	0	0.0	0.0	0.0
4	9.7	10.4	1.4	3	1948.7	1347.6	7.2
5	11.9	13.3	2.9	2	1299.1	440.6	6.1
6	18.1	22.9	9.5	3	1948.7	204.2	5.3
7	37.1	51.4	28.5	18	11692.1	409.6	6.0
8	60.8	70.1	18.7	14	9093.8	486.6	6.2
9	75.8	81.5	11.3	6	3897.4	343.5	5.8
10	86.2	90.9	9.5	15	9743.4	1028.8	6.9
11	95.2	99.5	8.6	10	6495.6	758.6	6.6
12	106.4	113.3	13.8	4	2598.2	188.1	5.2
13	121.2	129.0	15.7	10	6495.6	413.0	6.0
14	138.0	146.9	17.9	4	2598.2	145.1	5.0
15	155.5	164.0	17.1	4	2598.2	152.1	5.0
16	172.6	181.3	17.3	0	0.0	0.0	0.0
17	187.8	194.4	13.1	0	0.0	0.0	0.0
18	209.0	223.6	29.2	1	649.6	22.2	3.1
19	241.7	259.8	36.2	1	649.6	17.9	2.9
20	272.1	284.3	24.5	1	649.6	26.5	3.3
21	324.7	365.0	80.7	0	0.0	0.0	0.0

=====

survey	station	temp	julian	local	staged(21)	catch	#/m <sup>2</sup>
2MF81	G090A	4.5	99	1014	94	46672	34563.3



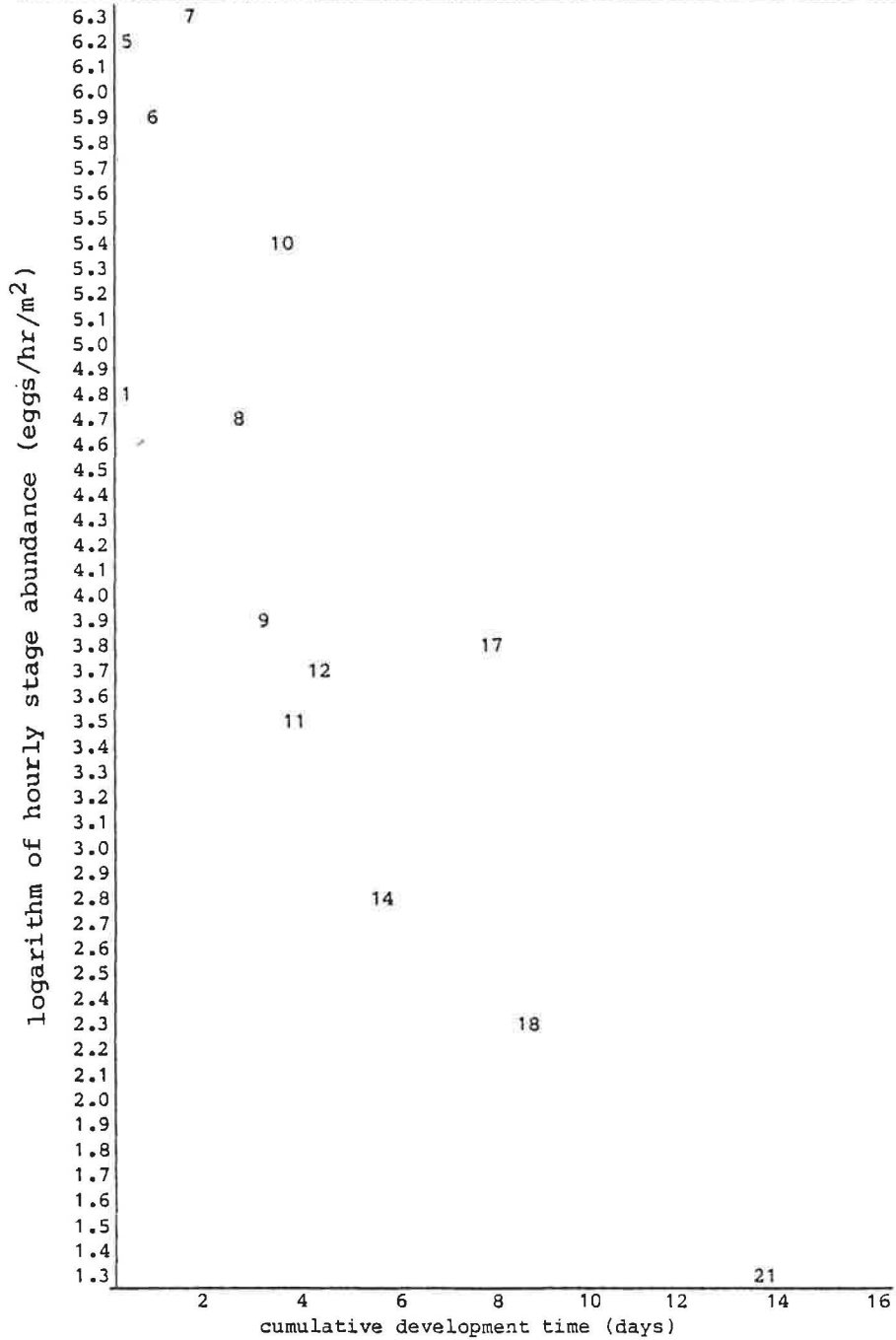
Appendix Figure A.18. Station abundance-age plot for eggs of walleye pollock obtained at station G090A of survey 2MF81. The logarithms of hourly stage abundances are plotted against the cumulative development times to stage midpoints. Each stage is identified by a stage number. See Appendix Table A.18 for intermediate values in the computations.

=====  
 Appendix Table A.18. Intermediate values in the calculations of  
 average hourly stage abundance for eggs of walleye pollock obtained at  
 station G090A of survey 2MF81.  
 =====

stage	mid	end	length	n staged	#/m <sup>2</sup>	#/hr/m <sup>2</sup>	ln(#/hr/m <sup>2</sup> )
1	2.6	5.3	5.3	3	1103.1	209.7	5.3
2	6.0	6.8	1.6	0	0.0	0.0	0.0
3	8.2	9.5	2.7	1	367.7	137.9	4.9
4	10.3	11.0	1.5	0	0.0	0.0	0.0
5	12.6	14.2	3.1	6	2206.2	704.7	6.6
6	19.2	24.3	10.1	3	1103.1	108.8	4.7
7	39.4	54.6	30.3	1	367.7	12.1	2.5
8	64.5	74.4	19.8	1	367.7	18.5	2.9
9	80.5	86.5	12.0	4	1470.8	122.1	4.8
10	91.5	96.5	10.1	7	2573.9	255.9	5.5
11	101.1	105.6	9.1	9	3309.3	364.0	5.9
12	113.0	120.3	14.7	9	3309.3	225.7	5.4
13	128.7	137.0	16.7	7	2573.9	154.1	5.0
14	146.5	156.0	19.0	10	3677.0	193.3	5.3
15	165.1	174.2	18.1	3	1103.1	60.8	4.1
16	183.3	192.5	18.3	3	1103.1	60.2	4.1
17	199.5	206.4	14.0	14	5147.7	368.8	5.9
18	221.9	237.5	31.0	10	3677.0	118.5	4.8
19	256.7	275.9	38.4	2	735.4	19.1	3.0
20	288.9	301.9	26.0	1	367.7	14.2	2.6
21	344.7	387.6	85.7	0	0.0	0.0	0.0

=====

survey	station	temp	julian	local	staged(21)	catch	#/m <sup>2</sup>
2MF81	G091A	4.9	99	843	98	55822	28648.6



Appendix Figure A.19. Station abundance-age plot for eggs of walleye pollock obtained at station G091A of survey 2MF81. The logarithms of hourly stage abundances are plotted against the cumulative development times to stage midpoints. Each stage is identified by a stage number. See Appendix Table A.19 for intermediate values in the computations.

=====  
 Appendix Table A.19. Intermediate values in the calculations of  
 average hourly stage abundance for eggs of walleye pollock obtained at  
 station G091A of survey 2MF81.  
 =====

stage	mid	end	length	n staged	#/m <sup>2</sup>	#/hr/m <sup>2</sup>	ln(#/hr/m <sup>2</sup> )
1	2.5	5.1	5.1	2	584.7	115.7	4.8
2	5.8	6.6	1.5	0	0.0	0.0	0.0
3	7.8	9.1	2.6	0	0.0	0.0	0.0
4	9.9	10.6	1.5	0	0.0	0.0	0.0
5	12.1	13.6	3.0	5	1461.7	485.9	6.2
6	18.5	23.3	9.7	12	3508.0	360.3	5.9
7	37.9	52.5	29.1	55	16078.3	552.1	6.3
8	62.0	71.5	19.1	7	2046.3	107.3	4.7
9	77.3	83.1	11.6	2	584.7	50.5	3.9
10	87.9	92.8	9.7	7	2046.3	211.8	5.4
11	97.1	101.5	8.7	1	292.3	33.5	3.5
12	108.5	115.6	14.1	2	584.7	41.5	3.7
13	123.6	131.6	16.0	0	0.0	0.0	0.0
14	140.8	149.9	18.3	1	292.3	16.0	2.8
15	158.6	167.3	17.4	0	0.0	0.0	0.0
16	176.1	184.9	17.6	0	0.0	0.0	0.0
17	191.6	198.3	13.4	2	584.7	43.6	3.8
18	213.2	228.1	29.8	1	292.3	9.8	2.3
19	246.6	265.1	36.9	0	0.0	0.0	0.0
20	277.6	290.0	25.0	0	0.0	0.0	0.0
21	331.2	372.4	82.4	1	292.3	3.5	1.3

=====

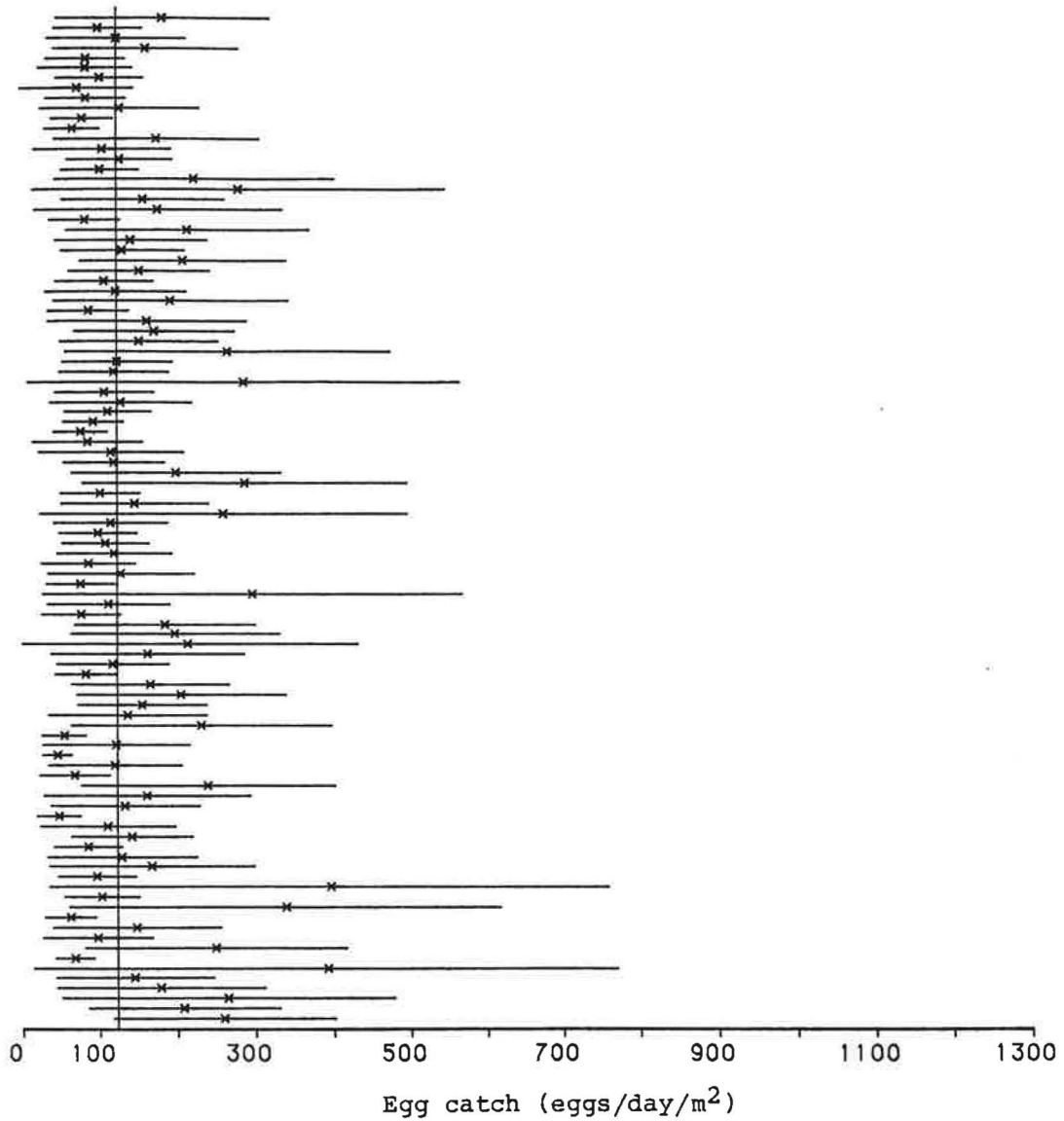




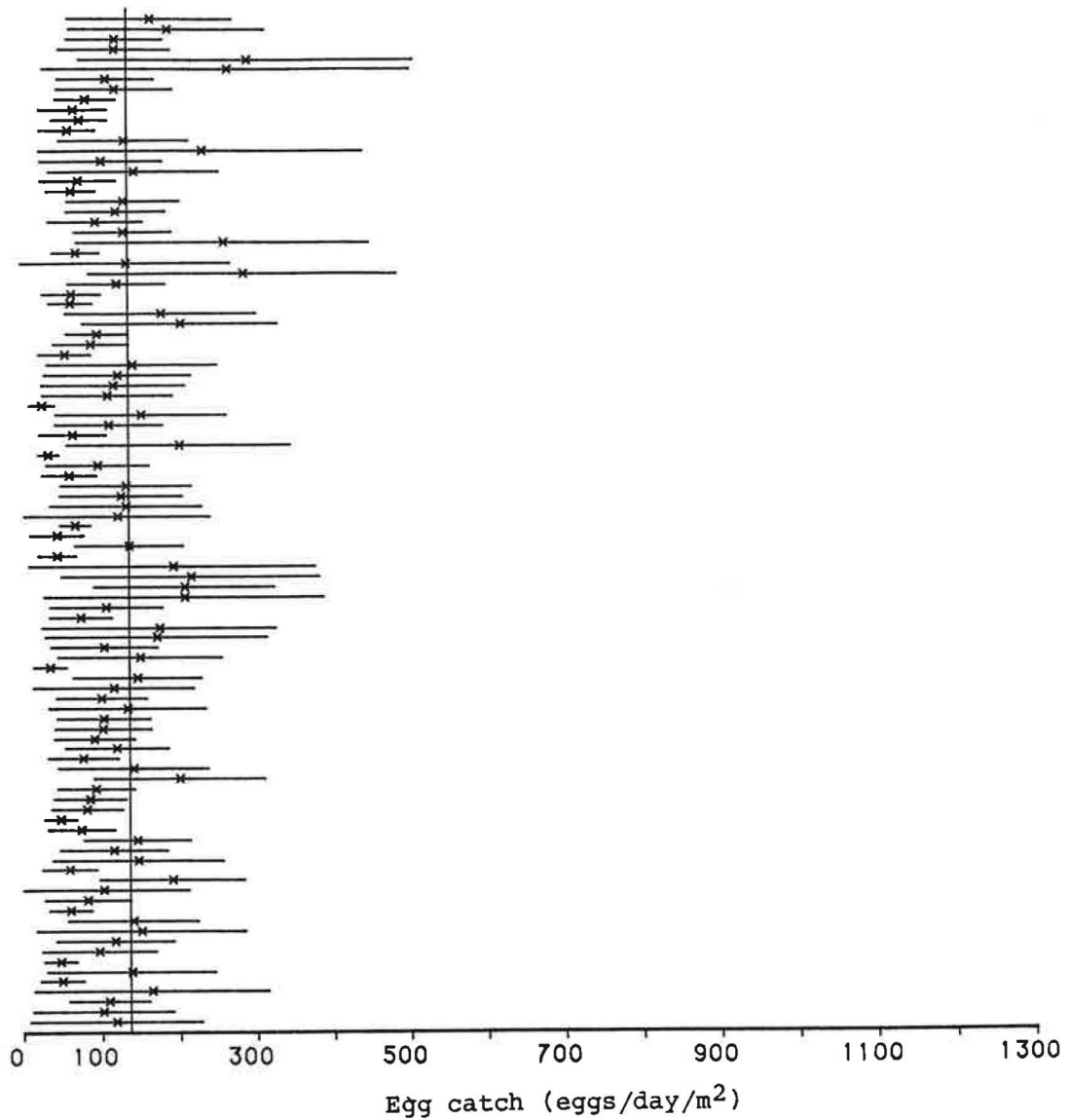
Appendix B. Confidence intervals for simulations of the sampling experiment.

Surveys were simulated from two models of egg abundance within the survey area (abundance surfaces A and B). Egg catch data from survey 2MF81 were used to construct abundance surfaces. The coefficient of local variation for egg catches at a sampling station was set to 0%, 25%, and 50% for the simulation of egg catches. Sampling design was random with a sample size of  $n=90$ , or systematic (gridded), using a grid template with a sample size of  $n=85$ .  $Q=100$  surveys were simulated for selected permutations of abundance surface, coefficient of variation, and sampling design. Egg catches from the simulated surveys were summarized using the delta distribution (DLN), negative binomial distribution (NB), and simple random sampling (SRS) design. Confidence limits were constructed (two standard deviations of mean) and plotted on the following pages. A horizontal line depicts the confidence interval for each of the 100 simulated surveys, and the "X" at the center of each interval indicates the magnitude of the estimated mean (eggs/day/m<sup>2</sup>). The vertical line indicates the magnitude of the true mean for the corresponding abundance surface.

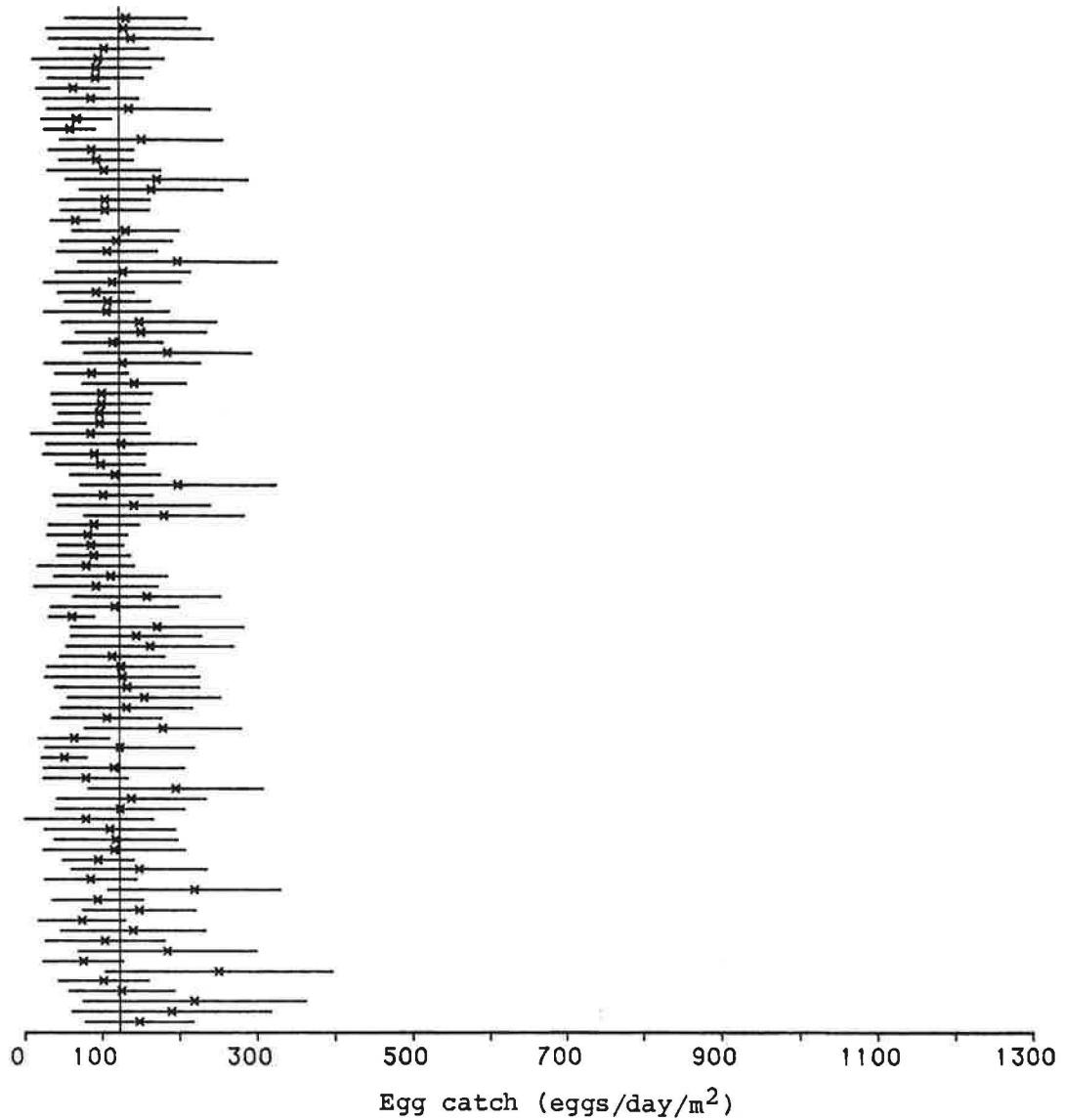




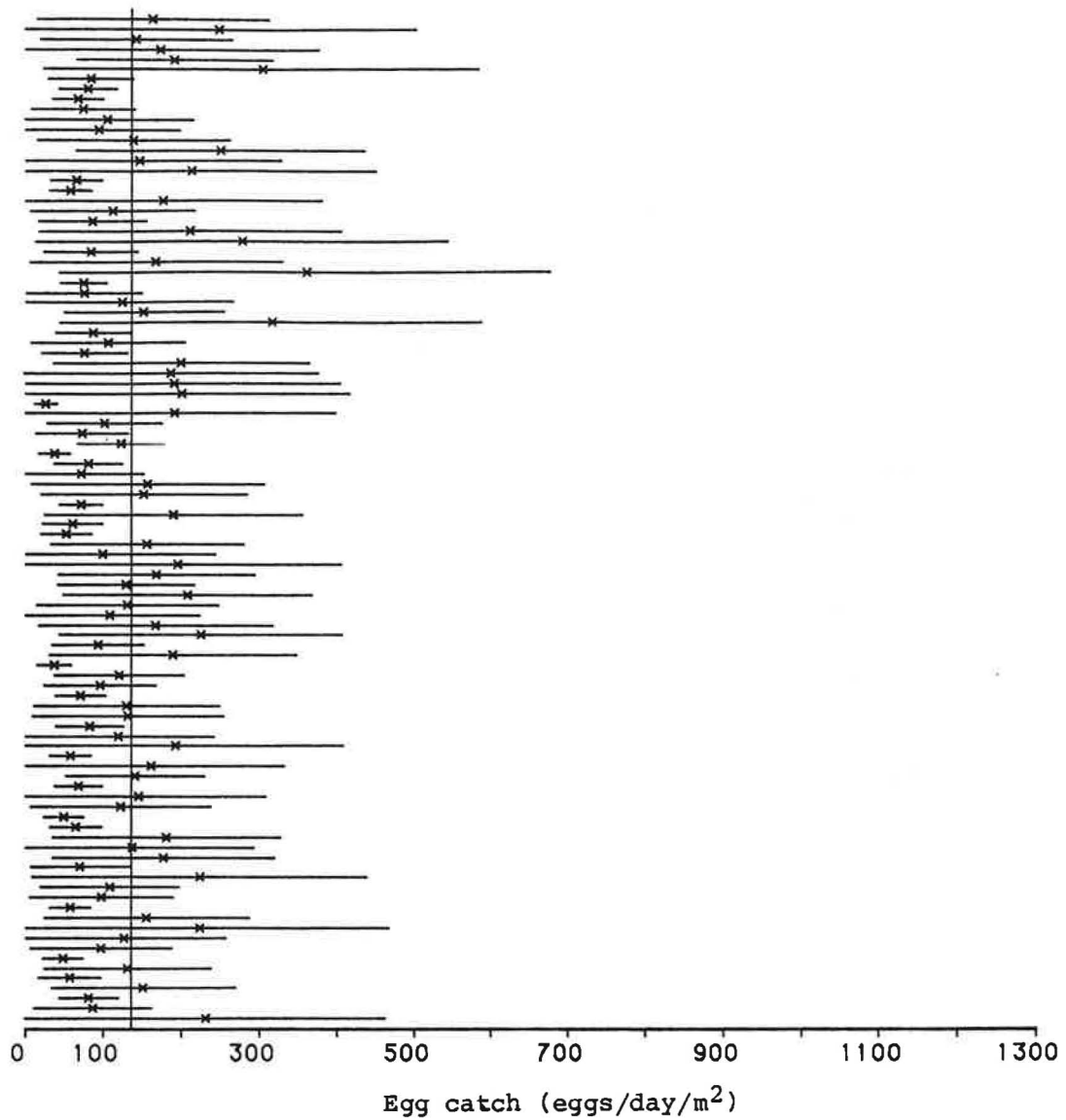
Appendix Figure B.1. Confidence intervals under the DLN model for 100 simulated surveys from abundance surface A, with random sampling, and with 0% local CV. The magnitude of the estimated mean for each survey is indicated by an "X" and the confidence limit extends two standard deviations from the mean. The magnitude of the true mean is indicated by the vertical line.



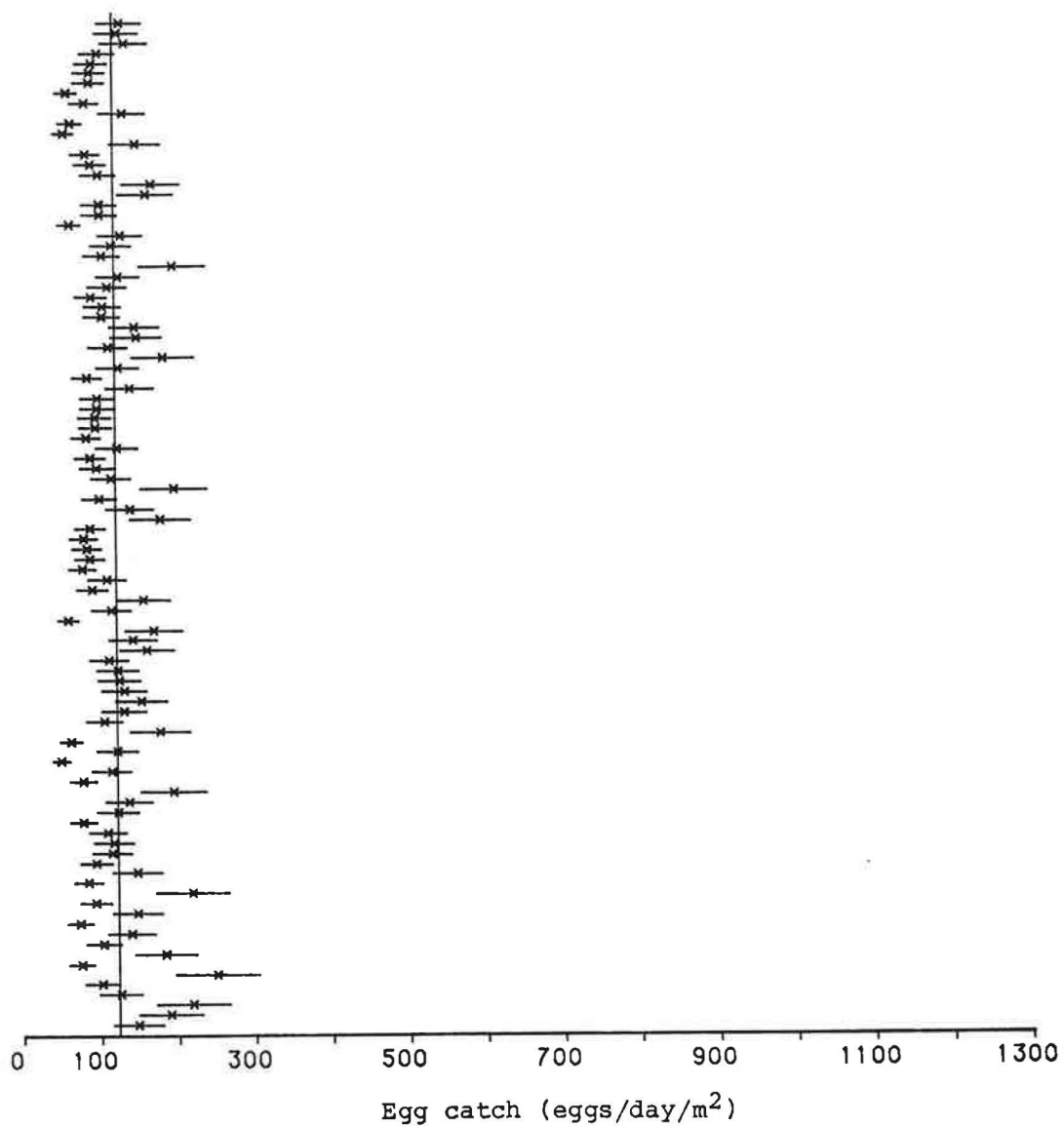
Appendix Figure B.2. Confidence intervals under the DLN model for 100 simulated surveys from abundance surface B, with random sampling, and with 0% local CV. The magnitude of the estimated mean for each survey is indicated by an "X" and the confidence limit extends two standard deviations from the mean. The magnitude of the true mean is indicated by the vertical line.



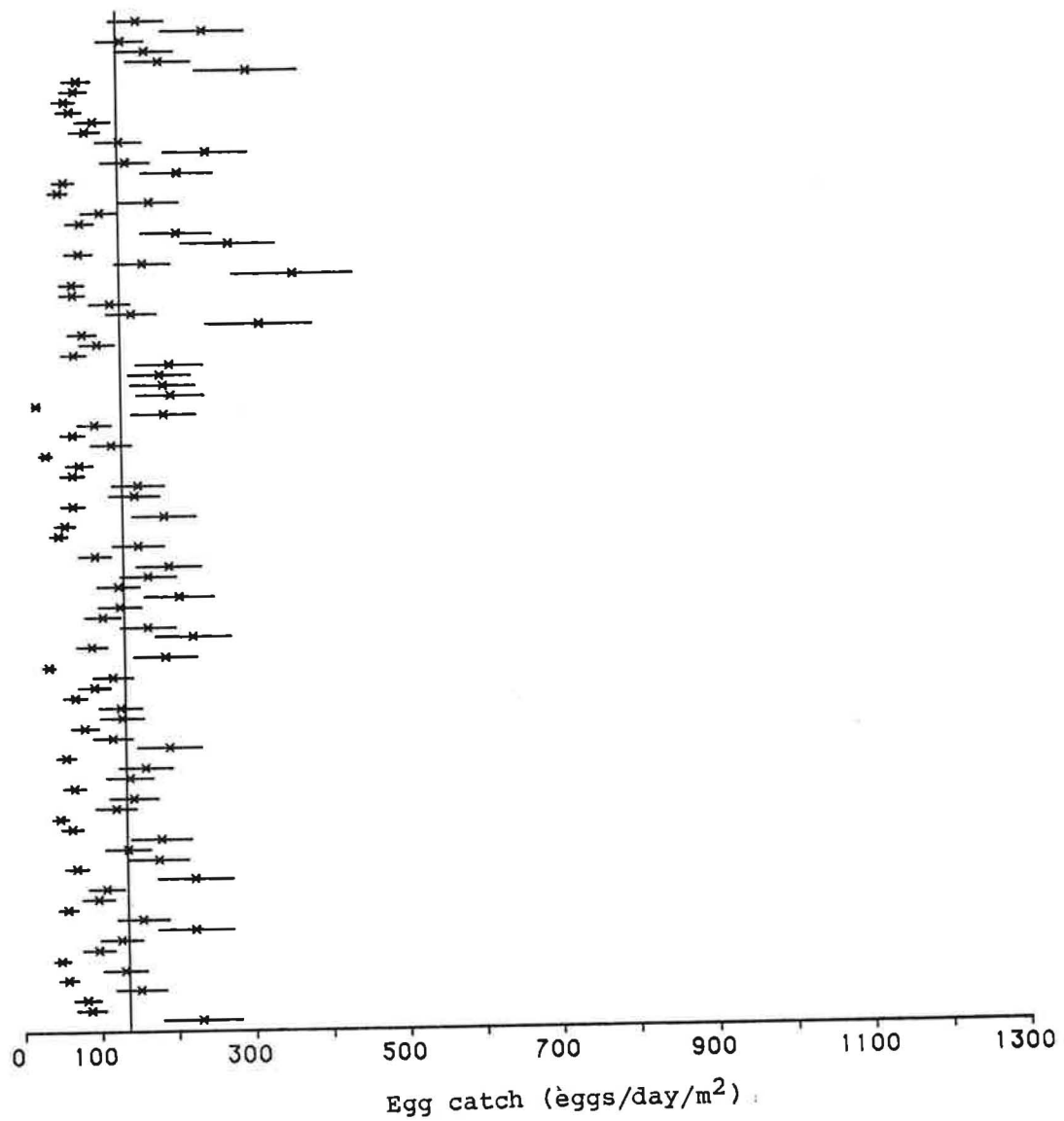
Appendix Figure B.3. Confidence intervals under the SRS model for 100 simulated surveys from abundance surface A, with random sampling, and with 0% local CV. The magnitude of the estimated mean for each survey is indicated by an "X" and the confidence limit extends two standard deviations from the mean. The magnitude of the true mean is indicated by the vertical line.



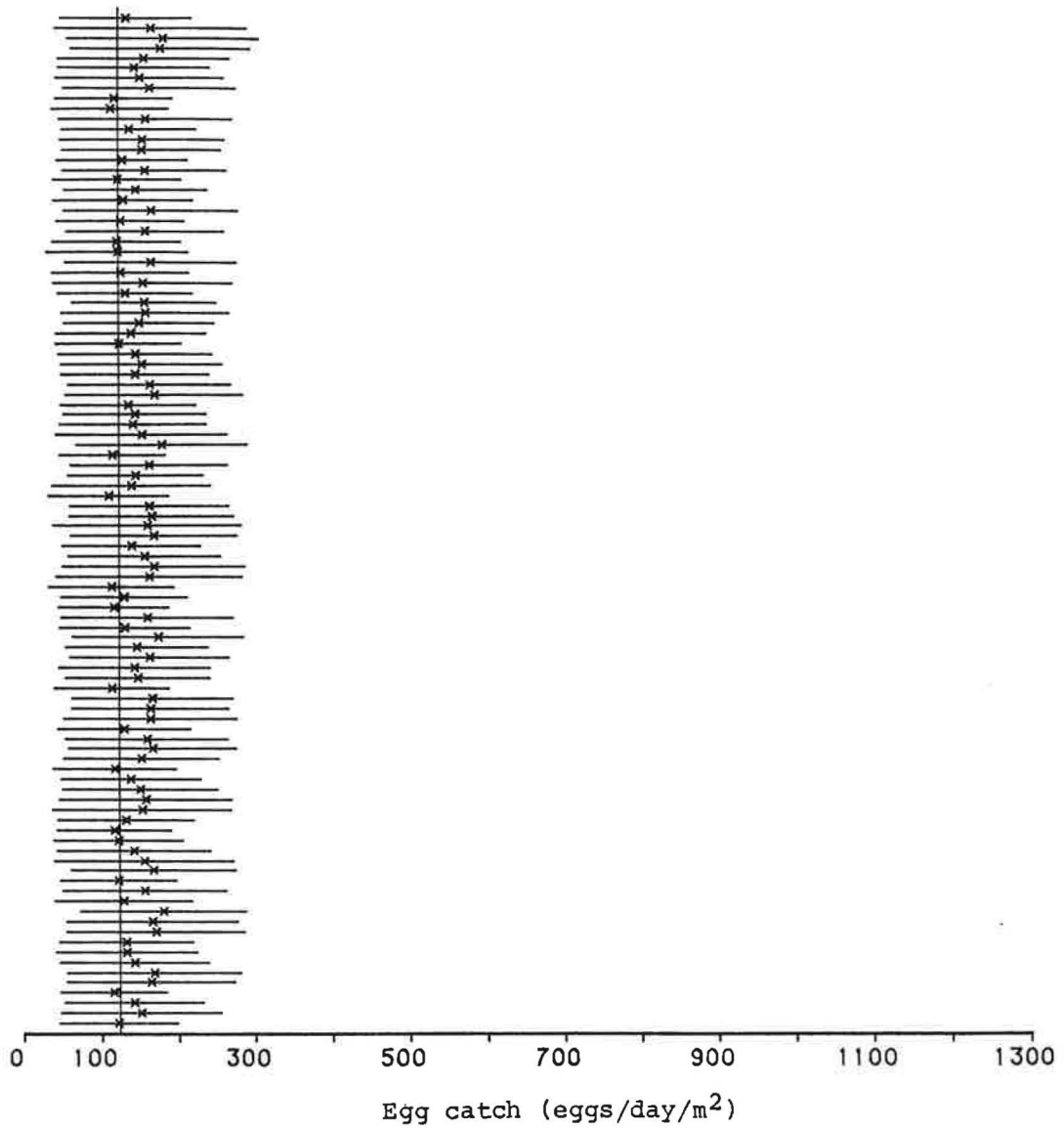
Appendix Figure B.4. Confidence intervals under the SRS model for 100 simulated surveys from abundance surface B, with random sampling, and with 0% local CV. The magnitude of the estimated mean for each survey is indicated by an "X" and the confidence limit extends two standard deviations from the mean. The magnitude of the true mean is indicated by the vertical line.



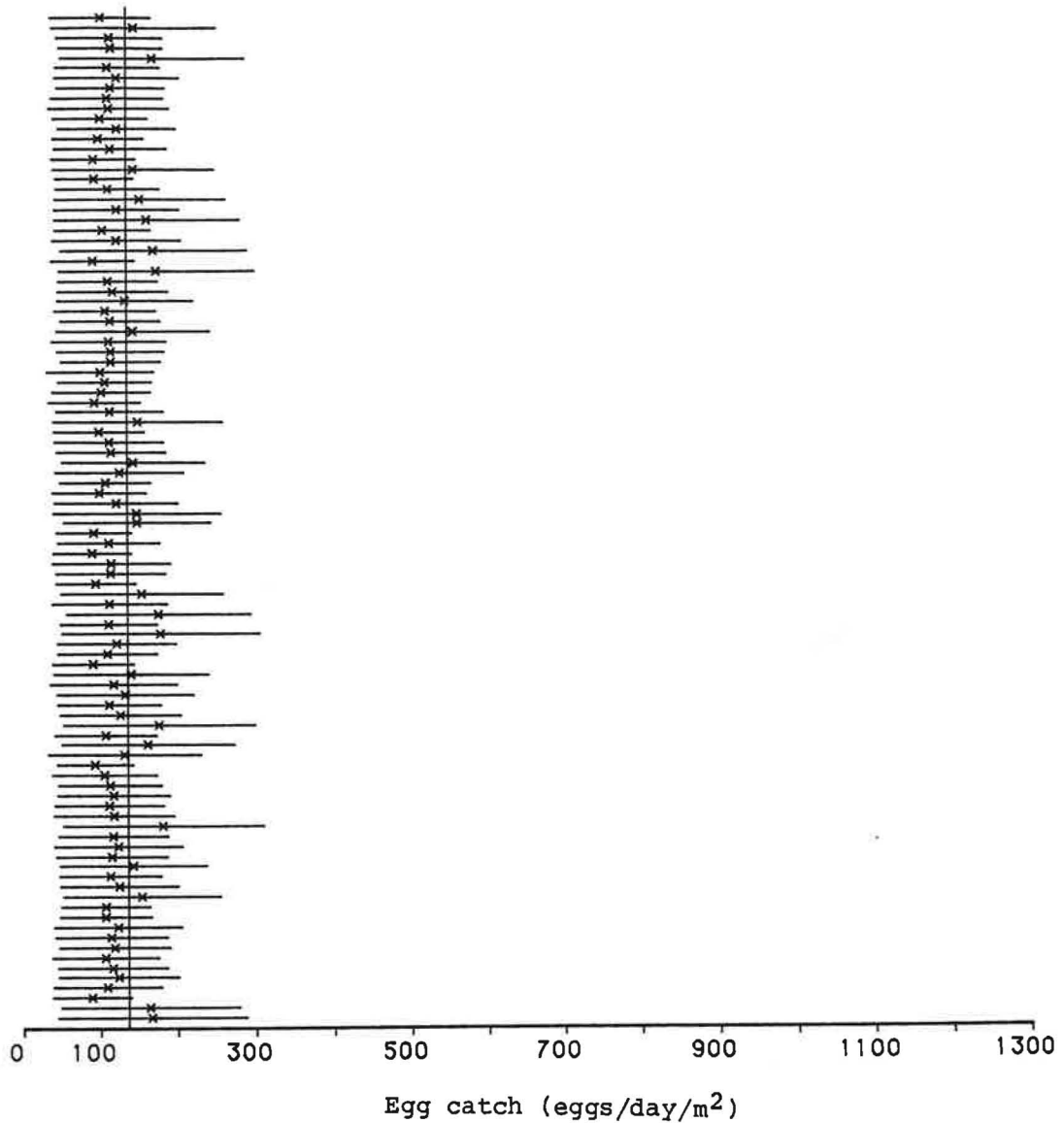
Appendix Figure B.5. Confidence intervals under the NB model for 100 simulated surveys from abundance surface A, with random sampling, and with 0% local CV. The magnitude of the estimated mean for each survey is indicated by an "X" and the confidence limit extends two standard deviations from the mean. The magnitude of the true mean is indicated by the vertical line.



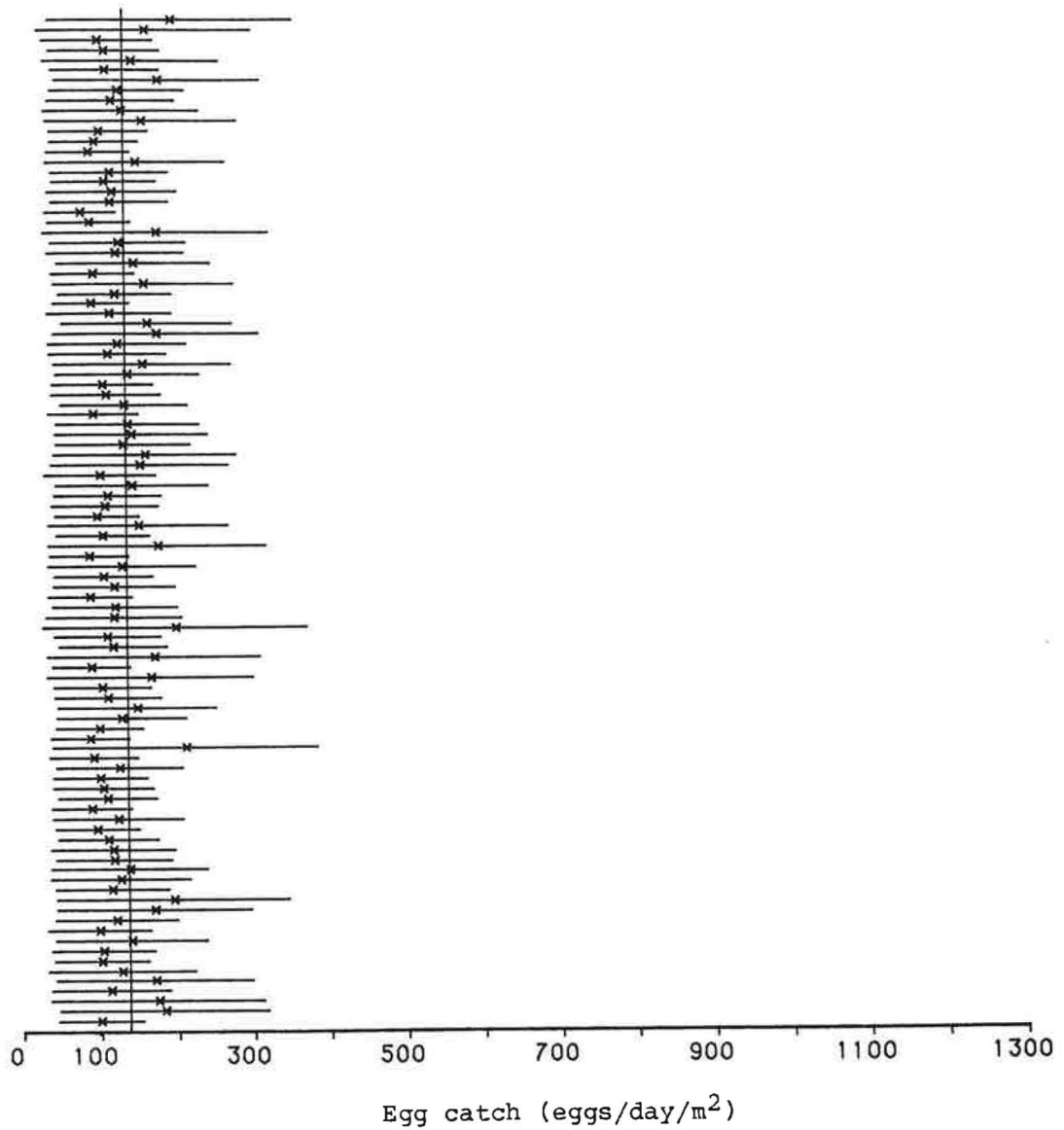
Appendix Figure B.6. Confidence intervals under the NB model for 100 simulated surveys from abundance surface B, with random sampling, and with 0% local CV. The magnitude of the estimated mean for each survey is indicated by an "X" and the confidence limit extends two standard deviations from the mean. The magnitude of the true mean is indicated by the vertical line.



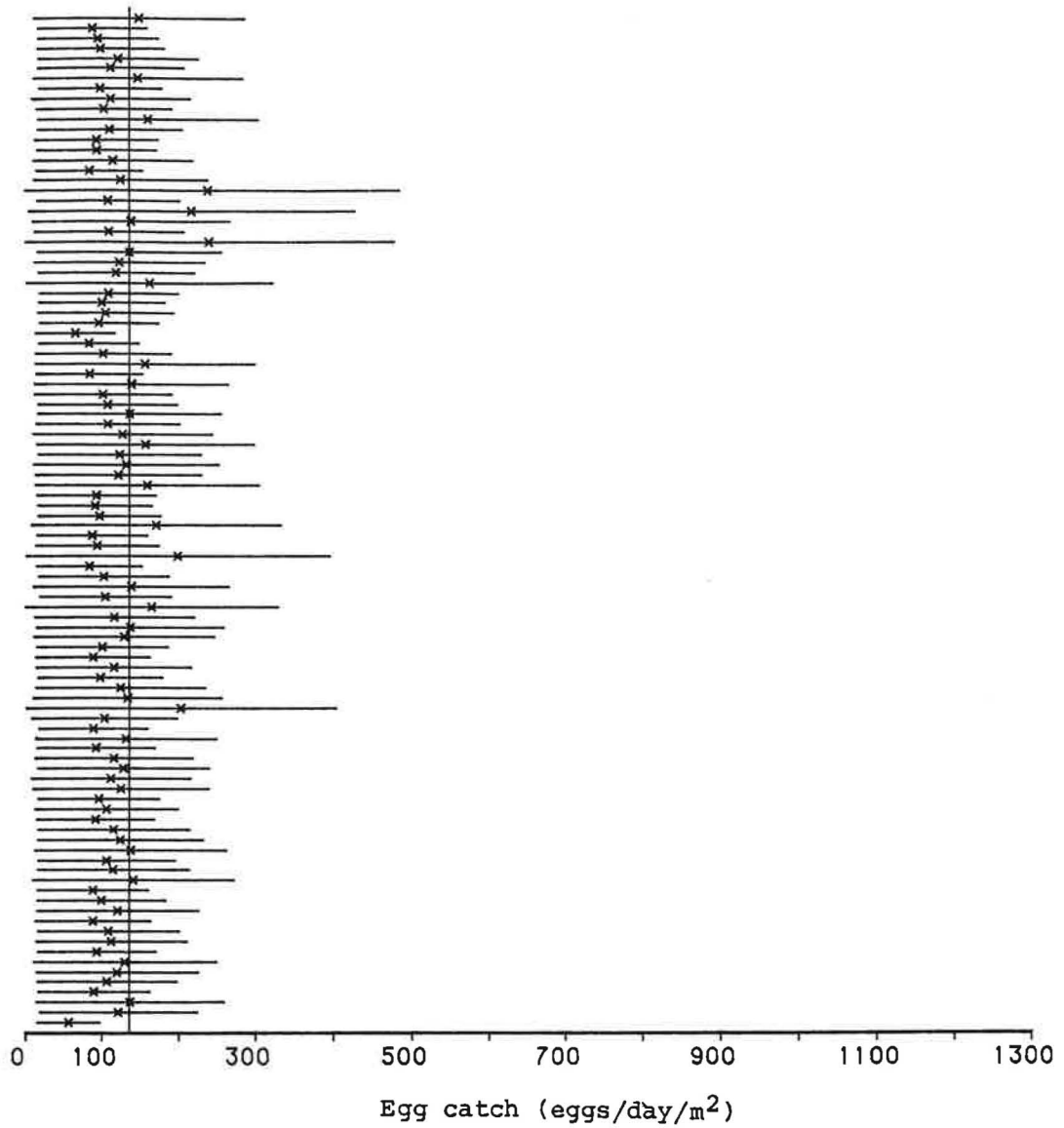
Appendix Figure B.7. Confidence intervals under the DLN model for 100 simulated surveys from abundance surface A, with grid sampling, and with 0% local CV. The magnitude of the estimated mean for each survey is indicated by an "X" and the confidence limit extends two standard deviations from the mean. The magnitude of the true mean is indicated by the vertical line.



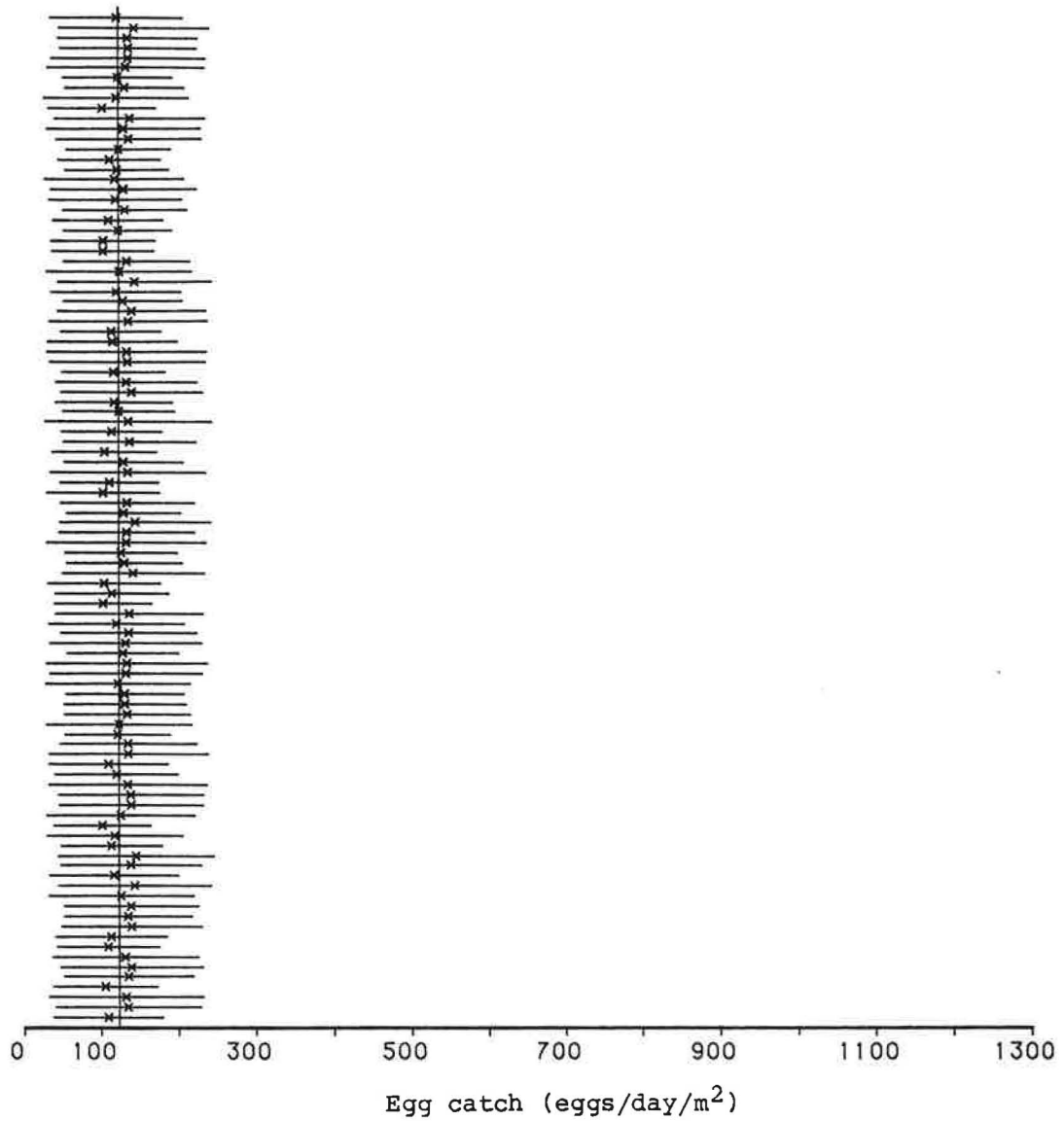
Appendix Figure B.8. Confidence intervals under the DLN model for 100 simulated surveys from abundance surface B, with grid sampling, and with 0% local CV. The magnitude of the estimated mean for each survey is indicated by an "X" and the confidence limit extends two standard deviations from the mean. The magnitude of the true mean is indicated by the vertical line.



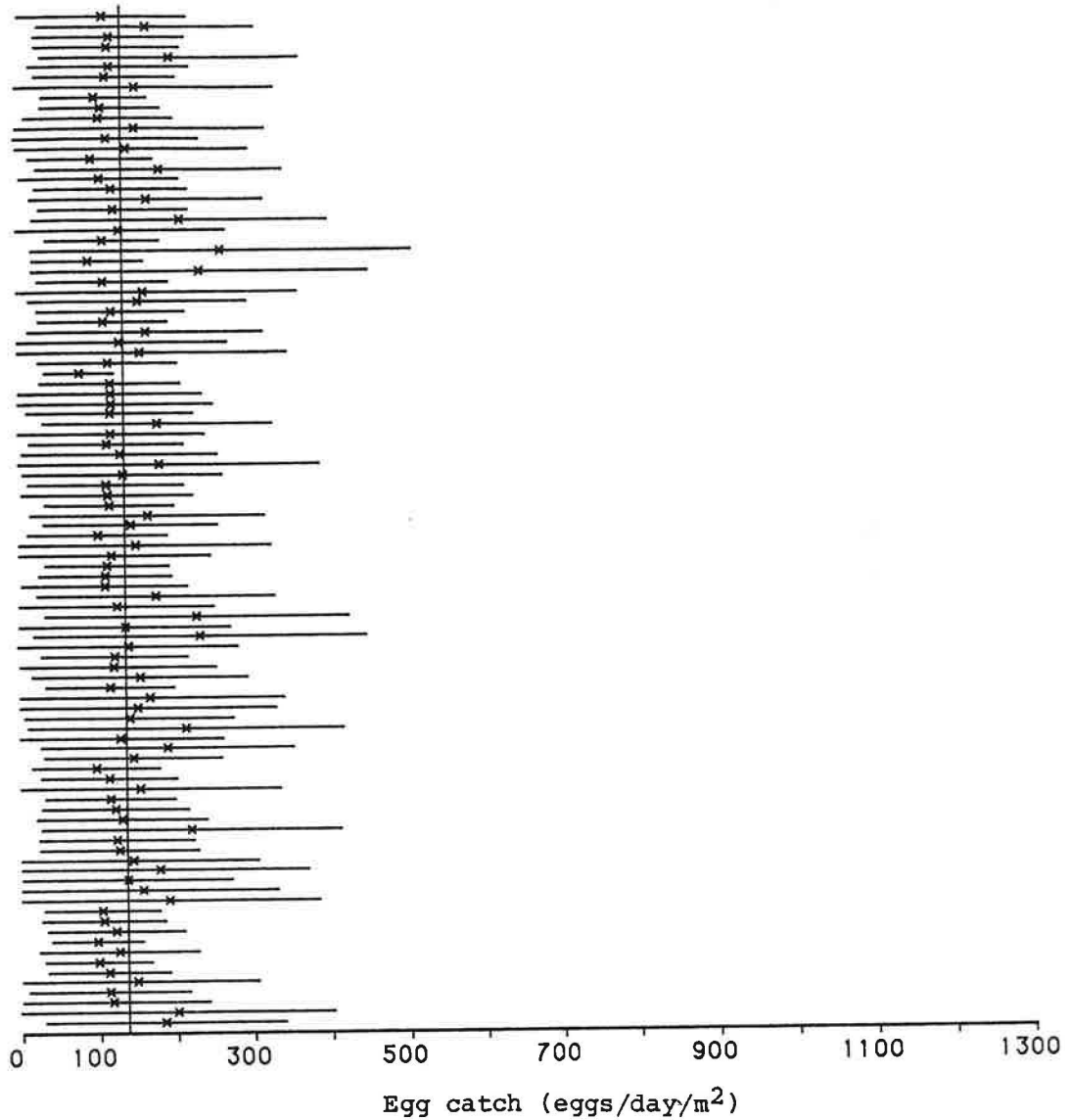
Appendix Figure B.9. Confidence intervals under the DLN model for 100 simulated surveys from abundance surface B, with grid sampling, and with 25% local CV. The magnitude of the estimated mean for each survey is indicated by an "X" and the confidence limit extends two standard deviations from the mean. The magnitude of the true mean is indicated by the vertical line.



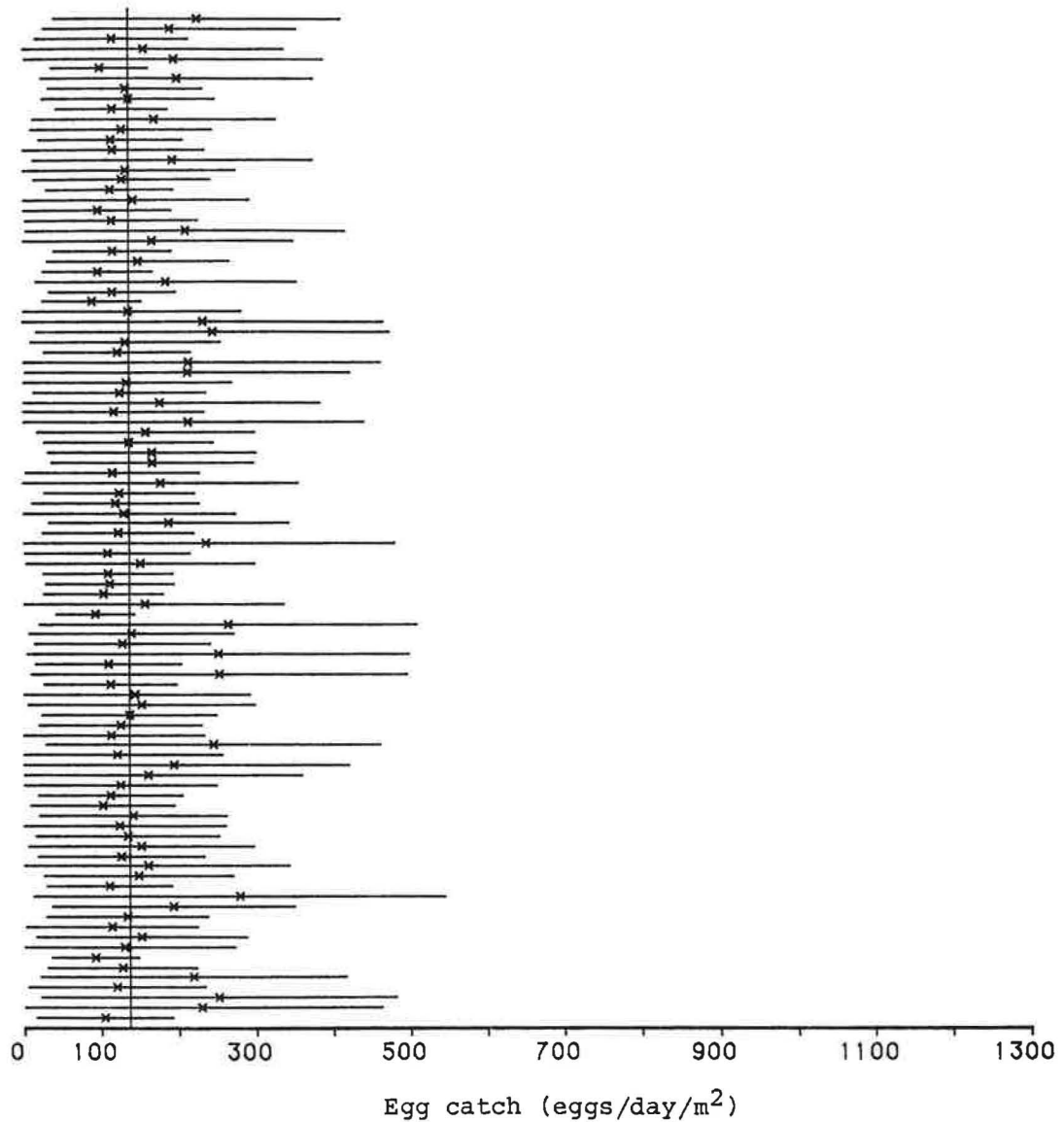
Appendix Figure B.10. Confidence intervals under the DLN model for 100 simulated surveys from abundance surface B, with grid sampling, and with 50% local CV. The magnitude of the estimated mean for each survey is indicated by an "X" and the confidence limit extends two standard deviations from the mean. The magnitude of the true mean is indicated by the vertical line.



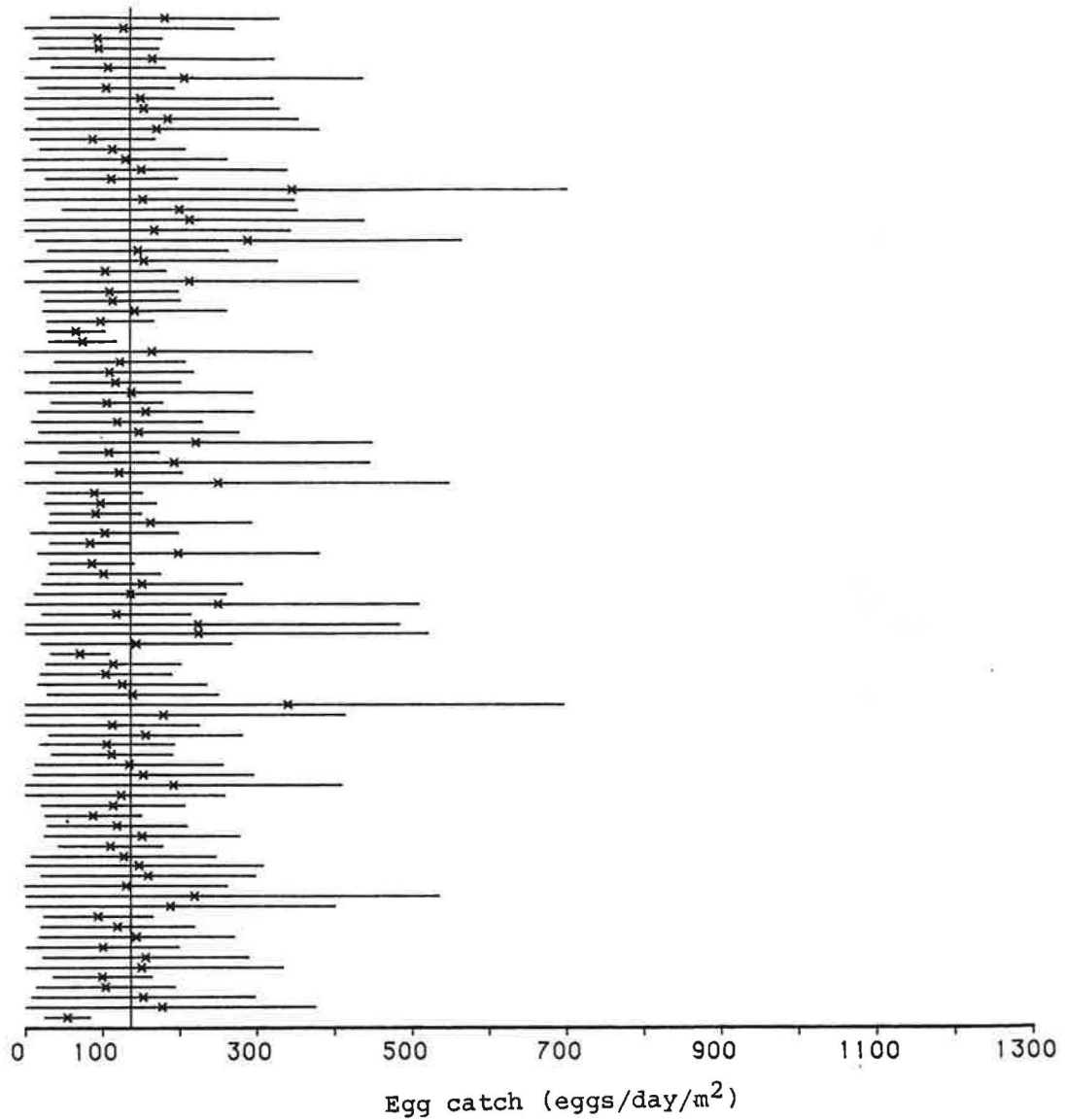
Appendix Figure B.11. Confidence intervals under the SRS model for 100 simulated surveys from abundance surface A, with grid sampling, and with 0% local CV. The magnitude of the estimated mean for each survey is indicated by an "X" and the confidence limit extends two standard deviations from the mean. The magnitude of the true mean is indicated by the vertical line.



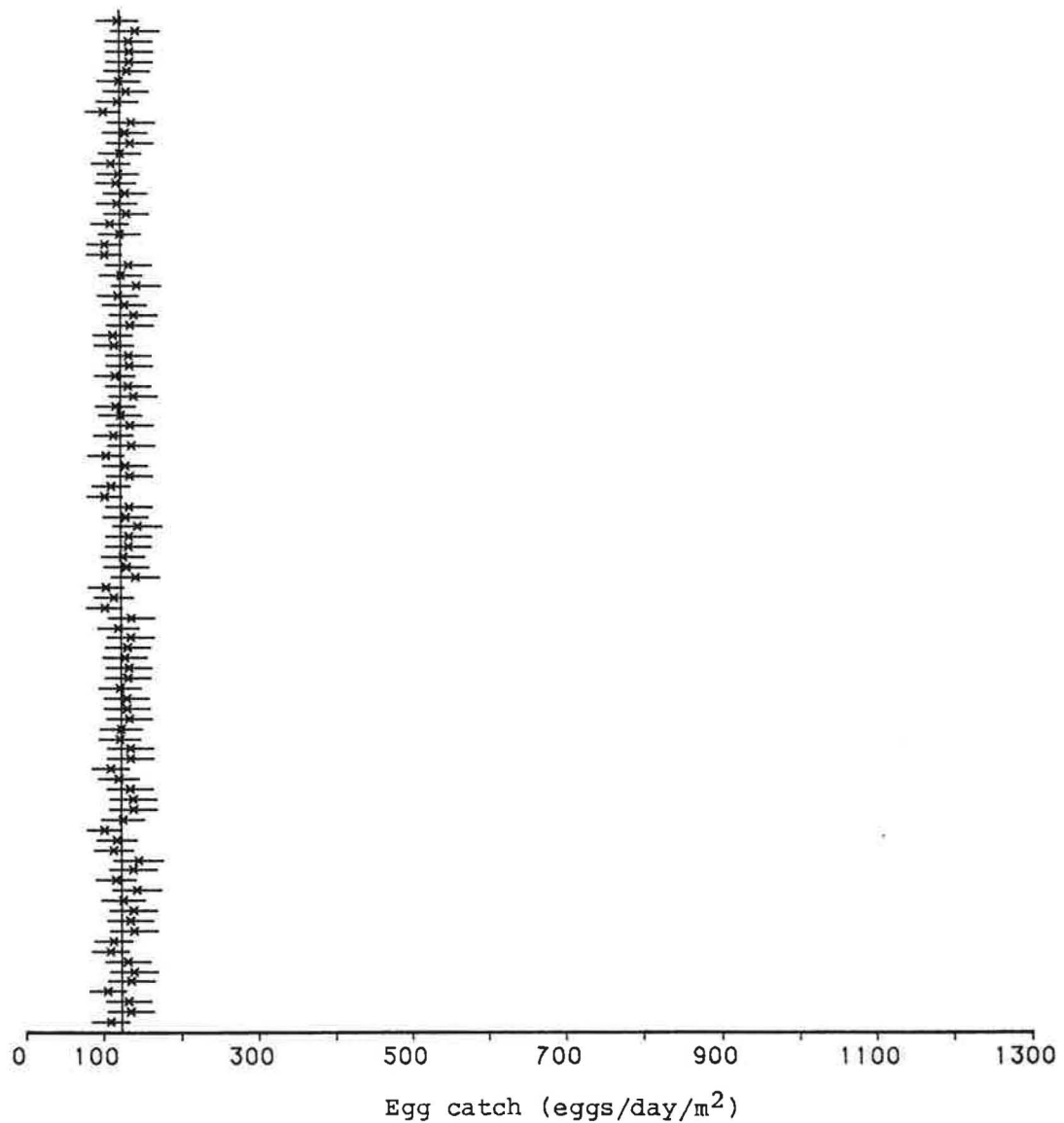
Appendix Figure B.12. Confidence intervals under the SRS model for 100 simulated surveys from abundance surface B, with grid sampling, and with 0% local CV. The magnitude of the estimated mean for each survey is indicated by an "X" and the confidence limit extends two standard deviations from the mean. The magnitude of the true mean is indicated by the vertical line.



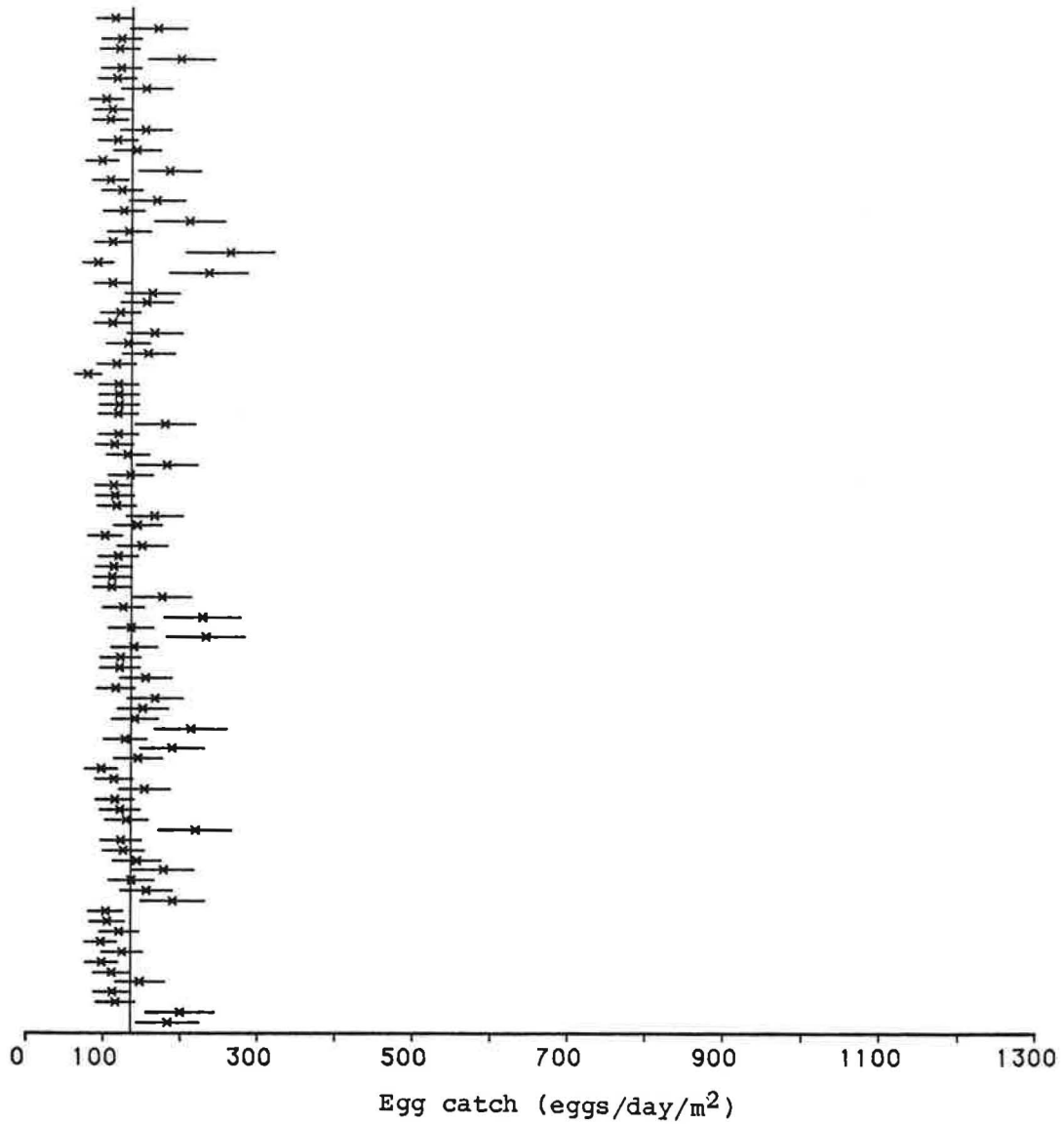
Appendix Figure B.13. Confidence intervals under the SRS model for 100 simulated surveys from abundance surface B, with grid sampling, and with 25% local CV. The magnitude of the estimated mean for each survey is indicated by an "X" and the confidence limit extends two standard deviations from the mean. The magnitude of the true mean is indicated by the vertical line.



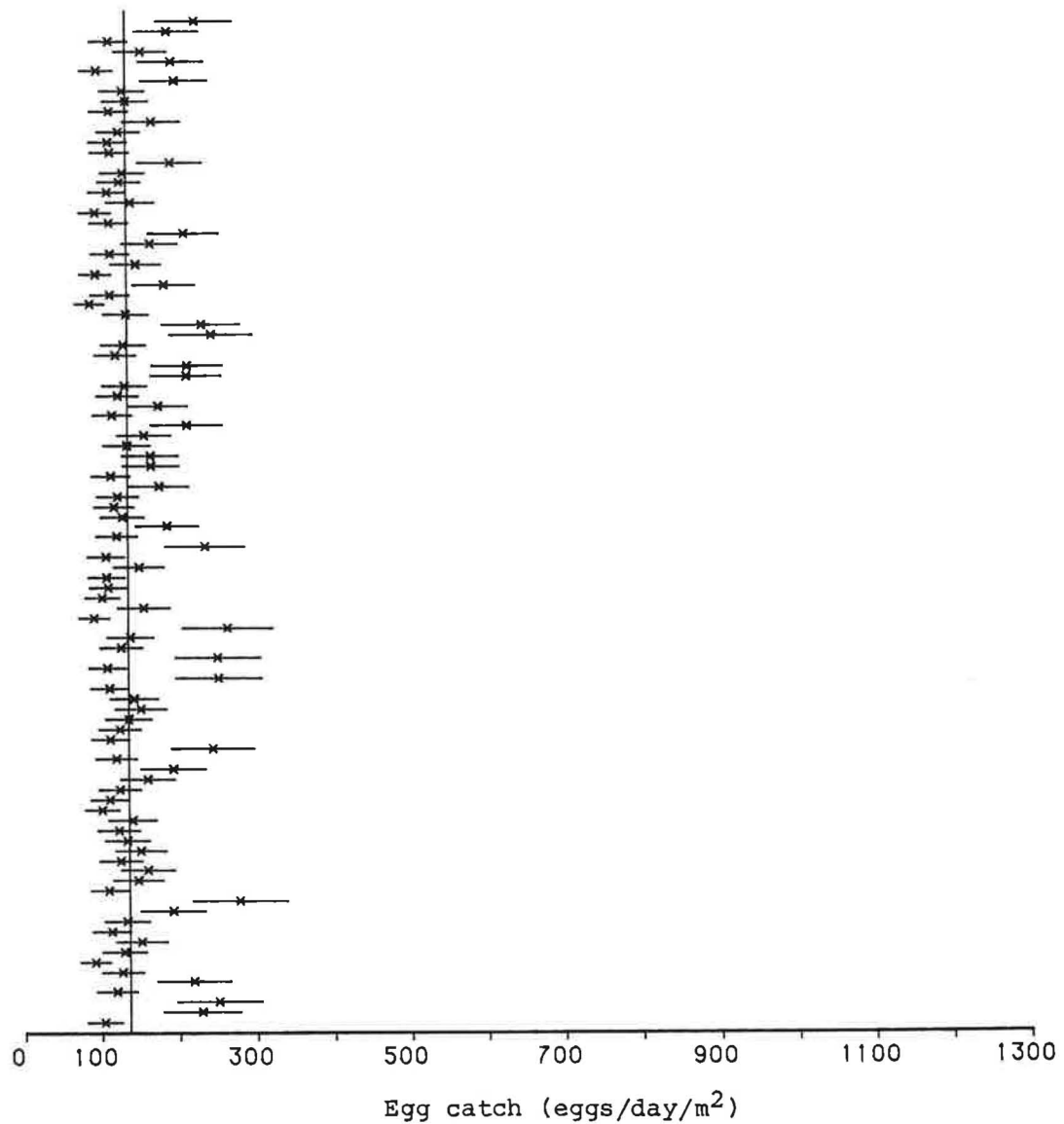
Appendix Figure B.14. Confidence intervals under the SRS model for 100 simulated surveys from abundance surface B, with grid sampling, and with 50% local CV. The magnitude of the estimated mean for each survey is indicated by an "X" and the confidence limit extends two standard deviations from the mean. The magnitude of the true mean is indicated by the vertical line.



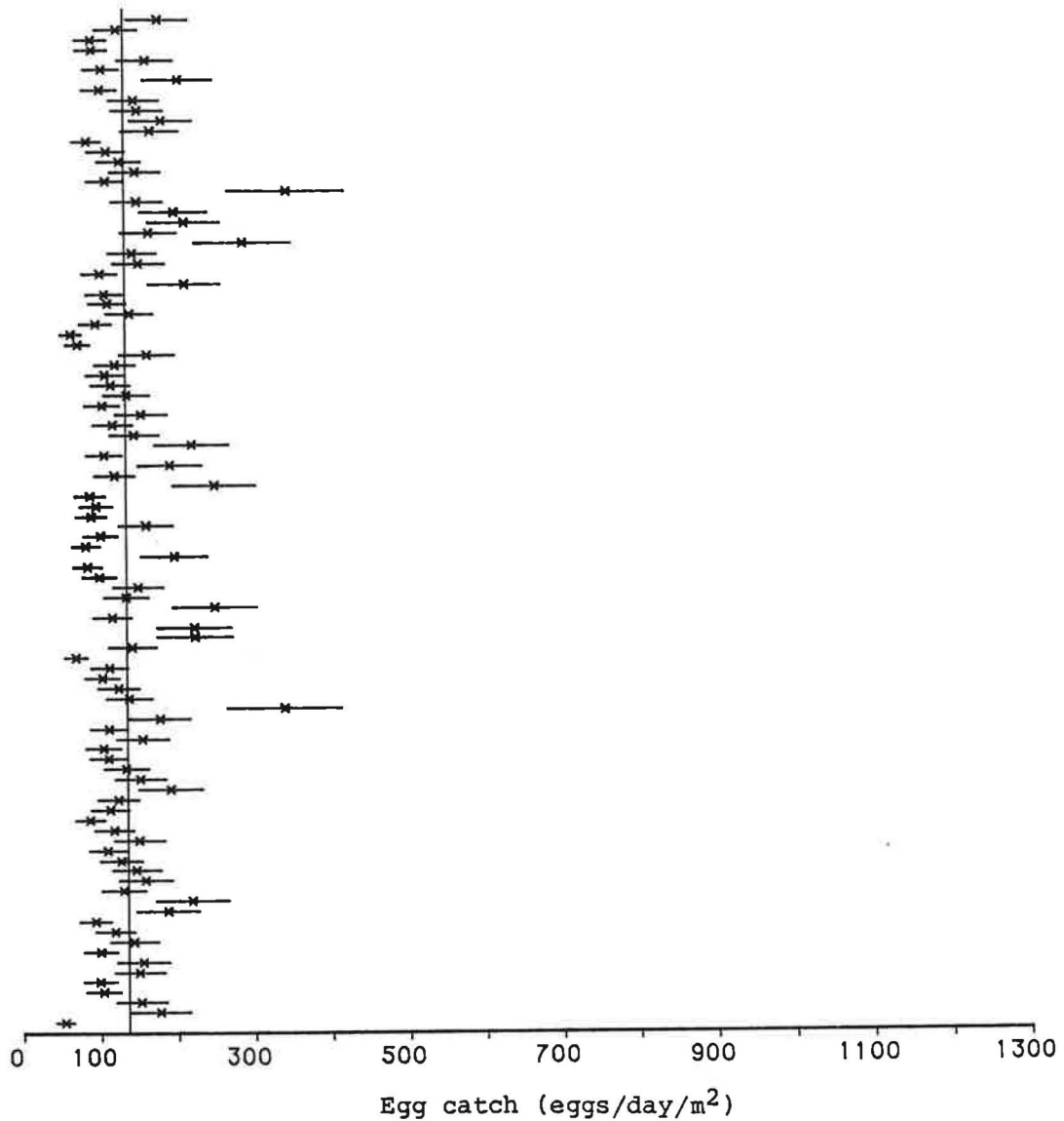
Appendix Figure B.15. Confidence intervals under the NB model for 100 simulated surveys from abundance surface A, with grid sampling, and with 0% local CV. The magnitude of the estimated mean for each survey is indicated by an "X" and the confidence limit extends two standard deviations from the mean. The magnitude of the true mean is indicated by the vertical line.



Appendix Figure B.16. Confidence intervals under the NB model for 100 simulated surveys from abundance surface B, with grid sampling, and with 0% local CV. The magnitude of the estimated mean for each survey is indicated by an "X" and the confidence limit extends two standard deviations from the mean. The magnitude of the true mean is indicated by the vertical line.



Appendix Figure B.17. Confidence intervals under the NB model for 100 simulated surveys from abundance surface B, with grid sampling, and with 25% local CV. The magnitude of the estimated mean for each survey is indicated by an "X" and the confidence limit extends two standard deviations from the mean. The magnitude of the true mean is indicated by the vertical line.



Appendix Figure B.18. Confidence intervals under the NB model for 100 simulated surveys from abundance surface B, with grid sampling, and with 50% local CV. The magnitude of the estimated mean for each survey is indicated by an "X" and the confidence limit extends two standard deviations from the mean. The magnitude of the true mean is indicated by the vertical line.



